**University of Plymouth**

**PEARL** **https://pearl.plymouth.ac.uk**

04 University of Plymouth Research Theses 01 Research Theses Main Collection

2006

# Investigation of the Joint Probability of Waves and High Sea Levels along the Cumbrian Coastline

Hames, Dominic Paul

http://hdl.handle.net/10026.1/2324

http://dx.doi.org/10.24382/3660
University of Plymouth

*All content in PEARL is protected by copyright law. Author manuscripts are made available in accordance with publisher policies. Please cite only the published version using the details provided on the item record or document. In the absence of an open licence (e.g. Creative Commons), permissions for further reuse of content should be sought from the publisher or author.*

# Investigation of the Joint Probability of Waves and High Sea Levels along the Cumbrian Coastline

by

**Dominic Paul Hames**

A thesis submitted to the University of Plymouth

in fulfilment for the degree of

**Doctor of Philosophy**

School of Technology

**June 2006**

# Abstract

**Investigation of the Joint Probability of Waves and High Sea Levels along the Cumbrian Coastline** by Dominic Paul Hames

The use of joint probability techniques for wave heights and sea levels to estimate potential damage and overtopping of flood defences is of vital importance in coastal defence work. Without the use of joint probability techniques, confidence in the appropriate design conditions are poor, and defences could be built to an incorrect design standard. This has the potential effect of a coastal or estuary scheme being under-designed, and therefore not suitable for the purpose it was built for or over-designed, and therefore built to a much greater cost than required.

With no research having considered the joint probability relationship between waves and high sea levels at nearshore locations, this study has therefore been defined to investigate this relationship spatially for an approximate 100km length of coastline for different nearshore beach levels in Cumbria. This should improve the understanding of the joint probability relationship nearshore, and enable this relationship to be reliably estimated for other coastlines where appropriate data is not available.

To investigate this relationship, 13.2 years of coincident waves and sea levels have been determined nearshore at regular 400m centres, and at 5 regularly spaced beach levels from 2m above and below Ordnance Datum. The wave transformation model REFDIF has been used to determine nearshore wave heights, using data from two deep water Met Office prediction points. Sea levels have been determined using recorded data from all known tide gauges and tide log books.

From an analysis of the results, clear relationships appear to exist over lengths of coastlines that have similar exposure conditions. Given the joint probability relationship at one location, the joint probability relationship at the second can be reliably estimated based on estimates of the extreme wave height and sea level at the second. Joint probability curves were noted to show a consistent shape within bays, as well as at headlands, steep beaches and for coastlines that had a change in direction away from the predominant wave direction. As beach levels increased, the joint probability curves became increasingly generic, and it was noted that at the most extreme sea levels return period wave heights generally increased for higher beach levels.

# List of Contents


**1. Introduction** **1**

1.1 Rational for Research 3

1.2 Investigation of the Joint Probability of Waves and High Sea Levels 4

1.3 Description of Thesis 7

**2. Literature Review of Joint Probability of Waves and High Sea Levels** **11**

2.1 Introduction 11

2.2 Sea Levels and Waves and their Correlation 13

2.3 Development of techniques of Joint Probability between Waves and Sea Levels 15

2.3.1 Independence or Dependence of Marginal Probabilities 15

2.3.2 Manual Analysis of Joint Probability Density 16

2.3.3 Extrapolation of Joint Probability Density above High Sea Level and Wave Height Thresholds 17

2.3.4 Intuitive Joint Probability Assessment 19

2.3.5 Extrapolation of Joint Probability Density (JOIN-SEA) 21

**3. Collection, Collation and Pre-processing of Raw Data Sets** **32**

3.1 Length of Data Record Analysed 33

3.2 Sea Level Data 33

3.2.1 Predicted Tide Level Data 34

3.2.2 Recorded Sea Level Data 34

3.2.3 Pre-processing of Sea Level Data 38

3.2.4 Compilation of Processed Time Series 40

3.2.5 Analysis of Trends in Sea Level Records 50

3.3 Wave Data 55

3.3.1 Data Availability 55

3.3.2 Met Office Wave Model 60

3.3.3 Validation of Met Office Wave Model 60
3.3.4 Wave Data Used in Study 62
3.3.5 Pre-processing of Wave Data and Compilation of Processed Time Series 63
3.3.6 Trends in Wave Heights 64
3.4 Currents 65
3.5 Bathymetry 65
3.5.1 Bathymetric Data Available for Study 66
3.5.2 Determination of Bathymetry Model Grids for Cumbrian Coastline 70

**4. Numerical Transformation of Offshore Waves 77**
4.1 Introduction 77
4.2 Wave Transformation Models Considered for Study 77
4.2.1 Ray Models 77
4.2.2 Mild Slope Equation Models 78
4.2.3 Non Linear Models 78
4.3 Wave Transformation Models 78
4.3.1 KrKs 79
4.3.2 SWAN 80
4.3.3 REFDIF 81
4.4 Verification of Models 83
4.4.1 Literature review of Comparison of REFDIF and SWAN 84
4.5 Choice of Suitable Wave Transformation Model 86
4.5.1 Limitations of REFDIF 87
4.5.2 Currents 93
4.5.3 Energy Dissipation 96
4.5.4 Sub Grids 97
4.5.5 General Comments 97
4.5.6 Verification Tests on REFDIF 98
4.6 Definition of Offshore and Inshore Wave Conditions 99
4.6.1 Wind Waves 101
4.6.2 Swell Waves 110
4.7 Specification of Offshore Wave Conditions 111

**5. Joint Probability of Waves and High Sea Levels** **114**

5.1 Introduction 114

5.2 Marginal Extremes 115

5.2.1 Extreme Sea Levels along the Cumbrian Coastline 116

5.2.2 Extreme Offshore Wave Heights along the Cumbrian Coastline 130

5.2.3 Extreme Inshore Wave Heights along the Cumbrian Coastline 137

5.3 Model Selection 145

5.3.1 Distribution of Wave Populations 145

5.3.2 Threshold Selection for Inshore Wave Steepness 151

5.4 Joint Probability Relationship 154

**6. Discussion** **164**

6.1 Introduction 164

6.2 Sea Levels 164

6.3 Offshore Wave Records 177

6.4 Model Grids 183

6.5 Wave Modelling 186

6.6 Investigation of Joint Probability Relationship 188

6.6.1 Marginal Distributions 188

6.6.2 Model Selection 196

6.6.3 Spatial Variation in Joint Probability at -2m@OD 198

6.6.4 Spatial Variation in Joint Probability at Higher Beach Levels 207

6.6.5 Accuracy of JOIN-SEA Estimates 209

6.6.6 Effect of Wave Period on Damage and Overtopping / Sea Level Rise 211

**7. Conclusions** **214**

**8. Recommendations** **222**

**References**

**Appendices**


| | |
|---|---|
| Appendix A | History of Known Sea Level Records for the Cumbrian Coastline |
| Appendix B | Verification of REFDIF |
| Appendix C | Sample Model Output for REFDIF Modelling |
| Appendix D | Joint Probability Curves at Selected Locations |

# List of Tables


| | | |
|---|---|---|
| 2.1 | Correlation factors for different levels of dependency | 20 |
| 3.1 | Locations where tide predictions are available | 34 |
| 3.2 | Recorded data sets available | 35 |
| 3.3 | Secular trends determined by applying low pass filter to digitally recorded data sets | 52 |
| 3.4 | Trends determined from PSMSL data base (as of February 2005) | 53 |
| 3.5 | Standardised trends applied to data sets | 55 |
| 3.6 | Wave records available around the Cumbrian coastline | 57 |
| 3.7 | Location of model and recorded data used in validation exercise | 61 |
| 3.8 | Met Office wave parameters | 63 |
| 3.9 | Missing Met Office data | 64 |
| 3.10 | Survey information used in bathymetry | 67 |
| 3.11 | Survey information identified but not used in bathymetry | 68 |
| 3.12 | Accuracy of bathymetric survey information | 71 |
| 4.1 | Wind wave discretization | 109 |
| 4.2 | Swell wave discretization | 111 |
| 5.1 | Extreme value estimates of sea levels at Barrow (m@OD) | 118 |
| 5.2 | Extreme value estimates of sea levels at Workington (m@OD) | 119 |
| 5.3 | Extreme value estimates of sea levels at Silloth (m@OD) | 120 |
| 5.4 | Extreme estimates of sea levels | 126 |
| 5.5 | Extreme estimates of $H_s$ at $MO_1$ and $MO_2$ | 135 |
| 6.1 | Typical format of recorded sea levels (Ramsden Dock 07/08/92) | 169 |
| 6.2 | Incorrectly formatted sea level records (Ramsden Dock 19/06/94) | 170 |
| 6.3 | Sections where spatial variation in joint probability was considered | 199 |
| B.1 | Wave transformation models used in verification exercise | |
| B.2 | Incident wave conditions for harbour approach | |
| B.3 | Storm conditions recorded by offshore waverider buoy at Perranporth | |
| B.4 | Test comparisons carried out together with participants | |

B.5 Wave height coefficients and percentage errors for Test A – Linear beach

B.6 Wave height coefficients and percentage errors for Test B – Elliptic shoal

B.7 Wave height coefficients and percentage errors for Test C – Harbour approach bathymetry

B.8 Wave height coefficients and percentage errors for Test D – Perranporth

# List of Figures


| | | |
|---|---|---|
| 1.1 | Location plan showing extent of study area | 9 |
| 1.2 | Location of prediction points | 10 |
| 2.1 | Typical spring / neap tidal cycle for Workington | 14 |
| 2.2 | Example of manually drawn joint probability contours (for Shoreham, Sussex) | 17 |
| 2.3 | Example of extrapolation above sea level and wave height thresholds (superimposed on manually drawn contours for Shoreham) | 18 |
| 2.4 | Joint density contours for the standardised bivariate normal distribution | 24 |
| 2.5 | Quantile plot for GPD of wave height for simulated data set DATA1 | 26 |
| | Quantile plot for GPD of sea level for simulated data set DATA1 | 26 |
| 2.6 | Linear regression model on steepness for simulated data set DATA1 (deviates) | 28 |
| 2.7 | Linear regression model on steepness for simulated data set DATA1 (values) | 28 |
| 2.8 | Joint density contours for a mixture of two bivariate normal distributions | 30 |
| 2.9 | Variation in correlation above threshold for simulated data sets DATA1 and DATA2 | 31 |
| 3.1 | Location of sea level measurements (Cumbrian coastline) | 37 |
| 3.2 | Comparison of recorded surges at Workington 23/01/02 to 02/02/02 | 41 |
| 3.3 | pdf and cdf of surges at Workington (POL tide gauge) and Ramsden Dock | 43 |
| 3.4 | Comparison of recorded sea levels at Roa Island and Ramsden Dock | 43 |
| 3.5 | Comparison of recorded sea levels at Halfway Shoal and Ramsden Dock | 44 |
| 3.6 | Comparison of recorded sea levels at Roa Island and Halfway Shoal | 44 |
| 3.7 | Comparison of recorded sea levels at Workington and Barrow | 45 |
| 3.8 | Comparison of recorded sea levels at Workington and Silloth | 46 |
| 3.9 | Comparison of recorded sea levels at Workington and Whitehaven | 47 |

| | | |
|---|---|---|
| 3.10 | Measured and hindcast wave data for the Cumbrian coastline | 59 |
| 3.11 | Surveys used to determine bathymetry along Cumbrian coastline | 69 |
| 3.12 | Bathymetric model grids for Cumbrian coastline | 75 |
| | | |
| 4.1 | Effect of small water depths on unreliability of REFDIF model | 88 |
| 4.2 | Effect of *G/L* ratio on edge effects in REFDIF model | 89 |
| 4.3 | Surface currents at high tide within the East Irish Sea | 93 |
| 4.4 | Average spring tide surface currents predicted from Irish Sea model | 94 |
| 4.5 | Maximum wave exposure for the Cumbrian coastline | 100 |
| 4.6 | Typical discretization of wave spectra using 5 frequency bins for conditions offshore Workington approximately 12:00 10/02/97 | 104 |
| 4.7 | Monochromatic to spectral wave height ratios for different numbers of spectral frequencies | 105 |
| 4.8 | Error density in determination of wave heights for different number of frequency components | 108 |
| 4.9 | Specification of offshore wave conditions | 113 |
| | | |
| 5.1 | Extreme estimates of sea levels at Barrow for different thresholds | 123 |
| 5.2 | Extreme estimates of sea levels at Workington for different thresholds | 123 |
| 5.3 | Extreme estimates of sea levels at Silloth for different thresholds | 124 |
| 5.4 | Extreme estimates of sea levels at Barrow, Workington and Silloth using recorded data | 125 |
| 5.5 | Quantile and probability plots for Barrow | 127 |
| 5.6 | Quantile and probability plots for Workington | 127 |
| 5.7 | Quantile and probability plots for Silloth | 127 |
| 5.8 | Spatial variation of extreme sea levels along the Cumbrian coastline | 130 |
| 5.9 | Mean residual life plots for $MO_1$ and $MO_2$ | 131 |
| 5.10 | Shape parameter of GPD above different thresholds for $MO_1$ and $MO_2$ | 132 |
| 5.11 | Scale parameter of GPD above different thresholds for $MO_1$ and $MO_2$ | 132 |
| 5.12 | Scatter plot of resultant $H_s$ at $MO_1$ and $MO_2$ | 133 |
| 5.13 | Extreme estimates of $H_s$ at $MO_1$ for different thresholds | 133 |
| 5.14 | Extreme estimates of $H_s$ at $MO_2$ for different thresholds | 134 |

5.15 Extreme estimates of $H_s$ at $MO_1$ and $MO_2$ 135
5.16 Quantile and probability plots for $MO_1$ 136
5.17 Quantile and probability plots for $MO_2$ 136
5.18 Spatial variation of extreme offshore wave heights along the Cumbrian coastline 137
5.19 Variation in shape (*k*) parameter for predicted inshore wave heights 139
5.20 Spatial variation of extreme wave heights (-2m@OD) (extrapolated from GPD, not considering depth limited effects) 139
5.21 Survey information used to determine bathymetry and seabed slopes (in region of north Walney Island) 141
5.22 Survey information used to determine bathymetry and seabed slopes (Whitehaven to Workington) 142
5.23 Nearshore beach slopes 142
5.24 Spatial variation of extreme wave heights (-2m@OD) (based on 'countback' from simulation of 10,000 years of data) 143
5.25 Spatial variation of extreme wave heights (-1m@OD) (based on 'countback' from simulation of 10,000 years of data) 143
5.26 Spatial variation of extreme wave heights (+0m@OD) (based on 'countback' from simulation of 10,000 years of data) 144
5.27 Spatial variation of extreme wave heights (+1m@OD) (based on 'countback' from simulation of 10,000 years of data) 144
5.28 Spatial variation of extreme wave heights (+2m@OD) (based on 'countback' from simulation of 10,000 years of data) 145
5.29 Scatter plot of resultant $H_s$ against sea level 146
5.30 Scatter plot of wave steepness against $H_s$ for individual components 147
5.31 Spatial variation in correlation for offshore conditions 148
5.32 Spatial variation in correlation at -2m@OD 148
5.33 Spatial variation in correlation at -1m@OD 149
5.34 Spatial variation in correlation at +0m@OD 149
5.35 Spatial variation in correlation at +1m@OD 150
5.36 Spatial variation in correlation at +2m@OD 150
5.37 Significant wave height against wave steepness (offshore Northing coordinate 498240m) 153
5.38 Significant wave height against wave steepness (+0m@OD Northing coordinate 498240m) 153
5.39 Significant wave height against wave steepness

(+2m@OD Northing coordinate 498240m) 154
5.40 Relationship between offshore and nearshore wave period (+0m@OD Northing coordinate 498240m) 154
5.41 Joint probability curves for standard return periods (offshore Northing coordinate 490640m) 158
5.42 Joint probability curves for standard return periods (-2m@OD Northing coordinate 490640m) 158
5.43 Joint probability curves for standard return periods (-1m@OD Northing coordinate 490640m) 159
5.44 Joint probability curves for standard return periods (+0m@OD Northing coordinate 490640m) 159
5.45 Joint probability curves for standard return periods (+1m@OD Northing coordinate 490640m) 160
5.46 Joint probability curves for standard return periods (+2m@OD Northing coordinate 490640m) 160
5.47 Joint probability curves for standard return periods (offshore Northing coordinate 546240m) 161
5.48 Joint probability curves for standard return periods (-2m@OD Northing coordinate 546240m) 161
5.49 Joint probability curves for standard return periods (-1m@OD Northing coordinate 546240m) 162
5.50 Joint probability curves for standard return periods (+0m@OD Northing coordinate 546240m) 162
5.51 Joint probability curves for standard return periods (+1m@OD Northing coordinate 546240m) 163
5.52 Joint probability curves for standard return periods (+2m@OD Northing coordinate 546240m) 163

6.1 Typical 'checked' time trace recorded by EA 165
6.2 Comparison of manual and digital surge records at Workington 167
6.3 Comparison of sea level record and port records for Workington 168
6.4 Approximate position of Met Office coastline superimposed on UK coastline 179
6.5 Scatter plot of wave heights and wave periods for swell conditions (offshore point 542240N) 182
6.6 Overlapping surveys at Maryport Harbour 185

6.7 Quantile plots (-2m@OD) at selected inshore locations 191
6.8 Extreme estimates of $H_s$ for different thresholds (-2m@OD, Northing coordinate 477440N) 192
6.9 Extreme estimates of $H_s$ for different thresholds (-2m@OD, Northing coordinate 538240N) 193
6.10 Spatial variation of extreme wave heights (100 year return period event) 195
6.11 Spatial variation in correlation for threshold of exceedance of 0.90 197
6.12 Spatial variation in correlation for threshold of exceedance of 0.95 197
6.13 Spatial variation in correlation for threshold of exceedance of 0.99 198
6.14 Generic joint probability curves for Cumbrian coastline (-2m@OD) 206
6.15 Generic joint probability curves for Cumbrian coastline (-+0m@OD) 206
6.16 Wave height ratio at +0m@OD compared to -2m@OD 208
6.17 Estimate of seabed level where joint probability curve is depth limited at extreme sea level 209
6.18 1 year return period curve determined by JOIN-SEA and countback of original time series (-2m@OD Northing coordinate 546240m) 210

A.1 Tide boards at Silloth
A.2 Tide boards at Workington
A.3 Radar reflection tide gauge (Whitehaven)
A.4 Location of tide gauges at Ramsden Dock, Roa Island and Halfway Shoal

B.1 Benchmark tests

C.1 Sample output for 180 grid
C.2 Sample output for 210 grid
C.3 Sample output for 240 grid
C.4 Sample output for 270 grid
C.5 Sample output for 210 grid
C.6 Sample output for 240 grid
C.7 Sample output for 270 grid
C.8 Sample output for 210 grid
C.9 Sample output for 240 grid
C.10 Sample output for 270 grid

D.1 Joint probability curves for Northing coordinate 465040m
D.2 Joint probability curves for Northing coordinate 469440m
D.3 Joint probability curves for Northing coordinate 472240m
D.4 Joint probability curves for Northing coordinate 475840m
D.5 Joint probability curves for Northing coordinate 476640m
D.6 Joint probability curves around Haverigg Point
D.7 Joint probability curves for Northing coordinate 505440m
D.8 Joint probability curves for Northing coordinate 505840m
D.9 Joint probability curves for Northing coordinate 513040m
D.10 Joint probability curves for Northing coordinate 515840m
D.11 Joint probability curves for Northing coordinate 518640m
D.12 Joint probability curves for Northing coordinate 533840m
D.13 Joint probability curves for Northing coordinate 535440m
D.14 Joint probability curves for Northing coordinate 539040m
D.15 Joint probability curves for Northing coordinate 544640m
D.16 Joint probability curves for Northing coordinate 547840m
D.17 Joint probability curves for Northing coordinate 551840m

# Glossary

*Annual Maxima*

A method of analysing a data set by considering only the highest recorded value for each year that records are available.

*Anthropogenic*

Human made. In the context of greenhouse gases, emissions that are produced as the result of human activities.

*Bathymetry*

Spatial variation of contours on the seabed.

*Benefit Cost*

The ratio of the present value benefits to the present value costs of a scheme.

*Chart Datum*

The level to which tidal levels are reduced on Admiralty Charts. This is usually approximately equal to Lowest Astronomical Tide.

*Class A Tide Gauge*

A UK tide gauge (of which there are 44) maintained by the Proudman Oceanographic Laboratory (POL) to the highest and most consistent standards.

*Correlation of non-exceedance (of the sea level)*

For this study, this is defined as the correlation between wave heights and sea levels considering only those combinations where the sea levels exceed a level that a specified percentage of sea levels 'do not' exceed.

*Countback*

A method of estimating return periods of extreme events from the empirical data set. In this study, the level of the extreme event is given as the effective number of years of data, taking into account missing records, divided by the descending order rank of the event.

*Design Condition*

The joint return period event designed for.

*Design Standard*

In the context of this study, it is defined as the maximum joint return period event that a coastal defence structure is built to withstand.

*Eustatic Trend*

Global trends in sea levels.

*Isostatic Rebound*

Rebound response of the land as a result of pressure exerted by ice during the last ice age.

*Joint Exceedance*

The probability of two variables simultaneously exceeding individually specified levels.

*Joint Probability*

The probability of more than one event occurring at the same time.

*JONSWAP*

Typical wave spectrum in growing deep waters.

*Leptokurtic Distribution*

A distribution of the same form as a normal distribution, but having a higher kurtosis (more peaked). This indicates, relative to a normal distribution, more occurrences near the mean, with fewer values away from the mean.

*Locally Generated Waves*

Wind waves generated within the immediate vicinity of the shoreline.

*Low Pass Filter*

A filter that removes all frequency terms above a defined cut-off frequency.

*Marginal Probability*

The probability of a single variable in the context of a joint probability analysis.

*Marginal Return Period*

The return period of a single variable in the context of a joint probability analysis.

*Mean Residual Life Plot*

Diagram indicating the mean excess of a threshold for different thresholds.

*Mean Sea Level*

The average level of the sea over a period of time.

*Nearshore*

The region intermittently covered by tidal action.

*Noise*

In the contest of this study it is a random or erratic fluctuation of a signal or curve.

*Nyquist Frequency*

The minimum frequency required to fully reconstruct a time series in a Fourier analysis. It is equal to twice the largest frequency present in a time series.

*Ocean Tide Loading*

Oscillation of land at the tidal frequency as a result of the weight of the ocean tides.

*Offshore*

The region beyond the nearshore region permanently submerged.

*Overtopping*

Water carried over the top of coastal defences as a result of wave and (or) sea levels.

*Peaks Over Threshold*

A method of analysing a data set by considering all records that exceed a set value regardless of the year they occur in.

*Return Period*

The average period of time between which an event is reached or exceeded

*Sea Level*

The observed level of the sea taking into account both astronomical and atmospheric effects.

*Secular Trend*

Trend in records relative to the location.

*Shallow Water*

Water depths where surface waves are noticeably affected by seabed bathymetry.

*Shoaling*

The increase of wave heights in shallow water as a result of the divergence in wave group velocity.

*Shoreline Management Plan*

A management plan of the coastline identifying the risks associated with coastal processes and long term policy frameworks to reduce these risks.

*Significant Wave Height*

The average height of the highest one third of the waves in a given sea state.

*Standardisation*

In the context of this study, it is the process whereby sea levels are corrected due to estimated changes in mean sea levels, so that they relate to a mean sea level at the study date (01/01/04).

*Stationarity*

This is where the expected value of successive records in a time series are the same, and there is no tendency (trend) to increase or decrease.

*Surge*

Difference between sea level and tide level as a result of atmospheric effects.

*Swell*

Wind waves generated some distance from the shoreline.

*Tide Level*

The level of the sea taking into account astronomical, but not atmospheric effects.

*TMA Spectrum*

Typical wave spectrum in growing limited water depth.

*Transit of the Moon*

The time interval between successive passes of the moon through a point (meridian) on the earth.

*Wave Transformation Model*

A computer program used to determine the variations in wave parameters across a body of water based on specified input conditions.

# Notation

| | |
|---|---|
| $a$ | constant for linear regression on wave height |
| $b$ | coefficient for linear regression on wave height |
| $C_\zeta$ | correlation between wave height and water level above threshold |
| $CD$ | chart datum |
| $C_F$ | intuitive correlation factor |
| $d$ | water depth |
| $d_{H_s}$ | deviate of wave height |
| $d_s$ | deviate of wave steepness |
| $d_\zeta$ | deviate of threshold |
| $f$ | wave frequency |
| $f_p$ | peak spectral wave frequency $(1/T_p)$ |
| $F$ | fetch length |
| $G$ | grid size |
| $H_b$ | 'binned' wave height |
| $(H_b)_i$ | inshore 'binned' wave height |
| $H_s$ | significant wave height |
| $(H_s)_b$ | limit on significant wave height breaking |
| $(H_s)_i$ | inshore significant wave height |
| $(H_s)_o$ | offshore significant wave height |
| $(H_s)_n$ | significant wave height for $n$ frequency components |
| $(H_s)^h_{Pi}$ | wave height at sea level percentile *h* on *i*th joint probability curve |
| $(H_s)^h_{+0m@OD}$ | wave height at sea level percentile *h* on *i*th joint probability curve at tide datum +0m@OD |
| $(H_s)^h_{-2m@OD}$ | wave height at sea level percentile *h* on *i*th joint probability curve at tide datum -2m@OD |
| $(H_s)^{\max}_{Pi}$ | maximum wave height for *i*th joint probability curve |
| $H_{swell}$ | swell wave height |
| $(H_{swell})_i$ | inshore swell wave height |
| $k$ | shape parameter of GPD |

| | |
|---|---|
| $K_s$ | shoaling coefficient |
| $L$ | wavelength |
| $L_0$ | linear deep water wavelength |
| $m_i$ | *i*th moment of wave spectrum |
| $MO_1$ | Met Office Prediction point 54.5°N 4.06°W |
| $MO_2$ | Met Office Prediction point 54.0°N 3.26°W |
| $msl$ | mean sea level |
| $n$ | number of data values |
| $n_e$ | number of joint probability events per year |
| $n_f$ | number of frequency components of wave spectrum |
| $n_y$ | years of observations of joint probability event |
| $OD$ | ordnance datum |
| $p_r$ | proportion of variables in first distribution of mixture distribution |
| $1-p_r$ | proportion of variables in second distribution of mixture distribution |
| $p(H_s,\eta)_i$ | *pdf* of *i*th distribution in mixture distribution |
| $q$ | parameter used in TMA spectrum |
| $r$ | rank of value in $n$ events (1=lowest, $n$=highest) |
| $(\ )_R$ | return period being considered |
| $t$ | wind speed duration |
| $T_{H_s}$ | return period of significant wave height |
| $T_{H_s,\eta}$ | return period of combined $H_s,\eta$ event |
| $T_p$ | peak spectral wave period $(1/f_p)$ |
| $T_z$ | zero crossing wave period |
| $T_\eta$ | return period of sea level |
| $u$ | threshold greater than $1-\varepsilon$ |
| $U_{10}$ | wind speed ay 10.0m above *msl* |
| $X$ | value in sample |
| | |
| $\alpha$ | nearshore seabed slope |
| $\beta$ | parameter used in TMA spectrum |
| $\beta_{max}$ | wave breaking parameter |
| $\beta_0$ | wave breaking parameter |

| | |
|---|---|
| $\beta_1$ | wave breaking parameter |
| $\gamma$ | peak enhancement factor |
| $1-\varepsilon$ | threshold |
| $\zeta$ | threshold (also location parameter of GPD) |
| $\zeta_s$ | threshold of deviate of wave steepness |
| $\sigma$ | parameter used in TMA spectrum |
| $\eta$ | sea level |
| $\eta_e$ | extreme sea level |
| $\theta$ | scale parameter of GPD |
| $\mu_{H_s}$ | mean of the $H_s$ distribution |
| $\mu_T$ | expected number of exceedances of the $T_{H_s,\eta}$ contour |
| $\mu_\eta$ | mean of the $\eta$ distribution |
| $\rho_{H_s,\eta}$ | correlation between $H_s$ and $\eta$ |
| $\sigma_{H_s}$ | standard deviation of $H_s$ |
| $\sigma_s$ | standard deviation of deviate of wave height |
| $\sigma_\eta$ | standard deviation of $\eta$ |

# Acknowledgements

In a study such as this it is often almost impossible to fully acknowledge all the help and assistance given over the years that it took to complete. Apart from the general time, help and advice given by a number of people to varying degrees, in the end it would not have been possible without the vast supply of free and often confidential data given by a number of institutions. The supply of free data has not been assessed, but it probably amounts to over 50% of the cost of my first house (which I bought 2 months before starting this PhD.).

A number of people have assisted in a form that normally would require a glowing acknowledgement. However, with the number of people to acknowledge fairly large, I have tried to keep the acknowledgements as short as possible. I apologise to anybody that I have left off, which will be an oversight. I also apologise to all those organisations that I have hassled and criticized (although possibly not unfairly) over the years. Please accept that this was solely as a result of my still continuing pursuit of quality information and results.

My main acknowledgement has to go to Professor Andrew Chadwick (University of Plymouth) who first made the suggestion to me of a PhD. Secondly I would like to thank Professor Dominic Reeve (University of Plymouth), who stepped into the breach after Professor Saralees Nadarajah (University of Nebraska, Lincoln) left to work in New Zealand. I have enjoyed my all too rare meetings with Andrew and Dominic immensely, and I look forward to working with them again in the future.

I would also like to give special thanks to Mark Breen (WA Developments), who during his time at Bullen Consultants (now Faber Maunsell) gave me the time to pursue my interest in Joint Probability, and Chris Davies (ex Bullen Consultants) who ultimately initially paid for it.

The last people that I would like to give special (academic) thanks to are Peter Hawkes (HR Wallingford Ltd), and the Harbour (and Deputy Harbour) Masters at the Ports of Barrow, Workington and Silloth (both present and retired). Peter has supplied a vast amount of help and information over the years, always willingly. I must apologize to him for two things, firstly for any non-glowing comments on his

work in this PhD, and secondly for buying a house last year within 10 minutes of where he works so he has not been able to avoid me. David Carpenter and his crew were a pleasure to get to know, and I look forward to the boat trip he promised me last time I was up there (but hopefully will not forget about now). Chris Puxley, who must be Harbour Master at one of the most beautiful sites in England, and to whom I owe a pint and some dog treats. Capt. Cousins et al, who didn't notice when I slipped over on the rock armour when (as a result of this fall) failed to inspect the tide gauges.

Other people that I would like to acknowledge are given below. These have been arranged randomly, not using a Monte Carlo simulation, so that no degree of acknowledgement can be inferred by the order, and that anybody missing will be harder to spot. I have also left off the array of various titles so as to avoid spurious titles, or more importantly missing ones.

| | |
|---|---|
| Karen Barfoot | The Meteorological Office |
| Russell Stead | Environment Agency |
| Bruce Porter | Bullen Consultants (retired) |
| Ian Hale | Environment Agency |
| Alistair Reid | Bullen Consultants (now Faber Maunsell) |
| Dave Wells | Bullen Consultants (now Faber Maunsell) |
| Alex Williams | Bullen Consultants (now Faber Maunsell) |
| Kevin Keating | Bullen Consultants (now Faber Maunsell) |
| Andrew Greenhalgh | Bullen Consultants (now Faber Maunsell) |
| Mike Faulkner | Allerdale Borough Council |
| Gary Clark | Copeland Borough Council |
| John Green | Associated British Ports (Barrow, retired) |
| Chris Clouter | Associated British Ports (Barrow) |
| Michelle Barrett | ex Associated British Ports (Barrow) |
| David Hulse | The Meteorological Office |
| David Allan | Port of Whitehaven (retired) |
| Neil Foskett | Port of Whitehaven |
| Susan Daffern | Environment Agency |
| Nigel Blofield | Ordnance Survey |
| Jonathan Tawn | University of Lancaster |
| Andy Tabor | Proudman Oceanography Laboratory |

| | |
|---|---|
| Polly Habziabdic | Proudman Oceanography Laboratory |
| Elizabeth Bradshaw | Proudman Oceanography Laboratory |
| Libby Macleod | Proudman Oceanography Laboratory |
| Lesley Rickards | Proudman Oceanography Laboratory |
| Nigel Tozer | HR Wallingford Ltd |
| Helen Stafford | ex Proudman Oceanography Laboratory |
| Jeremy Benn | Jeremy Benn Associates Ltd |
| Martin Holt | The Meteorological Office |
| Phil Woodworth | Proudman Oceanography Laboratory |
| Martin Wilson | Environment Agency |
| Alan Williams | Coastal Engineering UK Ltd |

Apart from the people given above, I would also like to thank the following organisations for whom no individuals are named.

The Hydrographic Office
BNFL
ABPMer
Halcrows

Aside from academic acknowledgements, I would also like to thank Ruth who has been with me for the duration of this study. I hope that I can now look after her for the next few months in the same way as she has looked after me.

# Dedication

## Honour Him

*How do you take the measure of a man?*

*Do you, with tape and plumb-line,*

*Gauge the length of his arms, and straightness of his back,*

*Or, with scales and callipers,*

*Determine the weight of his heart, and width of his mind?*

*No, for hearts are not constant,*

*Minds are variable,*

*Backs bend beneath burdens,*

*Arms stretch no further than their shoulders.*

*Measure a man by the affection held for him by others.*

*And should you discover a man that has given of his best,*

*and enjoyed the giving,*

*Found satisfaction in that, and sought nothing else,*

*Honour him,*

*For he will be loved by many.*

Goff Morgan

Newport Town Poet

February 1998

# AUTHOR'S DECLARATION

At no time during the registration for the degree of Doctor of Philosophy has the author been registered for any other University award without prior agreement of the Graduate Committee.

This study was self funded, and during the course of this study a number of conferences, seminars and workshops were attended including all relating to the development, testing and dissemination of the JOIN-SEA joint probability package.

Regular visits were made to external organisations, and a number of talks were given on this study as well as joint probability in general, and specifically relating to the Cumbrian coastline.

As a direct result of this study, so far one paper has been published, and contributions to a second have been made.

Word count of main body of thesis: 48,825 words.

Signed 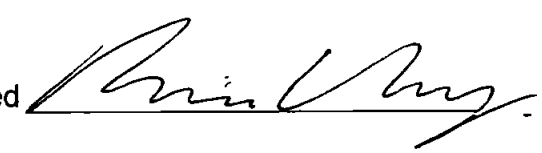

Date 16th June 2006

# 1 Introduction

Overtopping and damage at coastal locations are usually associated with periods of high sea levels combined with significant wave activity, and it is imperative that both are considered when designing coastal defence structures. Large waves will tend to occur during periods of low pressure and large wind speeds, resulting in an increase in sea levels above what is predicted (surge) in coastal regions. This increase is most pronounced when the winds are blowing onshore resulting in a positive correlation between onshore waves and sea levels and giving a correlated joint distribution. Although standard distributions for sea levels and wave heights are well established (see for example Coles and Tawn 1990 and Mathiesen et al 1994), little research has been carried out into their joint occurrence. Long term nearshore records of wave heights based on recorded, or transformed offshore data also do not exist. These need to be either generated from offshore recorded or predicted data to enable an assessment of the joint distribution to be analysed.

As it is impractical and uneconomic to design and build coastal defence structures so that no flooding or damage ever occurs, they are usually built to a design standard, with a specified level of overtopping and damage allowed. Beyond this, overtopping and damage may exceed the allowable levels. In the assessment of the required design standard, the joint distribution of the sea levels and wave heights, as well as their marginal distributions needs to be defined. Accurate definition of these distributions

enables the required design standard to be specified to a high level of confidence.

Within the UK, design standards are usually based on a benefit cost analysis. This is the approach adopted by the Department for Environment, Food and Rural Affairs (Defra) and the Environment Agency (EA), who are the main bodies responsible for damage (Defra) and flooding (EA) in the UK. Inherent in this risk / probability approach to damage and flooding, which is considered acceptable for a stretch of coast considered, is the accurate definition of design conditions (wave heights and sea levels). This applies not only for the present, but also for future years taking into account estimated rises in sea levels, as well as potential changes in wind, and therefore wave conditions.

The accurate assessment of the joint occurrence between wave heights and sea levels, termed joint probability, is therefore required to give not only the most accurate benefit cost analysis, but also confidence in design conditions, and the design standard. With environmental conditions often changing over short lengths of coastline, this implies that the joint probability relationship between sea levels and wave heights is also likely to vary over short lengths of coastline. The effect of nearshore coastal processes (such as shoaling, refraction and wave breaking) means that existing offshore wave records cannot be used. Wave transformation modelling is therefore required to represent the spatial variation in wave heights within nearshore areas as a result of bathymetric conditions. Further research into the joint probability between sea levels and wave

heights therefore needs to be considered spatially both along and within the nearshore zone.

## 1.1 Rational for Research

Although, as stated above, standard distributions for sea levels and wave heights are well established, the lack of a robust solution or understanding of the joint distribution of variables with a degree of correlation has resulted in the past in a lack of confidence in the design of coastal defence structures. This would often result in a conservative design leading to increased costs. With coastal defence structures costing in the region of at least £3000/m, and with approximately 1000km of defended coastline in Britain a typical overspend of perhaps 25%, would mean that vast sums could be saved if design conditions were specified with more confidence. An under-designed structure, although cheaper would not fulfil the purpose it was built for and could fail within a short time of being constructed. An over-designed structure, although built to an effective higher design standard would also result in a reduced benefit cost ratio and take money away from a limited coastal defence fund, leaving a less environmentally pleasing structure in its place.

For these reasons, and with knowledge in joint probability being identified as a major deficiency in first generation Shoreline Management Plans (Defra 2001), a better understanding of the joint probability between waves and sea levels is therefore required. This is particularly the case for nearshore conditions where coastal defence starts, yet it is believed has not been subjected to any joint probability analyses.

With maximum overtopping and damage at coastal defence generally occurring at high sea levels, this study has concentrated on the assessment of the joint probability relationship at high sea levels only. It was felt that little benefit would have been obtained considered the joint probability relationship across the tidal range. This would also have vastly increased the time required to complete the study, with little additional benefit.

## 1.2 Investigation of the Joint Probability of Waves and High Sea Levels

In defining a study to investigate the spatial variation in joint probability between high sea levels and wave heights, the unique nature of all coastlines meant that any study would have to concentrate on one specific area. The site chosen would need to be considered representative of many coastlines, with a prior appreciation of the factors affecting nearshore wave heights, such as predominant wind / wave directions and nearshore bathymetry. The data available for the study, and the logistics of obtaining it also needed to be considered.

Based on the factors outlined above, an approximate 100km stretch of the Cumbrian coastline in England from Walney Island in the south to Silloth in the north (as shown in Figure 1.1) was chosen. In terms of coastal processes, and their effect on the joint probability relationship, the main reasons for this choice are outlined below.

1. There is limited exposure to the most direct extreme wave activity from the Atlantic Ocean, particularly at the southern limit of the study area. The effect of shoreline orientation to a well defined predominant wave direction could therefore be investigated.
2. The headland at St. Bees Head splits the coastline into two distinct regions. For significant wave activity, this will result in an approximate direct wave approach south of St. Bees Head, and an angled wave approach north of St. Bees Head.
3. The reduced water depths of the Solway Firth enables the effect of reducing offshore water depths within estuaries to be investigated.
4. The bay centred on the village of Allonby, where detailed bathymetric data was known to exist, would enable the joint probability relationship to be investigated within large Bays.
5. The Cumbrian coastline has a significant and consistent tidal range (approximately 9-10m), with high tide occurring within ½ hour over the entire coastline. High tides can therefore be considered to be coincident, and at a similar level. The joint probability relationship can also be investigated over a significant range of levels (and therefore water depths).
6. Similar to point 5 above, the consistent tidal range also implies relative consistency between Ordnance and Chart Datum giving confidence in the conversion of nearshore bathymetric data to the required datum.

Aside from the reasons given above, the author had considerable experience of this area of coastline as a result of his employment when starting this study as a coastal engineer. Much of the data used in this

study had already been obtained, and most additional data required to complete the study had already been identified. The exact specification of the study area was chosen to match the two Shoreline Management Plans for this area (Bullen Consultants 1999a and 1999b), which the author was involved in producing.

Based on the study area chosen, and the tidal range, the spatial variation in joint probability curves for standard return periods has been investigated based on determining the joint probability relationship at 400m centres for five regularly spaced nearshore locations from beach levels of -2m@OD to +2m@OD (see Figure 1.2). The spatial variation has enabled the variation in the joint probability relationship to be investigated for typical shoreline features such as outlined in the points above. The variation in the beach levels was chosen so as to cover the range of levels within which it was believed the vast majority of waves, which ultimately define the joint probability relationship, would be likely to break.

To investigate the joint probability relationship, coincident time series of sea level and inshore wave records were required over as long a period as possible. Sea level records were obtained from all known sources covering as long a period of possible, and these were extensively pre-processed to check for errors and inconsistencies, and to correct data where possible. With no recorded wave data available, offshore wave predictions were obtained from the two nearest Met Office prediction points to the southern and northern limits of the study area. These were transformed inshore using the REFDIF wave transformation model (Kirby and Dalrymple 1994), using all known, and available, bathymetric data. This gave in the region of

13½ years of co-incident sea level and inshore wave records, at 229 locations, and 5 levels per location (see Figure 1.2).

Due to the spatial nature of this study, with results in three dimensions (location, sea level and wave height) results have concentrated on 'best estimates', with less emphasis placed on confidence. However, where considered appropriate, confidence bands are shown and discussed.

At the start of this study, no robust technique existed to describe the joint probability relationship between wave heights and high sea levels. However, shortly after starting this study, HR Wallingford Ltd and Lancaster University published details of the JOIN-SEA approach to joint probability (HR Wallingford 2000a and 2000b). This technique was therefore adopted for this study.

## 1.3 Description of Thesis

This thesis has been split up into 8 chapters, of which this is the first. A literature review of the different methods and techniques that have been used to investigate the joint probability between waves and high sea levels is given in Chapter 2, including full details of the JOIN-SEA approach. This chapter also outlines the reasons behind the correlation between waves and sea levels. Within Chapter 3, details of the raw data that was collected for this study is summarised. The pre-processing that was carried out on this data is given, together with how the data was collated to form the sea level data sets, as well as the input into the wave modelling package to determine the nearshore wave heights. With the model inputs defined,

Chapter 4 outlines the justification of the wave modelling package used in this study. Model restrictions and sensitivity of predictions are investigated, and based on the conclusions drawn; specifications of the model runs are defined. Chapter 5 outlines the methods used and the results obtained for both the marginal and joint predictions of the extreme events. Chapter 6 gives a detailed discussion of the results, including the justification for the input parameters to define the marginal data sets. The conclusions of the study are given in Chapter 7, with recommendations for further study, and the use of the results already obtained given in Chapter 8.

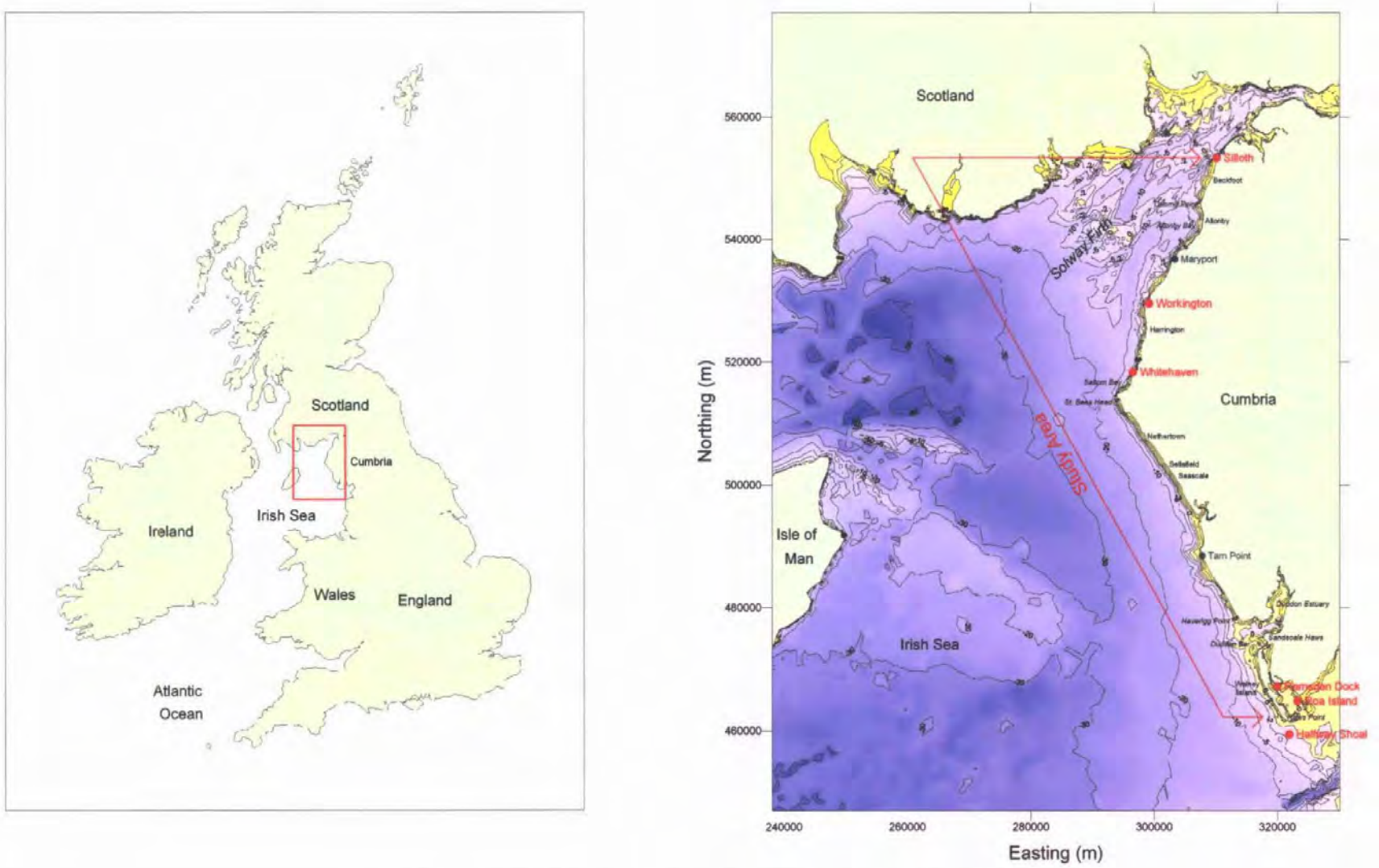


**Figure 1.1** : Location plan showing extent of study area

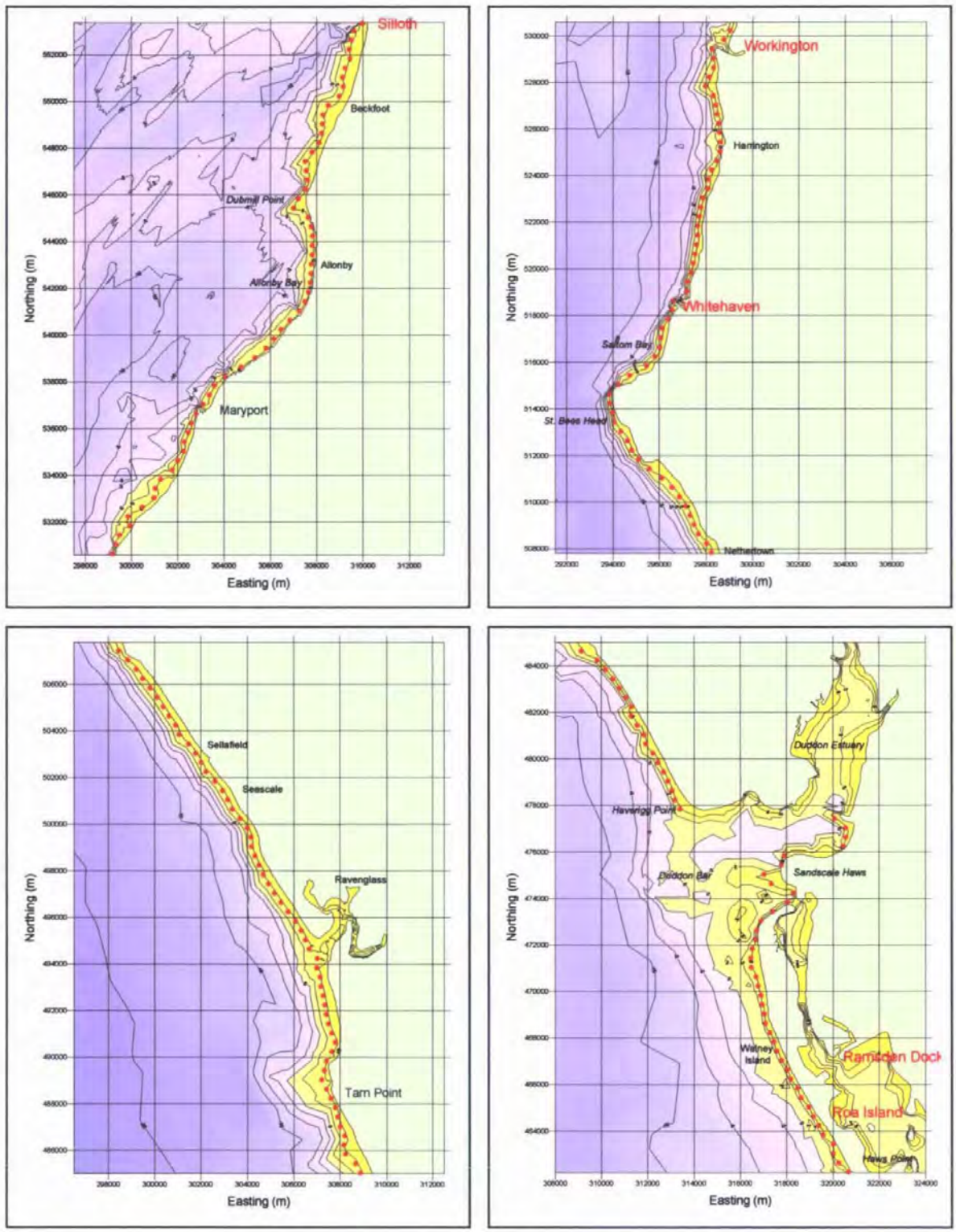


**Figure 1.2** : Location of prediction points

# 2.0 Literature Review of Joint Probability of Waves and High Sea Levels

## 2.1 Introduction

The design of coastal defence schemes to protect against flooding and damage is based on a design standard. This needs to take into account the joint extreme occurrence of both waves and sea levels, which is known as the joint probability of waves and sea levels. Methods of predictions of joint (multivariate) extremes naturally followed the development of predictions of single (univariate) extremes, a subject which developed from the 1940s, with environmental factors (sea levels, river flow, wave heights etc.) being the most common application. It wasn't until the 1950s that extreme value was expanded to multivariate extremes, and not until the mid 1980s that publications appeared dealing with applications of this theory (Kotz and Nadarajah, 1999). Similar to univariate extremes, early applications concentrated on environmental factors, with from the late 1980s onwards, applications in insurance, financial and more recently internet traffic management. However, these methods of multivariate extreme value analysis were based on a high level of dependency between all variables. This is not the case for many environmental factors, such as sea levels and waves, which have a low level of dependency. Methods were therefore proposed by Ledford and Tawn (1996 and 1997) which dealt with analysing multivariate extremes with a low level of dependency.

Considering this development in the analysis of multivariate extremes, it is therefore not surprising that joint probability methods in flood and coastal defence prior to the late 1980s were fairly rare. Although extreme sea levels and offshore wave heights were two of the main applications of extreme value theory, their joint occurrence in offshore areas were of little interest. Nearshore, few if any long term records of wave heights existed. With a lack of available data, but also probably due to a lack of knowledge and

understanding regarding the joint occurrence of sea levels and nearshore wave heights, many engineering studies were carried out on the basis of a design condition consisting of a standard sea level, and a standard wave height. A higher design condition would be defined by higher marginals, and a lower design standard by lower marginals. However, with the UK in particular having some of the largest tidal ranges, and therefore surges in the world, and with most flooding and damage occurring only during periods of extreme sea levels and significant wave activity, the incorrect assessment of joint probability effects can be significant, and possibly catastrophic.

The importance regarding the joint probability of waves and high sea levels within the UK was brought into sharp focus as a result of the Towyn floods in North Wales in late February 1990. A combination of large onshore wave heights and the largest sea levels ever recorded along this stretch of the North Welsh coastline at this time resulted in significant coastal flooding over a period of several days. As a result of this flood event, Hydraulics Research Limited (now HR Wallingford Ltd) was commissioned by the Welsh Office to establish the joint probability relationship between extreme high sea levels and wave heights along the North Welsh coastline. The urgency of this report can be appreciated by the fact that it was issued within three months of the Towyn disaster.

With the need for more work in joint probability a consistent theme in first generation Shoreline Management Plans (SMPs) issued in the mid-late 1990s (including the two SMPs covering the study area investigated in this study), considerable research into joint probability methods has been commissioned by MAFF over the last 10 years. This has resulted in new techniques being developed or revised, the most advanced of which are based on the work of Ledford and Tawn (1996 and 1997). Details of these techniques, together with other methods that have been traditionally used to determine the joint probability between waves and high sea levels are given in this chapter.

## 2.2 Sea Levels and Waves and their Correlation

Before considering the different joint probability techniques as applied to wave heights and sea levels, it is worth considering the input parameters separately, and the reasons for the correlation between them.

Sea levels are composed of two components, tides and surges. Tides are the alternating rise and fall of the water surfaces of the oceans and seas caused by the gravitational attraction of the moon and the sun. Typically there are almost two tides a day (known as semi-diurnal tides) corresponding to each transit of the moon, (every 12.42 hours). Superimposed on the tides are surges as a result of a spatial variation in pressure over a body of water and a build up of water caused by the wind blowing over the water surface. As tides are as a result of the gravitational attraction of the moon and the sun, due to their continually changing position relative to each other, this causes a modulation of the tidal cycle over a period of just over 14 days. At the peak of this modulation, you get the largest tides called spring tides, and at the trough of this modulation you get the smallest tides called neap tides. This is demonstrated on Figure 2.1 for predicted tides at Workington for February 1997. Also shown on this figure are the positions of the moon and sun relative to the earth during a spring and neap tidal cycle.

Predicted tides are traditionally determined by harmonic analysis, where a recorded time signal is interrogated for the different astronomic parameters. Extraction of the astronomic components from a tidal record will leave the surge component. This record will also contain any errors in the measurements, as well as astronomic components not accounted for, or incorrectly estimated by the harmonic analysis. The magnitudes of any errors in surge estimation are not known, but for a well maintained tide gauge and the use of reliable prediction methods using a significant number of astronomic parameters are unlikely to be significant. However, any errors will vary from site to site as a result of the prediction method and number of astronomic components considered, as well as the accuracy and reliability of

the recording device. It is worth noting that poorly maintained records can, without proper analysis produce significant errors in estimation of the predicted tides and the surge. This has been demonstrated in this study for predicted tides at Silloth (see Section 3.2.1), and by Hames et al (2004) for recorded tides at Whitehaven and Workington.

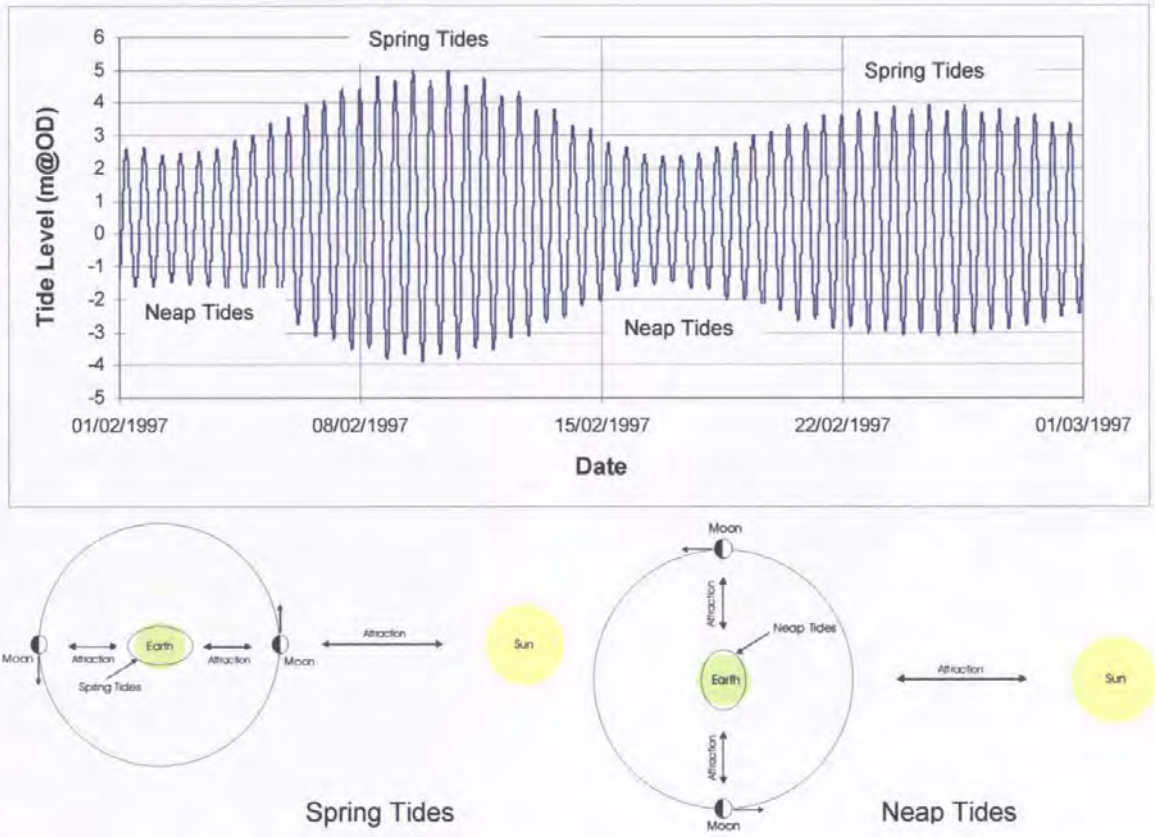


When the moon and the sun are in line with the earth, the forces act together and produce the largest tides.

When the moon and the sun are at right angles to the earth, the forces act out of phase, and produce the smallest tides.

**Figure 2.1** : Typical spring / neap tidal cycle for Workington.

Waves are mainly caused as a result of wind blowing across a body of water. This causes friction between the surface of the water and the bottom layer of the wind blowing across it, thus transferring energy from the air to the water surface. The height of the waves has a limited value dependent on the wind speed, but is also dependent on the length of time that the wind blows as well as the fetch length. Waves are altered in form as they move into shallow water areas as a result of their interaction with the sea bed surface. This can

cause waves to increase in height, but ultimately as a wave approaches a shoreline, this will result in the wave breaking due to depth limitation effects.

As tides are a result of astronomic effects, and waves meteorological effects, there is no relationship between them and no correlation between them would be expected. However, sea levels are a result of tides as well as surges which are caused by meteorological effects. With wind moving towards regions of lower pressure, this would be expected to cause a build up of water in the lower pressure region as a result of wind blowing across the water surface as well as the lower pressure itself. Surges and wave heights are therefore related, and the greater the wind speeds, the greater would be expected the surge. This therefore leads to a correlation between wave heights and sea levels. This correlation is however relatively weak, as in a sea level record the non correlated tide dominates, with the astronomic tide typically 97-98% of the total sea level, and even during the most extreme events, rarely less than 80-85% of the total sea level.

## 2.3 Development of techniques of Joint Probability between Waves and Sea Levels

Although the existence of a relationship between sea levels and wave heights will have been appreciated by the Coastal Engineering community in the past, the lack of a solution for partially correlated variables has resulted in a number of techniques to investigate the joint probability between sea levels and wave heights being developed. These techniques, which are outlined in approximate chronological order below, have ultimately led to the JOIN-SEA approach. This technique, which is based on sound and established mathematical techniques, is the approach that has been adopted in this study.

### 2.3.1 Independence or Dependence of Marginal Probabilities

These are the simplest approaches to a joint probability analysis and both

can easily be determined. These would have been the earliest joint probability methods applied to waves and high sea levels.

Independence implies that there is no relationship between the exceedance probabilities of the sea level and wave height distributions. The joint probability can therefore be given by the product of the marginal probabilities in the form:

$$p(H_s \geq y, \eta \geq x) = p(H_s \geq y)\, p(\eta \geq x) \qquad \textbf{(2.1)}$$

In reality this is an unrealistic assumption and some dependence would be expected. Generally this will produce an underestimate of the design conditions and a correspondingly under-designed structure. This would ultimately lead to a structure unlikely to fulfil its function on a long term basis.

Dependence implies that the exceedance probabilities of the sea level and wave height distributions are perfectly correlated, i.e., the largest wave heights always occur at the highest sea levels. The joint probability can therefore be given as:

$$p(H_s \geq y, \eta \geq x) = p(H_s \geq y) = p(\eta \geq x) \qquad \textbf{(2.2)}$$

Although a technique that was, and still possibly commonly used, it will almost certainly be an overestimate and produce an overestimate of design conditions. This would ultimately lead to over-designed and hence expensive coastal defence structures.

### 2.3.2 Manual Analysis of Joint Probability Density

This is a manual approach whereby the return period of an event can be determined directly from a scatter diagram of coincident pairs of wave height and sea level data. Using the scatter diagrams, return period curves up to the region of a tenth of the total length of the data set can be drawn in manually with rarer events sketched in maintaining the known shape of the contours.

An example of this is given below for high sea levels during a period of just over 9 years offshore of Shoreham in Sussex. Probability contours for return periods of 0.1 and 1 years are drawn in manually direct from the data. Return periods of 10 and 100 years are sketched in maintaining the shape of the joint probability curve with marginal extremes used to fix the largest wave heights and extreme sea levels.

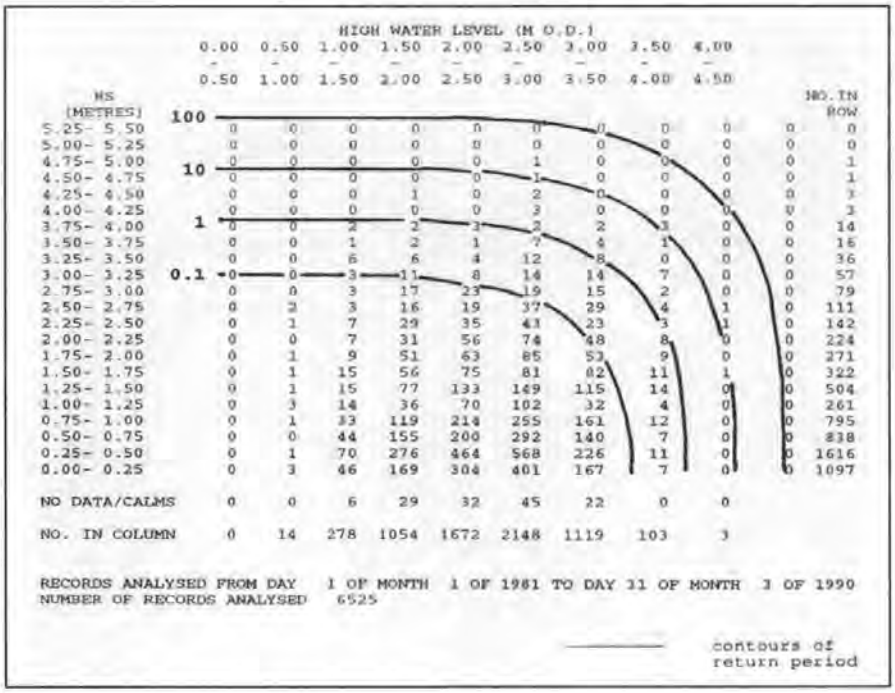


**Figure 2.2** : Example of manually drawn joint probability contours (for Shoreham, Sussex, HR Wallingford 1992).

### 2.3.3 Extrapolation of Joint Probability Density above High Sea Level and Wave Height Thresholds

This is a technique where several years of simultaneous wave height and sea level data are examined. Extremes are determined by extrapolating wave heights and sea levels for successively rarer sea levels and wave heights to produce contours of equal exceedance.

Although this technique is probably more robust than the techniques outlined

above, without available software it would be considered time consuming and in reality requires large data sets to work effectively. Also considering the highest sea levels, where it is likely that design conditions will be defined, the corresponding reduction in data available makes extrapolations unreliable.

An example of this technique is demonstrated in Figure 2.3 for the same data as given in Figure 2.2. In this example, extrapolated results are not shown where the results were considered unreliable, and no attempt has been made to 'sketch' in these curves based on an assumed shape. A direct comparison between the two sets of results should not be made as the techniques are not the same, and the scales may not be consistent.

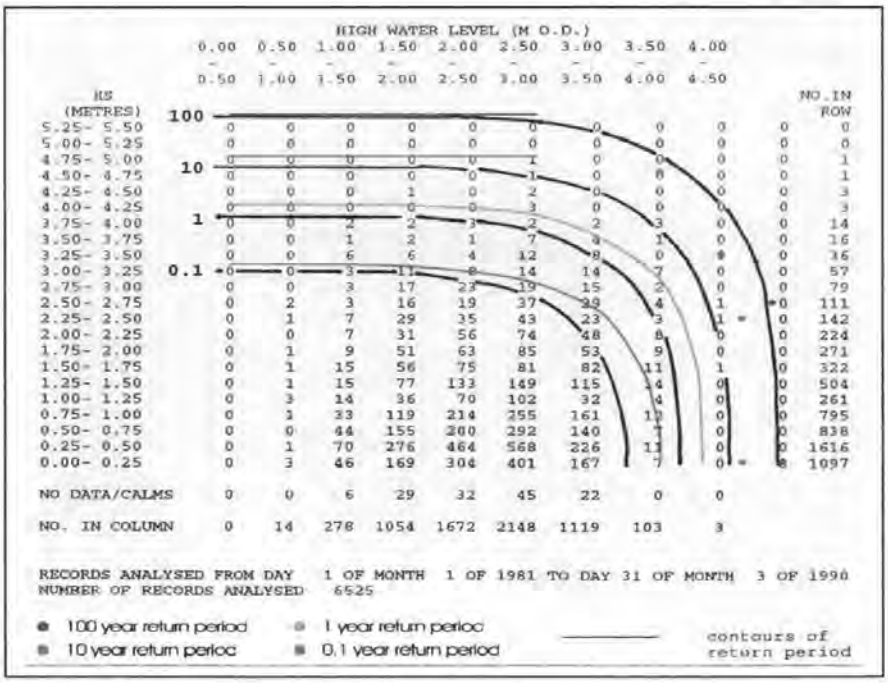


**Figure 2.3** : Example of extrapolation above sea level and wave height thresholds superimposed on manually drawn contours for Shoreham (after HR Wallingford Ltd 1992).

### 2.3.4 Intuitive Joint Probability Assessment

This is a simple technique originally put forward by Hawkes and Hague (1994). This technique took the rather straightforward approach that waves are "more (positive, possibly high correlation)" or "less (low or negative correlation)" likely to occur at extreme sea levels for any given site. This reduced the joint probability relationship to the product of the marginal probabilities multiplied by a correlation factor of the form,

$$p\left(H_s \geq y, \eta \geq x\right) = C_F \; p\left(H_s \geq y\right) p\left(\eta \geq x\right) \qquad \textbf{(2.3)}$$

where the correlation factor $C_F$ is an intuitive value, and is equal to the ratio of the actual joint probability to the joint probability based on independence of the marginal probabilities.

Equation (2.3) therefore gives an effective return period for waves and high sea levels as,

$$T_{H_s} = \min\left(T_{Hs,\eta}, T_{Hs,\eta} C_F \, p\left(\eta \geq x\right)\right) \qquad T_\eta = \min\left(T_{Hs,\eta}, T_{Hs,\eta} C_F \, p\left(H_s \geq y\right)\right) \qquad \textbf{(2.4)}$$

where,

$T_{Hs,\eta}$ = Return Period being considered
$T_{Hs}$ = Return Period of Wave Height
$T_\eta$ = Return Period of Sea Level

Using this technique, four levels of dependency were assumed - applied to the site of interest based on experience and knowledge of the site or nearby locations. For a 100 year return period, these were given as:

$C_F$ = 2 "no" correlation (independence)

$C_F$ = 20 "modest" correlation

$C_F$ = 100 "good" correlation

$C_F$ = 500 "strong" correlation

Although for independence the value of $C_F$ should be equal to 1, a value of 2 was chosen as this corresponded to a safer and realistic median wave height for a 100 year return period sea level.

Recently this work has been extended to map dependence around the coastlines of England, Scotland and Wales for extreme sea levels and wave heights, as well as other variable pairs potentially important in flood and coastal defence (including surge, river flow, rainfall, swell and wind), Defra (2005). It should be noted that different dependence models were used when considering combinations not related to sea levels and wave heights.

This introduced a new level of dependency (super), and associated levels of correlation relating to each correlation factor. These are given in Table 2.1 below.

| **Dependency** | **Correlation** | **Correlation Factor** | |
|---|---|---|---|
| Independent | ≤ 0.11 | 2 | (2-2.5) |
| Modest | 0.12 ≤ 0.37 | 20 | (2.5-25) |
| Good | 0.38 ≤ 0.53 | 100 | (25-125) |
| Strong | 0.54 ≤ 0.70 | 500 | (125-600) |
| Super | > 0.70 | 1500 | (600+) |

**Table 2.1** : Correlation factors for different levels of dependency.

Dependency around the coastline was based on 21 sea level and wave model locations for records over the period April 1990 to March 2002. This gave good spatial coverage around the coastline, which was determined for offshore areas. Estimated levels of correlation for Cumbria were given as

0.29 for Walney Island to St. Bees Head for all wave conditions, and 0.32 for the predominant wave direction (modest correlation). No levels of correlation were given between St. Bees Head and Silloth.

For return periods other than 100 years, the correlation factor is given by Equation (2.5).

$$(C_F)_R = 2\left(\frac{706T_R}{2}\right)^{\delta} \qquad \delta = \frac{\log((C_F)_{100}/2)}{\log(35300)} \tag{2.5}$$

where : $_R$ = return period being considered

If the design condition for independence is required, it is suggested (Defra, 2005) that Equation (2.5) should be restructured as follows, giving a minimum value of $C_F$ equal to 1.

$$(C_F)_R = (706T_R)^{\delta} \qquad \delta = \frac{\log((C_F)_{100})}{\log(70600)} \tag{2.6}$$

This technique was developed for use where only information on marginal extremes was available, and was not to replace the JOIN-SEA approach outlined below.

### 2.3.5 Extrapolation of Joint Probability Density (JOIN-SEA)

As a result of the lack of understanding with regard to joint probability, and the acknowledgement of its importance to flood and coastal defence issues (see Section 2.1), considerable research into joint probability methods has been commissioned by MAFF over the last 10 years. This has resulted in the development of the JOIN-SEA method (Hydraulics Research 2000a and 2000b) which is outlined here. This method is based on the methods developed by Ledford and Tawn (1996 and 1997).

In this method, based on proposals by Coles and Tawn (1994), a bivariate, or mixture of two bivariate probability distribution models is fitted to the upper tail of the wave height and sea level data sets. These models are then used to generate a large sample of random pairs of wave heights and sea levels based on the statistical distributions defined and the correlation between the two distributions. Below the upper tails, the data is assumed to follow the distribution of the input data. The joint probability curves are then determined by 'counting back' from the data set generated to the required return periods.

The choice between using the one (BVN) and two (MIX) bivariate normal distributions is determined by the fit to the data. Typically, the single BVN is stated as being adequate at locations where the extreme wave conditions all come from a single population (e.g. generated locally). The mixture of two BVNs is stated as generally being used at locations where the wave conditions are considered to come from two populations (e.g. significant swell waves as well as locally generated wind waves) or the correlation varies significantly at different percentage thresholds (Hydraulics Research Ltd. 2000b).

Wave periods are converted to wave steepness at the input stage, and a linear regression model is fitted to the wave steepness above a chosen threshold.

This technique therefore requires two similar but distinct methods which are outlined below.

As this method has been developed assuming that the upper tails of the marginal distributions follow established statistical techniques, it is considerably more rigorous than previous published techniques, and can currently be considered state of the art knowledge of this subject. It is also the technique that has been used in this study.

**Single Bivariate Normal (BVN) fit to Upper Tails**

This technique fits a BiVariate Normal distribution to the upper joint tail of the wave height and sea level data sets. The probability density function (*pdf*) of the bivariate normal distribution is given by Equation 2.7 below. Wave heights and wave periods are set to minima of 0.025m and 0.5s respectively at the input stage to prevent problems later on in the fitting procedure (details of these problems are not known). No alterations are applied to the sea level data set.

$$p(H_s,\eta)=\frac{1}{2\pi\sigma_{H_s}\sigma_\eta\sqrt{1-\rho^2_{H_s,\eta}}}e^{\left\{-\frac{1}{2(1-\rho^2_{H_s,\eta})}\left[\left(\frac{H_s-\mu_{H_s}}{\sigma_{H_s}}\right)^2-2\rho\left(\frac{H_s-\mu_{H_s}}{\sigma_{H_s}}\right)\left(\frac{\eta-\mu_\eta}{\sigma_\eta}\right)+\left(\frac{\eta-\mu_\eta}{\sigma_\eta}\right)^2\right]\right\}} \quad \textbf{(2.7)}$$

where:

$\rho_{H_s,\eta}$ = correlation between $H_s$ and $\eta$

$\sigma_{H_s}$ = standard deviation of $H_s$

$\sigma_\eta$ = standard deviation of $\eta$

$\mu_{H_s}$ = mean of the $H_s$ marginal distribution

$\mu_\eta$ = mean of the $\eta$ marginal distribution

Figure 2.4 overleaf shows the joint density contours of the standardized form of Equation 2.7 for different levels of correlation. These show that at the most extreme large or small values, as the correlation is reduced, the joint probability of the two variables also reduces. Conversely, as the correlation is increased, the joint probability of the two variables also increases.

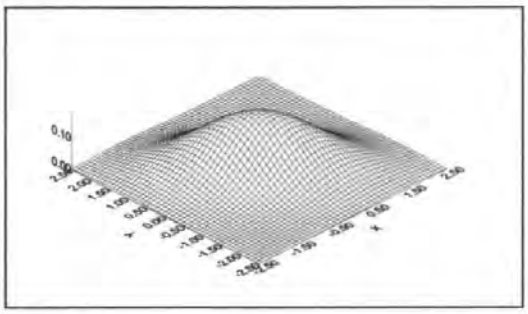

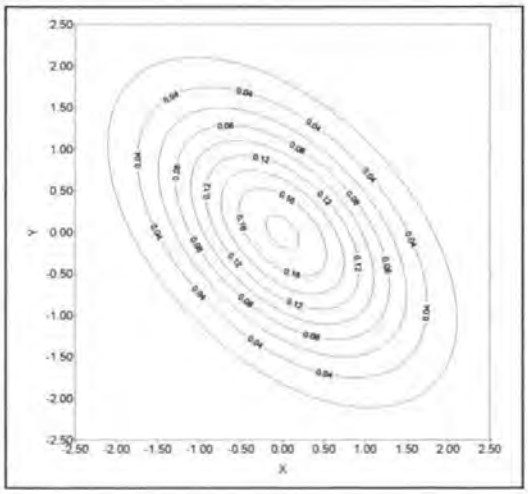

**Figure 2.4a** : Joint density contours for the standardised bivariate normal distribution for a correlation of –0.5.

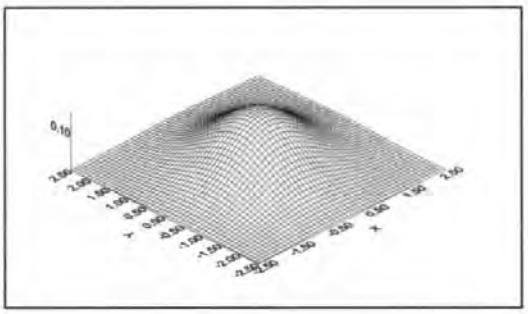

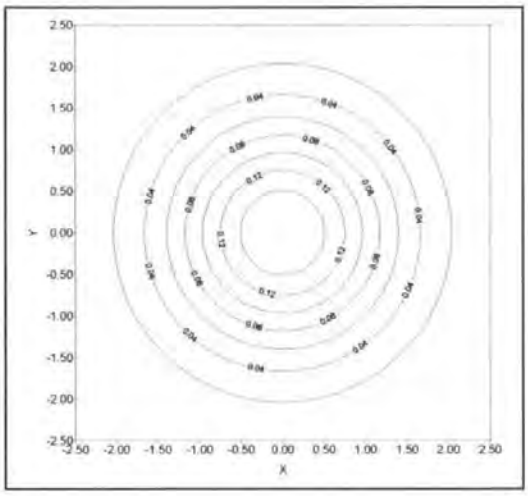

**Figure 2.4b** : Joint density contours for the standardised bivariate normal distribution for a correlation of 0.0.

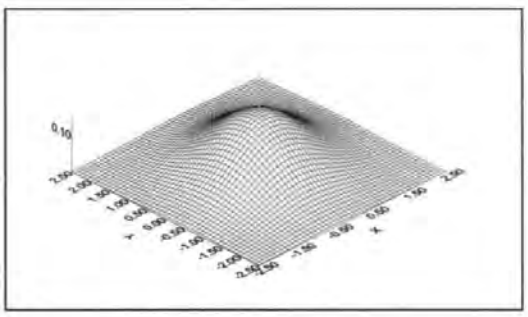

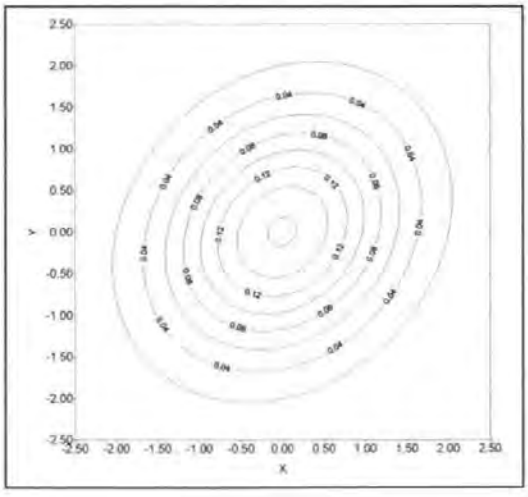

**Figure 2.4c** : Joint density contours for the standardised bivariate normal distribution for a correlation of +0.2.

The upper tails of the wave height and sea Levels are analysed by means of the Generalised Pareto Distribution (GPD), where the cumulative distribution function (*cdf*) of the wave height and sea level records is given by:

$$F(X) = \begin{cases} \dfrac{r}{n+1} & X < \zeta \\ \varepsilon\left\{1-\left(1-\dfrac{k(X-\zeta)}{\theta}\right)^{1/k}\right\}+(1-\varepsilon) & X \geq \zeta \end{cases} \quad \textbf{(2.8)}$$

where:

| | | |
|---|---|---|
| $X$ | = | sample being considered |
| $k$ | = | shape parameter |
| $\zeta$ | = | threshold (location parameter) |
| $\theta$ | = | scale parameter |
| $1-\varepsilon$ | = | threshold |
| $r$ | = | rank |
| $n$ | = | number of data points |

The parameters of the GPD are determined by means of a Maximum Likelihood estimation, details of which are given in for example Grimshaw (1993).

Figures 2.5 and 2.6 below show examples of quantile plots for the GPD's of wave height and sea level distributions using the simulated data set DATA1 (described later in this section), which was used in the beta-testing of the JOIN-SEA software (see Hawkes et al, 2004). These have been produced based on a chosen threshold of 95%.

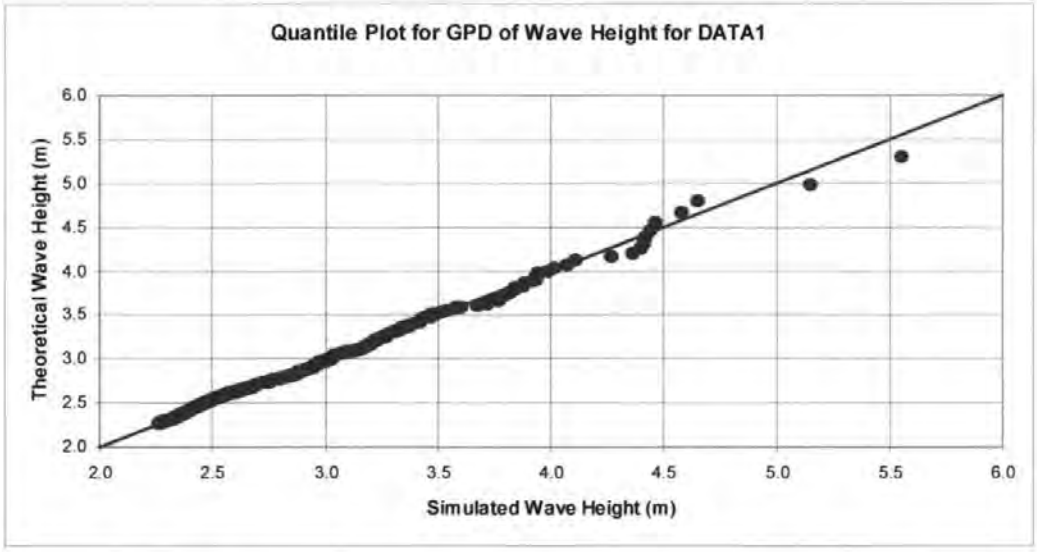


**Figure 2.5** : Quantile plot for GPD of wave height for simulated data set DATA1 (Hawkes et al, 2004)

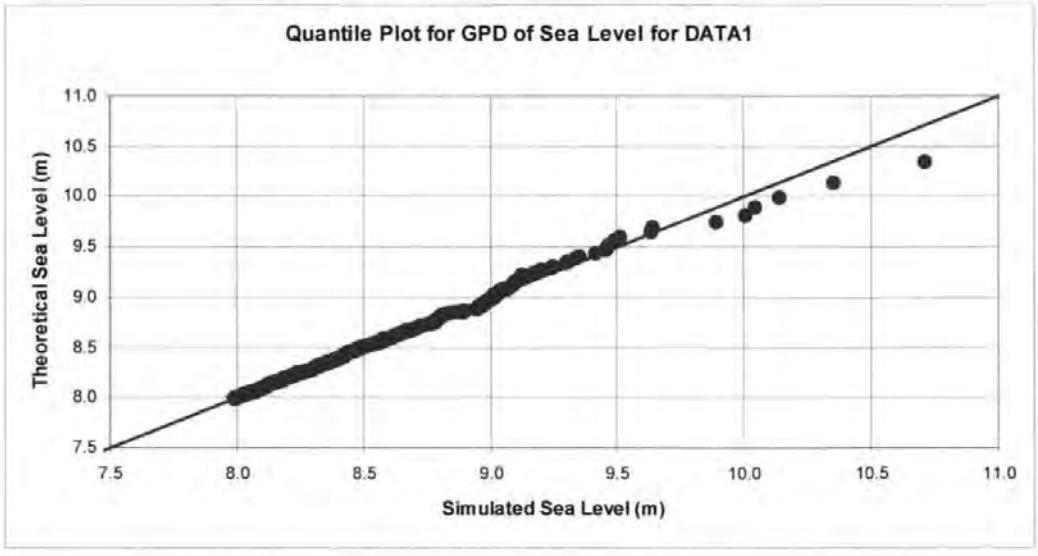


**Figure 2.6** : Quantile plot for GPD of sea level for simulated data set DATA1 (Hawkes et al, 2004)

The upper tail of the wave steepness is analysed by a linear regression model, where the deviate of the wave steepness is given by;

$$d_s = a + b\left(d_{H_s} - d_\zeta\right) \qquad H_s \geq \zeta \tag{2.9}$$

and the empirical distribution of steepness is modelled by a normal distribution on the wave height, where the deviate of wave steepness can be determined from Equation 2.10.

$$F(S) = \begin{cases} \dfrac{r}{n+1} = \displaystyle\int_{-\infty}^{d_s} \frac{1}{\sqrt{2\pi}\sigma_s} e^{\left[-\frac{(d_s-\zeta_s)^2}{2\sigma_s^2}\right]} dd_s & H_s \geq \zeta \\ \dfrac{r}{n+1} & H_s < \zeta \end{cases} \tag{2.10}$$

where:

| | | |
|---|---|---|
| $d_s$ | = | deviate of steepness |
| $d_{Hs}$ | = | deviate of wave height |
| $d_\zeta$ | = | deviate of threshold |
| $a$ | = | constant for linear regression |
| $b$ | = | coefficient for linear regression |
| $\zeta_s$ | = | threshold of deviate of steepness |
| $\sigma_s$ | = | standard deviation of deviate $d_H$ |

Figures 2.7 and 2.8 below show typical relationships determined by this linear regression model for the simulated data set DATA1, which was used in the beta-testing of the JOIN-SEA software (see Hawkes et al 2004). These have been produced based on a chosen threshold of 95%.

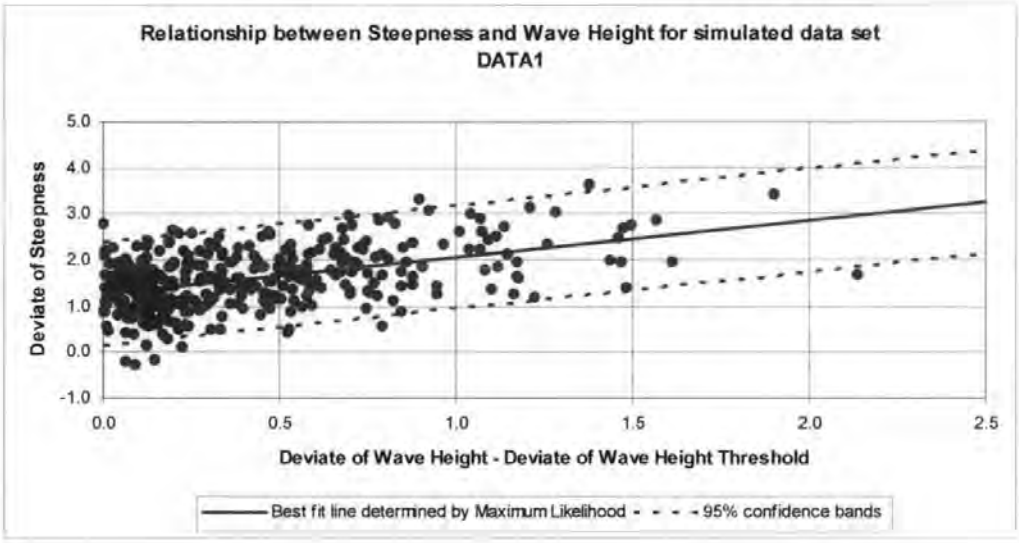


**Figure 2.7** : Linear regression model on steepness for simulated data set DATA1 (deviates), Hawkes et al (2004).

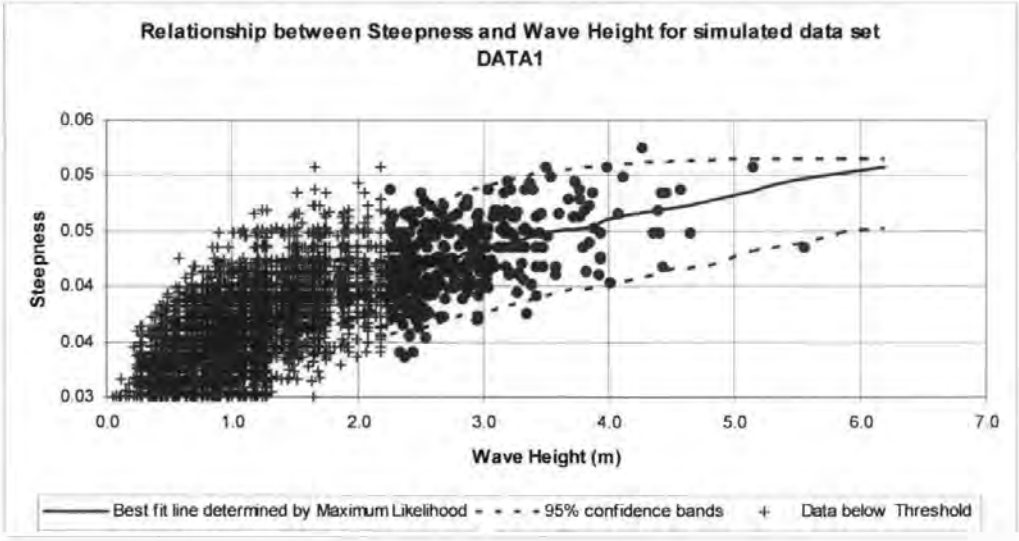


**Figure 2.8** : Linear regression model on steepness for simulated data set DATA1 (values), Hawkes et al (2004).

**Mixture of Two Bivariate Normals (MIX) fit to Upper Tails**

This technique fits a MIXture of two bivariate normal distributions to the wave height and sea level data sets. The *pdf* of the mixture distribution is given by Equation 2.11 below. Wave heights and wave periods are, similar to the BVN fit, set to minima of 0.025m and 0.5s respectively at the input stage to prevent problems later on in the fitting procedure. No alterations are applied to the sea level data set.

$$p(H_s,\eta)=(p_r)\,p(H_s,\eta)_1+(1-p_r)\,p(H_s,\eta)_2 \qquad \textbf{(2.11)}$$

where:

| | | |
|---|---|---|
| $p_r$ | = | proportion of variables in the first distribution |
| $1-p_r$ | = | proportion of variables in the second distribution |
| $p(H_s,\eta)_i$ | = | *pdf* of *i*th distribution of form Equation 2.7 |

Figure 2.9 overleaf shows the joint density contours of the standardized form of Equation 2.11 for different levels of correlation. These clearly indicate two different distributions. As with the single BVN fit, at the most extreme large or small values, as the correlation is reduced, the joint probability of the two variables also reduces. Conversely, as the correlation is increased, the joint probability of the two variables also increases.

The marginal distributions of the upper tails of the wave heights and sea levels are analysed by means of the GPD (see BVN fit to upper tails).

The upper tail of the Wave Steepness is analysed by a linear regression model (see BVN fit to upper tails).

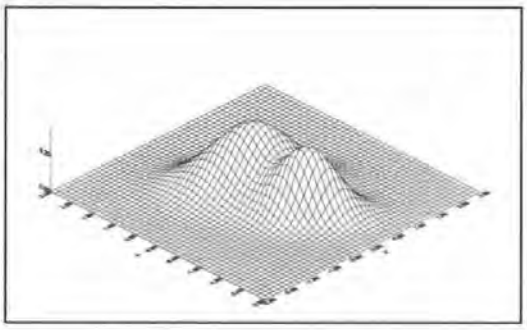

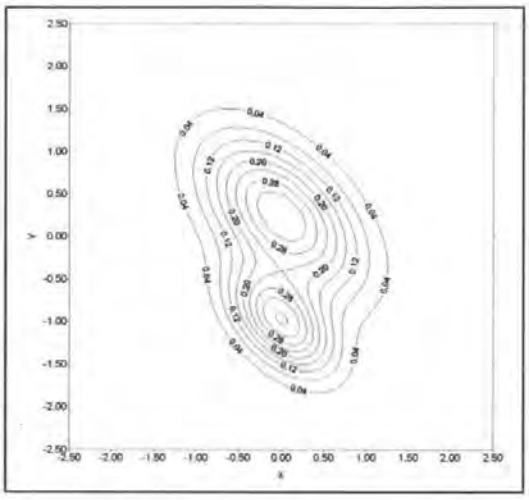

**Figure 2.9a** : Joint density contours for a mixture of two bivariate normal distributions both with a correlation of –0.5.

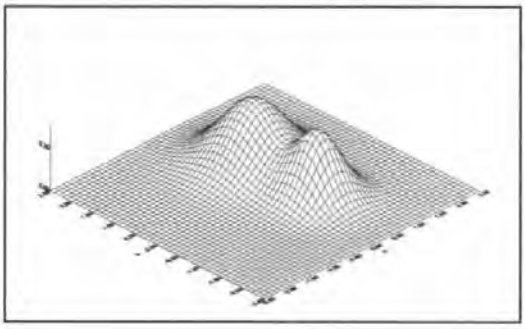

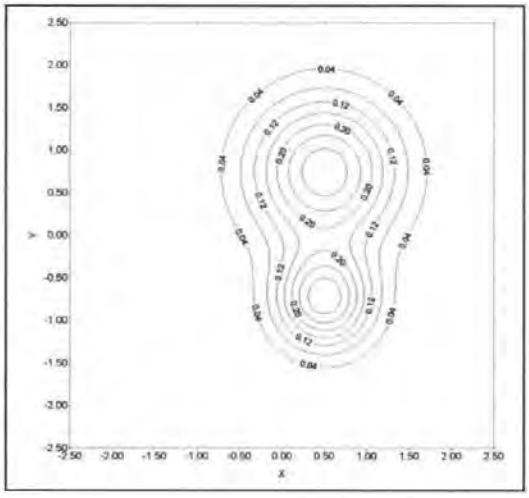

**Figure 2.9b** : Joint density contours for a mixture of two bivariate normal distributions both with a correlation of 0.0.

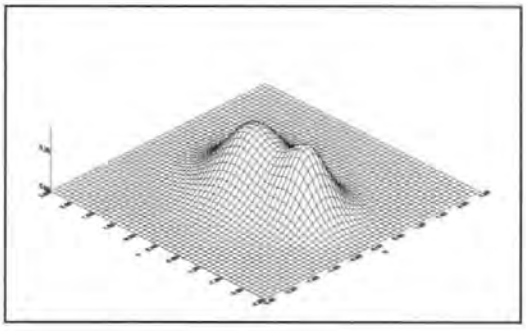

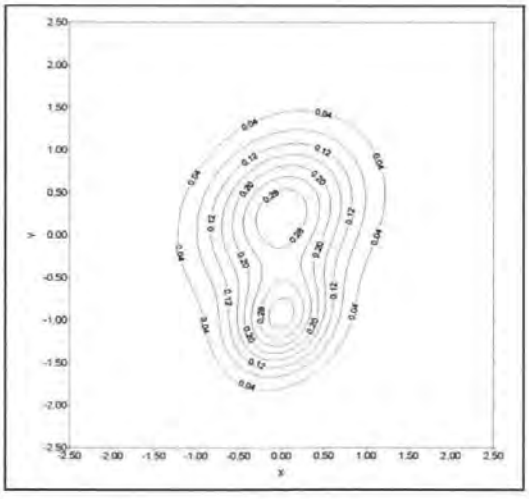

**Figure 2.9c** : Joint density contours for a mixture of two bivariate normal distributions both with a correlation of 0.2.

### Choice of Single or Mixture of BVN fit to Upper Tails

The choice of the MIX or BVN model is generally based on the variation of the correlation between wave heights and sea levels above different thresholds of non-exceedance of the sea levels. If the correlation tends to be constant above a threshold, then the BVN model is usually considered appropriate (Hydraulics Research Ltd, 2000b). If not, the more complex MIX model is more likely to represent the differing dependence at different thresholds.

This is demonstrated in Figure 2.10 below by means of the data sets DATA1 and DATA2, synthetic data sets based on underlying statistical distributions used in the beta testing of JOIN-SEA (see Hawkes et al 2004). These data sets were established so that one data set (DATA1) followed a BVN model and the other (DATA2) a MIX model. From these figures it can clearly be seen that the correlation shows little variation relative to threshold for DATA1, yet a constantly changing and increasing variation relative to threshold for DATA2.

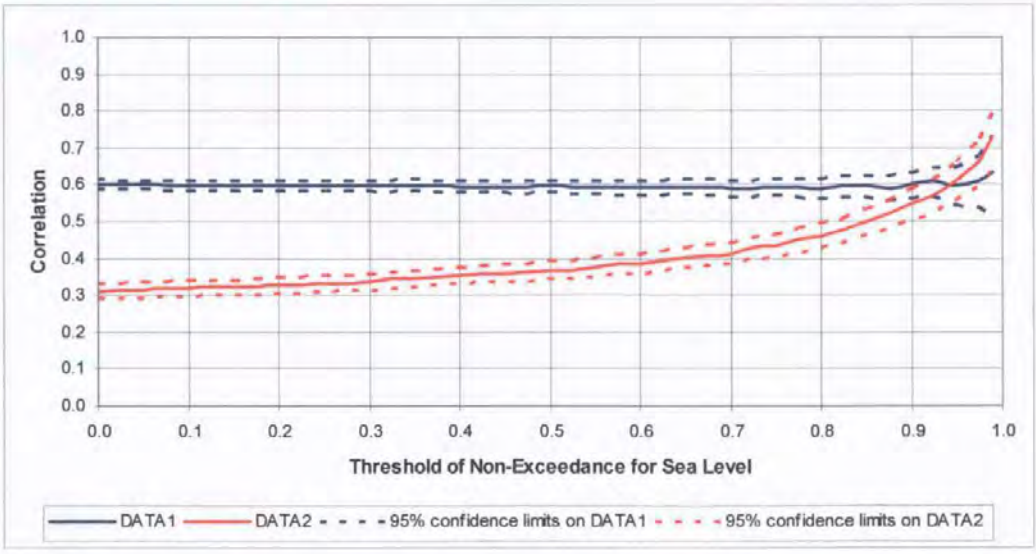


**Figure 2.10** : Variation in correlation above threshold for simulated data sets DATA1 and DATA2 (Hawkes et al, 2004)

# 3 Collection, Collation and Pre-processing of Raw Data Sets

Before considering the joint probability between waves and sea levels, relevant coincident records of waves and sea levels have either to be established, or obtained. Although sea level records have been recorded at a number of locations along the Cumbrian coastline for a significant number of years, no wave records suitable for a joint probability assessment have been previously measured or predicted. However, long term offshore predictions of wave heights are available from Met Office prediction points, and by transforming these inshore using an appropriate wave transformation model (WTM), nearshore predictions can be established.

This section therefore considers the collection, collation and pre-processing of the raw wave, sea level and survey data sets that were used in this study to establish the required coincident records. A detailed analysis of the sea level records outlines how the time series of high sea levels was established, which have been used as both an input parameter into the wave modelling as well as the joint probability data sets. This includes the pre-processing carried out on the sea levels to check for errors and inconsistencies, as well as techniques used to bridge any gaps in the data series. Offshore wave conditions are specified, which have been used in the wave transformation modelling, together with the sea level data to determine inshore wave heights, the determination of which is specified in Chapter 4. To determine nearshore wave heights, the wave transformation models considered for this study require bathymetric data to be specified on a regular, equally spaced horizontal grid of coordinates. Therefore this section outlines the survey information that was available for this study, and how it has been processed and collated to establish the bathymetry of the study area. With different bathymetric models used dependent on the offshore wave direction, finally this section outlines and justifies the bathymetric models that were established for this study. This section does not cover the grid spacing, which is considered in Section 4.0 based on the WTM used for this study.

## 3.1 Length of Data Record Analysed

To determine the joint probability relationship between sea levels and wave heights along the Cumbrian Coastline, the longest long term record of reliable co-incident sea level and wave height data was required.

Based on the available record of wave and sea level measurements / records - the determination of wave and sea level records for a joint probability assessment has been determined from 23/05/91 to 31/10/04. This matches the start of the earliest known digital record of sea levels for the Cumbrian coast from an EA gauge at Workington, and corresponds with the start of offshore predictions from the Met Office's European model of wave predictions (see Section 3.3). Although digital records from the Proudman Oceanographic Laboratory (POL) tide gauges at Workington and the Barrow locations (Ramsden Dock, Roa Island and Halfway Shoal) were not available until early-mid 1992, the EA gauge at Workington to this date is considered reliable (Hames et al, 2004), and the agreement of sea levels to nearby ports acceptable (see Section 3.2.4).

The finish date of 31/10/04 has been chosen to be as late as practically possible to enable the results to be based on the longest recorded data sets.

## 3.2 Sea Level Data

Using the recorded sea level data at Workington, Barrow, Silloth and Whitehaven and the predicted tides at the various locations along the Cumbrian Coast, has enabled the spatial variation of the sea levels (see Section 3.2.4). The location of the available sea level data sets is shown on Figure 3.1.

### 3.2.1 Predicted Tide Level Data

Predicted tides were determined by use of the tidal prediction program POLTIPS.3 (POL, 2001). Equal and high tide predictions were obtained for Ramsden Dock, Roa Island, Halfway Shoal and Workington based on the 103, 104, 96 and 108 most significant tidal constituents respectively. For secondary ports (see Table 3.1), high tides were determined by applying time and height differences for the nearby main port (Admiralty Tide Tables 2001). For Silloth, this was done using the leisure version of POLTIPS.2 (POL, 1998) as unresolved errors were evident in the Silloth predictions using POLTIPS.3 (POL, 2001)[1].

| Location | Predictions | Northing | Easting |
|---|---|---|---|
| Silloth | Time and Height | 553,340 | 310,159 |
| Maryport | Time and Height | 536,785 | 303,385 |
| Workington | Tidal Constituents | 529,580 | 299,170 |
| Whitehaven | Time and Height | 518,385 | 296,522 |
| Tarn Point | Time and Height | 488,465 | 307,782 |
| Duddon Bar | Time and Height | 473,527 | 312,926 |
| Ramsden Dock | Tidal Constituents | 467,190 | 319,980 |
| Roa Island | Tidal Constituents | 464,800 | 323,270 |
| Haws Point | Time and Height | 462,210 | 323,626 |
| Halfway Shoal | Tidal Constituents | 459,456 | 321,943 |

**Table 3.1:** Locations where tide predictions are available

### 3.2.2 Recorded Sea Level Data

The recorded data that were available is given in Table 3.2. Before any of the sea level data sets could either be analysed or processed, it was necessary to check them for errors or inconsistencies. These included large increases (spikes) in sea level over a single time step, time lags in recorded signals, an incorrect datum (drifts), and siltation of tide gauges.

[1] Personal Communications between Dominic Hames and Kevin Ferguson, Colin Bell and Philip Woodworth at Proudman Oceanographic Laboratory, 2003-2004.

More details on the checks carried out on these data sets, showing examples of the typical errors or inconsistencies found and their treatment was given in Hames et al (2004). Where possible, errors in the data sets were corrected so as to maintain as large a data set as possible for analysis (see Section 3.2.3).

| Location | Data available | Type[2] | Source | Availability | Collected |
|---|---|---|---|---|---|
| Silloth | Manually Recorded High Sea Levels | n/a | ABP | 01/11/87 – date | 01/11/87 – 31/10/04 |
| Workington | Manually Recorded High Sea Levels | n/a | ABP | 01/01/91 – date | 01/01/91 – 31/07/02 |
| Workington | Digitally Recorded every 1 hour | pneumatic bubbler | POL | 06/02/92 – 31/12/92 | 06/02/92 – 31/12/92 |
| | Digitally Recorded every 15 minutes | pneumatic bubbler | POL | 01/01/93 – date | 01/01/93 – 31/10/04 |
| Workington | Digitally Recorded every 15 minutes | pressure | EA | 23/05/91 – date | 23/05/91 – 31/10/04 |
| Whitehaven | Manually Recorded High Sea Levels | n/a | Port | 01/04/91 – 31/08/98 | 01/04/91 – 31/08/98 |
| Whitehaven | Digitally Recorded (no details available) | radar reflection | not known | unknown | none |
| Ramsden Dock | Digitally Recorded at two locations every 4 minutes | pneumatic bubbler | ABP | 01/05/92 – late 2005 | 01/05/92 – 31/10/04 |
| Ramsden Dock | Manually Recorded every 1 hour | n/a | n/a | ≈ 2001 to date | none |
| Ramsden Dock | Manually Recorded High and Low Sea Levels | n/a | n/a | not known (many years) | none |
| Roa Island | Digitally Recorded at two locations every 4 minutes | pneumatic bubbler | ABP | 01/05/92 - 16/02/00 | 01/05/92 - 16/02/00 |
| Halfway Shoal | Digitally Recorded at two locations every 4 minutes | pressure | ABP | 22/08/92 - 31/05/01 | 22/08/92 - 31/05/01 |

**Table 3.2**: Recorded data sets available

[2] Details of the different kinds of tide gauges are given on the National Tidal and Sea Level Facility at www.pol.ac.uk/ntslf/tgi/.

The pneumatic bubbler tide gauges are generally favoured over more traditional float gauges as they are 'perceived' to be superior (Woodworth et al 2004). POL tide gauges are stated as being accurate to 1cm (the GLOSS (Global Sea Level Observing System) standard) and 20 seconds in time (Woodworth et al 2004). This accuracy has recently been confirmed by Míguez et al (2005). Environment Agency tide gauges are probably accurate to several cms, although no confirmation of this has been sought. Manual sea level readings are at best accurate to 2-5cm.

A full history of the known sea level records available for the Cumbrian coastline is given in Appendix A.

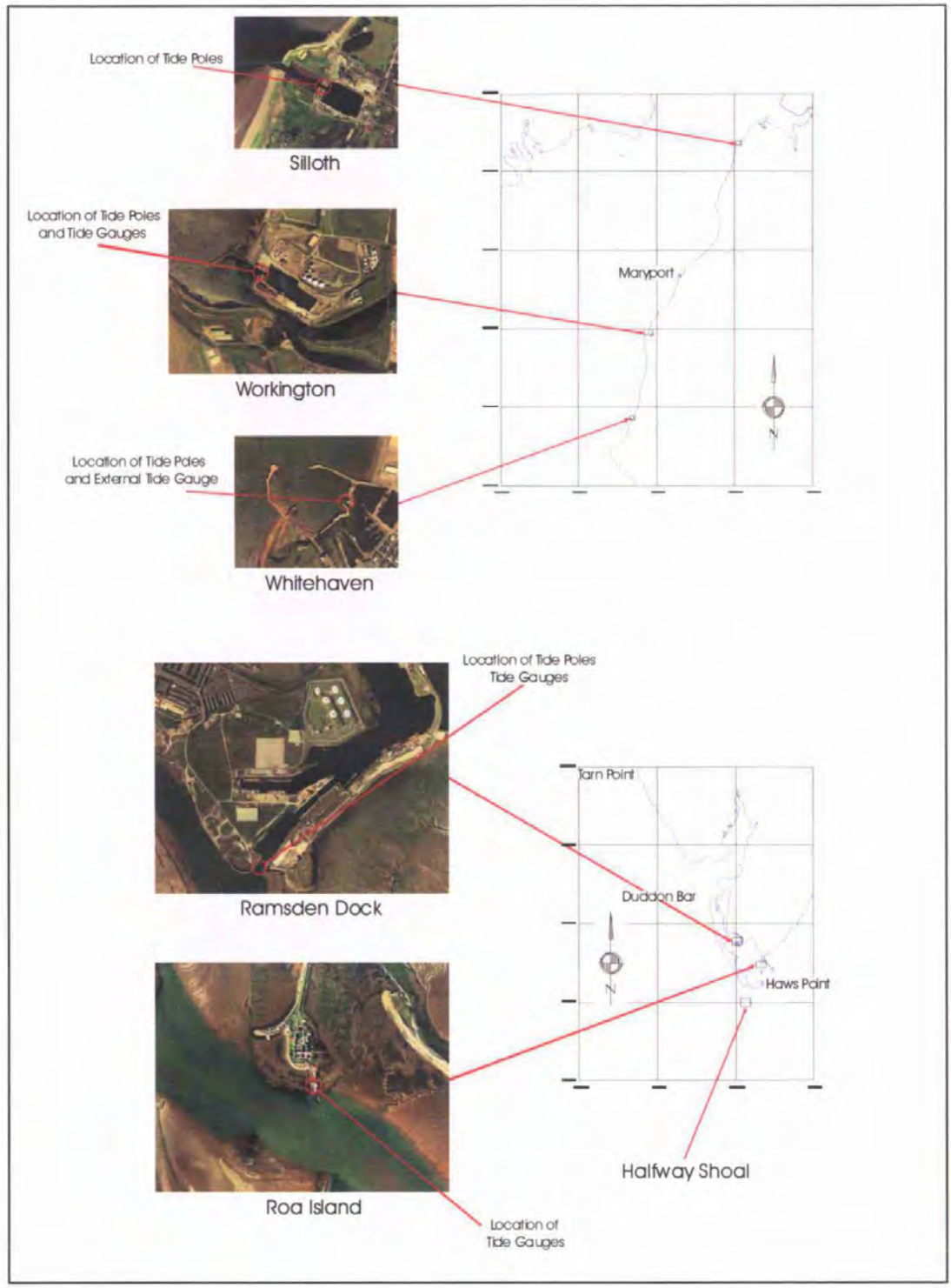


**Figure 3.1** : Location of sea level measurements (Cumbrian coastline)

### 3.2.3 Pre-processing of Sea Level Data

Before any of the sea level data sets could be used in this study, they had to be pre-processed to assess their quality, and to identify and (where necessary) to correct or eliminate incorrect data and to bridge gaps. The general checks carried out on the data sets are outlined below, together with how typical errors were treated. More detailed information on the quality of the data sets, including the typical errors detected are given in Hames et al (2004). It should be noted that the POL Workington data sets were supplied as checked, and the EA Workington data sets as 'mainly' checked[3]. No previous checks had been carried out on the digital Barrow data sets or any of the manual records, which had not been previously digitised.

1. The data sets were plotted against the predicted tide for the port and both the recorded sea level and the surge checked manually. For Silloth and Whitehaven, the manually recorded high sea levels and surges were compared against the processed high sea levels and surges at Workington as well as the predicted tides at these respective ports (see Section 3.2.4).

2. For short periods of missing or suspect values, a linear trend in the surge was assumed between 'correct' values, and regions of lag and shift corrected. Areas of the data set where the gauge appeared to slip, either suddenly or over a period of time were identified for comparison with nearby or co-incident locations. These were if possible corrected. Notes on the checking and maintenance of the recording device were further used to identify regions of suspect data.

3. For the Workington data sets, high sea levels were calculated and the surge at high tide compared with the co-incident surge determined from the high sea levels by the Port of Workington (see Section 3.2.4). Where high sea levels were seen to differ significantly, local manual checks were carried out on the relevant data set, including comparison

[3] The tide data from the EA gauge at Workington is marked as 'unchecked' from

against offshore wind speeds and directions. Regions of 'drift' in the EA data set were also able to be identified from this comparison, and where possible, these were corrected (see Section 3.2.4 and Hames et al 2004). The datum shifts for the POL data set were corrected (see Section 3.2.2).

4. For the Barrow locations, periods where the tide gauges were noted to silt up were identified and eliminated, as these data were unreliable, and could not be corrected. This mainly affected the Ramsden Dock tide gauges.

5. For the manual records, comparison with nearby digital records usually identified suspect values which would usually be as a result of incorrect reading off the tide board, or incorrect translation to the log book. The typical errors found and their treatment are highlighted in Hames et al (2004).

6. The surge for the digital data sets was determined, and sets of records identified where the time between successive up crossings was between 12-13 hours, i.e. coinciding approximately with the period of a semi-diurnal tide. This further enabled sections of the data record to be determined where any lag may be present which had been missed by the manual check. The sections which gave an excessive variation in surge over these periods were checked manually and compared to nearby or co-incident data sets.

7. Manual checks were carried out on the data records for the largest surges, the largest rate of change in successive surges and regions at high tides where significant 'kinks' in the data set were identified. All missing and suspect data records were also identified to see if any patching missed by the manual check could be carried out.

02/01/2001 to 29/02/2004, and for few other periods outside this range.

8. For the Barrow data sets, surges for both sensors at Ramsden Dock were checked against the corresponding surges at Roa Island and Halfway Shoal.

### 3.2.4 Compilation of Processed Time Series

To determine the spatial variation in sea levels along the Cumbrian Coastline, it was first necessary to establish reliable standardised records of recorded high sea levels from digital records at Workington and Barrow (see also Section 3.2.5). These were then compared against each other, and against the manually recorded high sea levels at Silloth and Whitehaven. Based on the comparisons, records of time series of high sea levels at the four locations along the Cumbrian coastline where sea levels were recorded were established. Based on published time and height differences (Admiralty Tide Tables, 2001), the relationship between sea levels at Maryport, Tarn Point and Duddon Bar could also be determined. Details of the analyses carried out to establish time series records of high sea levels at these locations are given below. With the time difference between high tide at Workington and Silloth (to the north), and Workington and Barrow (to the south) typically 7-17 minutes, or 20-35 minutes at the most, changes in atmospheric effects, and therefore surges were assumed not to occur, and tide and surge levels were therefore assumed to be coincident.

High sea levels from the digital records were determined based on a quadratic fit through the three highest sea levels centred on the highest recorded sea level. Sea level variation between the locations was assumed to be linear based on the Northing coordinate of each location given in Table 3.1.

The agreement between sea levels has been determined based on a standardised date of 01/01/04 (see Section 3.2.5) and on a minimisation of the absolute differences between the best fit line and the time series.

## Workington

To determine the record of high sea levels at Workington, all three records of high sea levels at this location (POL and EA digital records, and the manually recorded Port high sea levels) were visually compared. Generally the three records showed good agreement. The erratic nature of the EA sea level records at Workington (see Hames et al 2004) was noted to be a 'locally constant', yet variable datum shift. This is demonstrated by reference to Figure 3.2 below, which shows the recorded surge for high sea levels at Workington over the period 23/01/02 to 02/02/02. This coincides with the period when the EA sea level readings had the greatest variation between high sea levels recorded by the POL tide gauge and the manual readings.

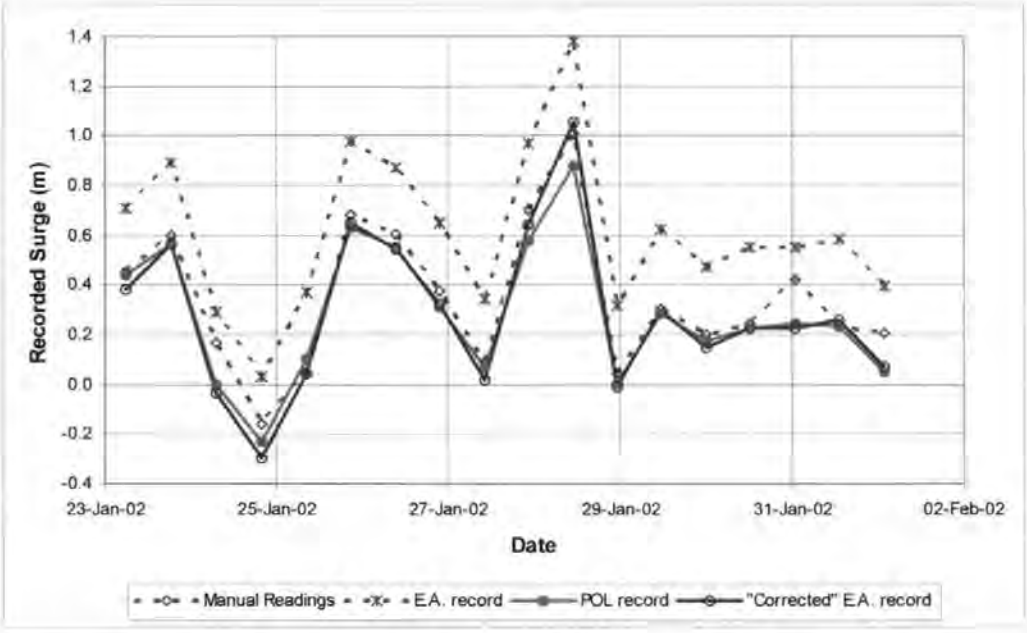


**Figure 3.2** : Comparison of recorded surges at Workington 23/01/02 to 02/02/02.

From this figure, it can be shown how, by assuming a locally constant shift in the datum for the EA gauge (from the POL gauge), the EA records could typically be corrected. The corrected records generally show good agreement with the POL records. The exception to this is the morning sea level of 28/01/02, which varies from the POL recorded high sea level by almost 0.2m. Assuming a locally constant shift in the EA tide datum relative

to the POL sea level records over several days was anticipated to correctly estimate the datum to ±0.05m more than 90% of the time.

Generally, the POL sea level records were used to determine high sea levels at Workington. Where these records were missing, or showed a large variation from the other two sea level records, the corrected EA sea level records or the manual records were used. When only 1 or 2 sets of records were available, a comparison was made with the recorded sea levels at Barrow.

**Barrow**

To determine the record of high sea levels at Barrow, all three records of high sea levels at Ramsden Dock, Halfway Shoal and Roa Island were compared. These were combined to form one composite record for Ramsden Dock (termed Barrow).

For all three locations, there is a pressure differential between the two gauges (see Appendix A). This is up to 23mm (16mm at high tide) for Halfway Shoal, see Hames et al (2004), and 4mm (2mm at high tide) for Ramsden Dock and Roa Island. The pressure differential is approximately proportional to the tidal pattern, although not necessarily the local tidal currents. This differential is believed to be as a result of a pressure gradient between the tubes to the instrument caused by the viscosity of the gases in the tubes. Recorded sea levels at the Barrow locations are taken to be the average of both gauge readings, or the remaining gauge reading if one reading is not available.

To establish the composite record for Ramsden Dock and the effect of the pressure differential between the two gauges, the surge records and the pdfs and cdfs of surge (Figure 3.3 below) at Ramsden Dock were compared to those for the POL tide gauge at Workington. These comparisons did not indicate that either of the two sea level records were under or over-recorded relative to each other. Recorded sea levels at

Ramsden Dock were therefore assumed to be accurate, with no datum correction required.

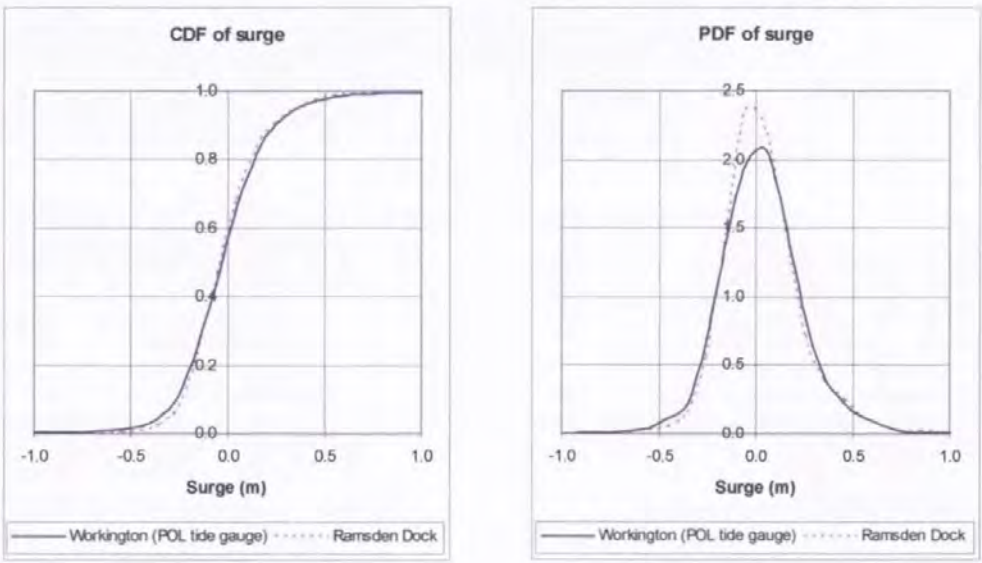


**Figure 3.3** : pdf and cdf of surges at Workington (POL tide gauge) and Ramsden Dock

The sea level records at Roa Island and Halfway Shoal were used to check the sea level records at Ramsden Dock, and (where necessary) replace missing records. The agreement between these locations is shown in Figures 3.4-3.6 below.

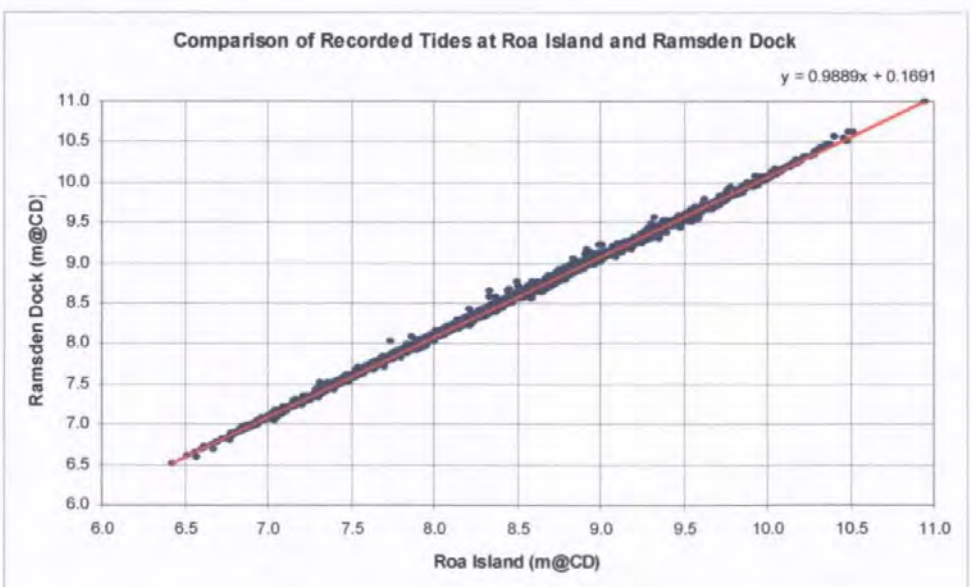


**Figure 3.4** : Comparison of recorded sea levels at Roa Island and Ramsden Dock

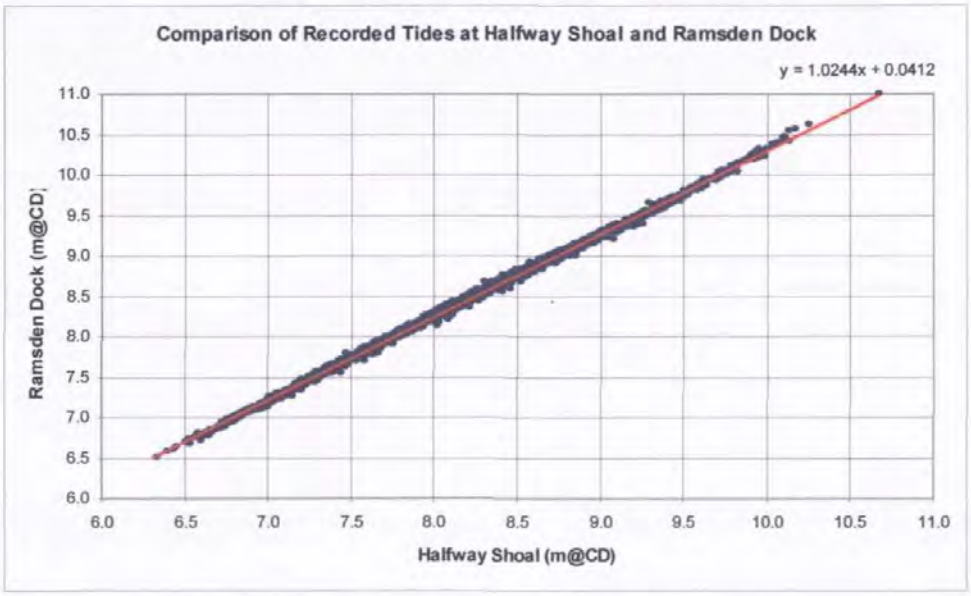


**Figure 3.5** : Comparison of recorded sea levels at Halfway Shoal and Ramsden Dock

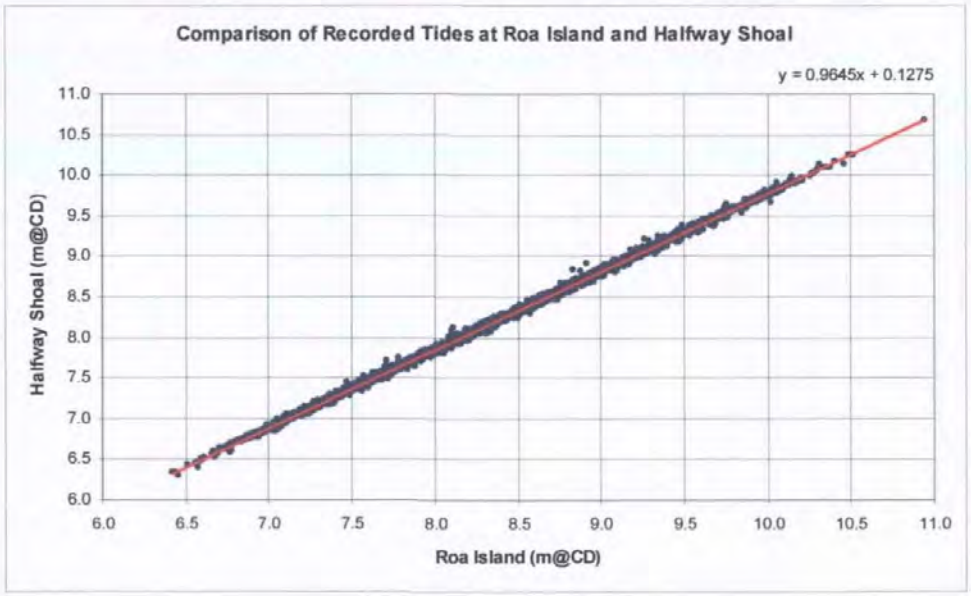


**Figure 3.6** : Comparison of recorded sea levels at Roa Island and Halfway Shoal

The agreement between sea level records at these three locations can therefore be seen to be very strong, and given the sea level at either Roa Island or Halfway Shoal, the sea level at Ramsden Dock can be estimated accurately. The effect of the pressure differential between the tide gauges

at Halfway Shoal is therefore not important, as its correction for Ramsden Dock will be inherent in the linear relationship given above. The potential under-recording of sea levels from the Roa Island gauges (see Hames et al 2004) will also be unimportant for the same reasons.

Missing records for Ramsden Dock were replaced using the linear relationship for Roa Island, and where necessary Halfway Shoal.

The agreement between the resultant composite sea level for Workington and Ramsden Dock (Barrow) is therefore given in Figure 3.7 below.

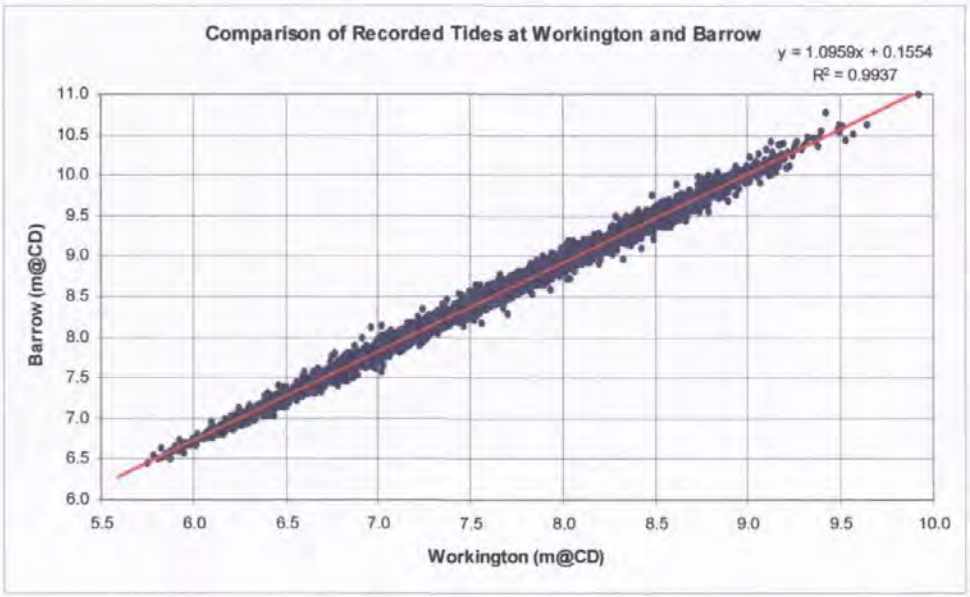


**Figure 3.7** : Comparison of recorded sea levels at Workington and Barrow

Using this relationship, sea levels at Barrow over the period 23/05/91 to 30/04/92 and 08/01/01 to 31/10/04 can be estimated from the sea level at Workington. Missing records between these dates (about 0.5% of records) can also be estimated in the same way. This can lead to errors in the estimate of the sea level at Barrow by over 0.1m approximately 10% of the time, and over 0.2m, approximately 0.5% of the time. However, the increased length of record to be analysed (about 13.5 years as opposed to 8.6 years) is considered to outweigh the disadvantages of the reduced accuracy in sea level estimates near Barrow.

## Silloth

To determine the time series of high sea levels at Silloth, the recorded high sea levels at Silloth were compared to those at Workington (Figure 3.8).

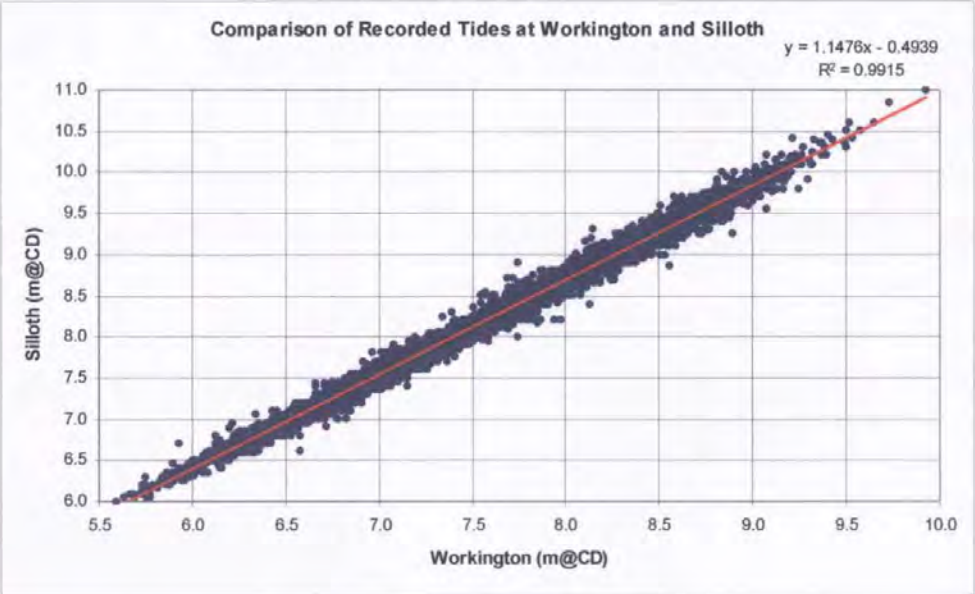


**Figure 3.8** : Comparison of recorded sea levels at Workington and Silloth

From Figure 3.8, it can be seen that the agreement between sea levels at Silloth and Workington is not as good as the agreement between sea levels at Barrow and Workington which would normally be unexpected considering the respective port locations and exposure conditions. The reason for the poorer agreement will be mainly down to the accuracy of measurement at Silloth (sea levels measured to the nearest 0.05m), but also down to the difficulty in reading sea levels off a tide board with possible swell present.

The differences between the recorded sea levels at Silloth and Barrow, and the corresponding simulated sea levels from Workington are approximately Gaussian distributed. Based on this distribution, the Barrow recorded sea levels are about 15-20% closer on average than the Silloth recorded sea levels to the relevant Workington simulation.

Therefore it would be expected that a comparison between the simulated sea levels at Silloth from the Workington sea level, would show better agreement to the 'actual' sea level than the manually recorded sea level. The sea level at Silloth is therefore estimated from the sea level at Workington using the linear relationship given below, Equation (3.1), and not from the recorded sea level.

$$\eta_{CD}^{Silloth} = 1.1476\eta_{CD}^{Workington} - 0.4939$$
$$\eta_{OD}^{Silloth} = 1.1476\eta_{OD}^{Workington} - 0.0740 \qquad \textbf{(3.1)}$$

**Whitehaven**

The comparison between the recorded sea levels at Whitehaven and Workington is given in Figure 3.9 below.

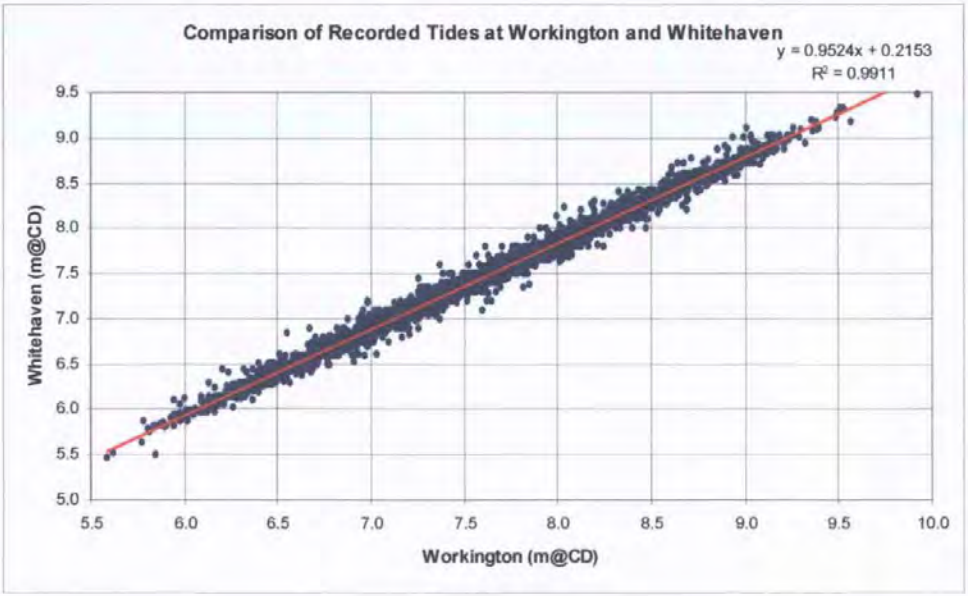


**Figure 3.9** : Comparison of recorded sea levels at Workington and Whitehaven

Similar to Silloth, the agreement between sea levels at Whitehaven and Workington is not as good as the agreement between sea levels at Barrow and Workington. This agreement is also not as good as the agreement

between Silloth and Workington. The reasons for any increased discrepancy are not significant, as they are almost certainly due to the inherent increased errors present from manual sea level readings as given earlier. This seems to be confirmed by comparing the Workington sea level records against the Workington Port manual readings which shows similar discrepancies to when comparing the manual Silloth and Whitehaven records against the Workington records. The manual records recorded at Whitehaven are also noticeably poorer in quality than the manual records recorded at Silloth and Workington.

Therefore it would be expected that a comparison between the simulated sea levels at Whitehaven, would show better agreement to the 'actual' sea level than the manually recorded sea level. The sea level at Whitehaven is therefore estimated from the sea level at Workington using the linear relationship given below, Equation (3.2), and not from the recorded sea level.

$$\eta_{CD}^{Whitehaven} = 0.9524\eta_{CD}^{Workington} + 0.2153$$
$$\eta_{OD}^{Whitehaven} = 0.9524\eta_{OD}^{Workington} + 0.0154 \quad \textbf{(3.2)}$$

**Maryport**

Sea levels at Maryport have been estimated based on the assumption of tidal similarity between Workington and Maryport. Standard tides have been determined from POLTIPS.3 (POL, 2001) and checked against standard tides from the Admiralty Tide Tables (2001). This gives the sea level at Maryport as:

$$\eta_{CD}^{Maryport} = 1.0823\eta_{CD}^{Workington} - 0.1778$$
$$\eta_{OD}^{Maryport} = 1.0823\eta_{OD}^{Workington} + 0.0679 \quad \textbf{(3.3)}$$

### Tarn Point

Sea levels at Tarn Point have been estimated based on the assumption of tidal similarity between Barrow and Tarn Point. Standard tides have been determined from POLTIPS.3 (POL, 2001) and checked against standard tides from the Admiralty Tide Tables (2001). Chart Datum at Tarn Point is not known. However, based on an assessment of standard tidal conditions at Workington and Barrow, Chart Datum is estimated as 4.25m below Ordnance Datum. The only known previous estimate of Chart Datum at Tarn Point is 4.30m (Hames 2002), an estimate determined by the author and re-specified for this study to 2 decimal places. This gives the sea level at Tarn Point as:

$$\eta_{CD}^{Tarn\ Point} = 0.9207\eta_{CD}^{Barrow} - 0.0159$$
$$\eta_{OD}^{Tarn\ Point} = 0.9207\eta_{OD}^{Barrow} + 0.1074 \qquad \textbf{(3.4)}$$

### Duddon Bar

Sea levels at Duddon Bar have been estimated based on the assumption of tidal similarity between Barrow and Duddon Bar. Standard tides have been determined from POLTIPS.3 (POL, 2001) and checked against standard tides from the Admiralty Tide Tables (2001). Chart Datum at Duddon Bar is not known. However, based on an assessment of standard tidal conditions at Workington and Barrow, Chart Datum is estimated as 4.37m below Ordnance Datum. There are no known previous estimates of Chart Datum at Duddon Bar. This gives the sea level at Duddon Bar as:

$$\eta_{CD}^{Duddon\ Bar} = 0.9454\eta_{CD}^{Barrow} - 0.0329$$
$$\eta_{OD}^{Duddon\ Bar} = 0.9454\eta_{OD}^{Barrow} + 0.0877 \qquad \textbf{(3.5)}$$

### 3.2.5 Analysis of Trends in Sea Level Records

The data series for this study have been standardised to 01/01/04. This is to ensure a stationary data set, with records invariant to time. The date chosen was the start of the last year where complete series of sea level (and wave) data were available.

To estimate the secular trend in the data sets, a low pass filter was applied to the regular time series data sets at Workington (POL), Ramsden Dock, Roa Island and Halfway Shoal to remove the dominant astronomical components. No calculations were carried out on the EA tide gauge at Workington as the non constant datum would result in unreliable estimates (see Section 3.2.2). For the Workington (POL) data set, data prior to June 1994 was not considered as the datum prior to this date is not reliable (see Section 3.2.2). The low pass filter was applied to the sea levels with and without the astronomical tide removed. Trend estimates should therefore not be biased by any long term astronomic component such as the 18.61 year nodal variation caused by the moon's declination to the earth.

However, Shennan and Woodworth (1992) indicate that for the length of records available for Cumbria (9-10 years), the standard deviation of the distribution of trends is approximately 5mm/year. This is determined from long-term MSL records. They indicate that approximately 35 years and 45 years of data are required to reduce these deviations to the order of 0.5mm/year and 0.3mm/year respectively. Although similar conclusions are also drawn by Douglas (1991) and Tsimplis and Spencer (1997) amongst others, it should be noted that these estimates are based on the analysis of either mean monthly or annual maxima sea levels, mostly manually recorded, and not digitally recorded twice daily high sea level records. Despite this, it is considered that any estimate of trend from the data sets using a low pass filter will only indicate the likely level, and a large but unknown deviation should be expected. The trends for the data sets therefore need to be considered in conjunction with historical global trends as well as locally determined trends for the Irish Sea region. Based on these analyses, and considering estimates of isostatic rebound for the area,

best estimates of eustatic trends have been estimated and applied to all data sets.

It should be noted that the data sets have been de-trended based on estimates of the mean sea level, although this study is concerned with the analysis of high sea levels only. Little work has been carried out on the trend of high sea levels, and no definite conclusions can yet be drawn on trends if any in high sea levels. This does appear to be a contradiction however, as trends in sea levels are usually based on annual maxima sea levels (i.e. high sea levels), and these do not produce consistent results as demonstrated for the Silloth data set in Hames et al (2004). Despite this, this study cannot address the issue of whether trends determined from high sea levels can be considered a reliable estimate of trends in mean sea levels, especially as this is a well established method. However, Hames et al (2004) did indicate that trends determined from sea levels recorded at a regular spacing was consistent, provided the spacing isn't near a multiple of the semi-diurnal period. This is the technique that has been considered for the Cumbrian data sets.

**Calculated Trends in Data Sets**

Several low pass filters were applied to the Workington (POL), Ramsden Dock, Roa Island and Halfway Shoal data sets. These were applied at frequencies below 0.03 hours$^{-1}$ to remove all high frequency terms (e.g. semi-diurnal and diurnal tides), leaving only low frequency terms which will include any trend. Subtracting the predicted tidal spectrum to leave the surge spectrum, also removes any significant long period lunar components.

Assuming a constant 'linear' trend, the best estimate of trends for these data sets is given below in Table 3.3.

| Location | Sampling Rate | 'Years' Analysed | Trend | |
|---|---|---|---|---|
| | | | Recorded Sea Level | Surge |
| Workington | 1 hour | 10.4 years | -0.4 mm/year | 0.1 mm/year |
| Ramsden Dock | 4 minutes | 8.7 years | 5.7 mm/year | 7.3 mm/year |
| Roa Island | 4 minutes | 7.8 years | 3.9 mm/year | 1.0 mm/year |
| Halfway Shoal | 4 minutes | 8.8 years | 6.2 mm/year | 6.5 mm/year |

**Table 3.3:** Secular trends determined by applying low pass filter to digitally recorded data sets

**Historical Analysis of Trends**

The Intergovernmental Panel on Climate Change, IPCC (2001), gives an estimate of global eustatic sea level change over the last 100 years averaging 1.0-2.0mm/year with no significant acceleration over this time. This coincides with nearly all studies carried out over the last 10-20 years, as shown in a number of reviews on this subject (see also for example Pirazzoli 2000). Over the next 100 years, the IPCC estimate that this is likely to rise to between 0.8-8.0mm/year with a central value of about 3.7mm/year, but averaging approximately 2.0mm/year over the period 1990-2010. UNESCO (1985) and DETR (1999) indicate a general increase in mean sea levels of about 100-150 mm/century over the period of detailed measurements.

Long term secular trends in mean sea level at Liverpool, the longest data set around the Irish Sea are given in Woodworth et al (1999) as 1.23mm/year. This is based on a record of mean sea levels from 1858. Over the 20$^{th}$ century, this trend is given as 1.39mm/year. Currently they indicate that sea levels at Liverpool are increasing by approximately 1.8mm/year, although no conclusions were drawn by Woodworth et al (1999).

## Trends based on Latest Published Mean Sea Levels for the Irish Sea Region

Monthly mean sea levels are published on the web site of the Permanent Service for Mean Sea Level (PSMSL) at the Proudman Oceanographic Laboratory for over 2000 locations around the world. Considering locations where records greater than 30 years are available, current estimates of secular and eustatic trends (as of February 2005) for locations around the Irish Sea are given below. Eustatic changes are based on best estimates of isostatic rebound summarised in Shennan and Horton (2002).

| Location | Range | Years | Trend (mm/year) | | Standard Deviation / Error (mm) |
|---|---|---|---|---|---|
| | | | Secular | Eustatic | |
| Holyhead | 1938-2003 | 54 | 2.87 | 2.58 | 0.46 / 0.06 |
| Liverpool (Georges and Princes Pier) | 1858-1983 | 88 | 1.08 | 0.87 | 0.36 / 0.04 |
| Heysham | 1960-2003 | 38 | 2.28 | 2.97 | 0.24 / 0.04 |
| Douglas | 1938-1977 | 34 | 0.35 | 0.80 | 0.04 / 0.01 |
| Portpatrick | 1968-2003 | 35 | 1.87 | 1.37 | 0.19 / 0.03 |
| Belfast | 1917-1963 | 46 | -0.17 | n/a | 0.02 / 0.00 |
| Malin Head | 1958-2003 | 43 | -1.22 | n/a | 0.15 / 0.02 |

**Table 3.4:** Trends determined from PSMSL data base (as of February 2005)

These records tend to indicate similar trends as indicated by IPCC (2001) and others, although no clear consistent trend for this region. Little research on isostatic rebound rates for Ireland has been carried out, although work is currently being done based on core samples from Giant's Causeway at the Universities of Maine and Belfast. These are expected to show that land in the region of Belfast and Malin Head is rising.

## Standardised Trends Applied to Data Sets

There has been a considerable amount of work carried out on trends in sea levels over the last 15-50 years. Most of this work has focussed on trends from the last century, leading to estimates of likely trends into the current

century. Most of the work over this time has indicated that eustatic sea levels have risen at a rate averaging 1-2mm/year over the last 100 years, and it is likely considering the conclusions of the IPCC (2001) and POL (e.g. Woodworth et al 1999) that sea levels are currently rising at an eustatic rate of approximately 2mm/year ±0.5mm/year.

Considering eustatic trends in the Irish Sea basin from the PSMSL archive, these range from 0.8-3.0mm/year, with an average trend of approximately 1.7mm/year centred on the early 1960s. This coincides with the work carried out by Woodworth et al (1999) on the Liverpool sea level data, which indicates a current eustatic trend at Liverpool of about 1.8mm/year.

An analysis of the trends from the Workington, Ramsden Dock, Roa Island and Halfway Shoal data sets indicates no secular trend at Workington, yet a secular trend averaging about 5mm/year at the Barrow locations. However, data sets of short duration are subject to large discrepancies in estimates of trends, not least caused by maintenance of the tide gauges themselves. This was confirmed by Lloyd (2000) who estimates that re-calibration of the tide gauge at Hilbre Island near Liverpool for example can result in a placement error of up to 2-3cms. A 'dip' in global mean sea levels in the early 1990s (Woodworth et al 1999), would also tend to overestimate any trends detected.

For the data sets considered in this study, it is assumed that local mean sea levels along the Cumbrian coastline have risen linearly at the same eustatic rate since 1992, and therefore the same estimate of linear trend is to be applied to all data sets. Considering the comments given above, and the analysis carried out, there is no reason to believe that local mean sea levels have not risen at the same rate as global mean sea levels. Therefore a trend in mean sea levels of 2mm/year is assumed, and applied to all data sets.

With the tide gauges used to measure the sea levels being fixed, the only variation in these trends would be as a result of isostatic rebound. For the north-west of England, this is given as approximately +0.25mm/year at

Barrow, +0.55mm/year at Whitehaven, +0.65mm/year at Workington and +0.95mm/year at Silloth, Shennan (1989).

Therefore the sea level data sets used in this study have been standardised as follows:

| Location | Before 01/01/04 | After 01/01/04 |
|---|---|---|
| Ramsden Dock | +1.75 mm/year | -1.75 mm/year |
| Roa Island | +1.75 mm/year | -1.75 mm/year |
| Halfway Shoal | +1.75 mm/year | -1.75 mm/year |
| Whitehaven | +1.45 mm/year | -1.45 mm/year |
| Workington | +1.35 mm/year | -1.35 mm/year |
| Silloth | +1.05 mm/year | -1.05 mm/year |

**Table 3.5:** Standardised trends applied to data sets.

## 3.3 Wave Data

Records of wave height along a coastline are basically obtained from 3 different sources, wave measurements, visual observations and hindcast from numerical models. Generally, the only long term record of wave heights along a coastline are for the Met Office Wave Model (see Section 3.3.2).

### 3.3.1 Data Availability

For the Cumbrian coastline, few records of wave data are available whether measured, observed or hindcast. The full list of known measured and hindcast wave data is given in Table 3.6 below, and shown on Figure 3.10. No known observed wave data are available.

| Location | Easting | Northing | Type | Instrument / Model | Depth (m) | Period from | Period To | Organisation (see Figure 3.10) |
|---|---|---|---|---|---|---|---|---|
| Barrow-in-Furness | 314,991 | 458,484 | recorded | wave rider tower | -12m CD | 27/12/93 | 31/08/94 | $BAE_7$ |
| | | | | | | 08/10/92 | 11/11/93 | |
| Barrow-in-Furness | 321,521 | 459,278 | recorded | pressure gauge | 8m depth | 15/12/87 | 17/11/88 | $MOD_6$ |
| Met Office | 266,613 | 513,598 | predicted | MOWM | | 23/05/91 | to date | $MO_1$ |
| | 291,856 | 485,103 | | | | 23/05/91 | to date | |
| | 317,418 | 456,752 | | | | 23/05/91 | to date | |
| Barrow-in-Furness | 301,171 | 442,973 | predicted | HIND WAVE | 8m depth | 15/12/87 | 17/11/88 | $MOD_5$ |
| Maryport | | | | JONSEY | -10m CD | 1970 | 1988 | $HR_3$ |
| Barrow-in-Furness | 10 points | | predicted | OUTRAY | -8.5m CD | 1988 | | $HR_9$ |
| Fleetwood - River Eden | 316,787 | 465,527 | predicted | REFPRO & | -2m CD | 1994 | | $HC_2$ |
| | 311,981 | 475,273 | predicted | SANDS | -2m CD | | | |
| | 305,928 | 493,819 | predicted | | -2m CD | | | |
| | 297,434 | 521,673 | predicted | | -2m CD | | | |
| | 298,887 | 532,017 | predicted | | -2m CD | | | |
| | 308,486 | 553,257 | predicted | | -2m CD | | | |

| Location | Easting | Northing | Type | Instrument / Model | Depth (m) | Period from | Period To | Organisation (see Figure 3.10) |
|---|---|---|---|---|---|---|---|---|
| Workington | | | predicted | ENDEC | +0m CD | 1991 | | $PD_4$ |
| Cumbrian Coast | whole coast | | predicted | KRKS v1 | +0m CD | 23/05/91 | 31/12/98 | Bullen Consultants |
| Barrow-in-Furness | 324,504 | 462,529 | recorded | wave rider<br>tower | -12m CD<br>+0m CD | 08/92 | 12/93 | $HC_8$ |
| Solway Firth | 283,904 | 534,491 | recorded | wave rider | | 10/10/91 | 12/10/92 | $HC_{10}$ |

**Table 3.6:** Wave Records available around the Cumbrian coastline
(Harford 1998, Ramsey and Harford 1995 and Reeve and Bin 1994)

The lack of any observed and the limited amount of measured wave data available, both duration and locations, means that these data can only be used as validation for hindcast predictions. The only long term wave data set available to be analysed is therefore the Met Office data at the locations indicated.

The suitability and accuracy of these data sets is therefore examined below.

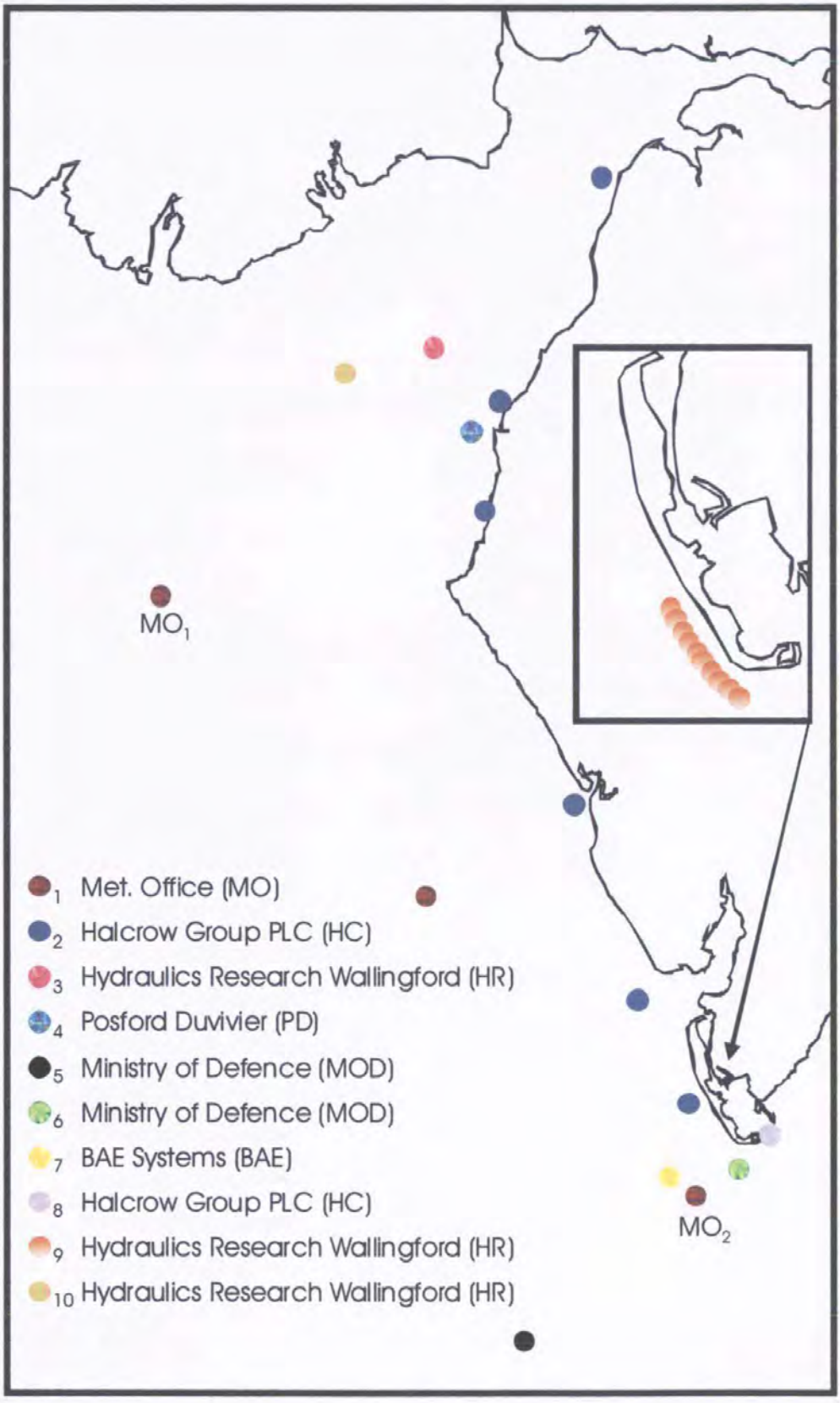


**Figure 3.10** : Measured and hindcast wave data for the Cumbrian Coastline

### 3.3.2 Met Office Wave Model

The Met Office provides the sole source of operational wave data forecasts around the whole of the coast of England and Wales. These forecasts are run twice daily with the results archived to form a unique long-term data set.

The Met Office operational wave model is a second-generation depth-dependent model based on the wave model first developed and described by Golding (1983). A full description of this model was given in Met Office (1995).

The model covers the European continental shelf from 30.5°N to 66.75°N at a resolution of 0.4° longitude by 0.25° latitude, and includes the effects of shallow water on the waves, but not wave-current interaction. Outputs from this model are at 3 hourly intervals, and consist of both locally generated waves and swell. The wave period quoted is the zero crossing period.

Wind data used in the Met Office models are provided as hourly and six-hourly values from a numerical weather prediction model (Met Office 1995).

The wave direction is calculated as the mean direction of the waves at the frequency with the most energy.

### 3.3.3 Validation of Met Office Wave Model

Verification of the Met Office Wave model is carried out against observations from moored buoys and weather ships. For the European model, wave heights are typically 0.1m lower than observations, and periods 0.2s lower (Met Office 1995). There are no verification points within the vicinity of the Irish Sea and no validation of the wave model in the region of the Irish Sea has been carried out by the Met Office.

The accuracy of the Met Office wave model was validated against actual wave measurements at or near to three model grid points used for operational wave forecasts by Reeve and Bin (1994). This study also

validated a wave transformation model for determining inshore wave spectra.

The three model points used in the validation exercise are given in Table 3.7 below. The first of these (Morecambe Bay) corresponds to the second Met Office prediction point used in this study ($MO_2$).

| Location | Offshore | | | | Inshore | | Duration |
|---|---|---|---|---|---|---|---|
| | Model Point | | Recorded Point | | Recorded Point | | |
| | Easting | Northing | Easting | Northing | Easting | Northing | |
| Morecambe Bay | 317,418 | 456,752 | 317,448 | 458,440 | 324,504 | 462,529 | 08/92→12/93 |
| Lyme Bay | 339,014 | 67,109 | 339,014 | 67,109 | 399,215 | 85,935 | 08/92→04/94 |
| Boygrift | 555,191 | 402,943 | 558,327 | 402,119 | 554,791 | 380,107 | 08/92→06/93 |

**Table 3.7:** Location of model and recorded data used in validation exercise

From the validation carried out by Reeve and Bin (1994), the main conclusions drawn from the study, with particular emphasis on $MO_2$, are given below.

1. The Met Office forecasts on average give conservative estimates of the measured wave heights (usually within 0.3m) and periods, especially during storm events. This appears to be the case for the Morecambe Bay predictions.

2. The Morecambe Bay recorder is situated near the crest of a submarine shoal and is in the shallowest water of the 3 sites. Modulation of the inshore wave height at the frequency of the tidal oscillation is pronounced in the time series data. The omission of surge and wave set-up from the sea levels for wave transformation modelling may thus be expected to have the largest relative effect at this, or similar sites.

3. With regard to the results at Morecambe Bay in particular and for shallow water sites in general it should be noted that non-linear wave processes may be expected to be significant. This includes processes such as

wave-wave interaction, partial breaking and dissipation through bottom interaction.

4. Mean directional differences are low (<10°) for direction sectors travelling towards the shore.

5. At the three study sites considered, the Met Office wave model provides a reasonable estimate of the measured wave climate, forecasting wave heights best, followed by wave period and then direction with mean differences of approximately 0.5m, 1s and 30° respectively.

### 3.3.4 Wave Data Used in Study

Based on the comments given above, it appears that the Met Office wave model gives robust and accurate values of wave conditions at the prediction points. There appears to be some contradiction on the accuracy of the predictions, although the wave height accuracy of 0.5m quoted by Reeve and Bin (1994) appears to be appropriate for this study. This is generally taken to be an over-estimate. Some concern should be expressed at the high directional variability quoted by Reeve and Bin (1994), although for Morecambe Bay this appears to be mainly as a result of waves approaching the site 'not' from the predominant wave direction sector (210-270°).

Based on the data available, and the comments given above, data were therefore obtained at two locations for this study. These locations were 54.5°N 4.06°W ($MO_1$) and 54.0°N 3.26°W ($MO_2$) which are shown on Figure 3.10. Significant benefit was not expected to be achieved from obtaining data from the remaining Met Office location shown on Figure 3.10. Despite the increased confidence that data from this point would have had on predictions, they were not obtained for the reasons given in Section 6.3.

### 3.3.5 Pre-processing of Wave Data and Compilation of Processed Time Series

The data provided by the Met Office are based on model predictions calibrated with measured offshore data. No pre-processing of these predictions is therefore necessary or practically possible.

The values from the model are valid at the time stated. To determine values of the wave parameters between time steps, it is considered adequate to assume a linear interpolation for the wave height, steepness and direction between the time steps, Holt (1999). This also applies to short regions of missing data. For longer periods, interpolation cannot be considered reliable, and the values were discarded (see Table 3.9 below).

The data supplied were a time series at a three hour resolution, the smallest available. The information supplied for each time step is outlined in Table 3.8 below.

| Parameter | Units |
|---|---|
| Wind Speed | knots |
| Wind Direction | ° |
| Resultant Significant Wave Height | m |
| Resultant Zero Crossing Wave Period | s |
| Resultant Wave Direction | ° |
| Wind Significant Wave Height | m |
| Wind Zero Crossing Wave Period | s |
| Wind Wave Direction | ° |
| Swell Significant Wave Height | m |
| Swell Zero Crossing Wave Period | s |
| Swell Wave Direction | ° |

**Table 3.8 :** Met Office wave parameters.

It should be noted that the Met Office wave model is based on a coarse grid which does not include the Isle of Man. Wave heights in the shadow of the

Isle of Man will therefore be overestimated. This is discussed in more detail in Section 6.3.

Regions where model data were unavailable, and therefore the joint probability relationship could not be carried out are given in Table 3.9 below.

| Missing Wave Records | Sea Levels Affected |
|---|---|
| 17/07/92 3:00 to 18/07/92 0:00 | 17/07/92 PM |
| 13/01/94 3:00 to 14/01/94 12:00 | 13/01/92 PM |
| 21/11/97 3:00 to 25/11/97 0:00 | 21/01/97 PM to 24/01/97 PM |
| 04/10/98 3:00 to 05/10/98 12:00 | 04/10/98 AM to 04/10/98 PM |
| 18/03/02 3:00 to 21/03/02 0:00 | 18/03/02 PM to 20/03/02 PM |
| 19/05/03 3:00 to 22/05/03 0:00 | 19/05/03 PM to 21/05/03 PM |
| 03/11/03 3:00 to 22/12/03 0:00 | 03/11/03 PM to 21/12/03AM |

**Table 3.9 :** Missing Met Office data

### 3.3.6 Trends in Wave Heights

Little research has been carried out into the determination of past trends in waves heights and (or) wave and wind directions. Research that has been carried out appears to be based on secular trends, and unlike sea levels (see Section 3.2.5), it is unlikely that any firm conclusions can be made relating to global changes in wave heights with time. Research has proved to be inconclusive, and decadal variability is high. This can be partially confirmed by comments by the Chairman of the ICE Coastal Engineering Advisory Panel, Professor William Alsop at a half day meeting on 28/03/01 at the Institute of Civil Engineers (ICE) on Long Term Wave Recording. He stated that measurements taken at Seven Stones Light Vessel over the period 1960 to 1986 had shown an annual increase in wave height of 0.12m. This would have been referring to results published by Carter and Draper (1988), although the stated increase was 0.034m. However, it is not believed that this point was clarified by stating that since this date, from about the 1990s onwards, wave heights at this location have levelled off

probably as a result of the North Atlantic Oscillation as indicated for example in Alexandersson et al (2000).

Although this comment may be considered political, in terms of a desire to promote a long term wave recording network for the UK (since put in place), it does indicate the general lack of positive conclusions that can be drawn on any past trends in wave heights and directions. As far as the governmental position on past trends in wave heights, Hulme and Jenkins (1998) stated that past gale activity, and therefore extreme wave heights for the UK year on year is highly variable, showing decadal variability and no noticeable long term trend.

With no conclusive evidence on any long term, let alone recent trends in wave heights globally or within the North Atlantic or Irish Sea, it was not considered practical or correct to attempt any detrending of the Met Office data sets to ensure stationarity. Wave heights are therefore assumed to be stationary over the analysis period.

## 3.4 Currents

The only information available on currents at the start of this study was from Admiralty tidal diamonds[4]. Although currents are now routinely modelled by POL, this model has only been in operation since 2003. Currents have not been included in this study (for reasons discussed in 4.5.2), and are therefore not included here.

## 3.5 Bathymetry

Records of bathymetry for this study have been obtained in three different formats. These are Ordnance Survey Strategi Tiles, localised surveys carried out mainly for consultancy studies and Admiralty Charts. Ordnance Survey Strategi Tiles have mainly been used to define the coastline (which is taken to be at MHWS), islands and local sand banks. Digitisation is typically 100-200m. Localised surveys give great detail for the region of

[4] Marks on Admiralty Charts used to indicate direction and speed of tidal streams.

interest, and are typically digitised to tens of metres. Admiralty Charts provide the main set of spatial data to define the bathymetric model. Digitisation is very broad, and can be anything from 50-1000m.

For the surveys obtained for this study, the survey that was deemed the most reliable was used where surveys overlapped. To limit sudden sharp gradients in the bathymetry due to either different survey dates (and subsequent movement of bed material) or more likely errors in the grid coordinates of the survey, a region was applied in which no bathymetric data was recorded.

### 3.5.1 Bathymetric Data Available for Study

The full list of bathymetric data available for the model grids used in this study (see Section 3.5.2) is given in Table 3.10 below. This includes the number of data points used in the bathymetric modelling. This also includes one survey (Chart E4993) where no bathymetric data was eventually used as more reliable overlapping data was available from other surveys. Detailed survey information in the region of the Scottish coastline outside of the Solway Firth and around the Isle of Man were not initially sought (see Sections 3.5.2 and 6.4) as these will have insignificant effect on model predictions along the Cumbrian coastline.

All surveys that had been carried out in the region of the model grids were checked. National grid co-ordinates of localised surveys were checked against known features where grid co-ordinates were available (e.g. local buildings or port structures). Localised surveys supplied to an arbitrary local grid were transformed to national grid co-ordinates.

Where survey information was deemed inaccurate, the survey information was not used. Two surveys identified, but not obtained for this study (together with the reasons), are outlined in Table 3.11. It is believed that as of 2004, these 2 tables contain a list of all significant surveys carried out along the Cumbrian coastline in recent years. The location and extent of surveys used in this study are also shown on Figure 3.11.

| Survey | Scale | Year | Levels | Data Points |
|---|---|---|---|---|
| Admiralty Chart 1346 | 1:100,000 | 1989 | Manually extracted soundings[1] | 1018 |
| Admiralty Chart 1346 (Solway Firth) | 1:100,000 | 1989 | Estimated from bathymetry levels[1] | 9 |
| Allonby Bay Survey | N/A | 1998 | GPS survey for Cumbria County Council | 3811 |
| Admiralty Chart 1346 (Ravenglass Estuary) | 1:15,000 | 1989 | Manually extracted soundings[1] | 46 |
| Admiralty Chart 1320 | 1:100,000 | 1992 2002 | Manually extracted soundings[1] | 1472 |
| Admiralty Chart 1826 | 1:200,000 | 2002 | Manually extracted soundings[1] | 163 |
| Admiralty Chart 2013 (Silloth Harbour) | 1:10,000 | 1987 | Manually extracted soundings[1] | 124 |
| Admiralty Chart 2013 (Port of Workington) | 1:7,500 | 1987 | Manually extracted soundings[1] | 89 |
| Admiralty Chart 2013 (Whitehaven Harbour) | 1:10,000 | 1987 | Manually extracted soundings[1] | 45 |
| Admiralty Chart 2013 (Harrington Harbour) | 1:10,000 | 1987 | Manually extracted soundings[1] | 27 |
| Admiralty Chart 2013 (Maryport Harbour) | 1:10,000 | 1987 | Manually extracted soundings[1] | 30 |
| Chart E4993 (Workington Bank to Silloth Channel) | 1:75,000 | 1937 | Manually extracted soundings[1] (not used) | 0 |
| Duddon Estuary Tidal Barrage Preliminary Feasibility Study | 1:75,000 | 1994 | Estuary bathymetry estimated from Land Survey (1992)[1] | 58 |
| Admiralty Chart 1961 | 1:75,000 | 1979 | Manually extracted soundings[1] | 25 |
| Walney Island Survey | N/A | 1995 | Reproduced from Ordnance Survey Map for Barrow Borough Council[2] | 7014 |
| Ordnance Survey Strategi Tile SDNW | N/A | 1997 | Margins, Islands and Coastline | 1602 (Margins) |
| Ordnance Survey Strategi Tile NXSE | N/A | 1997 | Margins, Islands and Coastline | 4156 (Coastline) |
| Ordnance Survey Strategi Tile NYSW | N/A | 1997 | Margins, Islands and Coastline | 381 (Islands) |
| Ordnance Survey Strategi Tile NXNE | N/A | 1998 | Margins, Islands and Coastline | |
| Ordnance Survey Strategi Tile NYNW | N/A | 1997 | Margins, Islands and Coastline | |
| Ravenglass Estuary Survey | N/A | 1994 | Survey for National Rivers Authority | 1248 |
| Selker Bay Survey | N/A | 1993 | Survey for Copeland Borough Council | 2051 |
| Chapelcross Survey | N/A | 1991 | Survey for BNFL | 40063 |

[1] Converted to National Grid Reference (NGR) by a transverse mercator projection based on software written by A.J. Morton, Imperial College, London.

[2] Orientation of Island deemed to be suspect, therefore only soundings and low tide information used.

**Table 3.10 :** Survey information used in bathymetry.

| Survey | Details |
|---|---|
| Eamse Bay Survey (1993) | Survey for Barrow Borough Council. No details available to tie in Survey. |
| Silloth Harbour (date unknown) | Survey carried out by James Banks Surveys Ltd for Posford Duvivier. Survey not pursued as details would have been replicated by Chapelcross Survey. |

**Table 3.11** : Survey information identified but not used in bathymetry

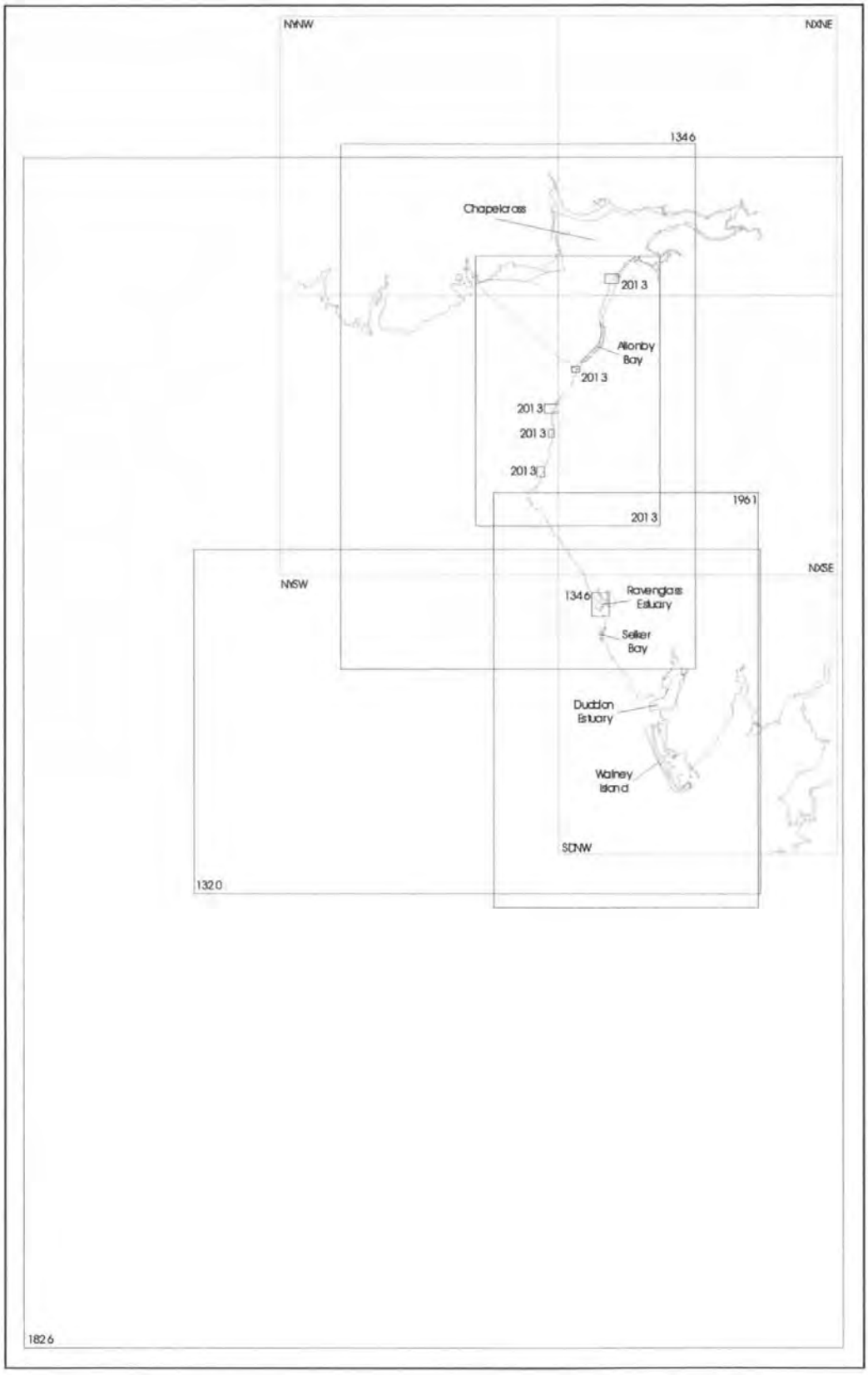


**Figure 3.11** : Surveys used to determine bathymetry along Cumbrian coastline.

### 3.5.2 Determination of Bathymetry Model Grids for Cumbrian Coastline

To determine the seabed bathymetry for the model grids, all available sources of bathymetry were identified. Since 1998, when the initial bathymetric model was set up, it is not believed that any significant surveys have been carried out on the Cumbrian coastline. The Admiralty Charts have all been updated since this date, but these updates have not been included in the model grids. The exception to this is for regions around the Isle of Man, and south of Walney Island where extensions to the model grids required additional peripheral survey information.

The model grids have been set to Ordnance Datum to ensure a horizontal water surface across all grids. Varying rates of isostatic rebound around the Irish Sea have been ignored as logistically they cannot be included. Being the order of a few millimetres, compared to the survey accuracy outlined below, they would not noticeably affect the results.

The accuracy of the data in the bathymetric models is very much dependent on the source and its interpretation. The likely levels of accuracy of the data acquired both in the horizontal and vertical alignment is indicated in Table 3.12 below. For manually recorded data, this is the perceived accuracy for this study. Levels of accuracy of Ordnance Survey and localised surveys are based on discussions with Brian Whiting and Richard Latham (Principal / Senior Lecturer in Surveying, University of East London) and Robert Lloyd (Chief Hydrographer, Mersey Docks and Harbours).

| Survey Type | Scale | Accuracy | | | |
|---|---|---|---|---|---|
| | | Horizontal | | Vertical | |
| | | Maximum | Typical | Range | Typical |
| Admiralty Chart | 1:200,000 | 200-1000m | 50-250m | 0.5-2.0m | 0.2-0.6m |
| | 1:100,000 | 100-500m | 50-250m | 0.3-1.0m | 0.2-0.6m |
| | 1:75,000 | 75-175m | 40-95m | 0.2-0.5m | 0.2-0.3m |
| | 1:15,000 | 15-45m | 7-25m | 0.1-0.2m | 0.05-0.15m |
| | 1:10,000 | 10-25m | 5-10m | 0.10-0.15m | 0.05-0.12m |
| | 1:7,500 | 7-25m | 4-8m | 0.10-0.15m | 0.05-0.10m |
| GPS survey | N/A | 30mm | 10-20mm | 0-100mm | 50mm |
| Ordnance Survey Maps | N/A | 30m | 10m | 0-5m | 2m |
| Surveys levelled to local Bench Marks | N/A | 1m | 0.0-0.5m | 0-20mm | 10mm |

**Table 3.12 :** Accuracy of bathymetric survey information

To set up the model grids, triangulation was used with grid nodes linearly interpolated over the plane of the triangle that each grid point was contained within. This was deemed to be the most appropriate gridding method considering the large number of points to be interpolated. The method of triangulation used was the optimal Delaunay Triangulation, details of which are given in, for example, Lee and Schachter (1980). The model grid size chosen was 40m*40m (see Section 4.5.1).

Six model grids were set up to cover the study area, at 30° separation. Wave predictions were carried out at up to ±15° of the grid direction. No predictions were carried out within 15° of the boundaries to eliminate edge effects (see Section 4.5.1).

Wave predictions were made at regular 400m intervals from Walney Island in the south to Silloth in the North (see Figure 1.2). Predictions were made at 5 levels (-2, -1, 0, +1 and +2m@OD) so as to investigate the effect of the joint probability relationship with depth.

The model grids used, and the reasons for their choice and limitations are given below. These grids are described in order of their perceived importance to the joint probability results. Wave heights travelling from

345° to 165° were taken to have minimal effect on the joint probability relationship, and the wave heights at these points were taken to be zero.

**240 Bathymetric Model Grid (see Figure 3.12c)**

This is the main grid used in this study, as it is anticipated to predict the most significant wave conditions to define the joint probability relationship. The offshore boundary has been set where possible to coincide with the 30m depth contour.

There are no anticipated limitations to this model grid.

**210 Bathymetric Model Grid (see Figure 3.12b)**

A number of model conditions from this grid would be expected to define the joint probability relationship. The offshore boundary has been set along the most consistent deep water boundary of 20m.

The left hand boundary of this grid coincides with the Isle of Man (i.e. land). However, resultant inshore predictions will be within the 15° edge effects, and this is therefore not anticipated to be a problem. The right hand boundary is in relatively shallow water. However in this region, the 210° model grid is less likely to influence the joint probability relationship as the North Welsh coastline acts as a barrier to significant wave activity from the Atlantic Ocean, and most significant wave activity will be modelled by the 240° model grid.

**270 Bathymetric Model Grid (see Figure 3.12d)**

The offshore boundary is set at what is considered the most consistent deep water boundary of typical depths of 20-30m.

The top boundary edge of this grid is on land. Waves approaching the coastline from 255-270° will not be expected to be affected by this boundary. Waves approaching from 270-285° will, as a result of this land,

be diffracted into the Solway Firth, and little wave activity would be expected from this region. However, predictions around Allonby Bay are likely to be overestimated, although not significant in a joint probability assessment.

This grid is expected to define some of the joint probability relationship around the region of Walney Island, where there are anticipated to be no model limitations to this model.

**180 Bathymetric Model Grid (see Figure 3.12a)**

This is a minor grid, as the results are not expected to noticeably affect the joint probability relationship. The offshore boundary has been set in the region of 5km offshore of Walney Island.

There are no anticipated limitations to this model grid.

**300 Bathymetric Model Grid (see Figure 3.12e)**

This is a minor grid, as the results are not expected to noticeably affect the joint probability relationship. The offshore boundary has been set in what is considered the most consistent deep water boundary between Scotland and the Isle of Man.

The top boundary edge of this grid is on land. Waves approaching the coastline from this region will, as a result of this land, be diffracted into the Solway Firth, and no wave activity would be expected from this region. However, predictions from around Allonby Bay to Workington are likely to be overestimated, although not significant in a joint probability assessment.

The bottom boundary is on land. This will probably affect results up to about Tarn Point (see Figure 1.1) for waves approaching the coastline from 300-315°. However, waves from these directions will be insignificant in relation to the joint probability relationship. Swell waves for this grid would also be intercepted by the Isle of Man. Setting the bottom boundary on

land therefore eliminates swell waves from this location, limiting effects to diffracted swell waves around the North of the Isle of Man.

**330 Bathymetric Model Grid (see Figure 3.12f)**

This is a minor grid, as the results are not expected to affect the joint probability relationship. Predictions above St. Bees Head are likely to be overestimated and erratic, especially in the region of the Solway Firth.

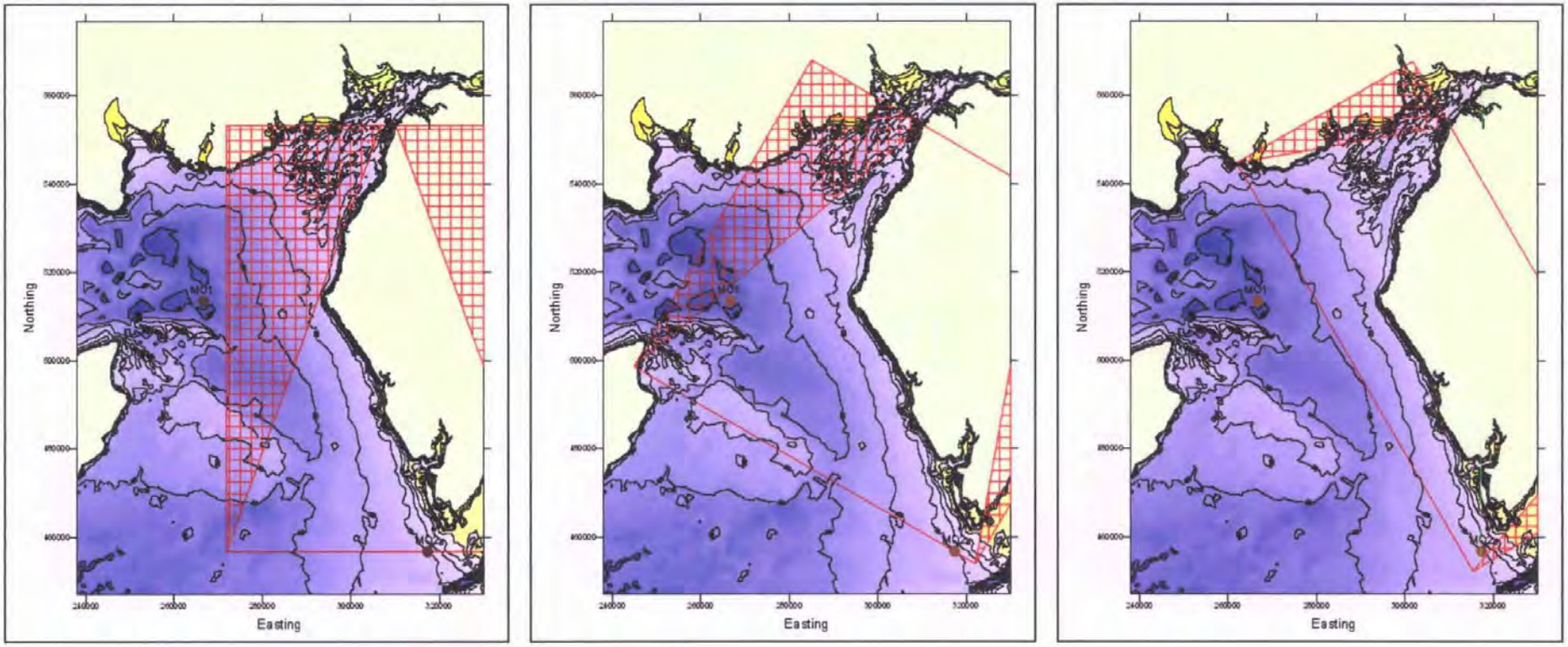


a) 180° grid

b) 210° grid

c) 240° grid

**Figure 3.12** : Bathymetric model grids for Cumbrian coastline
(more detailed bathymetric detail is given on Figure 1.1)

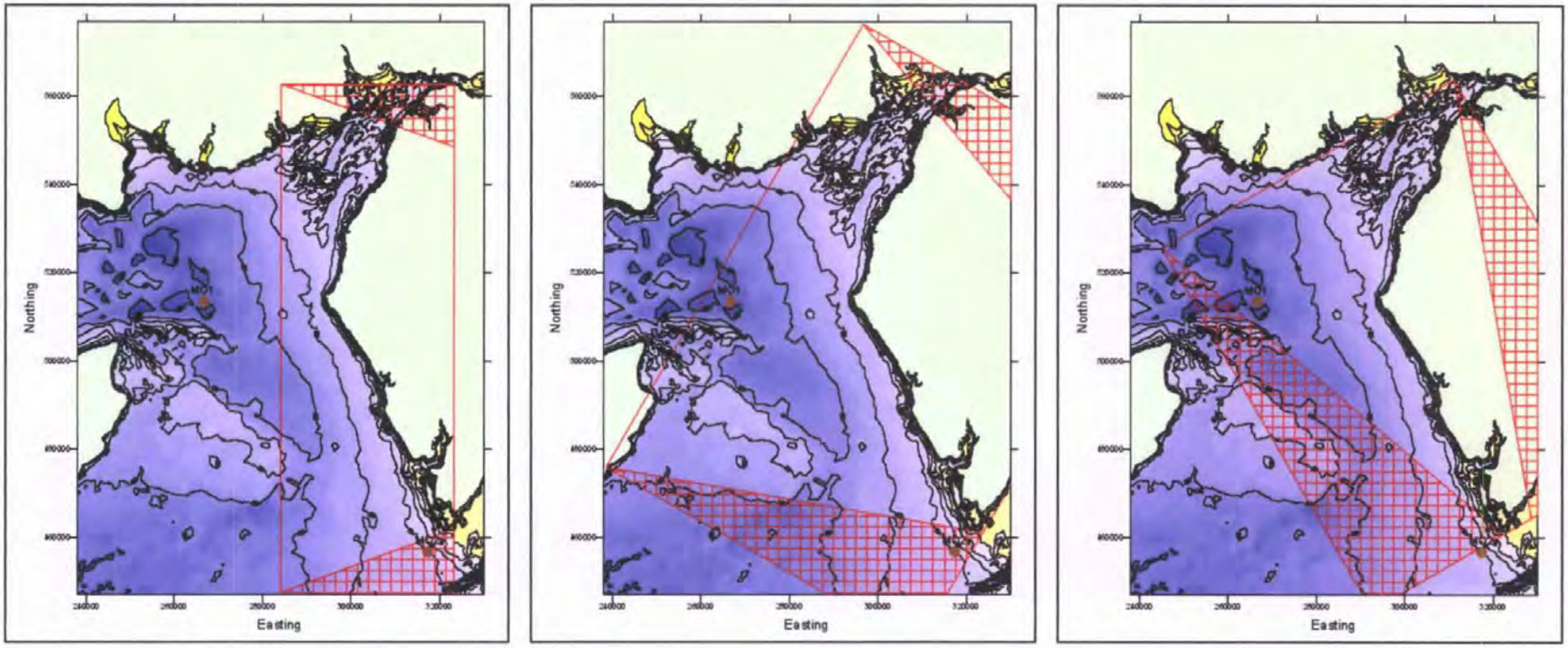


d) 270° grid

e) 300° grid

f) 330° grid

**Figure 3.12** : Bathymetric model grids for Cumbrian coastline

(more detailed bathymetric detail is given on Figure 1.1)

# 4 Numerical Transformation of Offshore Waves

## 4.1 Introduction

To determine the long term wave height distributions along the Cumbrian coastline, the offshore wave data needed to be transformed inshore using an appropriate WTM. This section therefore considers the choice of the most suitable WTM based on the specific nature of the study area and the model computational requirements and availability. For the WTM used, model restrictions and sensitivity of predictions have been investigated, and from the conclusions drawn, specifications of the model runs have been defined. This includes the bathymetric model grids, which specify the bathymetric of the study area and the model prediction points (see Section 3.5.2).

## 4.2 Wave Transformation Models Considered for Study

The choice of the most suitable WTM for use in this study was considered based on the three types of wave models most generally used in coastal engineering research and studies. All of these models, which are outlined below, can be implemented in monochromatic or spectral form.

### 4.2.1 Ray Models

These are the earliest types of wave models, and use the theory of refraction of light to trace wave rays from deep water offshore regions to shallow water nearshore regions. Wave rays in the absence of currents indicate the direction of propagation of wave crests, and wave energy is conserved between all pairs of rays. Wave ray models can be run in either forward or back tracking mode. Individual frequency components are combined to determine nearshore wave heights as demonstrated for example by Abernethy and Gilbert (1975).

Although wave ray models can be considered accurate in regions where refraction and shoaling dominate, they do not model diffraction.

### 4.2.2 Mild Slope Equation Models

The mild slope equation was introduced by Berkhoff (1972). This equation enabled the solution of a two-dimensional differential equation to take into account the combined effects of refraction and diffraction as well as shoaling and reflection. Mild slope models are considered to be relatively accurate, although computationally are very demanding.

Due to the complexity, and computer time and memory constraints in solving the mild slope equation, several variations to the solution of this model have been proposed, details of which are given in for example Reeve et al (2004).

### 4.2.3 Non-Linear Models

Non-linear models were models introduced to account for non-linear processes such as wave breaking or wave-wave interaction not accounted for explicitly in models based on the mild slope equation (see for example Dingemans 1997). The most popular type of non-linear models are Boussinesq like models, which are based on the solution of the Boussinesq type equations (Peregrine 1967).

Similar to mild slope models, they are considered to be relatively accurate and the most computationally demanding of the three types of models outlined. They cannot be applied in regions having both shallow and deepwater conditions (Schröter et al 1995).

## 4.3 Wave Transformation Models

Based on the choice of WTMs outlined above, the most suitable WTM model for use in this study was deemed to be one based on a mild slope model. Shallow water effects within the Solway Firth appeared to rule out

the use of ray type models, although their simple nature could be considered reliable below St. Bees Head for the most extreme conditions where wave fronts would approach the coastline across near parallel seabed bathymetry. The transformation of waves from deepwater to shallow water regions appeared to rule out the use of Boussinesq models, although the model grids would probably be too computationally demanding for this type of model.

However, the choice of a suitable WTM also had to be considered in relation to the model grids and the number of different wave conditions to be modelled. Model grids ranged from 4500-9500km$^2$ at a resolution of 40m*40m (see Figure 3.12 and Section 4.5.1). The number of wave conditions required was not known before the model was specified, however, with ultimately over 100,000 model runs required, computational speed was clearly an important consideration in terms of the choice of the most suitable WTM.

A further consideration in the choice of WTM was availability and (or) cost. Many commercial and academic WTMs are developed internally, and are not meant for external use. If available, these are often expensive, and suitable documentation may not be available, or is possibly inadequate. Also as internal software, these may not have been subject to external review (and hence validation and verification) and restrictions on publication of their use and suitability may have been imposed.

Ultimately, the choice of a suitable WTM was based on available models that had been independently reviewed, and were generally accepted within the coastal engineering community. With no funding available to purchase any WTMs, two models were initially considered, as well as a model developed by the author. These consisted of a ray model (KrKs), a non linear model (SWAN), and a form of the mild slope model (REFDIF). The option of using two models in combination, for example a mild slope model on a large grid feeding into a finer grid Boussinesq type model nearshore was not considered. This was considered computationally impractical considering the large area to be modelled, and the spatial variation of the nearshore region.

### 4.3.1 KrKs

KrKs is a forward tracking WTM developed by the author whilst an employee of Bullen Consultants Ltd in Birkenhead, which was re-validated for this study. It enables refraction and shoaling coefficients to be determined at specified locations along a coastline based on both a time and spatial variation in wave and sea level parameters. Wave breaking and wave growth, assuming a smooth sandy bottom, are included in the model, but not diffraction, reflection or wave-current interaction. Like all forward tracking WTMs, KrKs suffers from the formation of caustics. This leads to unreliability of results near these regions, and reduced accuracy past these regions.

The governing assumptions on which KrKs is based are:

1. Wave heights, wavelengths and periods are based on linear wave theory. Waves are assumed to be sinusoidal of small steepness and have an amplitude small in comparison with the local water depth.

2. Snell's Law is assumed throughout, which is exact for zero wave heights and flat sea-beds.

3. Waves are assumed to propagate inshore with a constant wave period and are monochromatic and of small amplitude.

4. The direction of the wave orthogonals is perpendicular to the wave crests.

5. The model assumes that the variations in the bottom occur over distances that are long in comparison to the wavelength (less than about 1 in 10).

6. Wave energy is confined between the orthogonals.

7. Wave reflection and diffraction are assumed to be negligible.

### 4.3.2 SWAN

SWAN is a third generation spectral WTM developed by Delft University of Technology. The model is based on the spectral wave action balance equation. The model takes into account shoaling, refraction, reflection, wave growth, energy dissipation (due to white capping, wave breaking and bottom friction) and wave-current interaction, but neither diffraction nor wave induced currents, (Holthuijsen et al 2004). Different spectral conditions can be defined at different points along the open boundary, as well as wind, water levels and currents over the model domain (Kelley et al 1999). It is anticipated that considerably more memory would be required to run SWAN than REFDIF, and this was confirmed by Kelley et al (1999). There are no limits on the wave propagation direction. The version of SWAN considered for this study was V40.3, the latest as of August 2004, and probably in use since at the earliest March 2001.

The governing assumptions on which SWAN is based are:

1. The model assumes that the variations in the bottom occur over distances that are long in comparison to the wavelength (less than about 1 in 10).

2. The model only considers linear wave refraction.

3. Diffraction is negligible.

SWAN can be slow in computation; however grid sizes can be large with little loss of accuracy (Maa et al 2004). These, combined with the restriction on grid sizes placed on REFDIF (see Section 4.3.3), can, regardless of the comments given above, make SWAN faster and less computationally demanding than REFDIF.

### 4.3.3 REFDIF

REFDIF is a WTM that is a parabolic approximation of the mild slope wave equation (Berkhoff 1972) originally developed by Kirby and Dalrmyple of the

University of Delaware from 1982. It determines the forward scattered wave heights and directions on a regular grid of slowly varying depths and currents taking into account shoaling, refraction, energy dissipation (due to surface friction and bottom friction, turbulence and porosity), wave-current interactions, wave breaking and diffraction. However, REFDIF cannot consider reflection, wave growth, white capping and wave-wave interaction. The main advantages of REFDIF over elliptic mild slope models are that it does not require boundary conditions at the down-wave end of the grid and because of the parabolic approximation, efficient solution techniques can be carried out in finite difference form (Kirby and Dalrymple 1994). Two versions of REFDIF were considered for this study, the monochromatic version (REFDIF/M V2.5), and the random wave version (REFDIF/S V1.2). These were the latest versions of these models as of August 2004. They have probably been in use since at the earliest April 1995.

The governing assumptions on which REFDIF is based are:

1. The model is based on a Stokes expansion of the water wave problem and includes the third order correction to the wave phase speed.

2. The model is restricted to cases where the wave propagation direction is within ±60° of the grid direction (for REFDIF/M) and ±45° of the grid direction (for REFDIF/S) for the minimax coefficients used.

3. The model assumes that the variations in the bottom occur over distances that are long in comparison to the wavelength. Based on work by Booij (1983), mild slope models are accurate up to 1:3, and for steeper slopes, wave heights and reflection coefficients are still predicted accurately.

4. Diffraction effects are only considered perpendicular to the prescribed principal direction.

5. As the model is based on a Stokes perturbation expansion, it is strictly restricted to cases where Stokes waves are valid.

REFDIF/M is stated as requiring the grid size to be less than $^1/_7$ of the wavelength (the shortest wavelength for REFDIF/S) to have reasonable accuracy on wave phase, from which wave direction is determined (Maa et al 2004). This coincides with conclusions reached by Martin et al (1987) (see also Section 4.5.1). This can obviously create a model slow in computation, although in general REFDIF is considered to have excellent computing efficiency (Kirby and Dalrymple 1994). However, it should be noted that REFDIF is stated as being implemented to have a maximum grid size of $^1/_5$ of the wavelength (Kirby and Dalrymple 1994), although it is actually implemented to have a maximum grid size of between $^2/_5$ and $^1/_5$ of the wavelength. It is not known whether the $^2/_5$ or $^1/_5$ ratio is correct, and attempts to confirm the correct value have been unsuccessful. REFDIF is also memory efficient since values only need to be retained along the current columns being considered as the solution moves forward.

It should be noted that although REFDIF/M and REFDIF/S are two separate programs, running REFDIF/M for each individual frequency component and combining the results, simulates the results from REFDIF/S. Depth limited effects are checked when combining the individual frequency components (see Section 4.6.1).

## 4.4 Verification of Models

REFDIF and SWAN are probably the most widely used and accepted WTMs by the Coastal Engineering Community. The main reasons for this are probably because they are both supplied freely on a General Public License, although their use would not be widespread if they were considered unreliable. This also means that they are also probably the most widely verified models. KrKs has never been released on a public license, and has had little commercial use. The only verification checks carried out on KrKs were for internal Bullen Consultants quality procedures, and those contained in this study (see Appendix B).

A brief literature review of comparisons between wave predictions using both REFDIF and SWAN is given below. It should be noted that all

reviewed versions of SWAN do not contain wave reflection, which is now included in SWAN.

### 4.4.1 Literature review of Comparison of REFDIF and SWAN

Andrew (1999) carried out a bibliographic review of WTMs including SWAN (version not stated) and REFDIF/S (version 1.1). Comparisons against simulated results and recorded (SWAN) and model (REFDIF/S) data were reviewed, but no direct comparisons between the two models were made. Both models were stated as simulating wave heights well. However, poor agreement was observed between recorded and simulated wave periods for the SWAN model, and wave heights were stated as being under-recorded by REFDIF/S nearshore due to the model not simulating wave set-up. Both SWAN and REFDIF/S were recommended for complex models, with REFDIF/S being recommended in situations where waves were no longer growing.

Kelley et al (1999) compared three WTMs, REFDIF/S (v1.2), SWAN (v30.74) and STWAVE (v2) to assess the impact of potential borrow sites on the wave climate at the coastline, and the resultant transport of sediment along the coast. The only wave process considered in this report was wave breaking. Simulations were compared for three different test cases where either laboratory or field measurements were available. These were waves breaking on a simple planar beach, wave refraction about a simple elliptical shoal and wave refraction along a prototype coastline. For waves breaking on a planar beach, both SWAN and REFDIF/S simulated wave breaking conditions more accurately than STWAVE, especially close to the coastline. Differences between predictions from SWAN and REFDIF/S were minor, with SWAN possibly having marginally better estimates. For wave refraction about the elliptical shoal, both STWAVE and REFDIF/S showed, as expected, symmetry about the centreline of the model domain, whereas SWAN showed asymmetry. For the two transects considered, agreement to laboratory data was poor with again more consistency between results from SWAN and REFDIF/S. However the laboratory results presented appear to be very erratic, and it is considered doubtful whether these can be considered

reliable. Behind the shoal, the inclusion of diffraction in REFDIF/S appears to provide more reliable estimates of wave heights, although no data is presented to confirm this. The final test case involved one test run on a 1:100 scale model test of wave conditions along the Ponce de Leon Inlet located on the east coast of Florida. Generally the results from the STWAVE and SWAN models were similar, with results from REFDIF/S slightly lower. Specific comparison of results at 30 locations indicated that REFDIF/S produced more reliable results nearshore where diffraction would be more significant, and STWAVE produced more reliable results offshore. Generally, REFDIF/S appeared to be the most reliable, and SWAN the least reliable. However, all three wave models could be considered to produce accurate estimates of wave heights compared to the recorded data. In conclusion, the model chosen to simulate wave breaking was STWAVE. This choice appears to be mainly driven by the author's employers (Applied Coastal Research) future commitment to STWAVE rather than the results of comparisons carried out.

Chawla and Baptista (2004) considered the wave–current interaction processes using SWAN and REFDIF/S (versions not stated) around the mouth of the Columbia River Estuary in Oregon. This is to develop accurate wave predictions for the region. Two test cases were considered, one with no current, and one with an opposing current. The results indicated that away from the estuary mouth, predictions using both models were very similar, although noticeable edge effects were noted using the SWAN model. However, large differences were observed at the mouth of the estuary, and particularly within the estuary itself where diffraction effects would become significant. In this region, predictions using SWAN were greater. No other test cases were considered, and no comparisons with recorded data were made. No conclusions were made on the accuracy of either model in comparison to the other, although it was stated that simulations needed to be compared against field data. Although field data is available from 1997-1999, this has not as yet been compared with simulated results, and it is not in the regions where the major differences between SWAN and REFDIF/S occurred (Chawla 2004).

Further comparisons between SWAN and REFDIF were carried out at Sandbridge Virginia by the Virginia Institute of Marine Sciences (VIMS). However, details or results of these comparisons are not available (Boon, Kim and Maa 2004).

## 4.5 Choice of Suitable Wave Transformation Model

Based on the properties of the wave transformation models considered, and the literature review carried out, it was initially decided to adopt REFDIF as the most suitable WTM to model inshore wave conditions along the Cumbrian coastline. From the literature review, little difference appeared to exist between REFDIF and SWAN except where diffraction became significant, which, for accuracy reasons, was the main advantage for choosing REFDIF over SWAN. The main advantage that SWAN was considered to have in comparison to REFDIF was its ability to consider further wave growth past the offshore boundary. However, the largest waves from the predominant south-west wave direction would generally be considered to be fully or almost fully developed by the time they reached the offshore boundary, and further wave growth is considered limited. KrKs was not considered further as test runs on the model indicated significant problems with caustics, especially in the region of the Solway Firth where water depths are in the region of 4-8m at high tide conditions.

From a practical viewpoint, REFDIF is a relatively simple model to run. Unlike SWAN, boundary conditions do not need to be specified down wave, and customisation of the program for the specific requirements for this study was fairly straightforward. With the size of the model required to model the Cumbrian coastline, memory requirements and speed are also a major consideration, and REFDIF is considered to be less memory intensive and probably quicker than SWAN. However, this was not tested.

For the Cumbrian coastline, each frequency component was run independently using REFDIF/M. This enabled individual frequency components to be shared between multiple model conditions therefore significantly reducing total run time.

### 4.5.1 Limitations of REFDIF

Before setting up REFDIF for model runs, checks were performed on the model to investigate any limitations, and to check those stated. These tests were mainly carried out on a constant depth model of many grid points for different wave heights and periods and propagation angles to the grid direction. All tests were carried out with no currents (see Section 4.5.2). Where problems were observed with REFDIF, these were not investigated further as the reasons for any problems were not of interest, only potential model restrictions.

All tests were carried out using the heuristic relationship developed by Hedges (1976) and the reflective boundary condition (see below). It should be noted that the parabolic nature of REFDIF means that waves are predicted on the current column as the solution marches forward. This means that current predictions are independent of predictions on any future column.

REFDIF was also tested for sensitivity of input parameters by Martin et al (1987). A series of 36 tests were carried out which evaluated the sensitivity to (amongst others) bottom friction, grid spacing, wave approach angle, wave periods, directional spreading, current and wave period. However, no or little comment on the effect of some of these parameters was given (such as bottom friction and wave approach angle). The objectives of these tests were to identify the relative importance of the various parameters and to give guidance on the most suitable choice of factors such as grid spacing. Based on the limitations detected, and those found by Martin et al (1987), model restrictions on multiple runs of REFDIF are outlined.

**Detected Limitations from Study**

From the analyses carried out, it was clear that calculations could become unstable for two conditions. The criteria for instability were mainly independent of the propagation angle, but the scale was generally more pronounced the greater the angle. Where the propagation angle was the same as the grid direction, noticeable instability of the model did not appear

to occur. The wave height appeared to have little or no effect on the reliability of the results.

The first criterion was water depth. At small water depths, the model would tend to become unstable as the model marched forward. This instability was sudden, and occurred sooner the smaller the water depth. This is demonstrated in Figure 4.1 which shows a wave of height 0.64m, period 4s and propagation angle 20° moving across a grid of constant depth. From this figure it can be clearly seen that for smaller water depths, the model has a tendency to suddenly become unstable sooner. Edge effects are also noticed at all points as the model marches forward, but generally these are restricted to no more than about 10°.

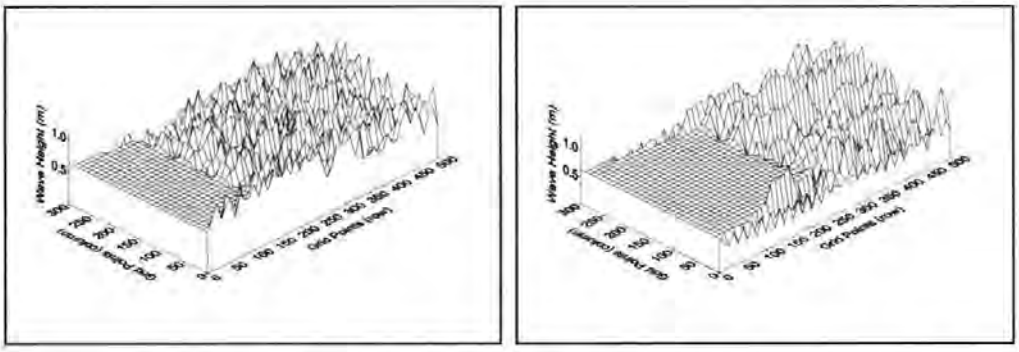

a) water depth = 2m (grid size 30m) b) water depth = 3m (grid size 30m)

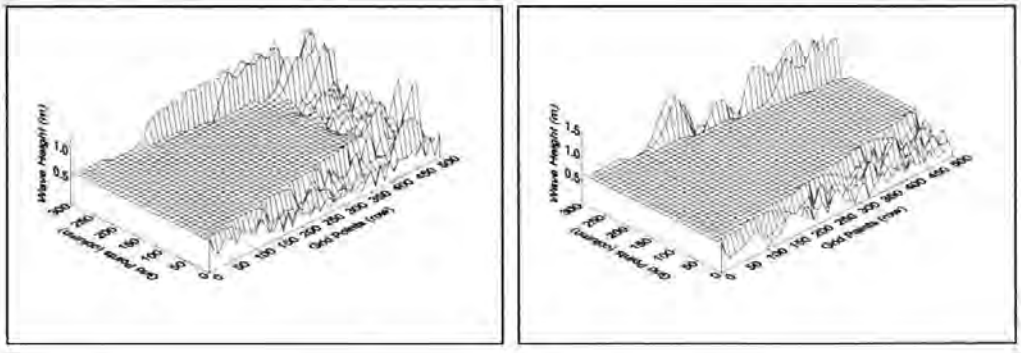

c) water depth = 4m (grid size 30m) d) water depth = 5m (grid size 30m)

**Figure 4.1** : Effect of small water depths on unreliability of REFDIF model (wave height 0.64m wave period 4s, propagation angle 20°)

The second criterion was edge effects. As the grid / wavelength ratio (*G/L*) was decreased, these became more noticeable. Unlike the previous condition, the instability was gradual, becoming more noticeable closer to

the model edges. This is demonstrated in Figure 4.2, which shows the same wave from the previous condition, but this time in deep water, moving across two different model grids of two different *G/L* ratios. From this figure it can be clearly seen that as the *G/L* ratio is decreased, edge effects become more noticeable. Also the 'wider' the model, the less these edge effects affect predictions in the middle of the model grid.

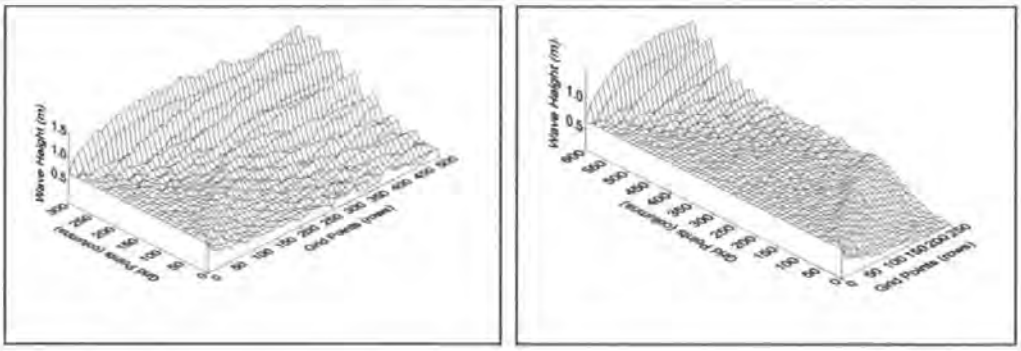

a) *G/L* = 0.04 (grid size 1m) water depth 50m

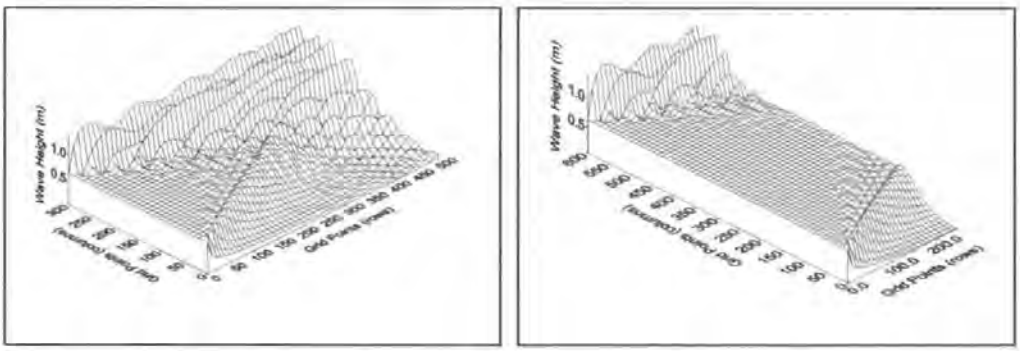

b) *G/L* = 0.20 (grid size 5m) water depth 50m

**Figure 4.2** : Effect of *G/L* ratio on edge effects in REFDIF model (wave height 0.64m wave period 4s, propagation angle 20°)

**Imposed Model Restrictions for Study**

To reduce, or eliminate the effect of these limitations, the following conditions were therefore imposed on multiple model runs of REFDIF. Any runs which exceeded these conditions were, where considered necessary, visually checked for reliability, and runs were further visually checked for

the largest deviations of the wave heights from the average within ±20° of the edges (see point 3 below).

1. REFDIF not to be run where depths anywhere in the model are less than 4m.

   For this study, models are to be run at high sea level conditions, and predictions are to be made between seabed levels of -2m@OD to +2mOD. The lowest high sea levels are at least 1.5m@OD, 3.5m above the lowest prediction point. Prior to reaching the prediction points, water depths may be less than 4m. However, these regions are generally limited to edge effects (see Figure 3.12). With more than 99% of sea levels at least 4.0m above the lowest prediction point, limitations due to limited depths at the lowest prediction point will not be noticeable. For the higher prediction points, depths less than 4m will only occur for the last few grid points and any instability would become evident in the results where they would be investigated. Based on the comments given above, this condition was not considered to be compromised (see also Section 4.5.5).

2. The *G/L* ratio not to be less than 0.2 for all model runs.

   For the two Met Office data sets used in this study, the maximum zero crossing period for wind waves is just under 10s, with 4 runs having a zero crossing period greater than 9s. Setting a grid size of 40m*40m, and running the wave conditions for 13 frequency components (see Section 4.6.1), would mean that only about 5 of the model run conditions would not meet this condition for the lowest frequency component. However, according to Martin et al (1987), they propose that this ratio should not be less than 0.14 (as does Maa 2004). However, they state that a larger grid spacing only has the effect of smoothing the bathymetry excessively. Considering the bathymetry used in this study, the vast majority of spatial bathymetry has come from Admiralty Charts of scale 1:100,000 and above (see Figure 3.11). The perceived accuracy of these data in the horizontal alignment is no greater than 100m (see Table 3.12), therefore a

40m*40m grid size should accurately reflect bathymetric conditions within the limitations of the input survey information. Nearshore, where localised surveys are estimated as having horizontal accuracies of between 30mm-30m (see Section 3.5.2), excessive smoothing of the bathymetry could be considered a problem. However, this is only likely to affect the last 50-100m at most, and is therefore not likely to significantly affect results.

3. To reduce / eliminate edge effects, model predictions not to be made within 20° of the end grid rows.

   Generally edge effects were found to be limited to not more than about 10° regardless of the wave propagation angle. With the maximum wave propagation angle within 15° of the grid rows, this limitation gave confidence that model predictions were unaffected by any potential edge effects.

**Stated Limitations**

The stated limitations of the REFDIF model are given below. Comments are made on these limitations, and how they have been dealt with in subsequent model runs of REFDIF.

4. The use of the parabolic approximation restricts the model to cases where the wave propagation direction is within ±60°.

   Although the model is stated as being accurate to ±60°, the model can also give reasonable results up to ±70° using different coefficients for the minimax approximation (Kirby 1986a). No noticeable loss of accuracy was observed running the model at wide angles, and a ±15° limitation on wave propagation direction was imposed (see point 3 above) and the original minimax approximations maintained. This is within the limitations suggested by Martin et al (1987) who state that consistent results are achieved for wave propagation angles up to ±30°. Based on model tests against the 'ideal' sea state for the Haringvliet Field Case

(Dingemans 1983), smaller minimax approximations are also preferred as these gave 'less noisy' results. However, these do refer to a previous version of REFDIF, and different minimax approximations.

5. The model is based on a Stokes perturbation expansion, and is therefore strictly restricted to cases where Stokes waves are valid.

   For the largest waves approaching the Cumbrian coastline, it is likely that the Stokes solution is not valid and the heuristic dispersion relationship developed by Hedges (1976) is more appropriate. Test runs on REFDIF indicated that model results vary little if the Hedges relationship is used where the Stokes solution is valid; whereas predictions using the Stokes solution can become erratic if anywhere on the model grid the Ursell parameter exceeds 40. The linear model, used for deep water conditions, was found to not be appropriate in test runs and was not considered an appropriate solution for the Cumbrian coastline. The Hedges solution has therefore been imposed on all REFDIF runs.

6. The lateral boundary conditions in REFDIF can be set either to be totally reflecting or partially transmitting (Kirby 1986b).

   Generally in REFDIF the totally reflecting condition is used. In test runs on REFDIF, little if any difference was generally noted whether the total or partial reflecting condition was used, and any reflection was limited to edge effects (see point 3 above). However for the partial transmitting condition, occasional results for the model grid became erratic. This was noted for example when running validation Test Case C (see Appendix B). The totally reflecting condition was therefore imposed on all REFDIF runs. Edge effects are within the limitations covered by point 3 above.

### 4.5.2 Currents

REFDIF can be run with and without current information included. Current information is read in by REFDIF for the same grid as the depths in Cartesian form, therefore increasing the information stored at each grid point by a factor of 3.

Little information on 'detailed' currents within the Irish Sea was available at the start of this study. Although POL now routinely model currents within the Irish Sea, this model has only been in operation since 2003. Currents within the Irish Sea were therefore considered based on surface current information from Admiralty tidal diamonds published on Admiralty Charts (see Table 3.10), details of which are shown on Figure 4.3 below.

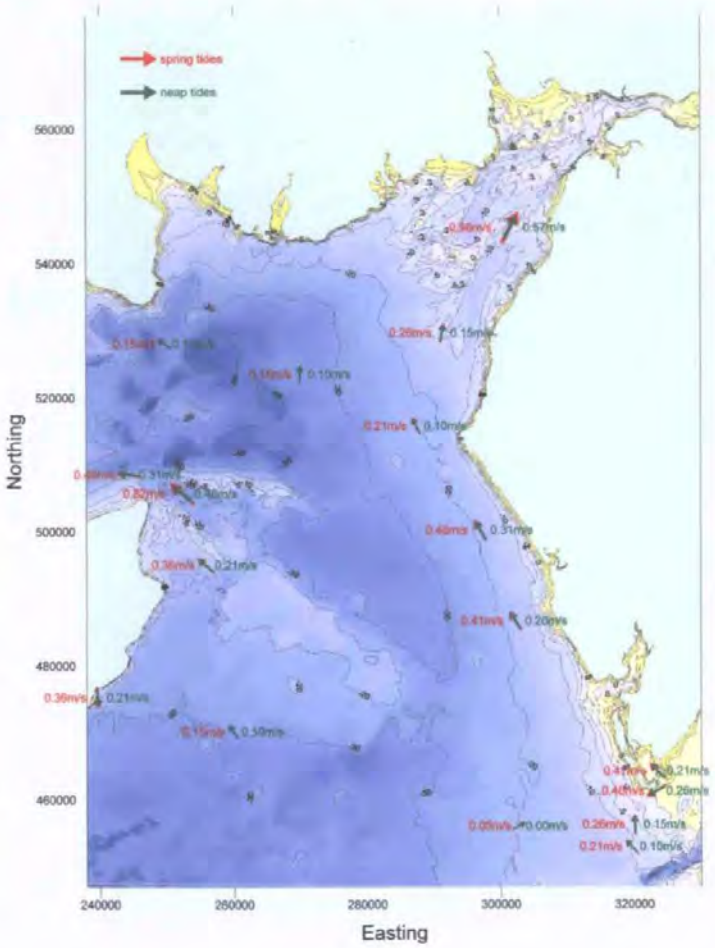


**Figure 4.3** : Surface currents at high tide within the East Irish Sea (information taken from Admiralty tidal diamonds on Admiralty Charts)

These currents are relative to high tide at Liverpool, which is approximately within ±20 minutes of high tide for all locations along the Cumbrian coastline. No correction was considered or applied for depth.

Further to the current information given by the Admiralty tidal diamonds, Figure 4.4 shows average spring tide surface currents predicted from the POL Irish Sea model at a resolution of 0.2m/s. This information was received too late to be considered for this study, but has been used to compare the original conclusions drawn about offshore surface currents.

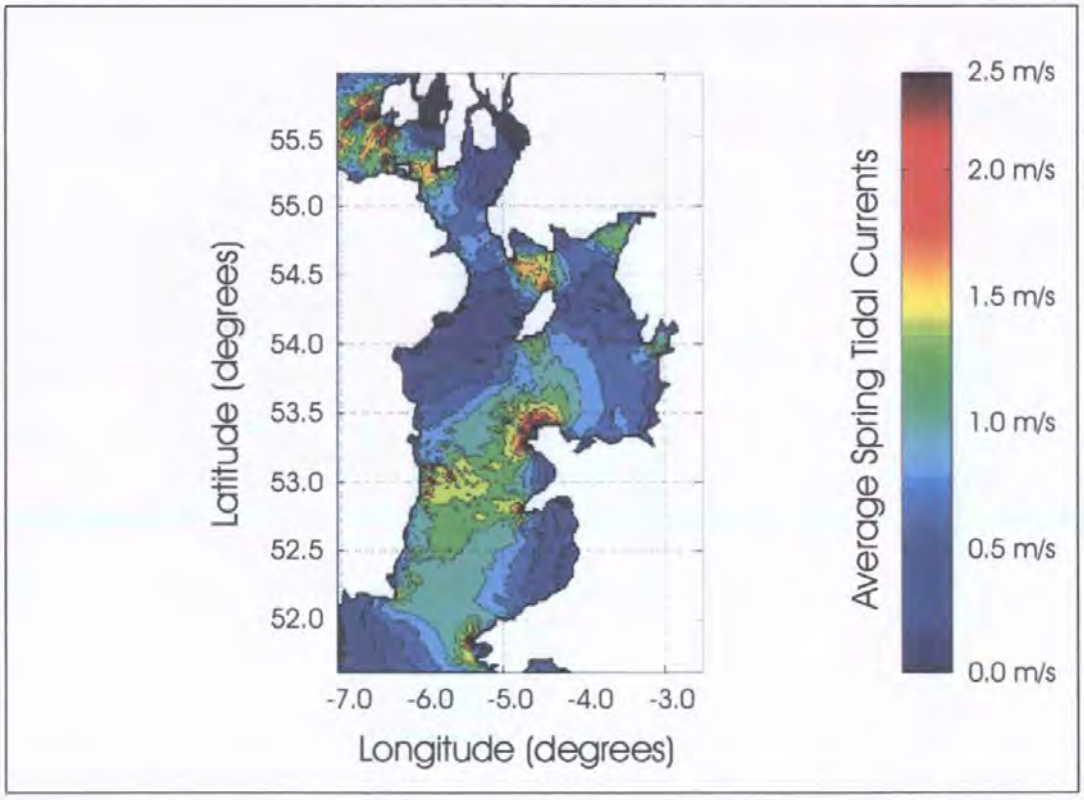


**Figure 4.4** : Average spring tide surface currents predicted from Irish Sea Model resolution 0.2m/s, 1.8km grid (results courtesy John Howarth, POL)

From Figure 4.3 it can be seen that at high tides, currents appear to travel parallel to the Cumbrian coastline in a clockwise direction, changing to an anti-clockwise direction as you travel further offshore towards the Isle of Man. Currents vary in speed from about 0.2-0.5m/s below St. Bees Head, to about 0.2-1.0m/s above St. Bees Head. This appears to be confirmed by reference to Figure 4.4, which show currents of a similar magnitude. However, the currents given in Figure 4.4 are 'average' spring tide surface

currents, which would be expected to be 2-3 times greater than surface currents at high tide.

To investigate the effects of currents on wave heights along the Cumbria coastline, several runs were carried out in spectral mode using 10 frequency components for different wave conditions and tide levels. The differences tended to follow a leptokurtic distribution with a kurtosis greater than 10 for even the largest currents (greater than 1m/s). This indicated that most of the time little variation was observed between predicted wave heights whether currents were included or not

From this analysis, considering currents using the Admiralty tidal diamonds, differences in predictions were generally estimated to be less than 5%, except for regions within the Solway Firth where the larger currents meant that differences could generally be up to approximately 9%. However, under extreme conditions, which are of main interest in this study, wave heights would be expected to approach the Cumbrian coastline approximately perpendicular to the current direction (particularly below St. Bees Head). This would be expected to have insignificant effects on wave heights, and therefore actual differences would be expected to be noticeably less than the approximations given above.

Furthermore, considering surface currents from the Irish Sea model, currents appear to be less than ½ the magnitude of those indicated by the Admiralty tidal diamonds. This appears to confirm original suspicions over the accuracy of the Admiralty current information, and the decision taken not to include current information in model predictions. With little information available to model currents, considering all the information given above, their inclusion could well have resulted in less accurate model predictions.

Although this decision may be incorrect, this decision does concur with conclusions reached by Martin et al (1987). Based on tests on a shoal and hollow bathymetry (similar to Test Case B in Appendix B, see Section 4.5.6), they indicated that for monochromatic waves of period 12s and height 3m, currents in both grid directions of up to 1.5m/s had little effect in

modifying wave conditions. This they stated was because current velocities were small relative to the wave celerity, and current shear was absent.

However, there were also other more practical reasons not to consider currents, not least the reasons outlined above. These reasons included the fact that current information would have been difficult to model practically with so little spatial information available, and the need to apply different current information for different runs. This latter point could have been mainly negated by simplified interpolation on current speed (but not direction) based on tide height and range, although the effect of the wind on induced currents could not have been modelled. However, based on model runs calibrated by measurements in the Irish Sea during the severe storm events of mid November 1977 (Jones and Davies 2003), it is anticipated that these would not be significant.

Regardless of the points given above, a further problem was encountered in modelling currents which was the occasional tendency for REFDIF to fail to run when currents were included. With a small number of runs, this problem could easily be overcome. However, with the number of runs required in this project (in excess of 100,000), this was not practical.

### 4.5.3 Energy Dissipation

Within REFDIF, energy dissipation can be applied for wave breaking or bottom or surface frictional losses. Bottom or frictional losses are specified by the user, and tests on model runs with or without these indicated little difference to the results output. This is indirectly confirmed by the Coastal Engineering Manual (2002) which states that no laboratory or field data sets clearly point to the need for including non wave breaking damping effects in model simulations. They also recommend that these damping mechanisms should not be included in model simulations. Indeed, little evidence was found in the literature of applying damping effects in REFDIF, although 1 test case was considered, although not commented on in Martin et al (1987).

In the model conditions considered in this study, it is likely that significant wind wave activity at the offshore boundary will coincide with strong onshore winds. Any non wave breaking frictional effects would be offset by growth, or re-growth caused by the wind and are therefore not included. For swell waves, these will have be generated by storms which no longer exist, and considering their long periods it was anticipated that non wave breaking frictional effects should be applied. However, as stated above, the application of frictional effects made little difference to the model simulations, and the inclusion of frictional effects in this case, although against the advice of the CEM, would have made no noticeable difference.

### 4.5.4 Sub Grids

An option to use sub grids is available within REFDIF. This is so that specified areas can be represented in greater detail. No sub-grids have been applied as no increased level of accuracy is anticipated, and condition 2 given in Section 4.5.1 would not be compromised.

### 4.5.5 General Comments

Land, surface piercing structures and natural features within REFDIF are handled by the 'thin film' technique of Dalrymple, Kirby and Mann (1984) and Kirby and Dalrymple (1986c). This procedure replaces areas above the sea levels by shoals of extremely shallow depth (1mm). The wave breaking routine reduces the wave heights over the shoal to less than ½ mm, resulting in a wave that has negligible wave energy, therefore not noticeably affecting any physical processes and maintaining water depths over the entire model grid. Although this technique will contradict the limitation placed on model runs in Section 4.5.1, this is a situation that cannot be avoided, and is a technique that is successfully employed within REFDIF.

Gravity within REFDIF has been set using the International Gravity Formula to $9.814635 m/s^2$, based on a sea level of *4m@OD* and mean latitude for Cumbria of $54.5°$.

Sea water density has been set to *1025.0kg/m$^3$*. This reflects average sea water density in the Irish Sea over the winter months when the largest wave activity would be expected.

### 4.5.6 Verification Tests on REFDIF

To verify the use of REFDIF as a suitable WTM model, it was tested against four of six benchmark tests outlined in Lawson et al (1994) and Lawson and Gunn (1996), and compared to the results of up to 17 other wave transformation models, including KrKs. Further details of these tests including the results and conclusions are given in Appendix B.

From these tests, REFDIF was seen to perform extremely well in monochromatic form when tested against the two tightly controlled numerical and physical model tests. These two test cases, a linear beach and an elliptic shoal, represent the two limits of extremes of the type of bathymetry along the Cumbrian coastline, and indicate that if input wave conditions are well defined, resultant predictions will also be well defined.

For the two cases where results are run in spectral form, the model does not perform as well. The first case, a Harbour Approach, is not of the form that exists along the Cumbrian coastline, and these results are therefore not of significant interest. For the second case (Perranporth), the poor performance of REFDIF, in common with the other WTMs, perhaps indicates model predictions are not suitably accurate. However, it could also indicate that for this case the offshore wave conditions may have been poorly defined. These test comparisons were carried out before a detailed analysis of the effect of the number of frequency components on wave transformation modelling was carried out. These indicated (see Section 4.6.1) that for the Cumbrian coastline, at least 10 frequency components were required to accurately represent the offshore spectrum, instead of the 5 used in this test case. An incorrect choice of the number of frequency components could also have been exacerbated by either an incorrect choice of the directional spreading function (wrapped normal) or, and, poor definition of the number of directional components (5). If this is the case,

then accurate definition of the offshore spectrum should result in an accurate definition of nearshore conditions, which is covered in Section 4.6.

However, considering the performance of REFDIF in monochromatic form and the nature of the bathymetry used in these test cases, it is anticipated that it is a valid model for use in transforming offshore waves nearshore for this study and was therefore adopted.

## 4.6 Definition of Offshore and Inshore Wave Conditions

Offshore waves generally contain a mixture of locally generated wind waves combined with swell waves from one or more distant storms. In a joint probability analysis, the greatest concern is in the accurate prediction of the most extreme wave heights and sea levels at the site(s) of interest. For the Cumbrian coastline, this will be as a result of wind waves generated over several hours emanating from the Atlantic Ocean and reaching the Cumbrian coastline through a narrow (maximum) 9° gap between Southern Ireland and Anglesey (see Figure 4.5). Under these conditions, swell waves are likely to approach from a similar direction, and swell waves generated from within the Irish Sea Basin would be expected to be minimal.

**Figure 4.5** : Maximum wave exposure for the Cumbrian coastline

Wind waves for the Cumbrian coastline are therefore considered to be random, with narrow directional spreading. This takes into account that the most extreme wave heights and sea levels along the Cumbrian coastline coincide with south-westerly storms. It also assumes that little diffraction takes place as the waves travel from the deep waters south of Anglesey (≈>60-80m deep), to the shallower waters (≈40-60m deep) north of Anglesey to the Met Office prediction points (≈40m and 25m depth respectively). All estimates and assumptions on wind waves in this study are based on extreme waves generated by south-westerly storms.

Similarly to the wind waves, the largest swell waves approaching the site will also come from the south-west sector. These will have been generated some distance from the British coastline, and as a result of frequency dispersion and angular spreading, would be expected to enter the east Irish Sea as a near monochromatic, uni-directional wave front. Swell waves are therefore considered to be monochromatic, with no directional variation. Swell waves generated within the Irish Sea, or just offshore of the British

coastline would, regardless of their 'spectral' shape and any directional variation, not coincide with the largest wind waves, and would therefore not noticeably affect the results of the joint probability calculations.

### 4.6.1 Wind Waves

The only known previous work on recorded wave spectra within the Irish Sea Basin was carried out by Reeve and Bin (1994). They evaluated the accuracy of Met Office wave model forecasts against wave measurements at three locations around the British Isles, including the second Met Office data point used for this study. Wave records were then transformed inshore using a back-tracking wave model and compared against nearshore wave measurements.

The spectrum used to define wave conditions was the JONSWAP spectrum (Hasselmann et al 1973), as they stated the emphasis was on storm conditions (i.e. fully developed seas) at locations which have elements of fetch limitation. The directional spreading function used was a cosine power function: the cos-2s (see Longuet-Higgins et al 1962). Waves transformed inshore were taken to follow the TMA spectrum (Bouws et al 1985), a depth dependent extension to the JONSWAP spectrum (see below).

Reeve and Bin (1994) concluded that no firm conclusions could be made between measured and predicted spectra at this location as a result of significant shallow water effects near the measuring location. This was exacerbated by the use of predicted tide levels as opposed to actual sea levels, therefore ignoring the effects of surge, which have a noticeable effect in this region.

Despite the comments given above, the use of the JONSWAP spectrum in fetch limited seas, and the TMA spectrum in fetch and depth limited seas is well established in the Coastal Engineering community. Indeed, Reeve and Bin (1994) do acknowledge from their analysis that where model assumptions are valid, inshore wave conditions are accurately represented using these techniques.

The TMA spectrum has therefore been adopted in this study, which is given in Equation 4.1. This takes into account that the offshore boundaries for the model grids used in this study are in 'non-deep' waters (see Figure 3.12).

$$S(f,\theta)_{TMA} = S(f,\theta)_{JONSWAP}\,\Phi(f) \qquad \textbf{(4.1)}$$

where:

$S(f,\theta)_{TMA}$ = TMA spectrum

$S(f,\theta)_{JONSWAP}$ = JONSWAP spectrum = $\dfrac{\beta g^2}{(2\pi)^4 f^5}\exp\left\{-\dfrac{5}{4}\left(\dfrac{f_p}{f}\right)^4\right\}\gamma^q$

$\Phi(f)$ = multiplicative depth and frequency dependent reduction factor

and:

$q$ = $\exp\left[-\dfrac{1}{2}\left(\dfrac{f-f_p}{\sigma f_p}\right)^2\right]$

$\beta$ = $0.032\left(\dfrac{f_p U_{10}}{g}\right)^{\frac{2}{3}}$

$\gamma$ = peak enhancement factor

$\sigma$ = $0.07;\ f < f_p$ = $0.09;\ f \geq f_p$

$f$ = frequency (*Hz*)

$f_p(1/T_p)$ = peak frequency (*Hz*) = $2.84 g^{0.7} F^{-0.3} U_{10}^{-0.4}$

$F$ = fetch length (m) (for fetch limited conditions)
= $0.008515 t^{1.298} g^{0.298} U_{10}^{0.702}$ (for duration limited conditions)

$U_{10}$ = wind speed (m/s) at 10.0m above *msl*

$t$ = duration limit (s)

The TMA spectrum is normalised so that the significant wave height offshore, $(H_s)_o$, is given as,

$$(H_s)_o = 4\sqrt{m_0} \qquad \textbf{(4.2)}$$

and considering the depth of water (including the sea level) at the offshore boundary, the spectral wave period ($T_p$) is set so that the zero crossing period is given as:

$$T_z = \sqrt{\frac{m_0}{m_2}} \qquad \textbf{(4.3)}$$

where,

$m_n$ is the $n$th moment of the spectrum

The peak enhancement factor, $\gamma$, typically lies between 1 and 7, but is usually taken to have a value of 3.3. This was the mean value determined for the North Sea, although this varies for different locations (and storms). No information specific to the Irish Sea (particularly for extreme storms) is available for this parameter. However, an analysis of the largest Met Office wave data indicates that a value of 3.3 is of the right order. This value has therefore been adopted, which is the same value used by Reeve and Bin (1994).

As for the directional spreading function, unlike the frequency spectrum, a standard form has not been universally agreed, and several are proposed. The most common are probably the cosine power, the wrapped normal (Borgman 1979) and the Von Mises distribution (Kobune 1986). Theoretical support for the wrapped normal has been put forward by Reeve (1992), which is also the function proposed for REFDIF/S. Krogstad et al (1998) indicate that the shape of the directional distribution is somewhere between another distribution (the Poisson) and the most common variant of the cosine power, the cos-2s. This was based on comparisons with

extensive data sets from the North and Norwegian Seas. However, considering the narrow directional spreading of the most extreme wave heights offshore of Cumbria, which are of most interest in this study (see Section 4.5), no directional spreading has been assumed for offshore conditions.

**Processing of Wind Wave Spectra**

Based on the calculated *Tp*, the input TMA spectrum was discretized into bins of constant volume between frequencies that contained 0.25% to 99% of the wave energy. This meant that computational time was not taken up determining the long tails of the frequency components, and also meant that the spectrum was well resolved near the peak of the wave spectrum.

An example of this discretization is shown below (Figure 4.6) for deep water conditions offshore of Workington at approximately midday 10/02/97. This shows the frequency spectrum divided into 5 equal energy bands, indicating good resolution near the spectral peak, with significantly less resolution away from the spectral peak.

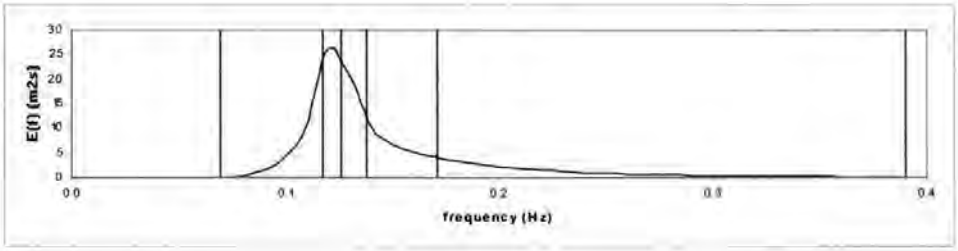


**Figure 4.6** : Typical discretization of wave spectrum using 5 frequency bins for conditions offshore Workington ≈ 12:00 10/02/97.

Based on the chosen number of frequency components (discussed later), the frequency limits of the bins were determined. This gave the offshore significant wave height for each bin as:

$$H_b = \frac{(H_s)_o}{\sqrt{2n_f}} \qquad \textbf{(4.4)}$$

where:

$H_b$ = binned wave height

$(H_s)_o$ = offshore significant wind wave height

$n_f$ = number of frequency components.

Expressing Equation 4.4 as the ratio,

$$\frac{H_b}{(H_s)_o} = \frac{1}{\sqrt{2n_f}}$$

This is shown graphically in Figure 4.7.

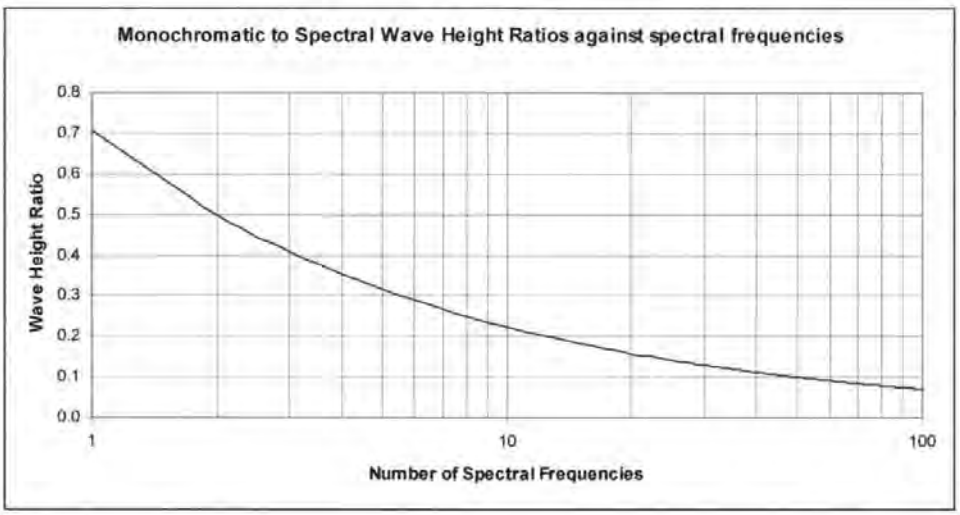


**Figure 4.7** : Monochromatic to spectral wave height ratios for different numbers of spectral frequencies.

The frequency associated with each binned wave height was the central frequency determined by moments of each bin between the individual frequency limits.

This gave the significant wave height inshore as Equation 4.5 below. The swell component has been treated as a separate energy component in this equation and combined as such.

$$(H_s)_i = \sqrt{2\sum_{j=1}^{n_f}(H_b)_{i,j}^2 + (H_{swell})_i^2} \quad \textbf{(4.5)}$$

where:

$(H_s)_i$ = inshore significant wave height

$(H_b)_i$ = inshore 'binned' wave height

$(H_{swell})_i$ = inshore swell wave height

Depth limited effects were checked using the approximation of Goda (2000), given in Equation (4.6) below:

$$(H_s)_b = \begin{cases} K_s(H_s)_o & : \ d/L_0 \geq 0.2 \\ \min\{\beta_0(H_s)_o + \beta_1 d, \ \beta_{\max}(H_s)_o, \ K_s(H_s)_o\} & : \ d/L_0 < 0.2 \end{cases} \quad \textbf{(4.6)}$$

where:

$(H_s)_b$ = limit on significant wave height breaking

$K_s$ = shoaling coefficient

$\beta_0$ = $0.028((H_s)_o/L_0)^{-0.38}\exp(20\tan^{1.5}\alpha)$

$\beta_1$ = $0.52\exp(4.2\tan\alpha)$

$\beta_{max}$ = $\max\{0.92, 0.32((H_s)_o/L_0)^{-0.29}\exp(2.4\tan\alpha)\}$

$\alpha$ = bed slope

The inshore zero crossing period is given by Equation (4.3), where the *0*th and *2*nd moments refer to the inshore wave spectrum. This assumes that the wave period squared follows a Rayleigh distribution.

**Number of frequency components**

The number of discrete frequency components required to define the TMA spectra had to be a partial compromise between the discretization of the offshore grid (see Section 4.5.1) and the accuracy of the input conditions (see below) and the time required to run the various wave models.

Wave conditions were predicted at 229 locations, for over 9000 different combinations of sea levels, wave heights, periods and directions. Running each condition separately for just 1 frequency component would have taken between approximately 3 and 30 minutes per condition, which with present computing power, would have required in the region of hundreds of years of computer time to complete. To alleviate this problem, and to cater for spectral runs, inshore wave conditions were determined for an array of sea levels, wave heights, periods and directions. For each frequency component, the array of inshore wave heights at the locations required was then interpolated to estimate the inshore wave height for the given frequency component, and these were then combined (Equation 4.5) to determine the total inshore wave height.

The array discretization was dependent on the number of frequency components required. The more frequency components, the greater the discretization and the increased accuracy for the output from the model runs. Also, the more frequency components, the increased range of wave periods required to cover the range required.

Taking all these factors into account, the effect of up to 19 different frequency components were compared for several different offshore conditions using the spectral version of REFDIF. Only the 240 bathymetric model grid was considered (see Figure 3.12). These were compared with the result using 20 frequency components, which was assumed to give the correct result.

Typical results of this analysis are shown below in Figure 4.8. These show the 'error' in the estimates in terms of frequency distributions, where the error is given as:

$$\text{Error} = \left[ \frac{(H_s)_{n_f} - (H_s)_{20}}{(H_s)_{20}} \right] 100\% \qquad \textbf{(4.7)}$$

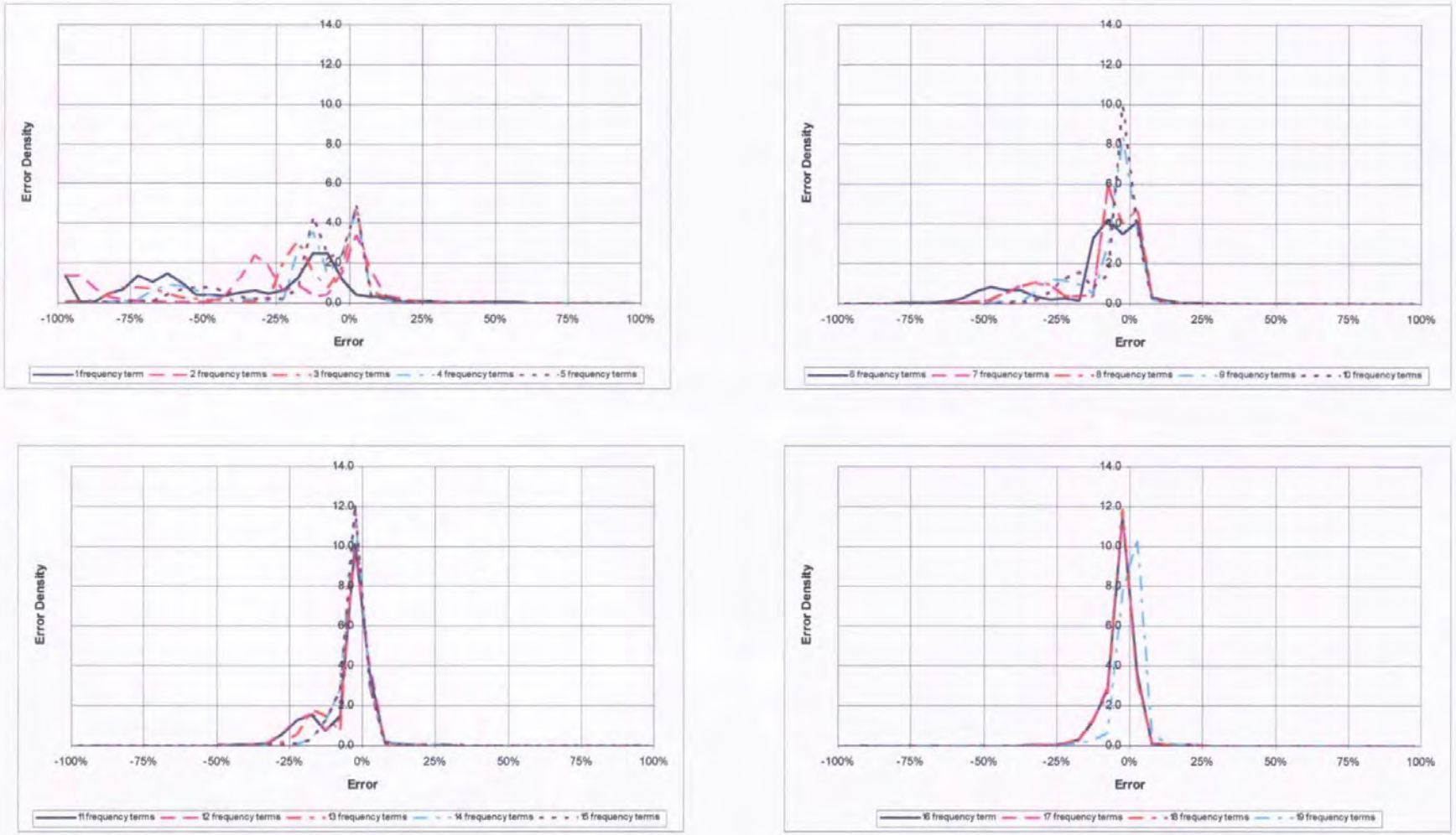


**Figure 4.8** : Error density in determination of wave heights for different number of frequency components.

These results indicate that good agreement is achieved using at least 9-10 frequency components. Less than this and the results are noticeably different. This is especially the case for the longer period events, and therefore the more significant wave heights, where wave heights were noticeably under predicted in the region of the Solway Firth. Therefore, considering the balance between increased accuracy and discretization, it was initially decided to use 10 frequency components to represent the offshore wave spectrum. However, late on in this study it was decided to adopt 13 frequency components. This was to match the number of frequency components used by the Met Office wave model to predict offshore wave heights. Although this would result in a slight decrease in accuracy in interpolating for the largest wave heights (as indicated by Figure 4.7), this would be more than offset by the increased accuracy of more frequency components. The disadvantage of using more frequency components was the greater range of periods required to simulate the tails of the frequency distribution. Wave heights less than 0.5m were modelled as a monochromatic wave, as the results would be insignificant in a joint probability assessment, and would save computational effort.

Sample model output, showing contours of wave heights are given in Appendix C. The model output concentrates on the main grids used in this study.

It should be noted that preliminary spectral runs using REFDIF were carried out using 10 frequency components, none of which were used in the final analysis. The added value of re-running these preliminary runs for 13 frequency components was considered negligible, and therefore not carried out.

**Discretization of Offshore Conditions**

As has already been stated above, to determine inshore wave conditions at each prediction point using the actual sea level and wave information would, based on current computing power, have taken in the region of hundreds of years of computer time using a high specification computer for just 1 frequency component. Using 13 frequency components for in excess

of 200 prediction points would probably have increased this time by approximately 200-1,000 times due to the disproportionate time required to run high frequency components.

Clearly therefore wave conditions had to be modelled as an array of standard wave conditions, with results interpolated between array values. The monochromatic version of REFDIF was used, as results could be superimposed, with results shared between multiple runs. Running the spectral version of REFDIF was not an option due to time constraints.

The chosen wind wave discretization is shown in Table 4.1 below:

| Parameter | Range | Stages | Comments |
|---|---|---|---|
| | | | |
| Wave Heights | 0.2m to 0.6m | 0.2m | High resolution required due to spectral representation of wave heights. |
| | 0.6m + | 0.1m | |
| | | | |
| Wave Periods | 3.0s to 7.0s | 2.0s | High resolution only required for periods corresponding to wave heights > 3.0m |
| | 7.0s + | 0.4s | |
| | | | |
| Sea Levels (@OD) | 1.2m to 5.2m | 1.0m | High resolution only required approaching extreme sea levels. |
| | 5.2m to 5.5m | 0.3m | |
| | 5.5m + | 0.1m | |
| | | | |
| Direction | -15° to +15° | 1° | |
| | | | |

**Table 4.1** : Wind wave discretization.

Considering interpolation between array values, linear wave theory would indicate that refraction is proportional to wave height, and shoaling independent of wave height. In intermediate depths, as is the predominant case in most significant model conditions, shoaling is more significant than refraction and is approximately proportional to wave period. No conclusions could be reached on sea level (as it is a proportion of depth), nor direction, so linear interpolation was deemed the most appropriate. Linear interpolation was therefore considered appropriate for interpolation

for all parameters, and the appropriateness of this was confirmed by model test runs.

Wind waves with a zero crossing period less than 3.0s were assumed to have a negligible effect on the joint probability relationship and were therefore set to zero.

### 4.6.2 Swell Waves

Swell Waves offshore the Cumbrian Coastline are assumed to be monochromatic with no directional spreading (Section 4.6).

**Discretization of Offshore Conditions**

For swell waves, a different array of values was chosen compared to wind waves. This was originally specified when wind waves were being considered as monochromatic waves. As swell waves were considered generally independent of surge, better resolution was considered necessary at higher sea levels. For wave periods, less resolution was considered at high wave periods due to the large range of wave periods to be considered. Resolution for direction was kept the same. The swell wave height resolution was kept relatively small to reflect the fact that under extreme wind wave conditions for the Cumbrian coastline, 'any' swell wave height could be present

The chosen swell wave discretization is shown in Table 4.2 below:

| Parameter | Range | Stages | Comments |
|---|---|---|---|
| | | | |
| Wave Heights | 0.4m to 0.8m | 0.4m | High resolution required to reflect fact that under extreme wind wave conditions, 'any' swell could be present. |
| | 0.8m to 1.4m | 0.2m | |
| | 1.4m + | 0.1m | |
| | | | |
| Wave Periods | 3.0s to 10.0s | 1.0s | Lower resolution at larger wave periods due to large range of periods. |
| | 10.0s + | 2.0s | |
| | | | |
| Sea Levels (@OD) | 1.4m to 4.4m | 1.0m | High resolution only required approaching extreme sea levels. |
| | 4.4m to 5.0m | 0.3m | |
| | 5.0m + | 0.1m | |
| | | | |
| Direction | -15° to +15° | 1° | |
| | | | |

**Table 4.2** : Swell wave discretization.

Interpolation between parameters (and the reasons) was the same as for wind waves (see above).

Swell waves with a period less than 3.0s[1] were ignored as their inclusion could lead to problems in the determination of the inshore wave periods.

## 4.7 Specification of Offshore Wave Conditions

Coincident offshore wave heights are available at two Met Office prediction points $MO_1$ and $MO_2$ (see Section 3.3). Offshore wave conditions at OP have been interpolated based on linear interpolation of wave height, direction and steepness as indicated in Figure 4.9. These have been transformed inshore to determine nearshore wave conditions, NP, at 5 levels (-2, -1, 0, 1 and 2m@OD). The wave direction indicated refers to the offshore wave direction interpolated from the Met Office data, and not the nearshore result. This gives unique, although similar offshore wave conditions corresponding to each inshore prediction point.

[1] Although in theory swell waves will have wave periods significantly greater than 3.0s, interpolation of the Met Office data will produce swell waves with periods less than 3.0s.

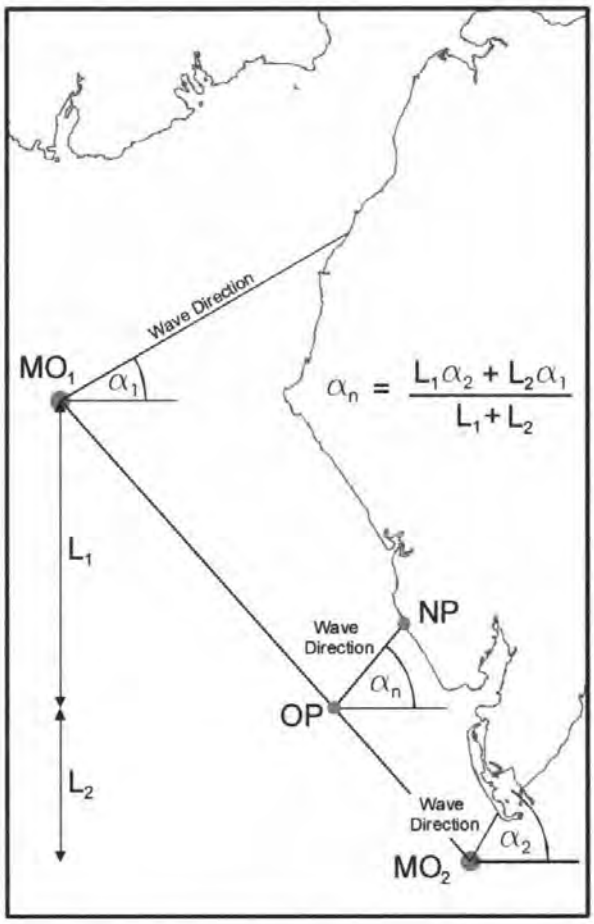


**Figure 4.9** : Specification of offshore wave conditions

# 5 Joint Probability of Waves and High Sea Levels

## 5.1 Introduction

Based on the sea level records outlined in Chapter 3 and the nearshore transformed wave heights from the WTM outlined in Chapter 4, this chapter outlines the methods used to determine the joint probability relationship between nearshore waves and high sea levels.

Although at the start of this study, no definitive technique to determine the joint probability between waves and sea levels existed, shortly after starting this study, HR Wallingford Ltd and Lancaster University published details of the JOIN-SEA approach, HR Wallingford Ltd, 2000a and 2000b[1]. JOIN-SEA, which follows established statistical techniques, is considerably more rigorous than previous methods and techniques that were being developed for this study. JOIN-SEA was therefore adopted for this study, and further work on an alternative solution was not continued.

Using the JOIN-SEA approach, marginal extremes have been specified using the GPD, with a justification for the appropriate single, or mixture of two BVNs given. Based on the analysis outlined, joint extremes are considered for return period events up to 200 years. This is the maximum return period event that is usually considered in flood and coastal defence work. However, marginal extreme sea levels are considered up to 10,000 years. This is to enable comparisons to be made with published results in this area. Marginal extreme wave heights are considered to the same return period level to maintain consistency.

From the results obtained, sample joint probability curves at two locations to the north and south of the study area are presented.

[1] Details of the JOIN-SEA approach are given in Section 2.3.5.

## 5.2 Marginal Extremes

The upper tails of the marginal extremes within JOIN-SEA are taken to follow the Generalised Pareto Distribution, which from Section 2.6.1.1 is given as:

$$F(X) = \varepsilon\left\{1-\left(1-\frac{k(X-\zeta)}{\theta}\right)^{1/k}\right\}+(1-\varepsilon) \qquad X \geq \zeta \qquad \textbf{(2.8)}$$

This formula approximates the Generalised Extreme Value (GEV) distributions for high thresholds, the proof of which is given in, for example, Coles (2001).

Setting *k=0* gives the Type I distribution, which is commonly referred to as the Gumbul distribution. This distribution is probably the most commonly used formula in the determination of extreme sea levels. The use of this distribution is mainly related to the analysis of annual maxima records, which is often the only readily available record of long term sea levels.

Setting *k* as alternately negative and positive gives the Type II and III distributions commonly referred to as the Fréchet and Weibull distributions respectively.

The Weibull distribution is widely used to determine extreme wave heights. Its suitability was confirmed based on results of a 2-year study by a working group of the International Association of Hydraulic Engineering and Research (IAHR) to achieve a better understanding of the methods used in extreme wave analysis. Based on this study, Mathiesen et al (1994) recommended the use of the 3 parameter Weibull distribution as the best method to determine wave heights. Earlier work (Van Vledder et al 1993 and Goda et al 1993) recommended that a suitable threshold should be applied, although it should be chosen with care and that the Maximum Likelihood Method, which has been used in this study, provided the best fit to the parameters.

The use of Equation 2.8 therefore gives more flexibility in the prediction of the marginal extremes. It represents the methods commonly used in threshold techniques, both for sea levels and wave heights, yet gives the added flexibility of enabling the data itself to determine the most appropriate distribution. To ensure that the asymptotic assumption for the GPD holds, threshold selection for both sea levels and wave heights were only considered above 0.80.

### 5.2.1 Extreme Sea Levels along the Cumbrian Coastline

Little work has been carried out on the analysis of extreme sea levels along the Cumbrian Coastline, and certainly no significant work over the last 8 years. Despite this, it is considered that there have been 4 significant reports on extreme sea level predictions including the Cumbrian coastline since 1990, which are described below. A summary of the published results is given in Tables 5.1-5.3.

**Site by Site Analysis for the UK (Coles and Tawn 1990)**

This paper considered an updated and corrected data set initially analysed by Graff (1981) of annual maxima sea levels recorded at 61 locations around the British coastline. Two locations were considered for the Cumbrian coastline, Barrow and Silloth.

**Site by Site Analysis for the UK (Dixon and Tawn 1995)**

This was the report on the second stage of a three stage process commissioned by MAFF (now Defra) to produce improved statistical methods for the analysis of extreme sea levels at regular intervals around the entire UK coast. It extended work from the earlier report (Dixon and Tawn 1994) to predict extreme estimates at individual locations, including Workington, which was not included in the first report.

**Spatial Analysis for the UK (Dixon and Tawn 1997)**

This was the third report of the three stage process outlined above, and built upon the two earlier processes. Although this report did not specifically give estimates of extremes at individual locations, its spatial technique meant that extremes could be determined for any location, including locations in Cumbria.

**Site by Site Analysis for the North West (Jeremy Benn Associates (JBA) 1998)**

This was a report commissioned by the Environment Agency to develop up-to-date estimates of extreme sea levels for 10 locations along the North West coastline using all available data and methods. For the Cumbrian coastline, three locations were considered, Barrow, Workington and Silloth.

The predictions for Workington were carried out using the incorrect POL readings, details of which are given in Section 3.2.4. As a result, these predictions should be approximately 0.18m higher than predicted.

**Summary of Results**

Based on the reports outlined above, Tables 5.1-5.3 below summarise the published extreme estimates of sea levels, including the range of data used. These estimates have been updated to the present (2004) based on conclusions on trends determined in Section 3.2.5. It should be noted that two figures are given for Dixon and Tawn (1997). This technique uses the 1 year return period level as the basis for predictions for higher return period levels. However, the report does state that where a better estimate of the 1 year return period level is available, this should be used. The second figure is therefore based on the 1 year return period level using the data from this study (see Table 5.4). Two figures are also given for Workington using the JBA (1998) figures. The second figure takes into account the expected 0.18m error in the estimate of extremes, as outlined above and in Section 3.2.4.

| Return Period (years) | Coles and Tawn (1990) Annual Maxima 1920 – 1978 (19 years) | Dixon and Tawn (1997) n/a | JBA (1998) Annual Maxima 1920 – 1978 (19 years) |
|---|---|---|---|
| 1 | | 5.72 (5.82) | 5.14 |
| 5 | | | 5.67 |
| 10 | 5.82 | 6.26 (6.36) | 5.81 |
| 20 | | | 5.95 |
| 25 | | 6.48 (6.58) | 6.00 |
| 50 | | | 6.16 |
| 75 | | | 6.26 |
| 100 | 6.42 | 6.62 (6.72) | 6.34 |
| 150 | | | 6.45 |
| 200 | | | 6.53 |
| 250 | | 7.07 (7.17) | |
| 500 | | 7.21 (7.31) | 6.81 |
| 1000 | 7.33 | 7.40 (7.50) | 7.05 |
| 10000 | | 8.05 (8.15) | |

**Table 5.1** : Extreme value estimates of sea levels at Barrow (m@OD)

(figures in brackets for Dixon and Tawn (1997) based on 1 year return period level used in this study)

| Return Period (years) | Dixon and Tawn (1995) Hourly 1992 – 1993 (2 years) | Dixon and Tawn (1997) n/a | JBA (1998) Annual Maxima 1992 – 1997 (6 years) |
|---|---|---|---|
| 1 | | 5.43 (5.26) | 4.23 (4.41) |
| 5 | | | 5.37 (5.55) |
| 10 | 5.69 | 5.96 (5.79) | 5.49 (5.67) |
| 20 | | | 5.58 (5.76) |
| 25 | 5.83 | 6.18 (6.01) | 5.60 (5.78) |
| 50 | 5.91 | 6.31 (6.14) | 5.68 (5.86) |
| 75 | | | 5.71 (5.89) |
| 100 | 6.02 | 6.53 (6.36) | 5.74 (5.92) |
| 150 | | | 5.77 (5.95) |
| 200 | | | 5.79 (5.97) |
| 250 | 6.13 | 6.75 (6.58) | |
| 500 | 6.18 | 6.89 (6.72) | 5.84 (6.02) |
| 1000 | 6.24 | 7.07 (6.90) | 5.88 (6.06) |
| 10000 | 6.32 | 7.69 (7.52) | |

**Table 5.2** : Extreme value estimates of sea levels at Workington (m@OD)

(figures in brackets for Dixon and Tawn (1997) based on 1 year return period level used in this study)

(figures in brackets for Benn (1998) take into account expected 0.18m error in estimates)

| Return Period (years) | Coles and Tawn (1990) Annual Maxima 1928 – 1978 (39 years) | Dixon and Tawn (1997) n/a | JBA (1998) Annual Maxima 1920 – 1978 (40 years) |
|---|---|---|---|
| 1 | | 5.61 (5.96) | 4.82 |
| 5 | | | 6.06 |
| 10 | 6.24 | 6.16 (6.51) | 6.22 |
| 20 | | | 6.35 |
| 25 | | 6.38 (6.73) | 6.39 |
| 50 | | 6.52 (6.87) | 6.51 |
| 75 | | | 6.57 |
| 100 | 6.70 | 6.74 (7.09) | 6.61 |
| 150 | | | 6.66 |
| 200 | | | 6.70 |
| 250 | | 6.97 (7.32) | |
| 500 | | 7.11 (7.46) | 6.81 |
| 1000 | 7.09 | 7.30 (7.65) | 6.88 |
| 10000 | | 7.94 (8.29) | |

**Table 5.3** : Extreme value estimates of sea levels at Silloth (m@OD)
(figures in brackets for Dixon and Tawn (1997) based on 1 year return period level used in this study)

To compare these estimates with estimates using Equation 2.8, the standardised data sets for Barrow (6100 records, 8.6 years), Workington (9519 records, 13.5 years) and Silloth (11991 records, 17.0 years) were analysed. The standardised recorded data set for Silloth was considered here, although in this study sea levels at Silloth are estimated from the sea level at Workington (Equation 3.1). It should also be noted that the full record of manually recorded high sea levels at Silloth goes back to November 1987, giving almost 17 years of recorded high sea levels.

In analysing sea level records, the most important factor to consider is the subjective choice of a threshold. This has to be chosen with care, as too high a threshold and there may be too few exceedances to accurately estimate the GPD parameters. Too low a threshold, and the asymptotic assumption for the GPD will no longer hold. The standard practice is to

adopt as low a threshold as possible (Coles 2001), therefore maximising the amount of data to be analysed, although reducing the asymptotic behaviour.

Although different thresholds could be considered for each data set, it would be considered unsafe to have different thresholds for each data set as a result of spatial interpolation of the threshold at individual joint probability locations. Therefore one common threshold selection has been considered for all data sets.

Historically three methods are usually considered in the choice of a suitable threshold, and these are outlined below.

1. Mean Residual Life Plots

   This is a measure of the mean excess of a threshold, given that the value is higher than the threshold. This is expressed (Davison and Smith 1990) as ($k>-1$):

$$E(X-u \mid X>u)=\frac{\theta-(u-(1-\varepsilon))k}{1+k} \qquad \textbf{(5.1)}$$

   where:

   $u$ is a threshold greater than $(1-\varepsilon)$.

   This equation is a linear function of $u$. Therefore, above a threshold $(1-\varepsilon)$ at which the GPD gives a valid approximation to the excess distribution, the mean residual life plot should be approximately linear.

2. Stability of Parameter Estimates Across Thresholds

   Considering the parameters across a range of thresholds for which the asymptotic assumption is valid, estimates of the shape ($k$)

parameter and scale ($\theta$) parameters should be approximately constant and linear respectively (Davison and Smith 1990).

3. Quantile / Probability Plots

   Quantile and probability plots are used for comparing the theoretical probability distributions with the actual probability distributions. This is a visual comparison, and comparing the plots in the extremes can indicate which threshold gives the best fit. In this study, the Weibull plotting position formula has been used which is the standard for probability plots.

These methods also have to be considered based on an approximate assumption of tidal similarity between the three locations where sea level records are available based on the equations given in Figures 3.7 and 3.8.

However, before considering any of the methods given above, estimates of the extremes using different thresholds from 0.80 to 0.99 at 0.01 intervals were compared. For all three locations, little variation in extreme estimates was observed for a threshold choice between 0.80 and 0.89. Considering the range of return periods given in Tables 5.1 – 5.3, the maximum differences were only 3.5cm, 2.5cm and 7.7cm for Barrow, Workington and Silloth respectively. Above a threshold of 0.89, these variations were noticeably higher and became increasingly erratic, particularly when a threshold greater than 0.96 was chosen. With in the region of 240-480 records for a threshold of 0.96 (60-120 for a threshold of 0.99), unreliability as a result of a lack of data points at high thresholds was not considered significant. Therefore with stability of extremes over a threshold range 0.80-0.89, a threshold in this region was deemed to be appropriate.

Considering the small variation in extreme predictions for the range of thresholds considered, the use of the first two methods in the choice of a suitable threshold was not considered to significantly assist the choice. This is particularly the case for mean residual life plots which are notoriously difficult to interpret (see for example Coles 2001, and Section 5.2.2). The choice of a suitable threshold therefore concentrated on the

third method, in comparison with how the extreme estimates compare with the tidal similarity equations given in Figures 3.7 and 3.8.

Figures 5.1 to 5.3 below show extreme predictions for 5 equally spaced thresholds for the three locations. From these predictions, it can be seen how similar estimates are for a choice of threshold below 0.90, and how they tend to become more variable for a threshold choice greater than 0.90.

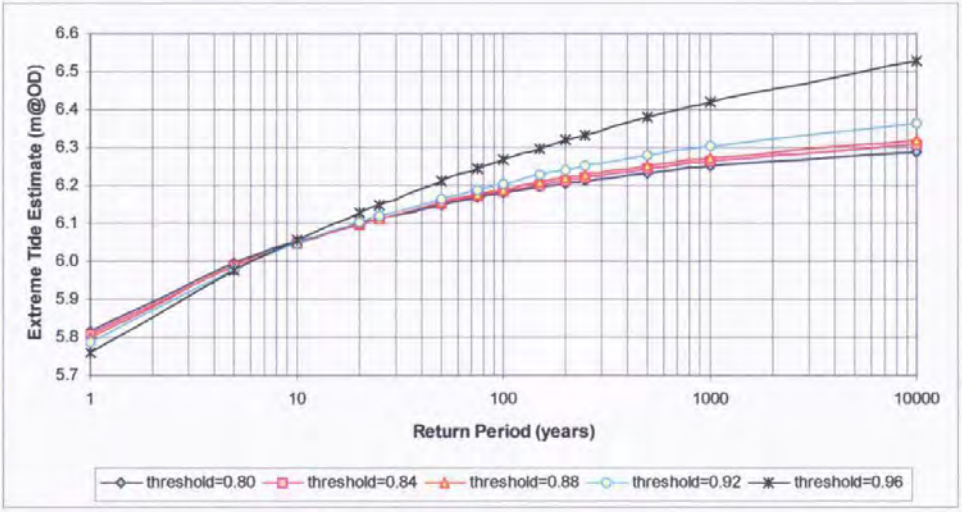


**Figure 5.1** : Extreme estimates of sea levels at Barrow for different thresholds.

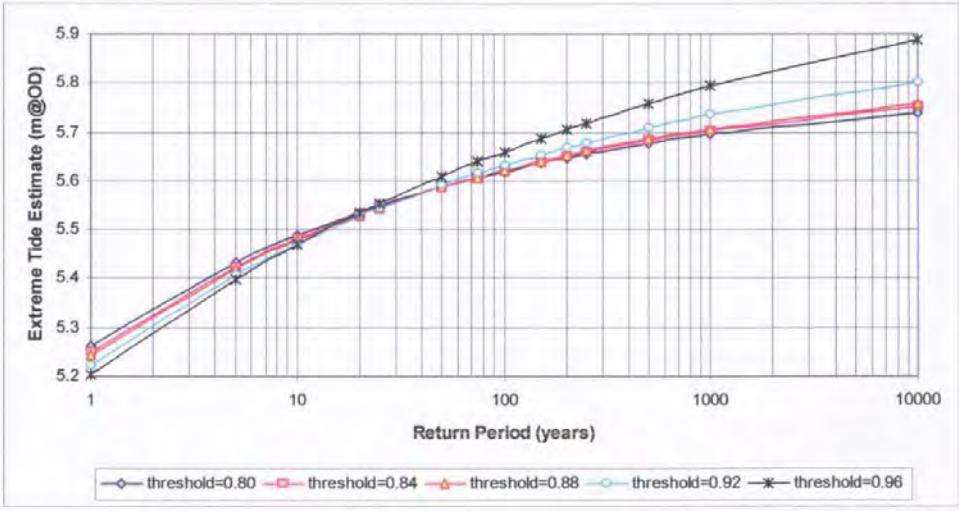


**Figure 5.2** : Extreme estimates of sea levels at Workington for different thresholds.

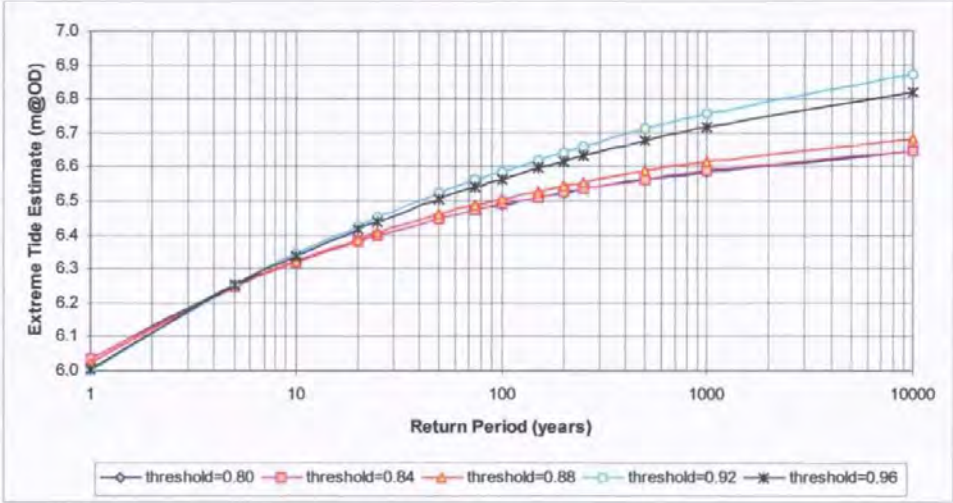


**Figure 5.3** : Extreme estimates of sea levels at Silloth for different thresholds.

Considering the agreement of the extreme predictions at Barrow and Silloth to the simulated extremes at these locations from the Workington predictions, the most suitable choice of a threshold appeared to be 0.80, particularly below return periods of 1000 years (which are of interest in this study). The 0.80 threshold also had the smallest variation in standard error estimates (and therefore confidence bands) for all considered return period events (shown on Figures 5.5 – 5.7). This produced maximum differences in predictions of less than 5cms and 13cms for Barrow and Silloth respectively.

The higher (although still small) discrepancy for Silloth was almost certainly due to the increased range of data that was analysed. The period November 1987 to April 1992 (before digital recordings were available) contains a disproportionate number of large sea levels for Silloth. This has had the effect of increasing predictions at Silloth within the range 7-9cm, reducing the maximum differences given above from less than 13cms to less than 4cms. This would indicate that the extreme predictions determined for Barrow, Workington and Silloth may be underestimated by approximately 8cm, 7cm and 9cm respectively. However, these data are the only data that were available for this study over this period, and based on the high emphasis placed in this study on quality and checking of data (see Hames et al 2004), could not be checked, and therefore not considered. Manually recorded sea level data is available for Ramsden

Dock over this period. However, awareness of its existence came too late for it to be included in this study (as outlined in Section 3.2.2).

The extreme predictions for Silloth have therefore been based on Equation 3.1, with the predictions for Barrow and Workington unchanged. Figure 5.4 shows the comparison between extremes outlined above, and Table 5.4 outlines the extreme predictions used in this study. The figures in brackets for Silloth are those given in Figure 5.4.

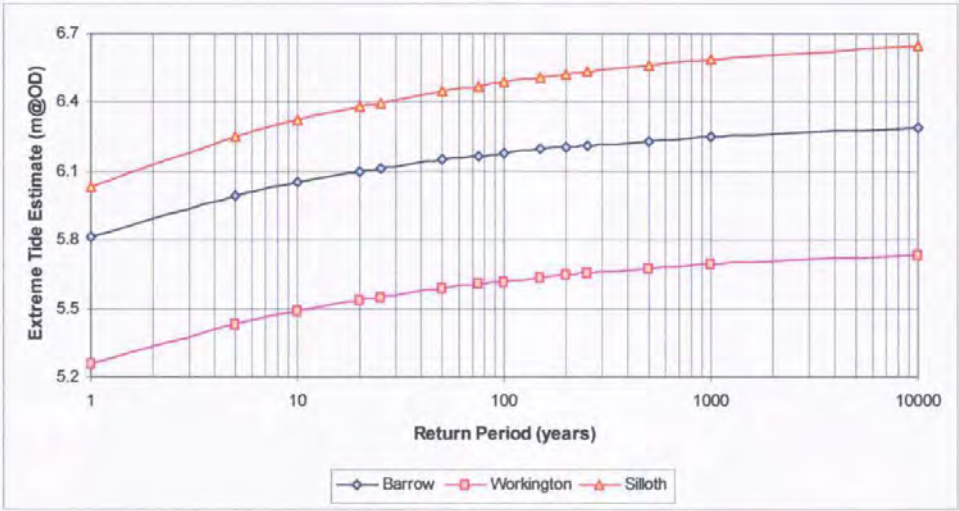


**Figure 5.4** : Extreme estimates of sea levels at Barrow, Workington and Silloth using recorded data.

| Return Period (years) | Barrow | Workington | Silloth |
|---|---|---|---|
| 1 | 5.818 | 5.261 | 5.963 (6.035) |
| 5 | 5.995 | 5.433 | 6.160 (6.250) |
| 10 | 6.051 | 5.488 | 6.224 (6.321) |
| 20 | 6.098 | 5.536 | 6.279 (6.381) |
| 25 | 6.111 | 5.549 | 6.294 (6.398) |
| 50 | 6.148 | 5.587 | 6.338 (6.447) |
| 75 | 6.167 | 5.607 | 6.360 (6.472) |
| 100 | 6.179 | 5.619 | 6.375 (6.488) |
| 150 | 6.195 | 5.636 | 6.394 (6.509) |
| 200 | 6.205 | 5.647 | 6.406 (6.523) |
| 250 | 6.213 | 5.654 | 6.415 (6.533) |
| 500 | 6.233 | 5.676 | 6.440 (6.562) |
| 1000 | 6.250 | 5.695 | 6.461 (6.586) |
| 10000 | 6.289 | 5.738 | 6.511 (6.644) |

**Table 5.4** : Extreme estimates of sea levels (figures in brackets for Silloth are based on the GPD fit to the full recorded time series)

Figures 5.5-5.7 below show quantile and probability plots for the predictions with 95% confidence bands shown on the quantile plots. These indicate that none of the distributions are a particularly good fit to the data, particularly at the higher levels. Generally from the bulk of the data it appears that the model predictions are likely to over-predict the extremes.

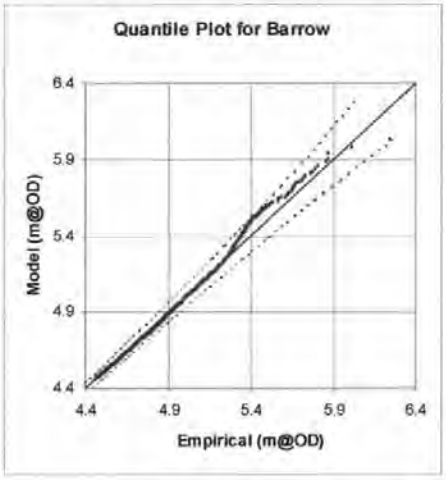


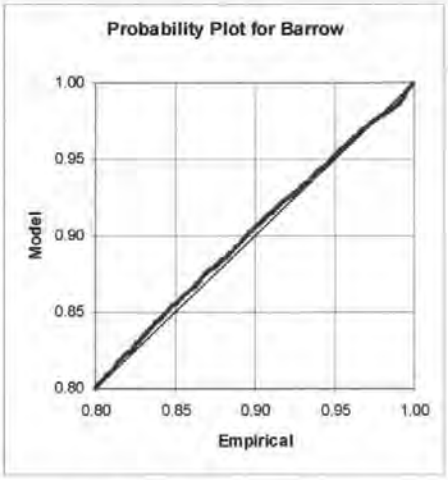


**Figure 5.5** : Quantile and probability plots for Barrow.
(Quantile plots show 95% confidence bands)

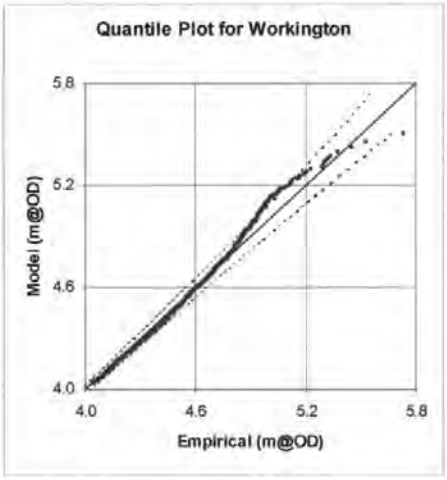


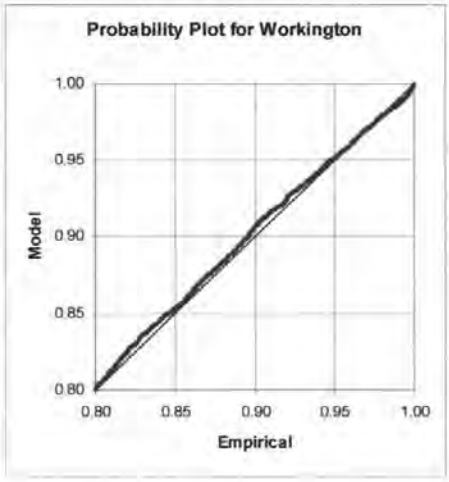


**Figure 5.6** : Quantile and probability plots for Workington.
(Quantile plots show 95% confidence bands)

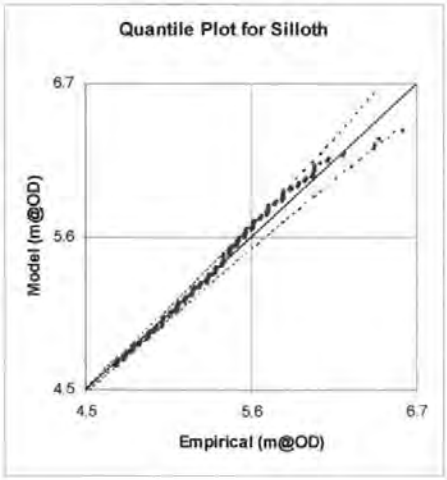


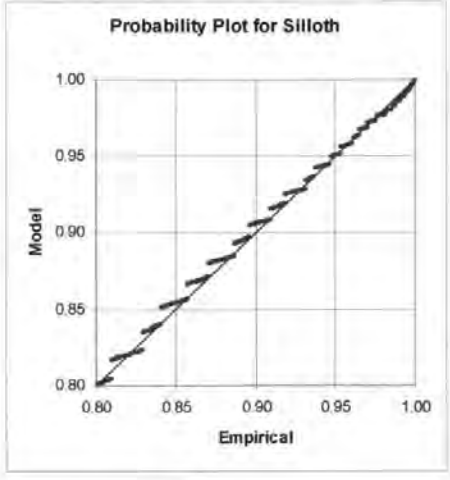


**Figure 5.7** : Quantile and probability plots for Silloth.
(Quantile plots show 95% confidence bands)

**Comparisons with previous estimates**

For Barrow, the predictions given by Dixon and Tawn (1997) are noticeably higher than all the remaining predictions, including the predictions from this study. These are typically 0.4m higher compared to JBA (1998), yet approaching the estimates of Coles and Tawn (1990) at the most extreme return periods. The predictions given in this study are generally higher for smaller return periods (up to approximately 50 years) compared to the JBA (1998) estimates, getting noticeably lower at more extreme return periods.

With over 8½ years of recorded data available, countback of the highest values indicates that return periods quoted by JBA (1998) below 10 years are almost certainly under-predicted. The quoted 1 and 5 year return period events are exceeded approximately 30 times and twice per year respectively, and the 10 year return period event is probably lower than the actual 2 year return period event. This also applies to the prediction by Coles and Tawn (1990).

Based on this analysis, return periods below 50 years quoted by JBA (1998) and Coles and Tawn (1990) are considered unreliable. Despite the variations between the predictions in this study and Dixon and Tawn (1997), especially at large return periods, no definite conclusions can be drawn as to the accuracy of either set of results relative to each other.

Similar to Barrow, the predictions for Workington by Dixon and Tawn (1997) are noticeably higher than all the remaining predictions, including the predictions for this study. These differences noticeably increase at larger return period events, with the 100 year return period event over 0.3m higher than all other predictions. Predictions by Dixon and Tawn (1995) are similar to the (corrected) predictions by JBA (1998), which are noticeably higher than the predictions for this study.

With approximately 13½ years of recorded data available, countback of the highest values indicates that the (corrected) 1 year return period event predicted by JBA (1998) is exceeded approximately 12 times a year. No definite conclusions can be drawn on the accuracy of any other predictions.

For Silloth, apart from the 10 year prediction by Dixon and Tawn (1997) and the 1 year prediction by JBA (1998), which is equivalent to MHWS, predictions by Coles and Tawn (1990), Dixon and Tawn (1997) and JBA (1998) for return periods less than 100 years show good comparison with results predicted by this study.

Considering the comments given above, apart from consistency, there are no firm conclusions that indicate that the predictions for this study are any more accurate than specific predictions given by other authors, and there is a general wide discrepancy at the highest (>100 years) return period events. However, the predictions in this study are based on significantly more extensive data sets than were considered by the other three authors. These data sets have also undergone extensive pre-processing, and are unlikely to include any noticeable discrepancies which occur for example in some of the JBA (1998) data sets.

With coastal defence work in Cumbria usually requiring a defence standard with a 50 year return period (and occasionally 100 year), and bearing in mind the strong spatial agreement between Barrow, Workington and Silloth, the predictions in this study can be considered acceptable for return period events up to 100 years, and the most appropriate to apply. However, these estimates are based on data sets up to $1/10^{th}$ of the extrapolation, and could be subject to significant, yet unknown variations in estimates of the most extreme events.

Based on these predictions, and the agreement to secondary locations outlined in Section 3.2.4, Figure 5.8 shows standard spatial extreme predictions for the Cumbrian coastline.

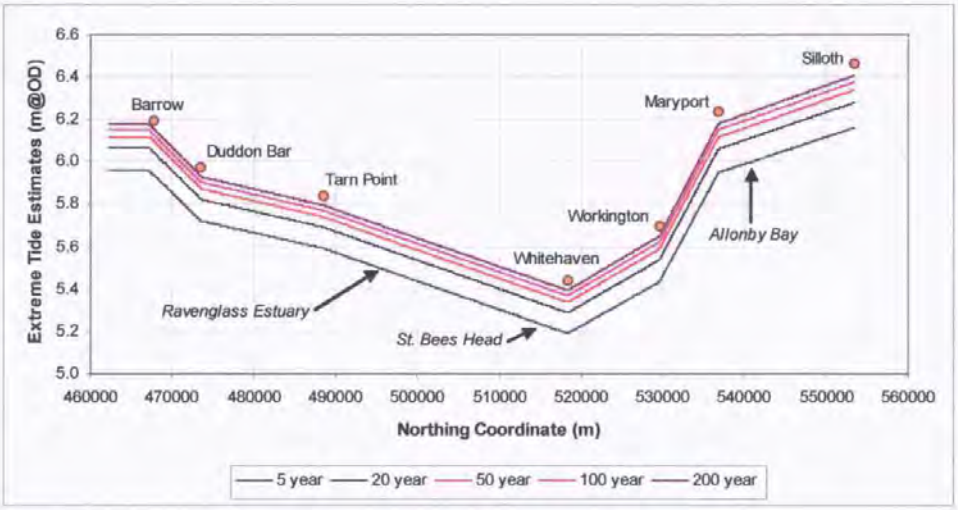


**Figure 5.8** : Spatial variation of extreme sea levels along the Cumbrian coastline.

### 5.2.2 Extreme Offshore Wave Heights along the Cumbrian Coastline

Typical of most locations around the UK coastline, little if any recording of offshore extremes has been carried out along the Cumbrian coastline (see Section 3.3.1). Offshore predictions at the Met Office locations are carried out by the Met Office. However, these have not been obtained for the two locations used in this study, which are believed to be the only predictions of extremes at Met Office locations offshore of Cumbria.

Extreme wave height predictions for the two Met Office locations have therefore been considered using the same approach as outlined for extreme sea levels. However, it should be noted that this study is particularly interested in inshore extreme wave heights, not offshore extreme wave heights (see Section 5.2.3).

For $MO_1$, similar to the sea levels, some stability of estimates was observed for thresholds between 0.80 and 0.90. However, little stability of estimates was observed for $MO_2$, with the shape parameter ($k$) oscillating around zero, indicating that the most appropriate fit to the data is uncertain (see Section 5.2).

All three methods outlined for the sea levels have therefore been considered in the choice of a most suitable threshold for the offshore wave

heights. Similar to sea levels, an approximate assumption of similarity of wave records has also been considered as both prediction points are exposed to similar exposure conditions within the same body of water.

Figures 5.9, 5.10 and 5.11 below show mean residual life plots and plots of the shape and scale parameters against different thresholds for both $MO_1$ and $MO_2$. From Figure 5.9, linearity of the mean excess curves appears to exist between approximate thresholds of 0.80 and 0.88. For $MO_1$, the shape parameter is constant, and the scale parameter linear below a threshold of about 0.92. No clear pattern is observed for $MO_2$ for these parameters. This indicates a threshold for $MO_1$ of approximately 0.88 or lower, yet no clear indication of the appropriate threshold for $MO_2$.

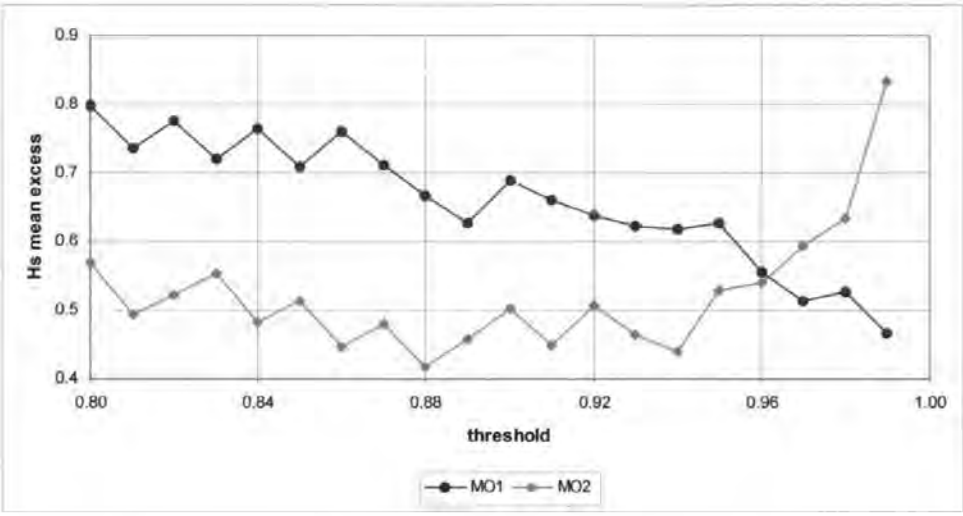


**Figure 5.9** : Mean residual life plots for $MO_1$ and $MO_2$.

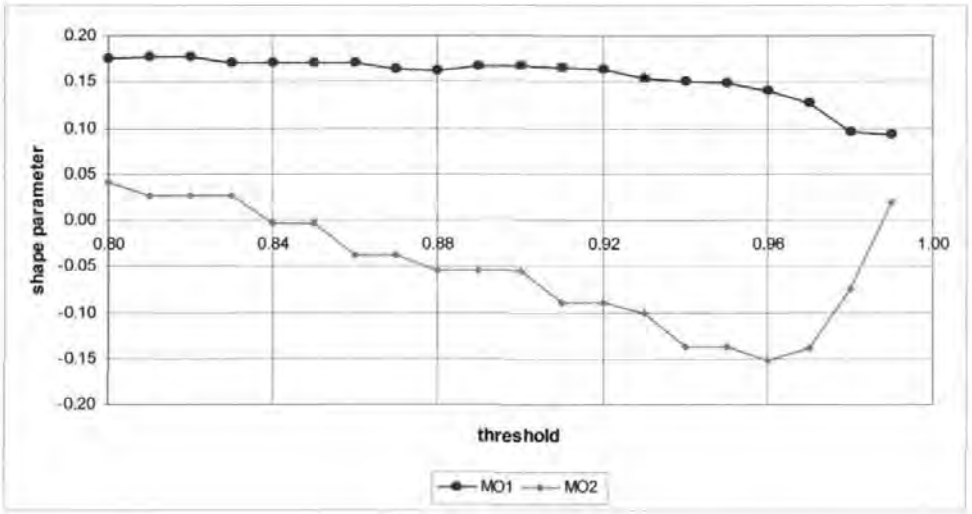


**Figure 5.10** : Shape parameter of GPD above different thresholds for $MO_1$ and $MO_2$.

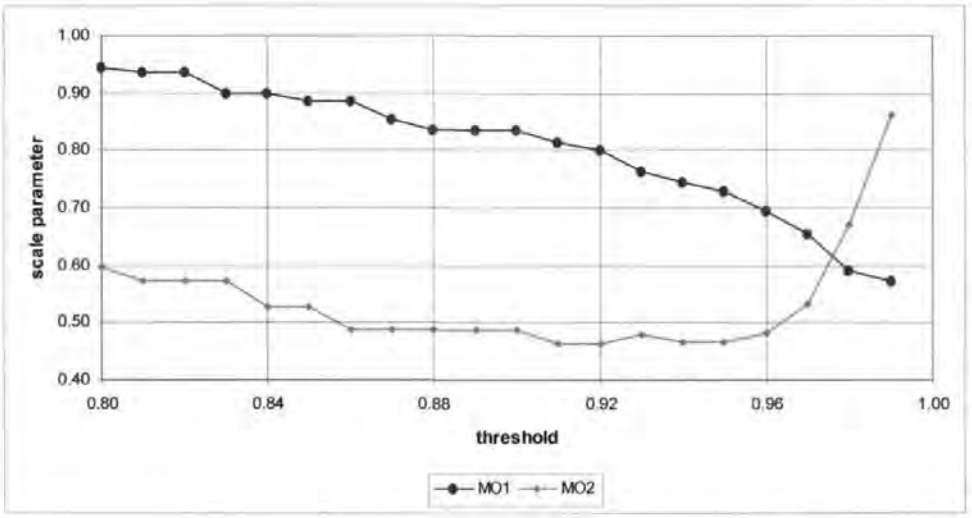


**Figure 5.11** : Scale parameter of GPD above different thresholds for $MO_1$ and $MO_2$.

With $MO_1$ and $MO_2$ in close proximity, and exposed to similar wave climates (see for example Figure 4.5), similarity of wave conditions and extremes would be expected. This would also imply that the distribution to describe the extremes would be the same. A scatter plot of resultant wave heights for $MO_1$ and $MO_2$ (Figure 5.12) indicates a clear relationship between wave conditions at $MO_1$ and $MO_2$. Although generally, wave heights at $MO_1$ are approximately 15% larger than wave heights at $MO_2$, unusually, for more extreme wave heights (Hs>4.0m), $MO_2$ has larger wave heights.

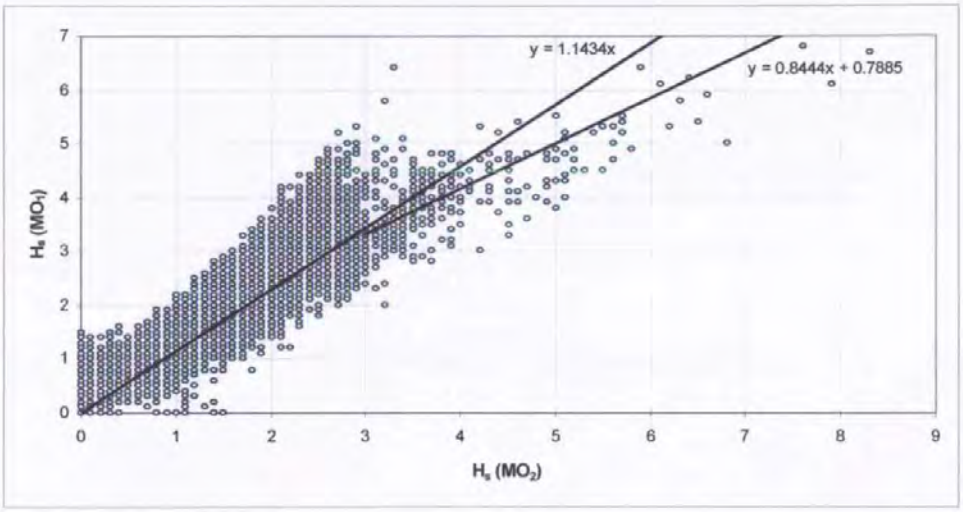


**Figure 5.12** : Scatter plot of resultant $H_s$ at $MO_1$ and $MO_2$.

Figures 5.13 and 5.14 below show extreme predictions at both locations for thresholds up to 0.90. For $MO_1$, Figure 5.13 indicates that the choice of threshold has little bearing on extreme predictions. However, from Figure 5.14, the choice of threshold for $MO_2$ is very dependent on the threshold, indicating a Weibull distribution below approximately 0.84 and, apart from a threshold of 0.99 (not shown), a Fréchet distribution above this.

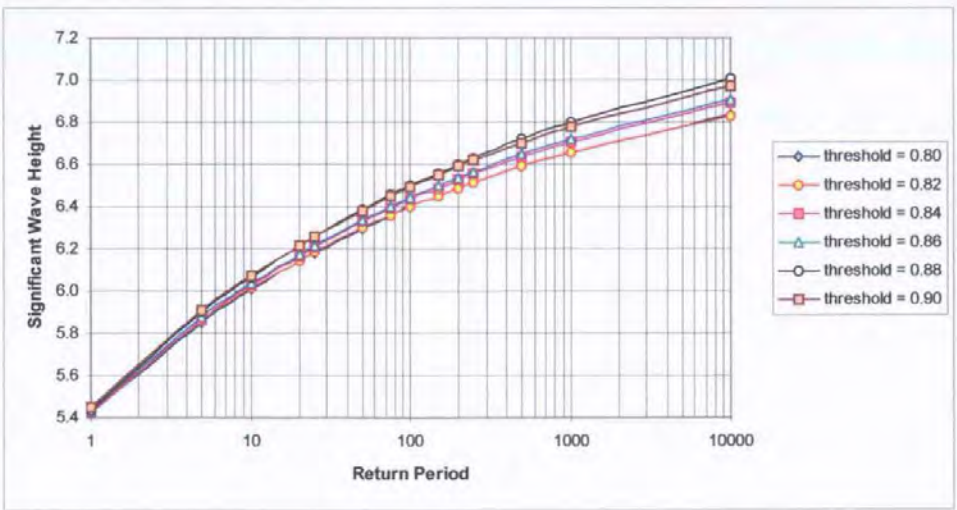


**Figure 5.13** : Extreme estimates of $H_s$ at $MO_1$ for different thresholds.

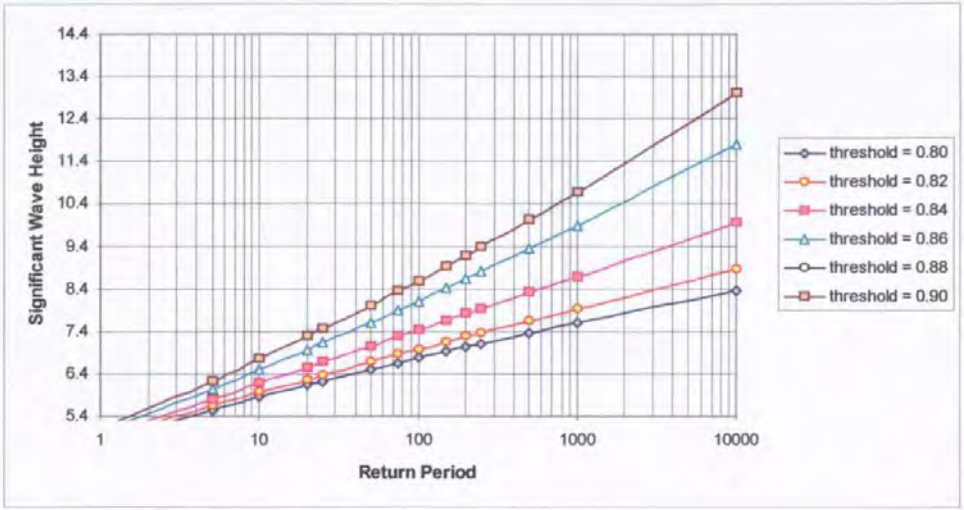


**Figure 5.14** : Extreme estimates of $H_s$ at $MO_2$ for different thresholds.

However, considering the comments given above about similarity of wave conditions at extremes, and the conclusions regarding the 'recommended' distribution to describe extreme wave heights by Mathiesen et al (1984) (see Section 5.2), a threshold for $MO_2$ below approximately 0.84 is considered appropriate. This gives a Weibull distribution, the same as for $MO_1$. The chosen threshold for both locations was therefore 0.80. The same threshold has been chosen for both locations for the same reasons as given in Section 5.2.1. This also maintains as much as possible the similarity of distributions between the two locations, and therefore spatially along the coastline.

Figure 5.15 therefore shows the comparison between extremes at $MO_1$ and $MO_2$, and Table 5.5 outlines the extreme predictions used in this study.

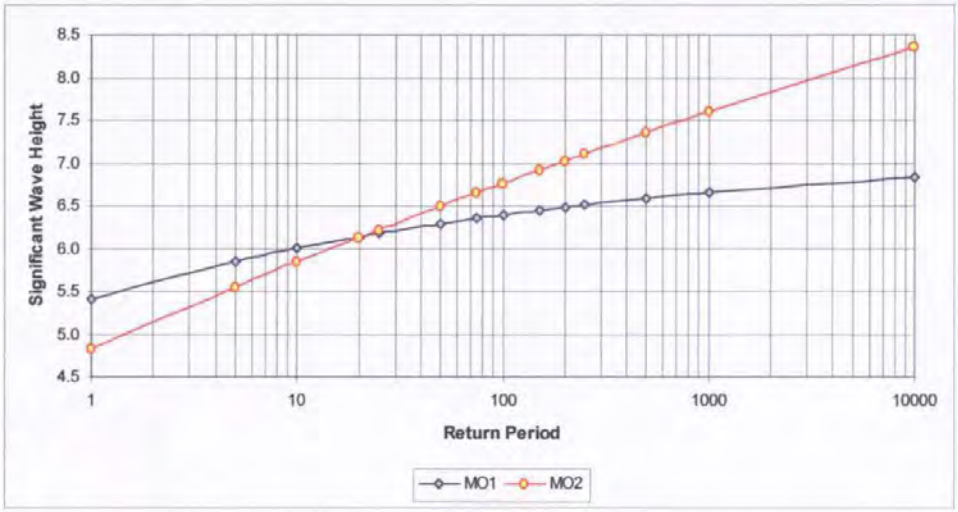


**Figure 5.15** : Extreme estimates of $H_s$ at $MO_1$ and $MO_2$.

| Return Period (years) | $MO_1$ (m) | $MO_2$ (m) |
|---|---|---|
| 1 | 5.42 | 4.84 |
| 5 | 5.85 | 5.56 |
| 10 | 6.01 | 5.85 |
| 20 | 6.14 | 6.14 |
| 50 | 6.30 | 6.50 |
| 100 | 6.40 | 6.77 |
| 200 | 6.49 | 7.03 |
| 500 | 6.59 | 7.36 |

**Table 5.5** : Extreme estimates of $H_s$ at $MO_1$ and $MO_2$.

Figures 5.16-5.17 below show quantile and probability plots for the predictions with 95% confidence bands shown on the quantile plots. These indicate similar to the sea levels that the distribution is not a particularly good fit to the $MO_1$, particularly at the higher levels. However, predictions are considered acceptable. For the $MO_2$ data, the distribution is a very poor fit to the data. The quantile plot in particular indicates that stability of predictions appears more likely at a higher threshold, although further investigation (not shown) indicates that this is not the case. It is therefore considered that a great deal of uncertainty exists on the prediction of

extremes for $MO_2$. This is easily demonstrated for example by counting back in the 13 years of wave records for which 3 records are greater than the 500 year extreme prediction.

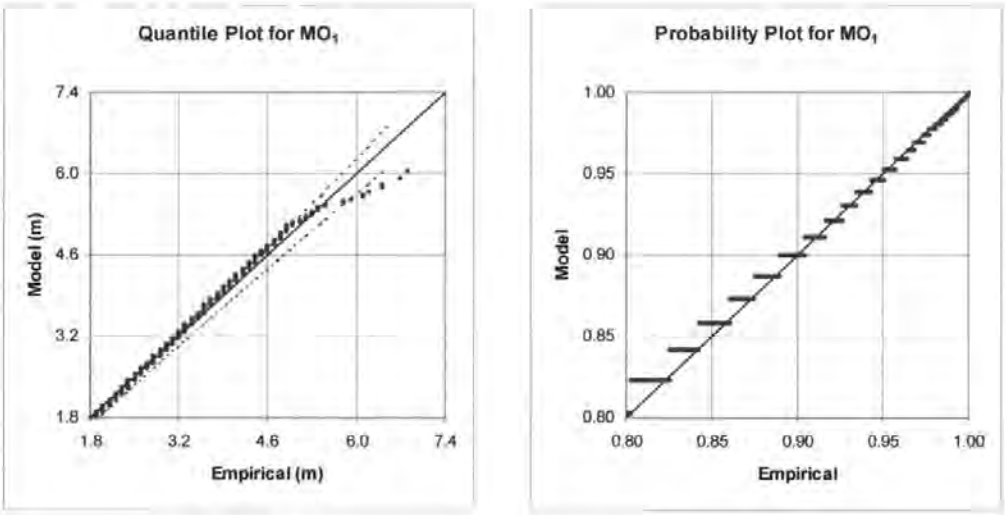


**Figure 5.16** : Quantile and probability plots for $MO_1$.
(Quantile plots show 95% confidence bands)

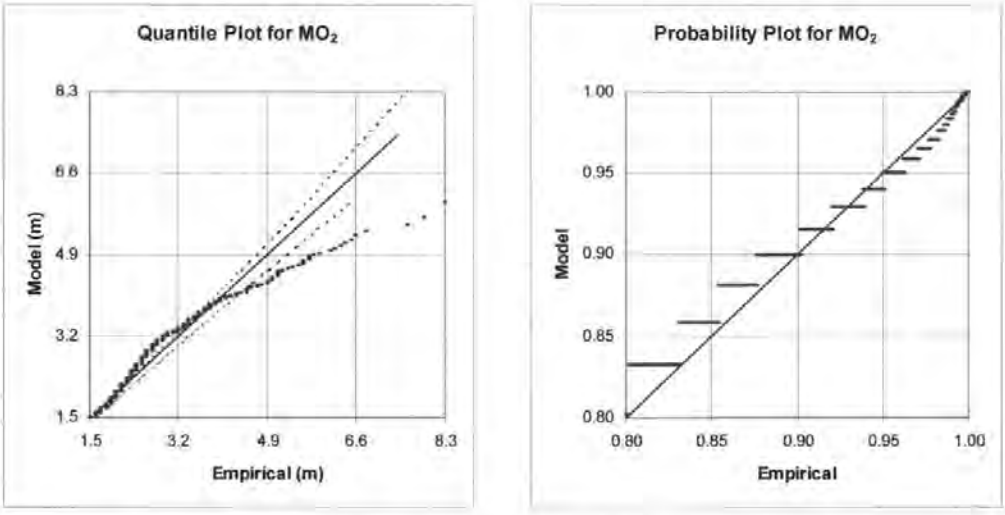


**Figure 5.17** : Quantile and probability plots for $MO_2$.
(Quantile plots show 95% confidence bands)

Based on these predictions, Figure 5.18 shows standard spatial extreme predictions of offshore $H_s$ for the Cumbrian coastline. Note that these predictions are based on the estimated $H_s$ at high tide, and not the 3 hourly values analysed in this section.

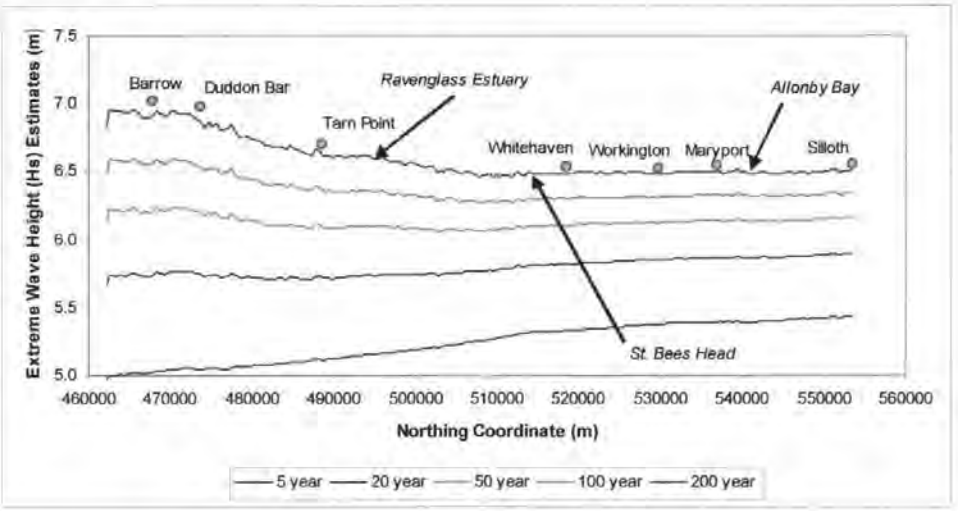


**Figure 5.18** : Spatial variation of extreme offshore wave heights along the Cumbrian coastline.

### 5.2.3 Extreme Inshore Wave Heights along the Cumbrian Coastline

Although some recording and prediction of offshore extremes has been carried out along the Cumbrian coastline (see Section 5.2.2), it is unlikely if any previous detailed assessment of nearshore extremes has ever been carried out. This section considers the prediction of extreme inshore wave heights at five bed levels (-2, -1, +0, +1 and +2m@OD) along the Cumbrian coastline. Using maximum likelihood estimation, a GPD is fitted to the data (Equation 2.8) which is then extrapolated to standard extreme events. However for nearshore wave heights, depth limitations leading to wave breaking needs to be considered, which is not implicitly included in the GPD distributions. Therefore nearshore extreme wave heights have been determined by counting back to the required return periods based on a simulation of 10,000 years of coincident wave and sea level data (see Section 6.6.5 and Figures 5.24 – 5.28). Wave heights in the simulations have been checked for depth limited effects (see Equation 4.6) taking into account not only the water depth and beach slope, but also the simulated wave periods based on the distributions determined (see Sections 2.6.1.1 and 5.3.2).

With nearshore, predictions at five depths and at 229 locations, it was not practical to rigorously consider all the methods outlined in the previous two sections to determine a suitable threshold. The choice of a threshold has therefore mainly been based on a comparison of extreme predictions at different thresholds. The comparison is based on the assumption that spatially, distributions would be expected to be the same (Weibull, see Section 5.2), with the same 'shape' and little variation. Similar to sea levels and offshore wave heights, similarity of extreme predictions over a range of thresholds would indicate the region for the correct choice of the threshold.

Based on this comparison, at -2m@OD and -1m@OD, stability of extremes was generally observed below a threshold of approximately 0.85, with increased variability in the region 0.85-0.90. Above a threshold of approximately 0.90, predictions became increasingly erratic, with the data following a Fréchet distribution.

At +0m@OD and above, general consistency of extremes was observed above all thresholds.

Based on the spatial analysis outlined above, and a comparison of selected locations, the choice of a suitable threshold in the region 0.80 to 0.82 appeared appropriate. The threshold chosen was 0.82 as this appeared to give slightly better stability spatially (although not significant) than either 0.81 or 0.80.

Using this threshold, Figure 5.19 below shows the variation in the shape ($k$) parameter for predicted inshore wave heights along the Cumbrian coastline at the 5 different bed levels. This is seen to be positive at all locations except for a region around Northing coordinate 475000m (which is discussed later in this section), which indicates that the most appropriate fit to the data is a Weibull distribution.

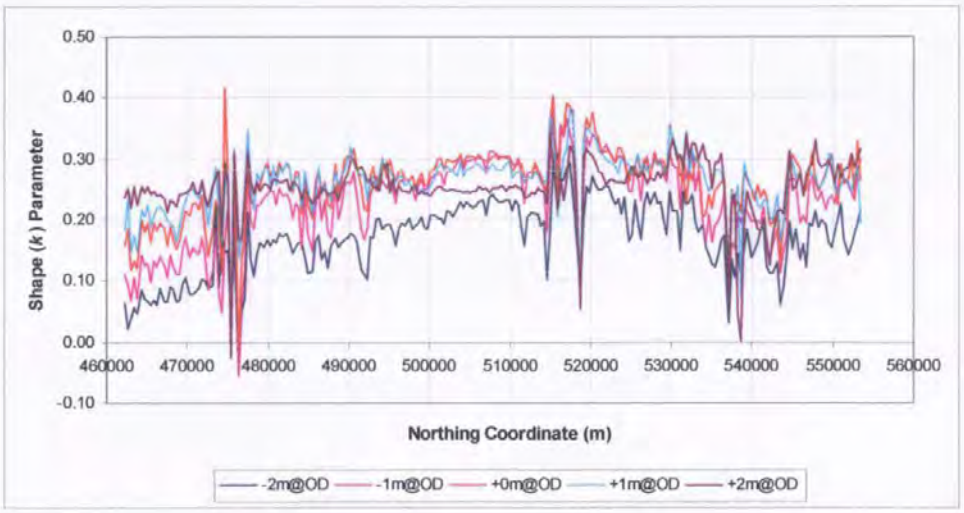


**Figure 5.19** : Variation in shape (*k*) parameter
for predicted inshore wave heights

Based on the analysis of the nearshore records, Figure 5.20 shows the marginal extreme predictions for nearshore wave heights at -2m@OD for a range of standard return periods. These predictions have been determined based on the extrapolation of the GPD, and do not consider depth limited effects (see Figures 5.24 – 5.28).

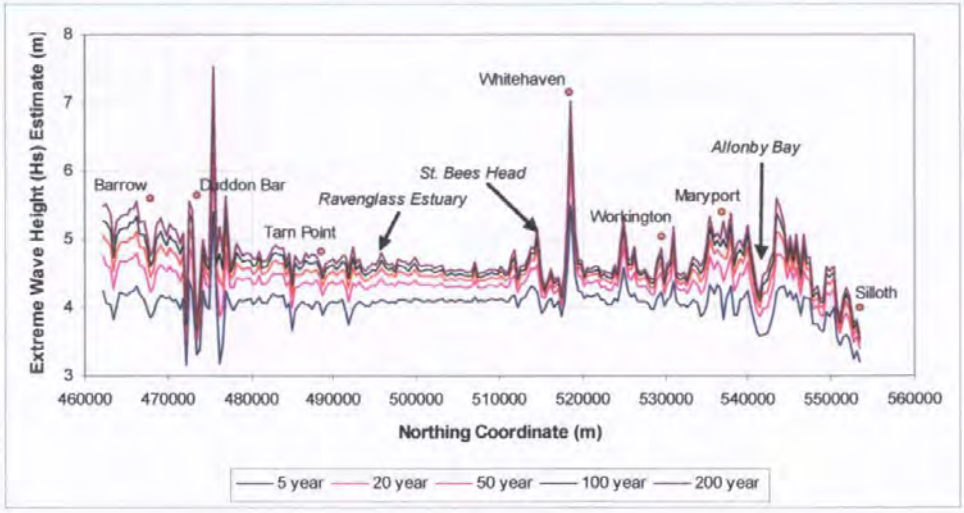


**Figure 5.20** : Spatial variation of extreme wave heights (-2m@OD)
(extrapolated from GPD, not considering depth limited effects)

From this figure, anomalies appear at extreme predictions for Northing coordinate 475440N, and centred around Northing coordinate 518640N. To investigate these further, Figures 5.21 and 5.22 show detailed contoured plots around these regions. Included on these plots are the spot heights

used to determine the bathymetry, and the nearshore seabed slope used to check for wave breaking conditions. For the first coordinate (475440N), it was clear that the large predictions here were due to an erroneous spot height near the coastline (near Sandscale Haws, circled). This has resulted in a steep beach (see next paragraph) in this region (1 in 5.5), and limited calculated wave breaking, giving large extreme predictions. For the second coordinate (around 518640N), the large predictions were again as a result of a steep beach in this region (1 in 6 to 1 in 10), although in this case the spot height information is believed to be correct. The apparent steep beach in this region is believed to be as a result of a lack of survey information near the seaward breakwater at Whitehaven. As this area is permanently submerged, it has not been possible to re-assess the beach slope in this region. However, based on a previous inspection of this breakwater, the seabed along the seaward base of this breakwater is estimated at between -4.2 to -5.2m@OD (Foskett, 2006). This gives an estimated beach slope of approximately 1 in 20 to 1 in 25, and confirmed that the calculated beach slope was incorrect. From the analysis carried out, results from Northing coordinate 475440N have been discounted from further analysis in this study. As the spot height information is not incorrect, results around Northing coordinate 518640N are left unchanged, although wave breaking due to depth limited effects has been based on a maximum beach slope of 1 in 18. This gives a degree of confidence in the predictions, and matches the maximum beach slopes determined for the seaward breakwater at Workington, which is similarly exposed.

Beach slopes were determined based on the median beach slope calculated between -2m@OD and +0m@OD, -1m@OD and +1m@OD and +0m@OD and +2m@OD using the horizontal gridded bathymetry. With beach slopes typically 1 in 40 or shallower, and a grid size of 40m, beach slopes were typically based on beach profiles 80m in length or more. For a linear beach (as has been assumed), this would typically correspond to at least 1 wavelength at extreme conditions, a distance considered suitable to determine nearshore beach slopes (see for example Besley 1999). Figures 5.21 and 5.22 also corresponded to the regions where the steepest beaches were observed (see Figure 5.23). Considering the potential effect of an erroneous beach slope on extreme predictions, these regions were

subject to further analysis. These checks indicated no reason to doubt the accuracy of the predicted beach slopes (and therefore the extreme predictions) within the limitations of the predictive techniques used.

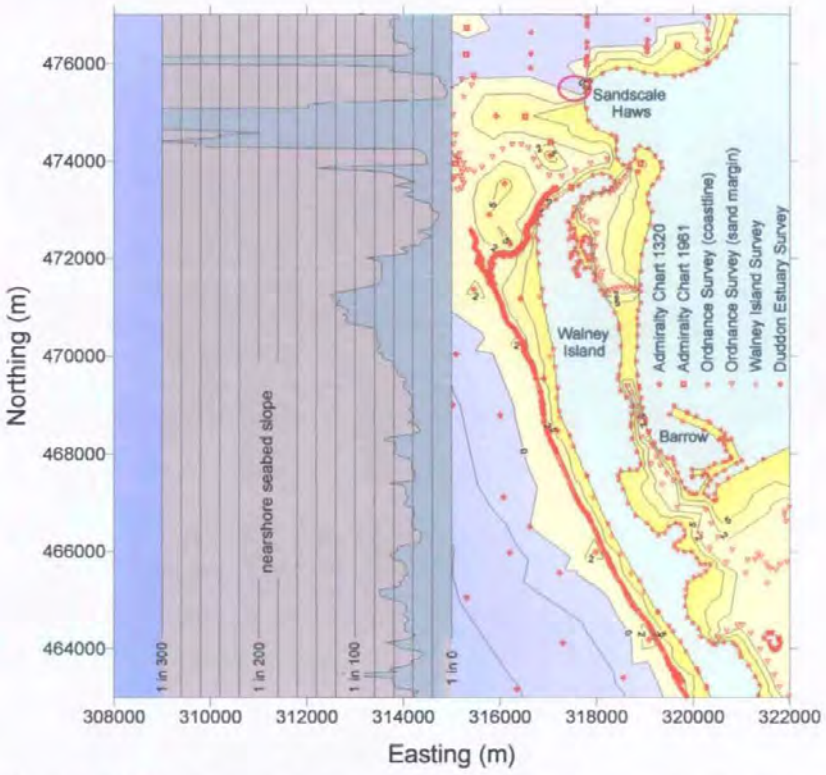


**Figure 5.21** : Survey information used to determine bathymetry and seabed slopes (in region of north Walney Island))

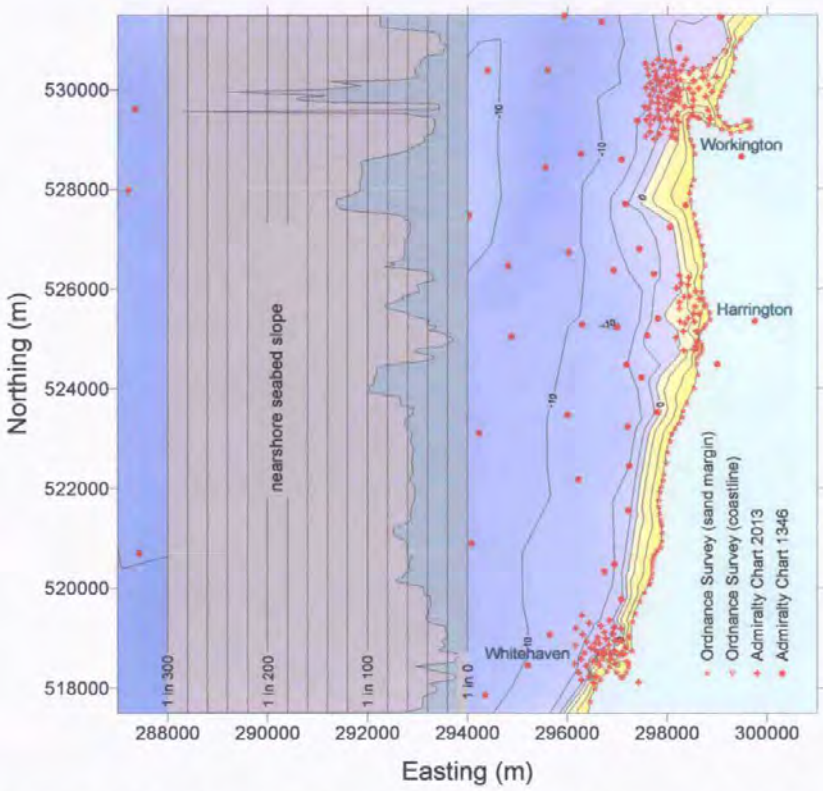


**Figure 5.22** : Survey information used to determine bathymetry and seabed slopes (Whitehaven to Workington)

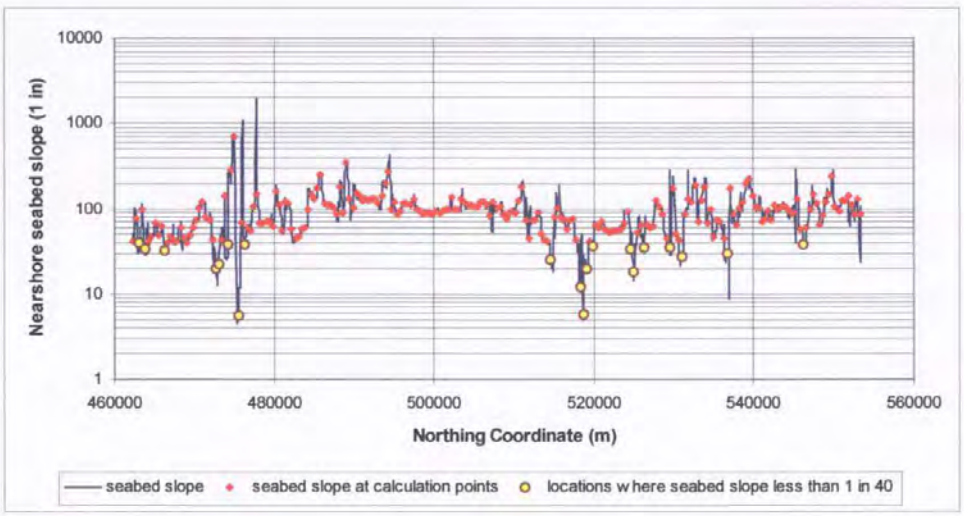


**Figure 5.23** : Nearshore beach slopes

Taking into account depth limited effects, and therefore wave breaking, Figures 5.24 to 5.28 show the inshore extreme wave height predictions for the different bed levels considered. The erroneous predictions at Northing coordinate 475440N have been excluded from these figures. These show little variation from the predictions in Figure 5.20 apart from at Whitehaven,

where as a result of the imposed seabed slope, predictions have significantly reduced (although still the largest along the Cumbrian coastline).

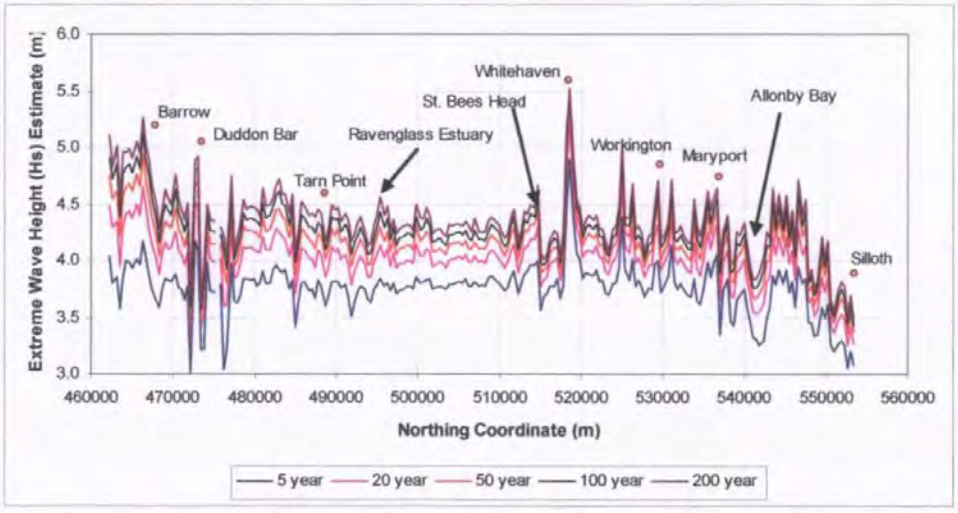


**Figure 5.24** : Spatial variation of extreme wave heights (-2m@OD) (based on 'countback' from simulation of 10,000 years of data)

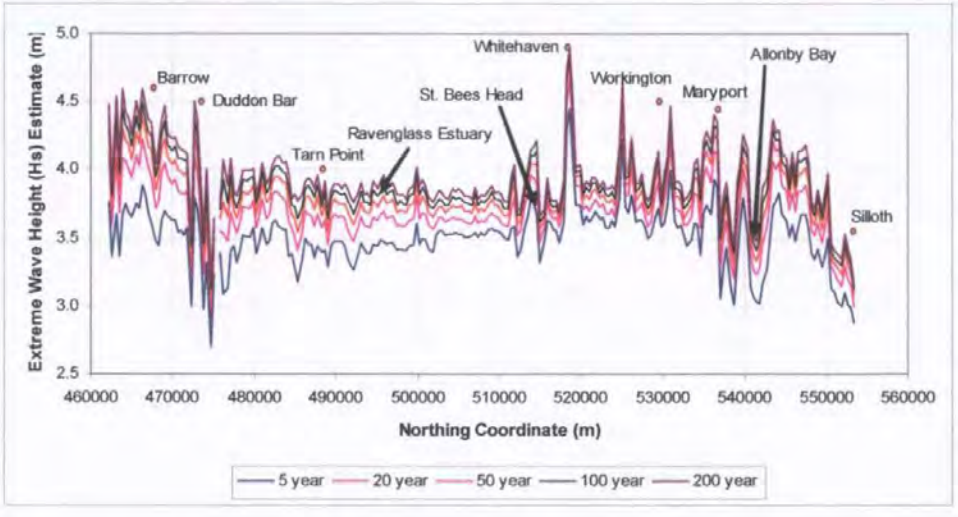


**Figure 5.25** : Spatial variation of extreme wave heights (-1m@OD) (based on 'countback' from simulation of 10,000 years of data)

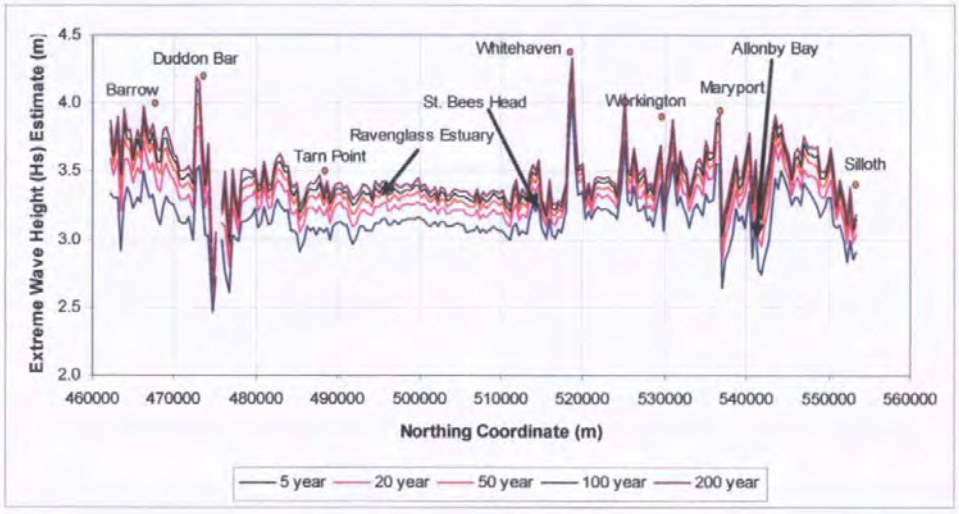


**Figure 5.26** : Spatial variation of extreme wave heights (+0m@OD) (based on 'countback' from simulation of 10,000 years of data)

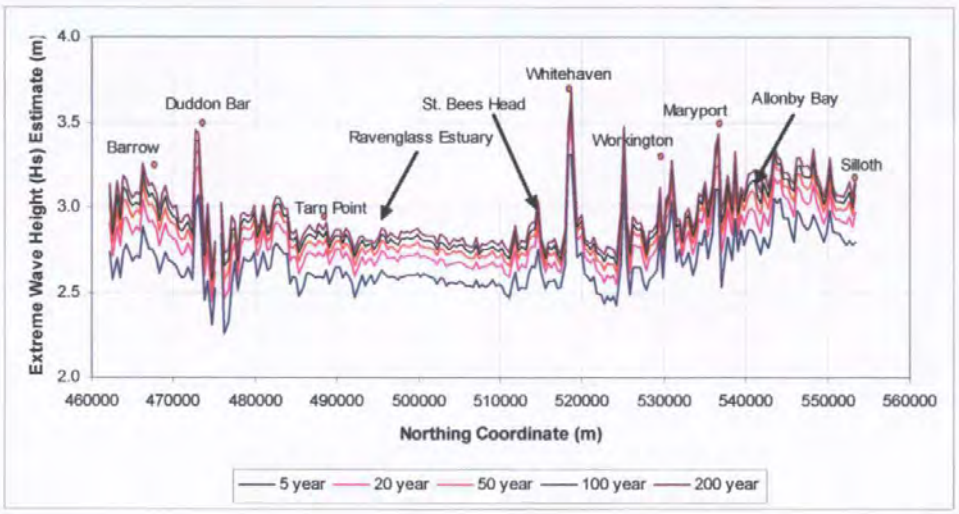


**Figure 5.27** : Spatial variation of extreme wave heights (+1m@OD) (based on 'countback' from simulation of 10,000 years of data)

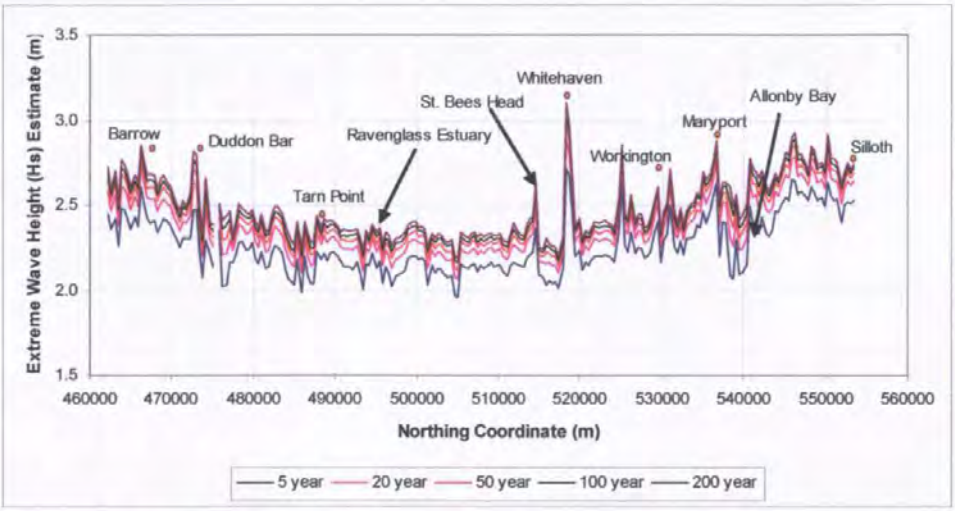


**Figure 5.28** : Spatial variation of extreme wave heights (+2m@OD) (based on 'countback' from simulation of 10,000 years of data)

## 5.3 Model Selection

Within JOIN-SEA, two different models are available (see Section 2.6). This section considers the choice of the most suitable model for the Cumbrian coastline, together with the model to represent wave steepness.

### 5.3.1 Distribution of Wave Populations

Within the eastern Irish Sea, two types of wave populations could be considered to exist. As a semi-enclosed sea, these would be swell waves generated through the narrow gap between the Isle of Anglesey and the south of Ireland (see Figure 4.5), and locally generated seas either from within the Irish Sea basin or from the south-west quadrant in the Atlantic Ocean.

This is demonstrated for the offshore conditions used for Northing coordinate 470000N in Figures 5.29 and 5.30 below. Figure 5.29 shows a scatter plot of the resultant significant wave height against the sea level.

Identified on this figure are conditions where the wind or swell wave is larger. This indicates some correlation between wave height and sea level when the wind wave dominates, particularly at higher sea levels, yet no clear indication of correlation when the swell wave dominates. Figure 5.30 shows a scatter plot of the wave steepnees against the significant wave height for the individual wind and swell wave components. This clearly indicates two populations of wave conditions, with the wind wave component having a steepness greater than 0.03 approximately 91% of the time, yet the swell wave component having a steepness less than 0.03 approximately 99% of the time.

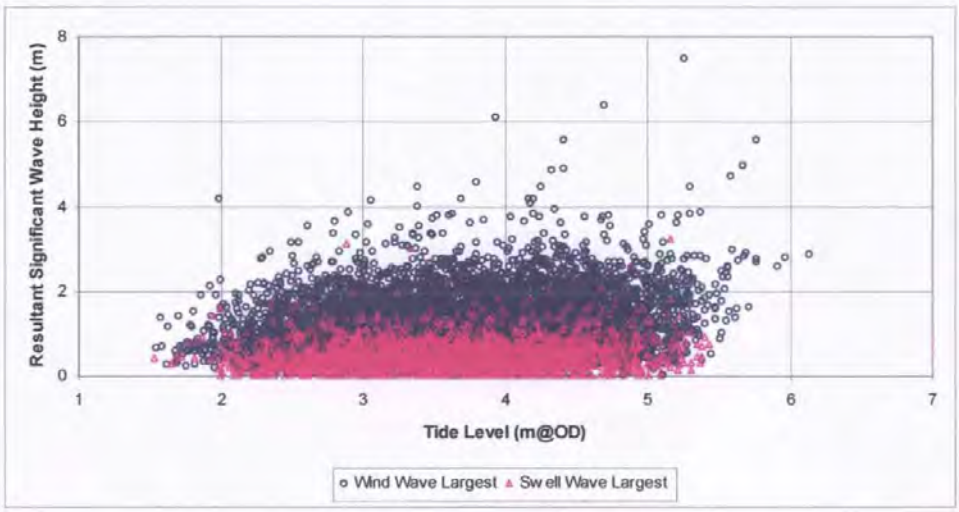


**Figure 5.29** : Scatter plot of resultant $H_s$ against sea level.
(offshore Northing coordinate 470000N)

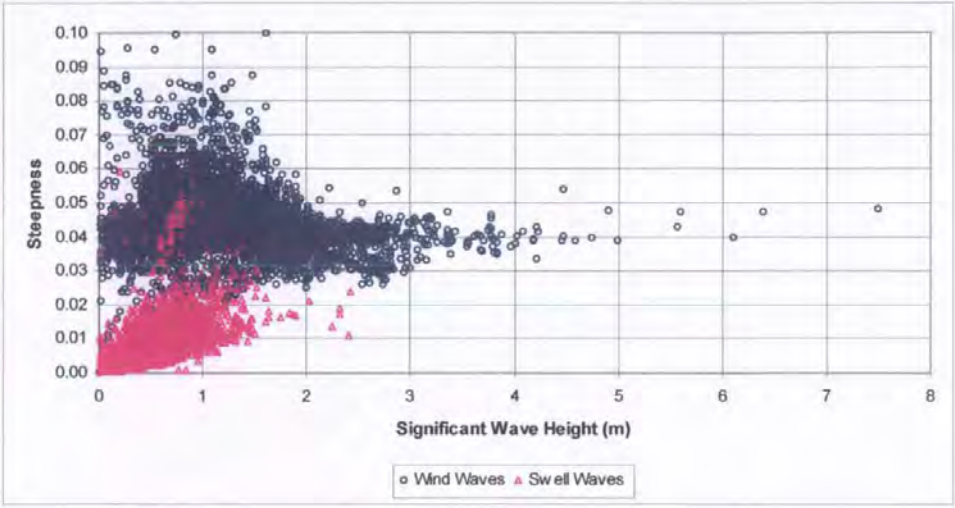


**Figure 5.30** : Scatter plot of wave steepness against $H_s$ for individual components (offshore Northing coordinate 470000N)

This would indicate that for offshore conditions, the correct model to describe the wave conditions would be a mixture distribution (see Section 2.6.3). This is confirmed by Figure 5.31 which shows the spatial variation in correlation along the Cumbrian coastline, varying for different thresholds of non-exceedance of the sea level. Nearshore, the wave conditions would also be expected to be a mixture distribution, not necessarily because of the different wave populations offshore, but as a result of the depth limited effects nearshore. This would result in large wave heights breaking at lower sea levels, yet similar wave heights being unaffected at higher sea levels. This effect would be expected to be more pronounced the further inshore you progress. This is confirmed by Figures 5.32-5.36, which are the same as Figure 5.31 but for nearshore conditions. These clearly indicate the increased levels of correlation between threshold of non-exceedance of sea levels and wave height for increased beach levels. These figures are discussed in more detail in Section 6.6.2.

The mixture distribution (MIX) has therefore been used to model wave conditions along the Cumbrian coastline.

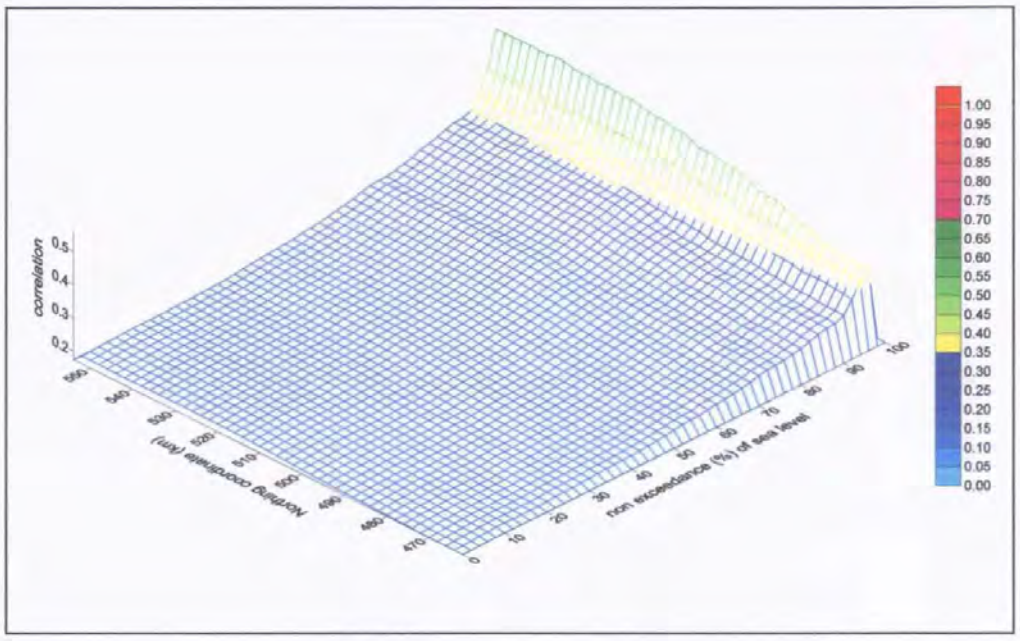


**Figure 5.31** : Spatial variation in correlation for offshore conditions for different thresholds of non-exceedance of the sea level

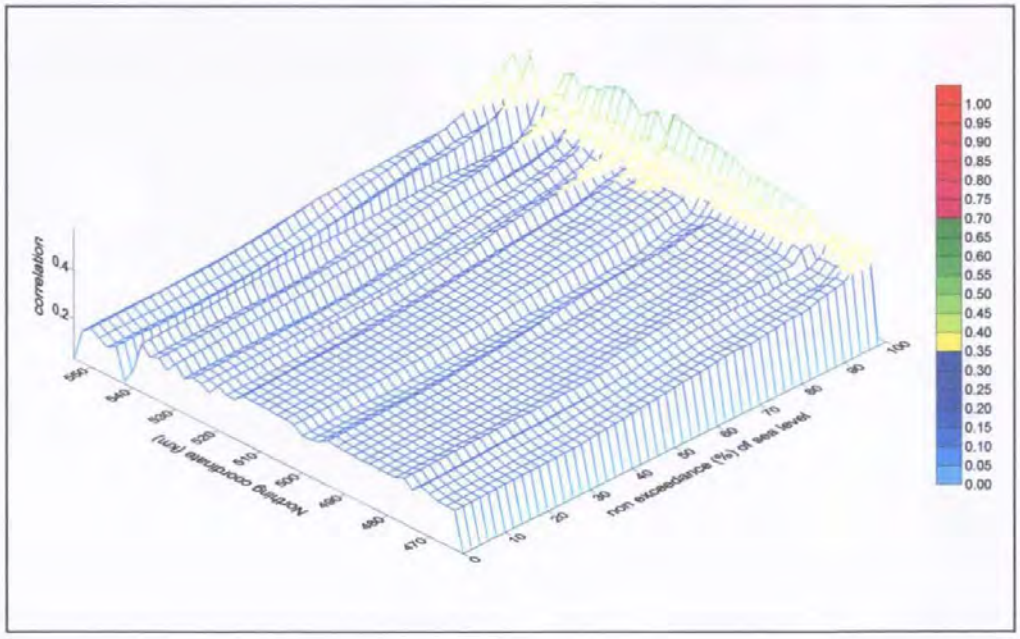


**Figure 5.32** : Spatial variation in correlation at -2m@OD for different thresholds of non-exceedance of the sea level

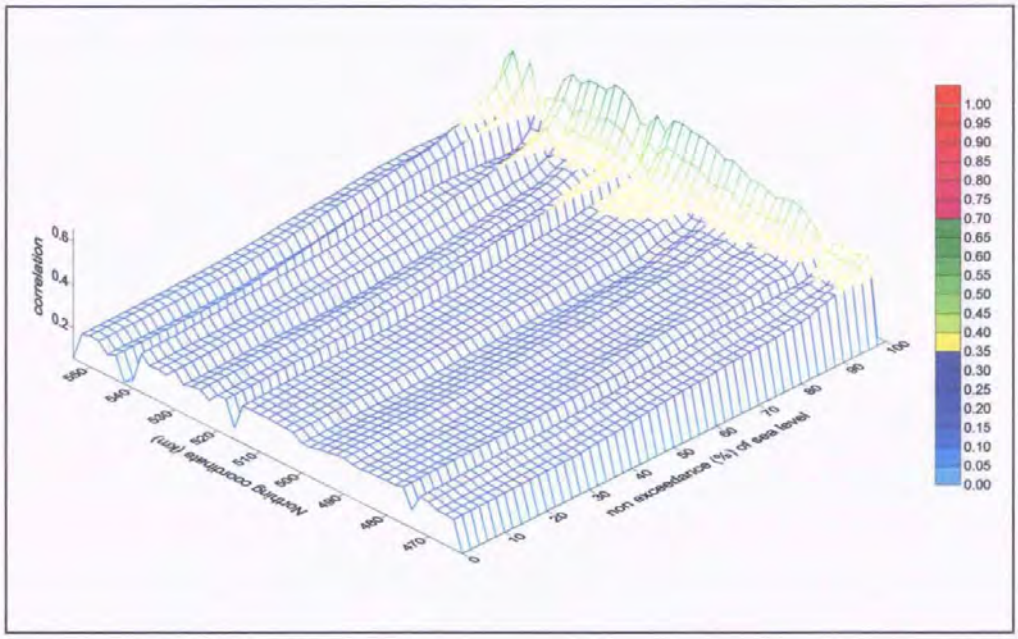


**Figure 5.33** : Spatial variation in -1m@OD
for different thresholds of non-exceedance of the sea level

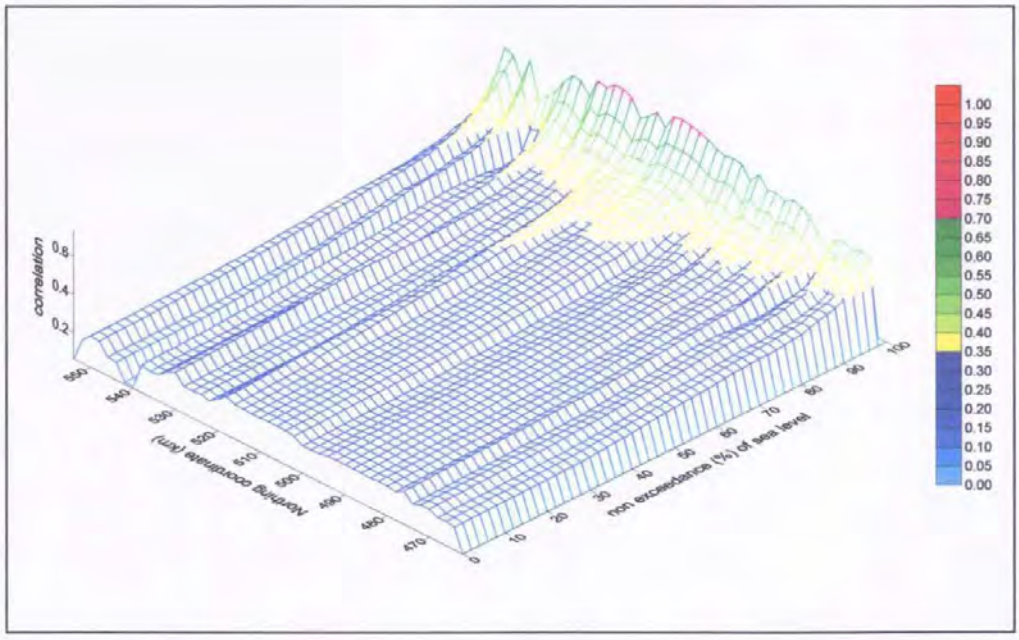


**Figure 5.34** : Spatial variation in correlation at +0m@OD
for different thresholds of non-exceedance of the sea level

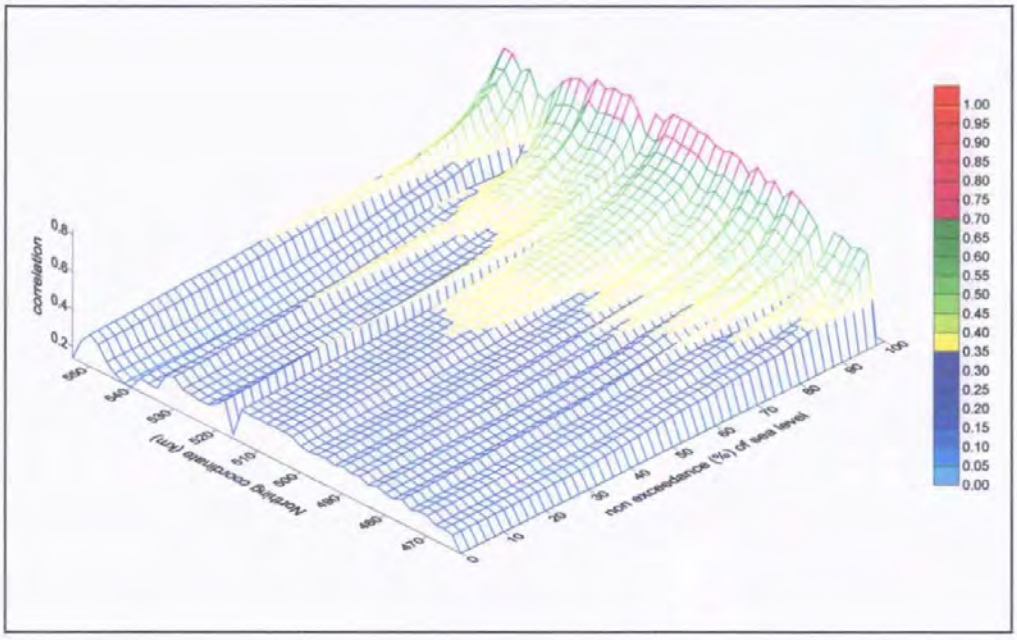


**Figure 5.35** : Spatial variation in correlation +1m@OD
for different thresholds of non-exceedance of the sea level

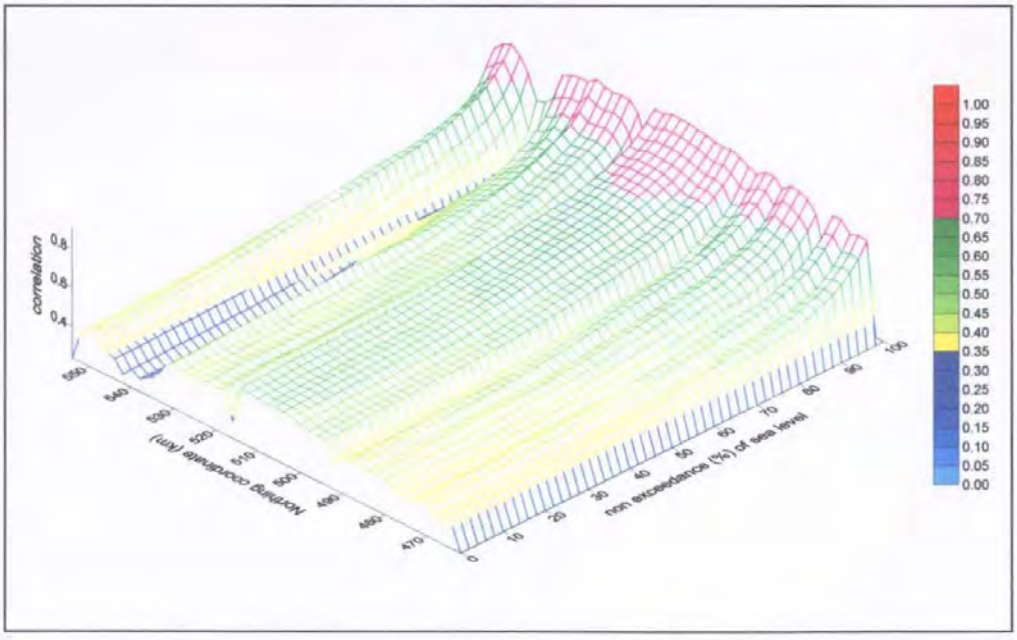


**Figure 5.36** : Spatial variation in correlation at +2m@OD
for different thresholds of non-exceedance of the sea level

### 5.3.2 Threshold Selection for Inshore Wave Steepness

The upper tail of the wave steepness has been modelled using the linear regression model outlined in Section 2.6.1.1 (Equation 2.10). Unlike the threshold selection for the wave heights and sea levels, the selection of the appropriate threshold for wave steepness is not directly concerned with extrapolation to extreme values, but the estimation of the wave steepness as a wave approaches an extreme value.

Usually wave steepness is modelled as a constant value for comparatively large wave heights in a region, and for waves from a single population has little variation. Typically for wind waves this is in the region 0.040-0.043, which is the case for the Irish Sea, as indicted for example on Figure 5.30. The use of the linear regression model gives a degree of flexibility to the modelling of wave steepness, allowing some variability as the wave height increases.

The choice of a threshold for wave steepness is therefore based on a level of exceedance of the wave height above which wave steepness is observed to be approximately constant. Based on an analysis of wave steepness both inshore and offshore at a number of locations, a threshold of non-exceedance of 99% for the wave height was considered appropriate (see below), enabling wave steepness to be modelled based on almost 100 values.

Figures 5.37-5.39 below show a typical relationship between wave height and steepness at three locations (offshore, +0m@OD and +2m@OD) for Northing coordinate 498240m. Identified on these figures are different levels of non-exceedance. It is noticeable from the two inshore locations that nearshore, waves appear to split up into two different populations of distinct wave steepnesses. This would tend to imply that wave heights offshore are from two different populations, wind or swell dominated, as indicated by Figure 5.37 and also Figure 5.30. However, identifying these populations on Figures 5.38 and 5.39 appears to indicate that this is not the case. Further investigation indicates that this apparent split into two populations is as a result of the determination of the nearshore wave period

(Equation 4.3). Nearshore, a large offshore wind wave (of typical wave steepness) would be significantly reduced due to wave breaking. However, a typical swell wave of a significant wave period (for example, 0.4m and 10s) may not be significantly changed in height. This would result in a noticeably increased nearshore $T_z$.

This is indicated on Figure 5.40 which shows the relationship between wave periods at +0mOD and offshore. This clearly indicates an increase in nearshore wave period for certain wave conditions, particularly in the region 3-6 seconds.

Unfortunately, this means that the identification of the nearshore wave period and therefore wave steepness is subject to a large error band based on a range of swell periods, independent of wind waves and sea levels. However, this study is expressly interested in specifying the joint probability relationship between high sea levels and wave heights. The determination of the third variable (wave steepness) is mainly used in this study to specify wave breaking conditions (Equation 4.6) at extreme conditions. However, wave period is specified based on a Gaussian random process (Equations 2.9 and 2.10). Assuming the variation in wave periods to be Gaussian distributed, this will simulate the typical range of wave periods identified (for example) in Figures 5.38 and 5.39.

The choice of the high threshold also often appears to reduce the influence of these two populations. This is demonstrated for example in Figure 5.38, where the lower population appears to be more dominant above the 99% threshold than the other thresholds identified.

Despite the comments given above, the accurate specification of wave steepness is of vital importance in coastal defence work, and overtopping and damage at coastal locations could be vastly over or under estimated if wave period is inaccurately specified. The purpose of the joint probability curves is to define extreme wave height and sea level combinations for use in coastal defence work. Therefore the importance of wave steepness and its relevance is discussed in more detail in Section 6.6.6.

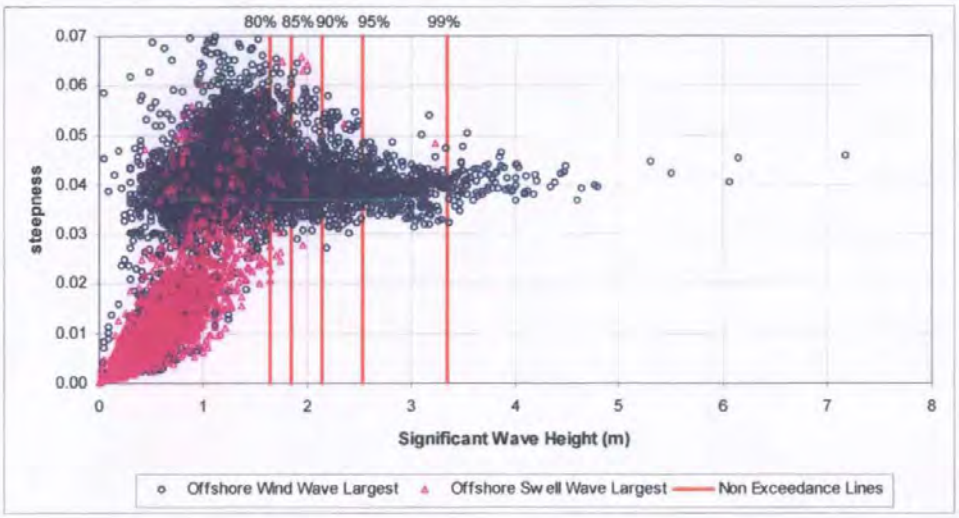


**Figure 5.37** : Significant wave height against wave steepness (offshore Northing coordinate 498240m)

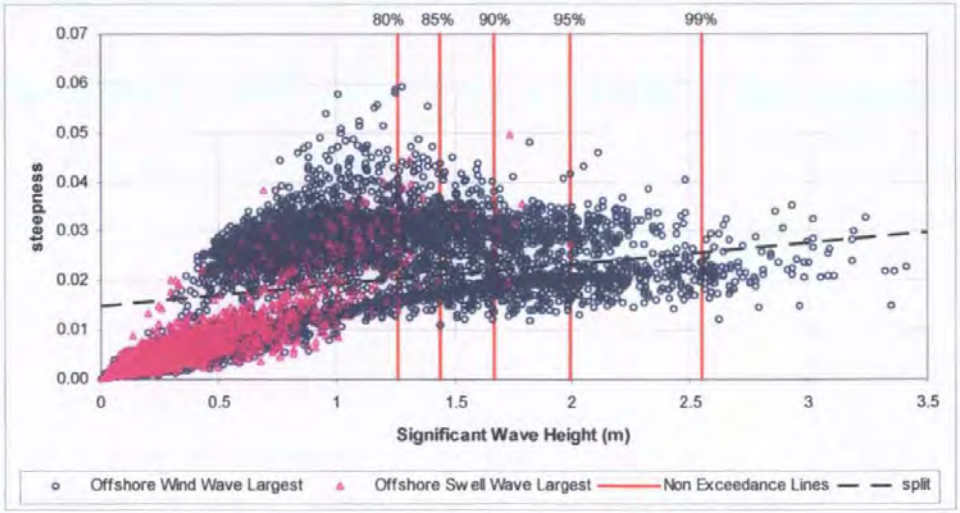


**Figure 5.38** : Significant wave height against wave steepness (+0m@OD Northing coordinate 498240m)

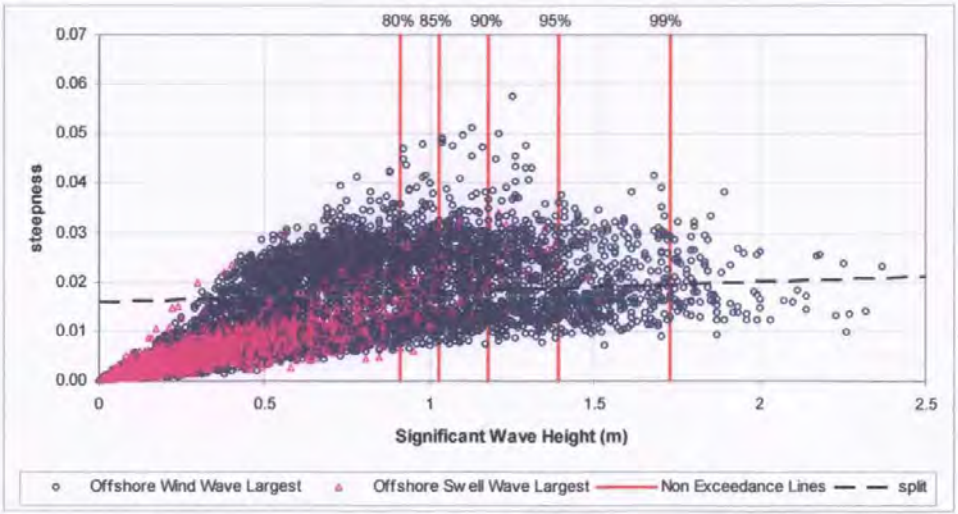


**Figure 5.39** : Significant wave height against wave steepness (+2m@OD Northing coordinate 498240m)

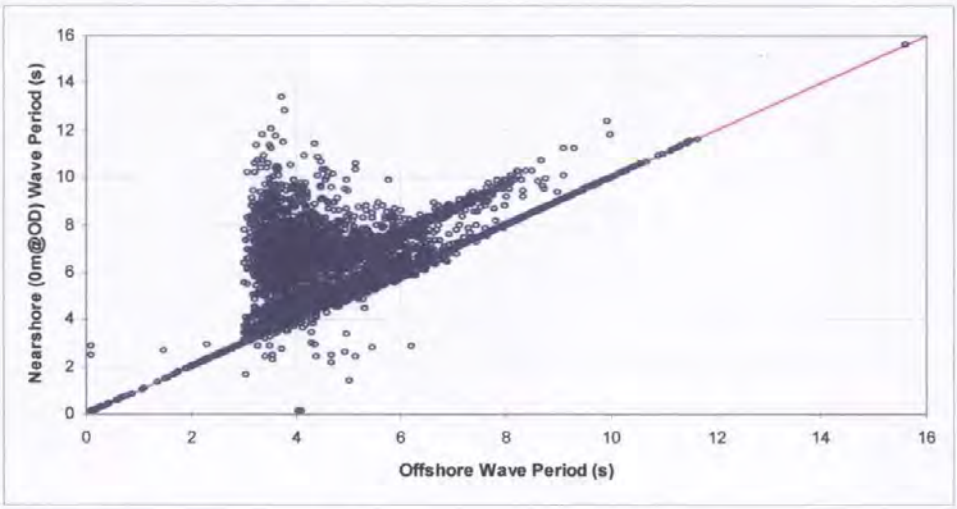


**Figure 5.40** : Relationship between offshore and nearshore wave period (+0m@OD Northing coordinate 498240m)

## 5.4 Joint Probability Relationship

To determine the joint probability between waves and sea levels, 10,000 years of wave conditions (wave heights, sea levels and wave periods) were simulated using the mixture distribution (Equation 2.11). These were then checked for depth limited effects (Equation 4.6). With coastal defence structures along the Cumbrian coastline typically designed to a 50 year standard (and occasionally 100 years), this gave a sample set 100 times the size of the maximum return period event usually considered, and 50 times

the maximum design standard usually considered by the Environment Agency (except for the lower reaches of the River Thames).

Below the individual wave height and sea level thresholds of non-exceedance, values were determined from the general distribution of individual wave height and sea level values. Above the individual wave height and sea level thresholds of non-exceedance, values were determined using the marginal distribution (Equation 2.8).

Return period curves were estimated by 'counting back' through the ranked data in descending order above individual thresholds. So (for example), to estimate the 100 year return period curve using the sea levels, this was estimated by counting back to the $100^{th}$ largest wave height that exceeded the chosen threshold. The same procedure was used for the wave heights giving strong definition in the upper tails of the wave and sea level extremes.

Example results of this analysis are shown in Figures 5.41-5.52 below for two locations (490640N and 546240N). These correspond to regions where data using $MO_2$ dominates (490640N) and where $MO_1$ dominates (546240N).

Conclusions related to these two locations are outlined below. Unless otherwise stated, these conclusions are likely to be generic for any location considered in this study.

1. There is a reduction in marginal extreme wave heights as you move into shallower waters (higher beach levels). This would be expected due to increased depth limitation effects.

2. The most extreme offshore wave heights have the greatest reduction in wave heights for nearshore locations. This would be expected due to nearshore depth limiting effects. This can be seen by considering the three largest offshore wave heights for coordinate 490640m, compared to the offshore wave heights that correspond to the three largest sea levels (Figure 5.41). The largest offshore wave

heights have reduced to approximately 60% of their height at a beach level of -2m@OD (Figure 5.42), yet the offshore wave heights that correspond to the largest sea levels only reduce to approximately 92% of their offshore height until you reach a beach level greater than 0m@OD, where depth limitation effects become more prominent.

3. For both locations, there are a disproportionate number of exceedances of the joint exceedance return period contours for the larger return period events. This should lie somewhere between the case of independence and dependence of the joint events given by, HR Wallingford (2000b):

$$\mu_T = \frac{n_y}{T_{H_s,\eta}} \ln\left(n_e T_{H_s,\eta}\right) \quad \text{for independence}$$

$$\mu_T = \frac{n_y}{T_{H_s,\eta}} \qquad \text{for dependence} \qquad \textbf{(5.2)}$$

where:

$n_e$ number of joint probability events per year

$n_y$ years of observations of joint probability event

$\mu_T$ expected number of exceedances of the $T_{H_s,\eta}$ contour

This is probably as a result of the GPD of the wave heights under-estimating the empirical distributions for the more extreme events, particularly for $MO_2$ (see Section 5.2.2).

4. As the beach level increases, there is a tendency as a result of depth limited effects for the largest wave heights to occur at the largest sea levels. This is consistent with the increased levels of correlation at higher beach and threshold levels as indicated on Figures 5.32 to 5.36.

5. As the beach levels increase, the variation between estimates of different return periods of the marginal extreme wave heights noticeably reduces.

6. At higher beach levels, the joint probability curves become noticeably 'squarer' approaching the extreme sea levels. This would be expected, as due to depth limiting effects, the largest wave heights are more likely to occur at larger sea levels as the beach levels increase.

7. As the beach levels increase, the effect of depth limitation effects can be clearly seen. This is indicated by the maximum wave heights increasing approximately linearly with increasing sea levels.

8. At nearshore locations, changes in wave heights appear to be mainly as a result of depth limitation effects as opposed to other wave processes such as wave shoaling and refraction.

9. The joint probability curves at the two locations are noticeably different for the same beach levels, with location 546240N noticeably more flat approaching the extremes, particularly at the higher beach levels. These shapes are specific to these locations, with the shape being dependent on the location and exposure conditions of the site. This is discussed in more detail in Section 6.6.3.

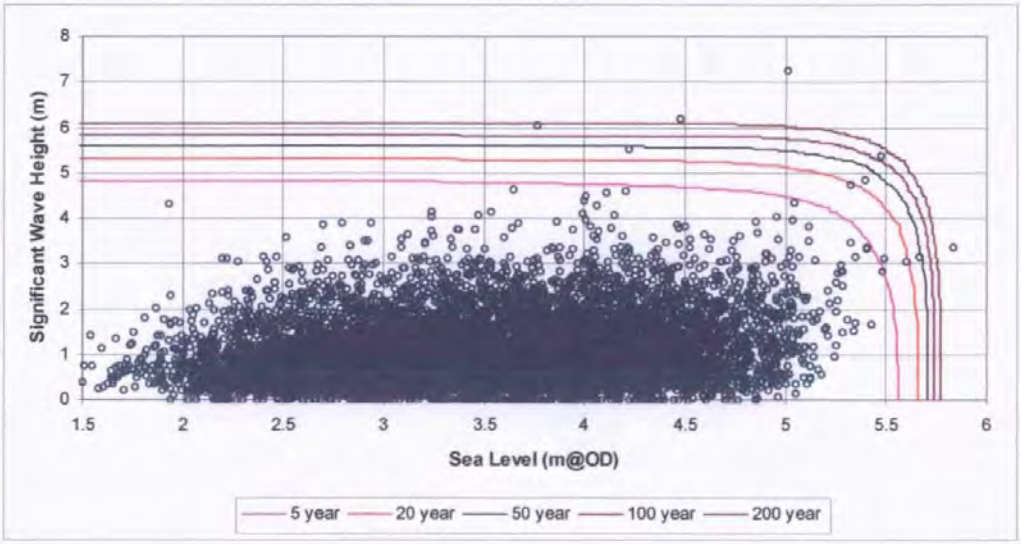


**Figure 5.41** : Joint probability curves for standard return periods (offshore Northing coordinate 490640m)

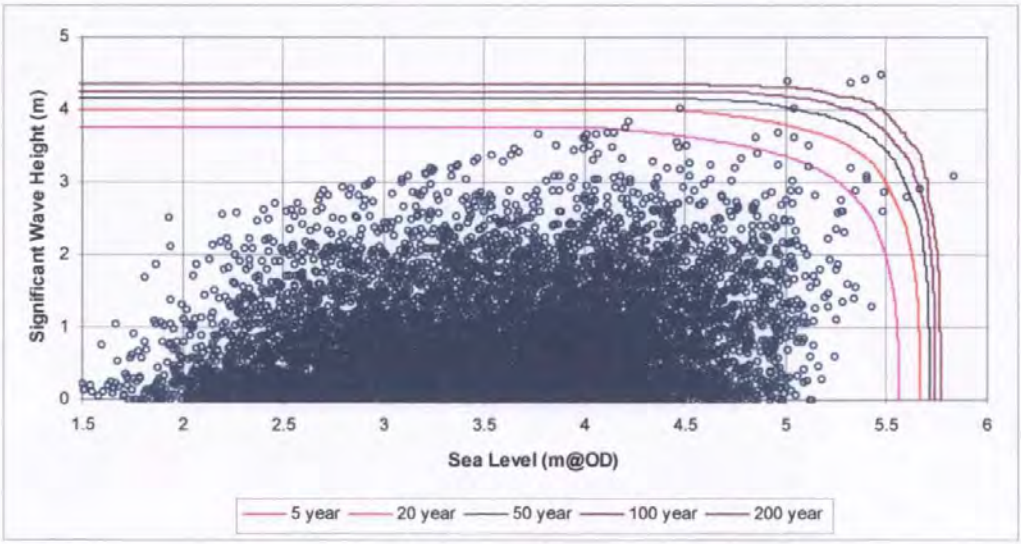


**Figure 5.42** : Joint probability curves for standard return periods (-2m@OD Northing coordinate 490640m)

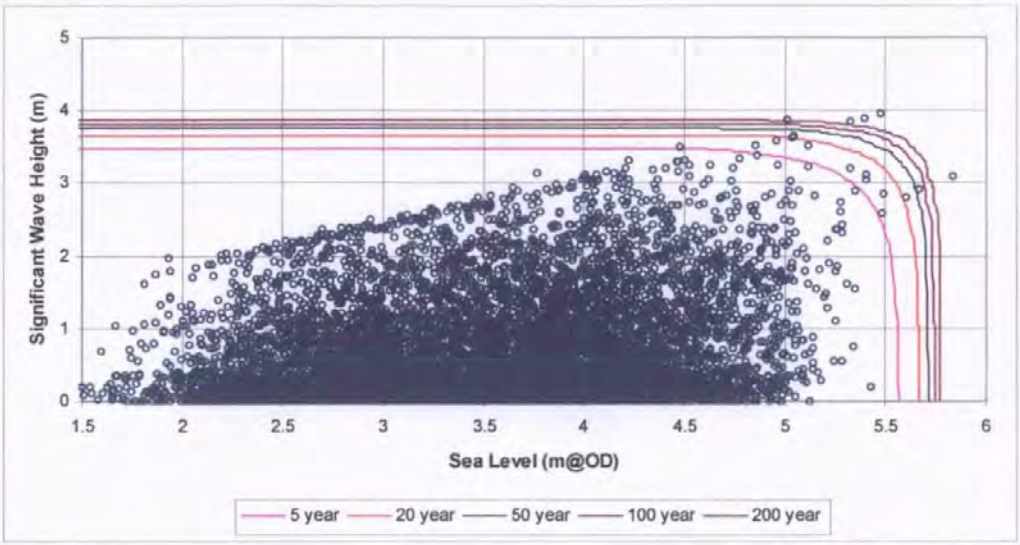


**Figure 5.43** : Joint probability curves for standard return periods (-1m@OD Northing coordinate 490640m)

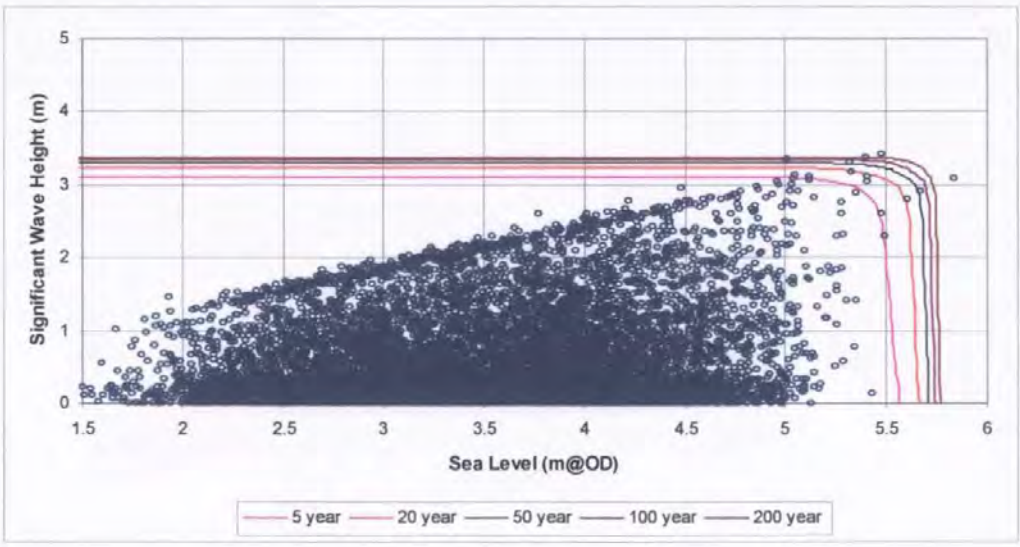


**Figure 5.44** : Joint probability curves for standard return periods (+0m@OD Northing coordinate 490640m)

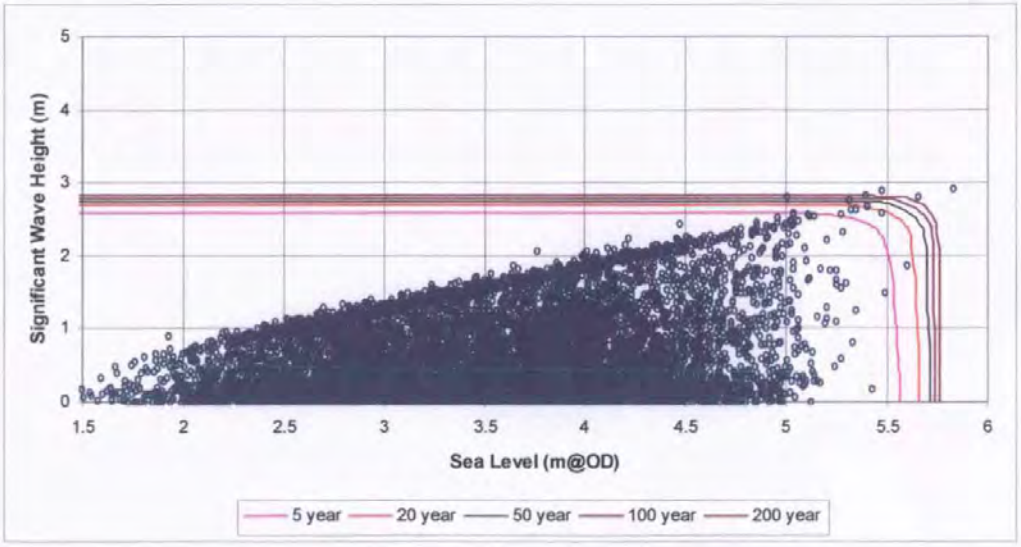


**Figure 5.45** : Joint probability curves for standard return periods (+1m@OD Northing coordinate 490640m)

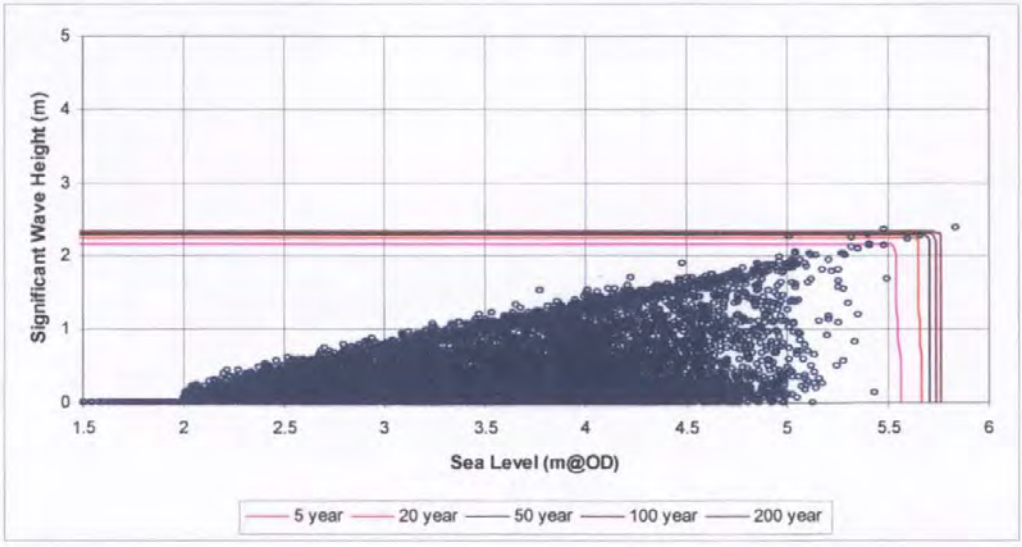


**Figure 5.46** : Joint probability curves for standard return periods (+2m@OD Northing coordinate 490640m)

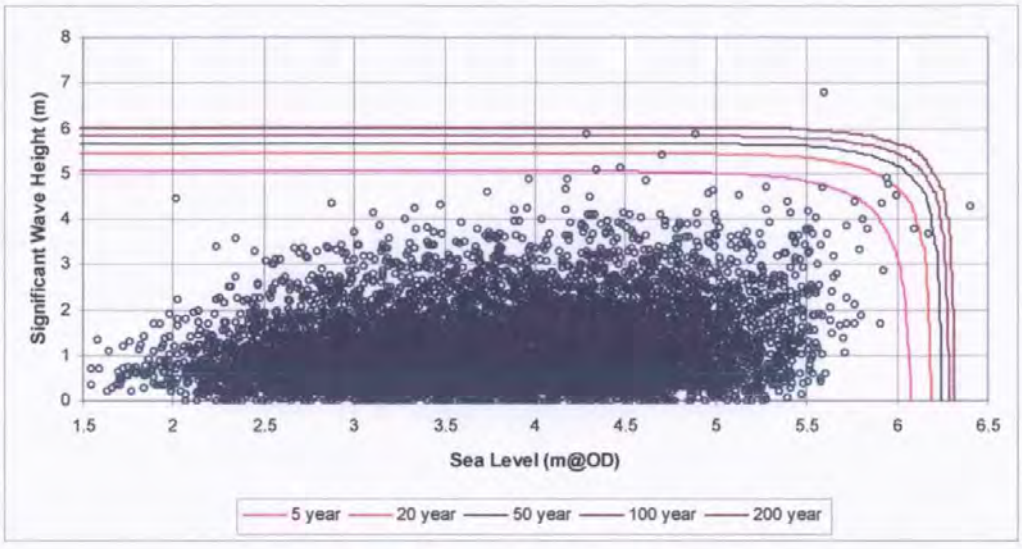


**Figure 5.47** : Joint probability curves for standard return periods (offshore Northing coordinate 546240m)

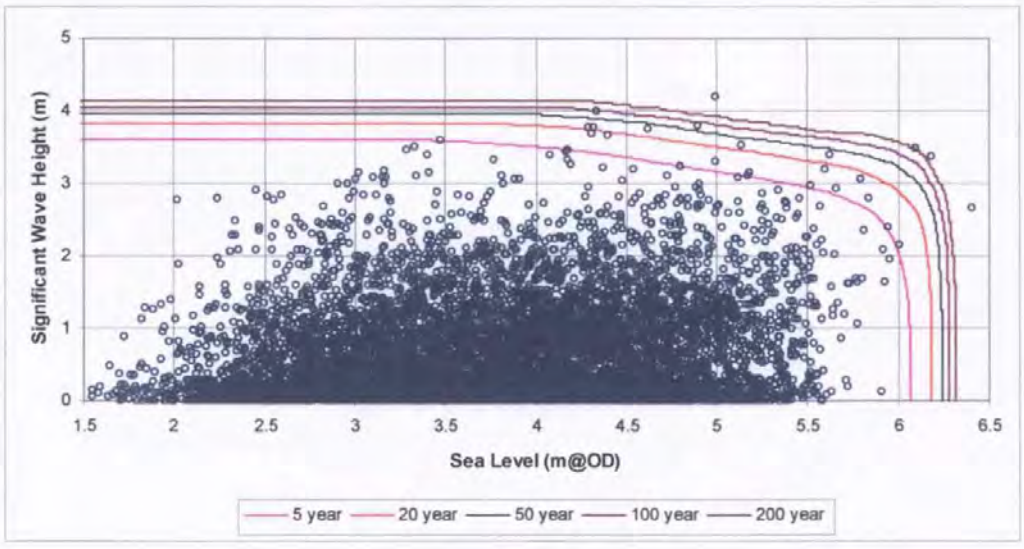


**Figure 5.48** : Joint probability curves for standard return periods (-2m@OD Northing coordinate 546240m)

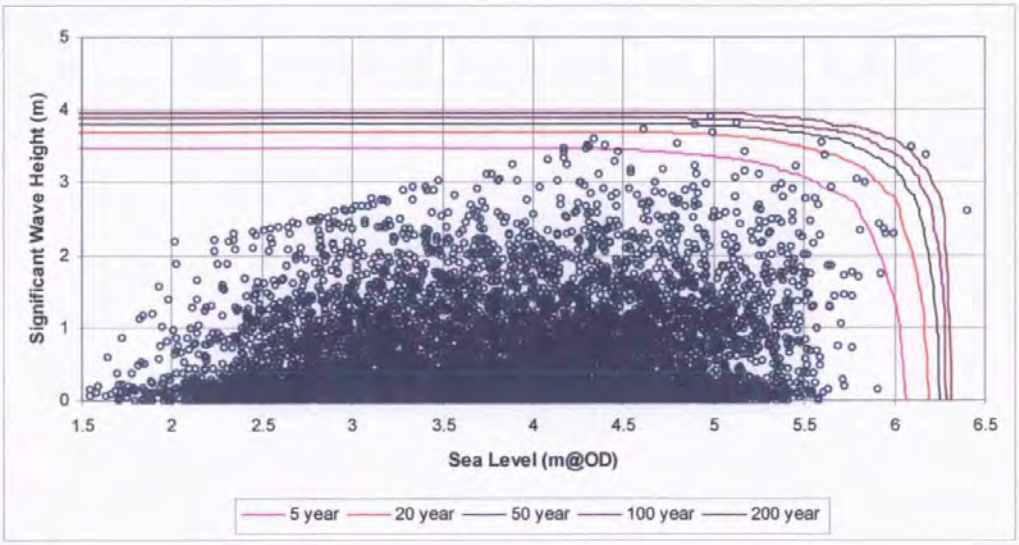


**Figure 5.49** : Joint probability curves for standard return periods (-1m@OD Northing coordinate 546240m)

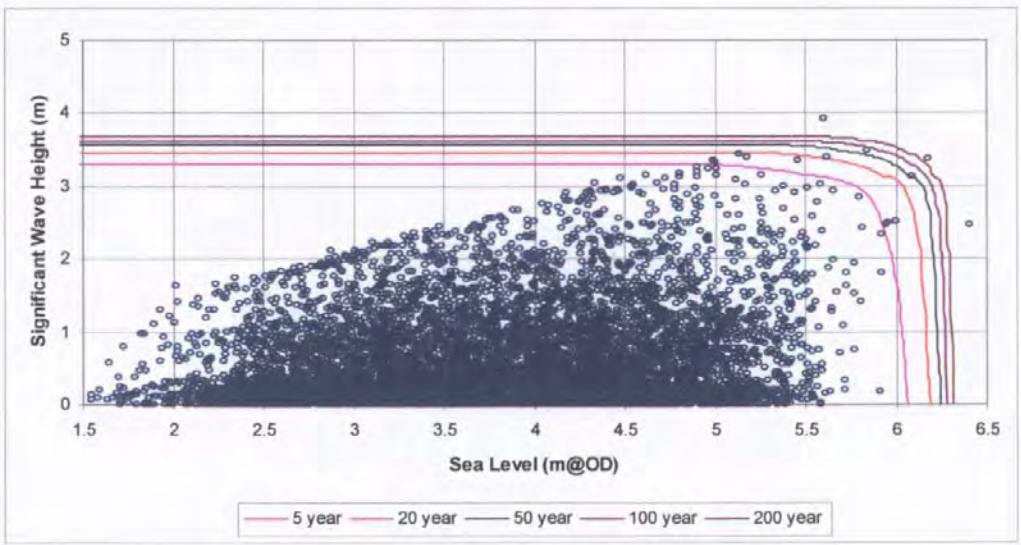


**Figure 5.50** : Joint probability curves for standard return periods (+0m@OD Northing coordinate 546240m)

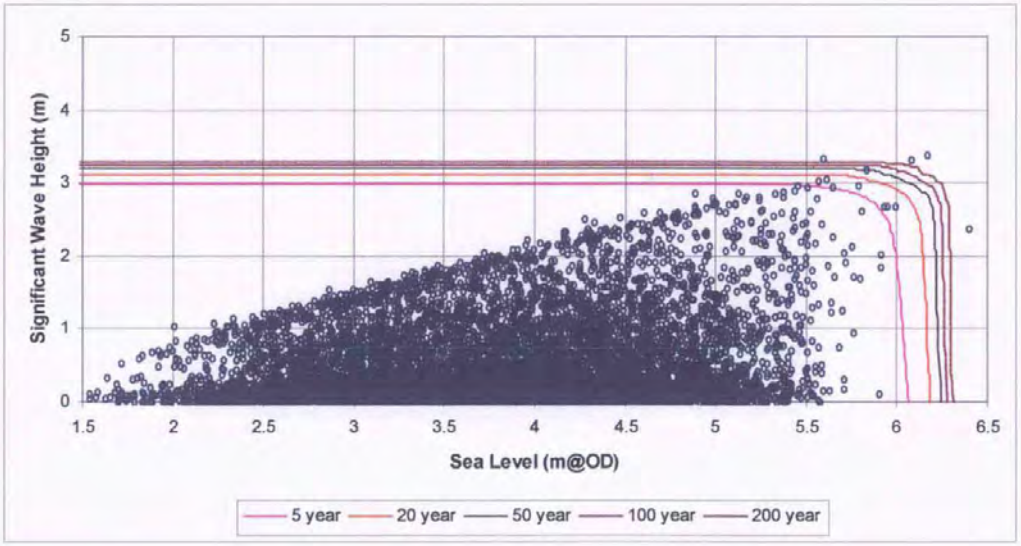


**Figure 5.51** : Joint probability curves for standard return periods (+1m@OD Northing coordinate 546240m)

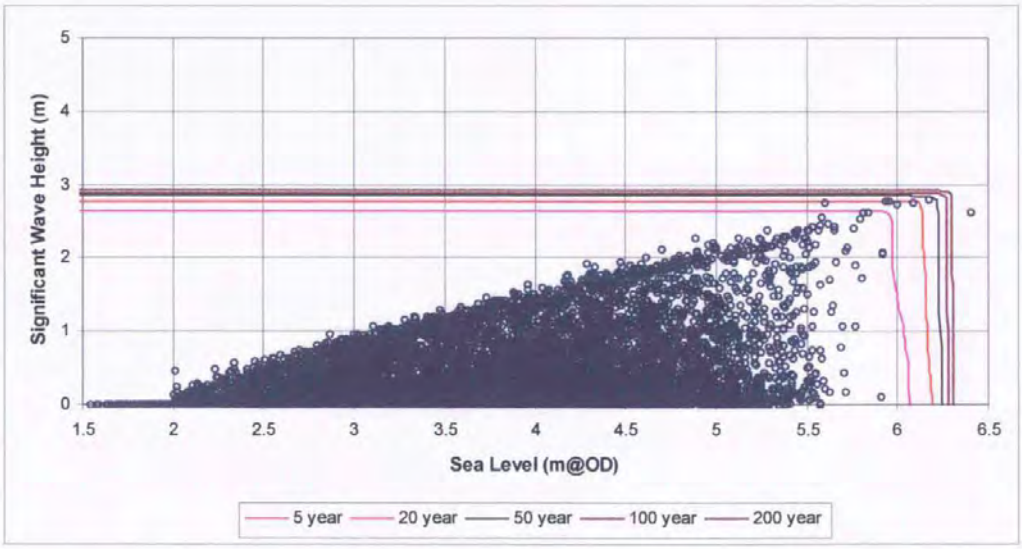


**Figure 5.52** : Joint probability curves for standard return periods (+2m@OD Northing coordinate 546240m)

# 6 Discussion

## 6.1 Introduction

This chapter discusses and analysis the results of the joint probability study carried out on the Cumbrian coastline using the JOIN-SEA approach (see Section 2.6). The discussion has been split into five sections, which reflects the input conditions, modelling approach and the joint probability results outlined in the previous 3 chapters. The first section discuses the quality of the sea level records obtained for this study, and the processing of these records to establish stationary time series records for input conditions into the wave modelling as well as the joint probability data sets. The second section discusses the establishment of the offshore records for use in the wave modelling, including the choice of the array discretisation of the various wave and sea level parameters. The third section discusses the bathymetric modelling of the Cumbrian coastline, and the choice and discretisation of the model grids used to model wave conditions. The fourth section discusses the choice of the WTM used in this study, and the establishment of the model input conditions, considering the sensitivity of the input conditions outlined in Chapter 4. The fifth section discusses the results of the joint probability study, including the model selection (BVN or MIX), the spatial variation in the joint probability relationship at different bed levels, and the accuracy of the JOIN-SEA estimates.

## 6.2 Sea Levels

When this study first started, the only known available records of sea levels along the Cumbrian coastline were the EA digital records at Workington and manually recorded high sea levels of unknown length at Workington, Silloth and Whitehaven. The POL records at Workington were, at this time, not readily available, only becoming available by mid-late 2002 (almost 4 years later). The sea level records at Ramsden Dock, Roa Island and Halfway Shoal were the property of the Ministry of Defence (MOD) and, as a consequence, their mere existence let alone their supply was confidential. However, these records were obtained, with the author at the time being

unaware of any confidentiality issues. However, confidentiality issues with regard to these data sets no longer exist. Awareness of the manually recorded sea levels at Ramsden Dock came too late for them to be considered for this study.

The digital records at Workington were supplied by the EA as checked, with incorrect or suspect data flagged. Further checking of these records by the author indicated that a number of discrepancies were present in this data set including, for example, data incorrectly marked as checked or suspect. This is demonstrated in Figure 6.1 which shows data recorded by the EA over a 2-day period (an EA 'tidal day' runs from 9:00 one day until 8:45 the next). These records are marked as checked, yet contain a period of approximately 1 day where the sea level is incorrectly recorded approximately 0.8m too high, as well as a sudden dip at the start of the 2nd 'EA' day.

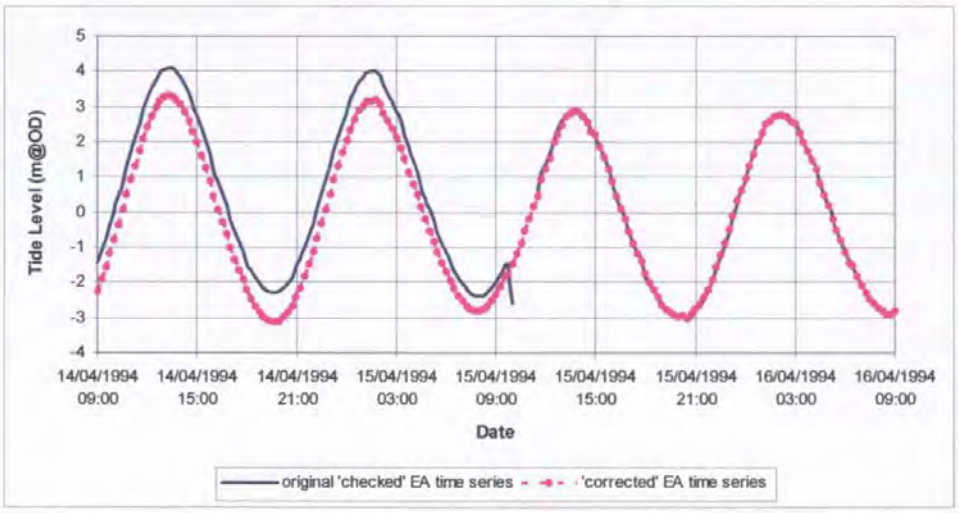


**Figure 6.1** : Typical 'checked' time trace recorded by EA

Quality flags, as with all other digitally recorded data sets were therefore only used as a guide and where possible, the EA data set was corrected so as to maintain as long a data set as possible. With this being the only known readily available record of digitally recorded sea level records along the Cumbrian coastline at the start of this study, it was deemed imperative that as much data as possible was retained. The general processing that was carried out on this data set, as well as subsequent digitally recorded data sets, is detailed in Section 3.2.3. Detailed information on the quality of

the data sets, including the typical errors detected is not given here, but is detailed in Hames et al (2004).

With the subsequent acquisition of the POL data set at Workington, and the manually recorded high sea levels at Workington, this gave three sets of independent records of sea levels at Workington. Initial problems were experienced 'detrending' the EA data set (see below), and there was an apparent under-recording of the sea level in the POL data set. The manually recorded high sea levels were therefore used as the basis for checking these records as this consisted of a time series of mutually independent records unaffected by mechanical or digital problems. With these records being used in Port operations every day, incorrect readings would have either been as a result of incorrect logging of the sea level, estimated by Hames et al (2004) to be approximately every 750-1500 readings, or within the normal bounds of error appropriate to the recording method. This was estimated by Hames et al (2004) to be 0.1-0.2m 90% of the time. An incorrect datum for the tide board, although possible, would soon get picked up by normal everyday Port operations.

The checking that was carried out on the POL and EA records was outlined in Hames et al (2004). This compared the difference in surge between the manually and digitally recorded high sea levels based on a 3 month moving average (see Figure 6.2). This comparison indicated that the POL data set had initially been set up to an incorrect datum, which had changed 3 times over the life of the gauge (see Section 3.2.2). Subsequent re-levelling of the POL tide gauge indicated that the gauge was under recording by 0.18m since approximately 27/05/94, and sea levels from this date were corrected accordingly. Under recording of sea levels prior to this date were estimated based on an analysis of Figure 6.2 and are outlined in Section 3.2.2. Although POL have subsequently corrected their sea level records, sea levels prior to 27/05/94 were incorrectly increased by 0.18m. POL have been made aware of the errors in sea level estimates prior to this date, although no response has been received as yet (see Section 3.2.2).

the data sets, including the typical errors detected is not given here, but is detailed in Hames et al (2004).

With the subsequent acquisition of the POL data set at Workington, and the manually recorded high sea levels at Workington, this gave three sets of independent records of sea levels at Workington. Initial problems were experienced 'detrending' the EA data set (see below), and there was an apparent under-recording of the sea level in the POL data set. The manually recorded high sea levels were therefore used as the basis for checking these records as this consisted of a time series of mutually independent records unaffected by mechanical or digital problems. With these records being used in Port operations every day, incorrect readings would have either been as a result of incorrect logging of the sea level, estimated by Hames et al (2004) to be approximately every 750-1500 readings, or within the normal bounds of error appropriate to the recording method. This was estimated by Hames et al (2004) to be 0.1-0.2m 90% of the time. An incorrect datum for the tide board, although possible, would soon get picked up by normal everyday Port operations.

The checking that was carried out on the POL and EA records was outlined in Hames et al (2004). This compared the difference in surge between the manually and digitally recorded high sea levels based on a 3 month moving average (see Figure 6.2). This comparison indicated that the POL data set had initially been set up to an incorrect datum, which had changed 3 times over the life of the gauge (see Section 3.2.2). Subsequent re-levelling of the POL tide gauge indicated that the gauge was under recording by 0.18m since approximately 27/05/94, and sea levels from this date were corrected accordingly. Under recording of sea levels prior to this date were estimated based on an analysis of Figure 6.2 and are outlined in Section 3.2.2. Although POL have subsequently corrected their sea level records, sea levels prior to 27/05/94 were incorrectly increased by 0.18m. POL have been made aware of the errors in sea level estimates prior to this date, although no response has been received as yet (see Section 3.2.2).

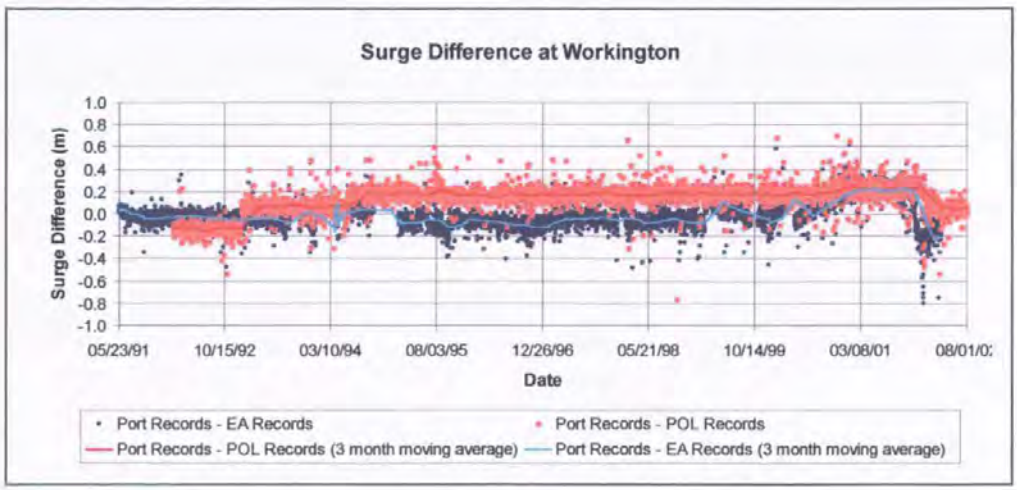


**Figure 6.2** : Comparison of manual and digital surge records at Workington (Hames et al 2004)

For the EA tide gauge, it was clear from Figure 6.2 that there was a severe problem with the sea level measurements at this location. The 'mean' sea level was clearly variable. Typically it was 0.05 to 0.15m too high until about 1999, and highly variable, up to 0.20m too high or low, after this date. However, the variable nature of the 'mean' sea level, masked to an unknown degree by the 3-month moving average shown on Figure 6.2, meant that problems with the EA tide gauge were not originally picked up by the visual comparison with predicted records. This was in contrast to the POL readings, where problems were immediately identified as a result of consistent and long term apparent negative surges.

The time series of high sea levels for Workington was therefore established based on the corrected POL time series. This showed good agreement to the Port records, yet would not have the variability observed in recording sea levels manually. Also as part of the UK National Network of 'Class A' tide gauges, these records would be expected to meet the GLOSS standard of 1cm (Woodworth et al, 2004). This was confirmed recently for the type of gauge used at Workington by Míguez et al (2005) based on a comparison of 7 different tide gauges over a period of 6 months at the port of Vilagarcía in Spain.

Despite the problems with the EA tide gauge, it was observed that EA records could be considered to have a locally constant datum if averaged over a period of several days as indicated on Figure 3.2. Based on this assumption, the EA record usually showed very strong agreement to the POL records. This meant that EA records could be used to compare against POL and the Port readings, and where necessary be used to fill any gaps. Where both the POL and EA records were missing (few records), the Port records were used after surge records were checked against the manual readings at Silloth and Whitehaven.

Figure 6.3 below shows the comparison between the sea level record used for Workington and the Port records. Although this indicates apparent good agreement between the records, there is a noticeable scatter in the region ±0.18m. This is a considerable scatter for the measurement of sea levels at the same location, especially when compared to the comparisons of the digital records at Ramsden Dock, Roa Island and Halfway Shoal (Figures 3.4-3.6). These show significantly less scatter, yet are 4-8km apart. Comparing the sea level record used for Workington with the sea level record used for Barrow (Figure 3.7) gives a similar level of scatter to Figure 6.3. With these two locations over 70km apart, this indicates that the use of the POL data set as the basis to describe sea level conditions at Workington was correct.

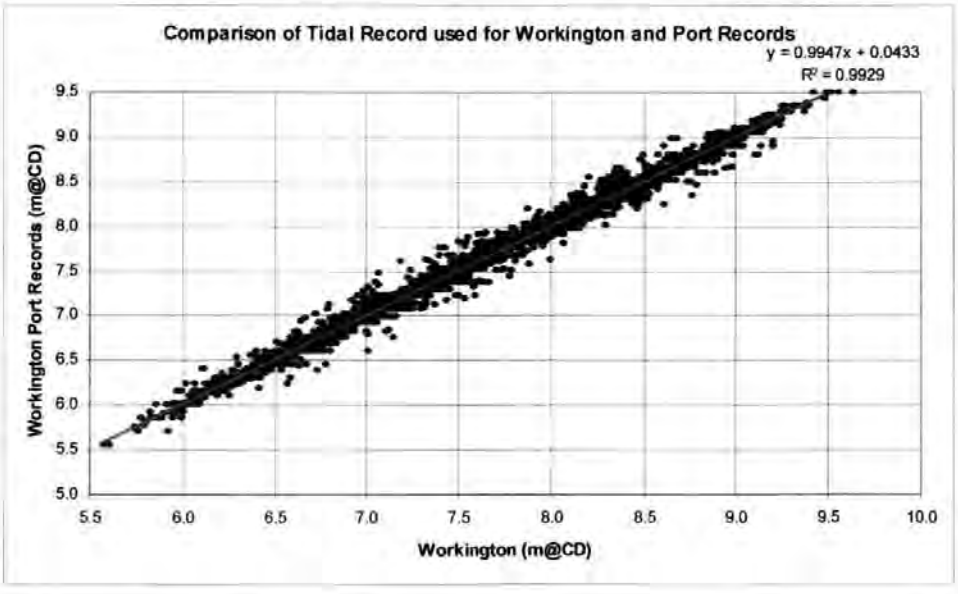


**Figure 6.3** : Comparison of sea level record and port records for Workington

The digital records supplied by ABP for Ramsden Dock, Roa Island and Halfway Shoal were supplied in the form of one file per day, with one subdirectory per month and year per location. Two records (in millimetres) were recorded for each location every 4 minutes by two gauges. This gave in the region of 9,600 files and 1,600 sub-directories. It is believed that this full data set had never been analysed before, and apart from a few periods, none of the digital records had even been looked at. The format of the data supplied is shown in Table 6.1. Therefore for example, the sea level recorded by the 2nd gauge at Ramsden Dock at 22:08 on 07/08/92 was 4.448m.

```
Ramsden dock data.
FRI  07 08 92 00 2611 2607|2614 2610|2616 2611|2623 2618|2635 2630|
                 2653 2648|2675 2669|2691 2686|2719 2713|2752 2748|
                 2784 2778|2818 2814|2850 2844|2883 2879|2927 2921|

FRI  07 08 92 01 2973 2967|3019 3013|3067 3062|3113 3108|3162 3157|
                 3217 3213|3277 3271|3337 3332|3401 3396|3471 3466|
                 3544 3538|3616 3611|3686 3681|3754 3751|3827 3823|
                                    .
                                    .
                                    .
                                    .
                                    .

FRI  07 08 92 22 4575 4570|4515 4509|4454 4448|4397 4391|4335 4330|
                 4271 4265|4206 4200|4145 4139|4093 4088|4043 4037|
                 3986 3981|3935 3929|3869 3862|3804 3798|3747 3741|

FRI  07 08 92 23 3692 3687|3642 3636|3596 3591|3547 3541|3501 3495|
                 3461 3455|3415 3410|3369 3363|3325 3320|3283 3277|
                 3248 3243|3212 3207|3172 3166|3127 3121|3082 3077|
```

**Table 6.1** : Typical format of recorded sea levels, Ramsden Dock 07/08/92

However, extracting the sea level records for analysis was not straightforward. Approximately 40% of the files were formatted incorrectly, with many erratic readings (some were even in the wrong sub-directory). An example of this is shown in Table 6.2 which is a sample of the original record from Ramsden Dock for 19/06/94. This shows how the sea level for the first hour is replicated twice, with the second occurrence offset. The first occurrence contains a number of erratic readings. For example, a reading of -11.995m at 00:04 is given by the first gauge, which is given as 2.857m for the second occurrence, compared to the predicted value of 2.530m. Therefore, before any pre-processing could be carried out, all files

that contained incorrect formatting had to be identified and manually edited with codes added to indicate any changes made. Where difficulty was experienced in identifying correct records, the predicted tide was used to indicate the likely sea level and gradient at any point in time. This whole process (including the pre-processing) took in the region of six months. However, with 3 sets of records available at this location and two gauges per location, a potentially very reliable long term record of sea levels was available for Barrow.

```
Ramsden dock data.
SUN  19 06 94 00 2869 2846|-11995 17166|27887 -96|5742 2728|32595 →
                 14679 -26717|30372 4476|27887 -217|5611 16933|170→
                 21469 -14856|-11800 27864|8241 -647|2658 2630|208→
                 SUN  19 06 94 00 2869 2846|2857 2835|2827 2804|27→
                 2718 2700|2721 2703|2682 2663|2682 2663|2662 2638|
                 2649 2628|2675 2644|2666 2637|2640 2615|2658 2630|

SUN  19 06 94 01 2665 2643|2651 2627|2688 2665|2663 2642|2676 2657|
                 2700 2677|2710 2696|2731 2714|-25007 9958|2770 27→
                 2802 2781|2835 2816|2863 2839|2884 2863|2903 2888|
                                    .
                                    .
                                    .
```

**Table 6.2** : Incorrectly formatted sea level records, Ramsden Dock 19/06/94

With these three records of sea levels in close proximity, it was decided to combine these into one data set based on the data set at Ramsden Dock (termed Barrow). Similar to Workington, this gave three records of sea levels at one location, although this time all digital. Although a further manual record of high and hourly sea levels is available at Ramsden Dock, awareness of this record came too late for it to be included in this study.

For all three locations, a difference in pressure was observed between the two gauges. It is believed that these pressure differences are a combination of the tidal currents over the gauges, and a pressure gradient as a result of the gas viscosity in the tubes to the pressure devices. This variation for high sea levels is of the order of 16mm at Halfway Shoal, and 2mm at Ramsden Dock and Roa Island. The effect of this variation, and any other unknown drop in pressure on sea levels is not known. However, any variation would be expected to affect mean sea levels which for Ramsden Dock did not appear present, although likely only to be of the order of a few millimetres. This is indicated by Figure 3.3 which looked at

the pdf of surge at the composite Ramsden Dock and Workington records. This indicated that neither of the two records were under or over recording relative to each other. Sea level records at each location were based on the mean of the two gauge readings, or one where one reading was missing.

Before combining the sea levels at Barrow, a visual comparison of the sea levels for the six gauges (three locations, two gauges per location) identified any anomalies which were either deleted or corrected (see Section 3.2.3). This included large sections in particular of the Ramsden Dock record that had to be discounted as a result of siltation. Gaps in the Ramsden Dock record were filled using the linear relationship given by Figure 3.4 for the Roa Island sea level record or where not available, by the linear relationship given by Figure 3.5 for the Halfway Shoal sea level record. These figures showed very strong agreement between the sea levels at these locations, indicating that given the sea level at either Roa Island or Halfway Shoal, the sea level at Ramsden Dock could be estimated with a large degree of confidence. The effect of the pressure differentials at Halfway Shoal or Roa Island was not important as its correction for Ramsden Dock was inherent in the linear relationship given.

For Silloth, only manual records were available. Like Workington and Whitehaven, these consisted of high sea level values that had never been digitised before. Manual sea levels at Silloth are available from 01/11/87 to date, and these were digitised and analysed until 31/10/04. Only one record from this period was missing. An assessment of the likely error in the recording of the sea levels at Silloth was made by Hames et al (2004) based on an analysis of surges from all eight records of sea levels analysed in this study. This indicated that sea levels at Silloth were recorded to an accuracy of 0.17m approximately 90% of the time and were recorded in error by 0.5m and above approximately 0.05-0.10% of the time (i.e. every 1000-2000 recordings). They also indicated that sea levels were on average recorded accurately, within 5cm, the smallest measured increment, although measurement errors of +0.5m and above were likely when offshore winds were greater than about 21m/s.

A comparison of high sea levels at Silloth and the composite record for Workington indicated that the agreement was not as strong as the comparison between high sea levels at the composite Ramsden Dock and Workington records. This would have been as a result of the expected scatter of manually recorded sea levels as indicated above and for Workington on Figure 6.3. This would not be expected on reliable digitally recorded data sets, as indicated on Figures 3.4-3.6 for the Barrow locations. Considering the location of the Ports of Silloth and Workington and their exposure conditions and orientation in relation to Ramsden Dock, this lower level of agreement was not considered likely. This indicated (as suggested in Section 3.2.4) that given the sea level at Workington, the linear relationship given by Equation 3.1 in Section 3.2.4 would show better agreement to the 'actual' sea level at Silloth than the manually recorded sea level. This linear relationship was therefore adopted at Silloth.

For Whitehaven, manually recorded records were available from 01/04/91 until 31/08/98 which were collected and digitised. These records are now believed to be lost, which means that the records considered in this study are the only known records of recorded sea levels at Whitehaven over this period. Sea levels at Whitehaven are now recorded by radar reflection at three locations, and these are believed to have been recorded since 01/09/98. Unfortunately during the course of this study it has not been possible to establish ownership details of these records, and therefore they could not be obtained. The records at Whitehaven were of significantly poorer quality than the records similarly collected at Workington and Silloth with a significant number of incorrectly translated sea levels. An assessment of the likely error in the recording of the sea levels by Hames et al (2004) indicated that sea levels at Whitehaven were recorded to an accuracy of 0.19m approximately 90% of the time and were recorded in error by 0.5m and above almost 1% of the time, which is a significant error rate. Despite this, sea levels at Whitehaven were on average recorded accurately (within 3 inches, the smallest measured increment). However, unlike Silloth, there was no noticeable increase in measurement errors when strong offshore winds were present, which is probably as a result of the more sheltered location of the tide board at Whitehaven compared to Silloth.

Similar to Silloth, a comparison of high sea levels with the composite record for Workington indicated that the agreement was not as strong as the comparison between high sea levels for the composite Ramsden Dock and Workington records. This was also the case for the comparison given above for Silloth. Therefore for the same reasons given for Silloth, the linear relationship given by Equation 3.2 was therefore adopted at Whitehaven.

For the spatial variation in sea levels along the Cumbrian coastline, tidal similarity was assumed between the secondary ports of Maryport and Workington, and Tarn Point, Duddon Bar and Barrow. The linear variations were based on predicted tides from POLTIPS.3 (POL, 2001) and standard tides from the Admiralty Tide Tables (2001), which are given in Section 3.2.4. A linear variation in sea levels was assumed between all locations based on the Northing coordinate. Quality of tidal estimates at secondary ports is highly variable. Estimates could be determined based on observations over a month or more, or on a few hourly records of sea levels. The quality of the tidal estimates at Maryport, Tarn Point and Duddon Bar are not known. However, a comparison of the sea levels used in this study for Silloth and Whitehaven (which are also secondary ports) indicate, that for these locations, tidal similarity would on average under and over estimate the sea levels by approximately 0.23m respectively (with a standard deviation of about 0.11-0.12m). This is a significant difference, and it is likely given the less strategic importance of Duddon Bar and Tarn Point in particular that potential errors for these locations could be even greater. This potential is magnified by the fact that the relationship between Chart and Ordnance Datum at these two locations is not known, and has had to be estimated based on an assessment of standard tidal conditions at Workington and Barrow. However, for the reasons given in Section 1.1, this study has concentrated on best estimates for the joint probability relationship (and therefore sea levels). The effect on any potential error in the sea level estimates on the joint probability relationship is covered in more detail in Section 6.6.5. With no further information known on the spatial variation of sea levels along the Cumbrian coastline, a linear variation between known, or predicted tides was assumed to be correct.

Sea levels along the Cumbrian coastline, like all time series of sea levels around the world, are not stationary. This can be as a result of several different factors, but which for the Cumbrian coastline are as a result of rising sea levels (common to all sea level records) and isostatic rebound. A third factor, ocean tide loading, is a sinusoidal motion at the same frequencies and relative amplitudes of tidal forces and is inherent to different degrees in all sea level records. Its effect therefore does not need to be considered, although for Cumbria it is less than 5mm due to its proximity to an amphidromic point (Dwarko 2004). Standardisation of time series to a set date therefore has to be carried out before further analysis, which for this study was set to the start of 2004 (see Section 3.2.5).

To estimate secular trends in the time series, a low pass filter was applied to the two time series data sets at Workington, and the three time series data sets at Barrow. Gaps were filled by assuming a linear variation in the surge between missing records, and different cut-off frequencies were analysed. The trend was estimated by fitting a best-fit line to the remaining time series, with the data used to fill any gaps removed. This would leave only high frequency terms which would include any trend. Trends using this approach could not be applied for the manually recorded records as more than two records are required for the lowest frequency (the Nyquist frequency).

Initially, this analysis could only be carried out on the EA data set at Workington and the three Barrow locations. At the time, the problems that existed with the EA data set were not known, and as a result considerable difficulty was noted in achieving reliable estimates of trends at Workington. As more data became available, estimates of trends became more variable, particularly as data towards the end of 2001 was added. Trends for the Barrow locations were less erratic, however, with records every 4 minutes, and the relative slow computing power at this time, individual runs could take a considerable time. Increasing the digitisation was not considered as although reducing the run time, would reduce the accuracy of the results. With the acquisition of the POL data set for Workington, clear and immediate problems with the datum resulted in checks on the time series,

together with the EA record, against the port records. As stated earlier, manually recorded sea levels are mutually independent and any datum error would have quickly been identified as a result of normal Port operations. This time series could therefore be considered as a reliable, although slightly erratic measure of sea levels over a long term basis. Despite the significant scatter observed (see Figure 6.2), the 3-month moving average clearly identified the problem with the EA records that had not previously been identified. This also indicated that the determination of a trend of a few millimetres in a time series that oscillated randomly by tens of cms was indeterministic. Analysis of the trend for the EA gauge at Workington was therefore not continued. For the POL time series at Workington, the trend was determined over the period June 1994 to October 2004. Data prior to June 1994 was not considered as it was based on an estimated datum. The trend was determined based on hourly records as 15 minute records were not originally released.

Based on the trend analysis carried out, Table 3.3 shows the secular trends determined for the four locations considered for both the recorded sea level and the surge record. This indicated some consistency for the recorded sea levels at the Barrow locations, but overall, no clear indication of the likely trend. However, these records are of relative short length, and trying to determine a trend amounting in total to approximately 20-40mm for regions with tidal ranges of 10m is likely to have a large error band. Eustatic trends were therefore estimated based on published mean sea levels for the Irish Sea, values estimated in this study, and past (and short term) future estimates of trends based on published information. Eustatic trends were determined by subtracting estimates of isostatic rebound at each location.

Based on published information of trends, the general consensus is that over the last 100 years, eustatic sea levels have increased by 100-200mm. This is the conclusion of the IPCC (2001), and coincides with nearly all studies carried out on this topic over the last 10-20 years (see Section 3.2.5). The trend rate is generally agreed to be increasing with time, although little work is available to indicate the trend over the last 10-15 years. Based on published work by the IPCC (2001) and others outlined in

Section 3.2.5, it is likely that over the period considered for this study (1991-2004), secular trends are in the region 1.5-2.5mm/years. Indeed, interpretation of results presented by Woodworth et al (1999) indicates that currently sea levels at Liverpool are increasing by approximately 1.8mm/year. Based on the analysis carried out, and past published information, it was felt likely that sea levels are currently rising at a rate of 2mm/year ±0.5mm/year, and a trend of 2mm/year was therefore assumed. The estimated error band of ±0.5mm/year was not significant, as it would only lead to a maximum error in the estimation of sea levels of up to 7mm. Isostatic rebound rates were taken from rates for the British Isles by Shennan (1989), and these, together with standardised trends applied to all data sets are given in Section 3.2.5.

Based on the availability and assessment of sea level records along the Cumbrian coastline, sea level records for a joint probability assessment were considered over the period 23/05/91 to 31/10/04. This matched the start of the EA tide gauge at Workington, and corresponded with the period when predictions from the Met Office's European model of wave predictions began. Although digital records from the POL tide gauges at Workington and the Barrow locations (Ramsden Dock, Roa Island and Halfway Shoal), were not available until early-mid 1992, checks on the EA gauge at Workington with port records over this period indicated that EA records over this period were acceptable. For Ramsden Dock, siltation problems mean that readings since 07/01/01 are considered unreliable, and were therefore not considered for this study. With readings from the Halfway Shoal tide gauge ending on 31/05/01, sea levels for Barrow after this date (and before May 1992) were estimated using the linear relationship given in Figure 3.7. The increased length of data that was available by using the EA dataset prior to the start of the POL and Barrow datasets, and the linear relationship for Barrow from June 2001 onwards increased the length of record to be analysed by over 4 years. The advantages of this increased record length were considered to far outweigh any disadvantage due to any potential loss of accuracy in sea level estimates. The finish date of 31/10/04 was chosen as it was the latest date that it was considered practical to enable the results to be based on the longest recorded data set possible.

## 6.3 Offshore Wave Records

Offshore records have been specified using data predicted by the Met Office wave model. This supplies data in the form of wind, swell and resultant wave heights, together with wave zero crossing periods and wave directions. Wind speed and direction were also supplied, but these were not explicitly used in this study.

The Cumbrian coastline is covered by three Met Office wave prediction points, which are shown on Figure 3.10. However only two points (the northern and southernmost points) were acquired for this study as it was felt that little benefit would have been achieved with the third, despite the increased confidence that data from this point would have had on predictions. This decision was also driven by commercial considerations, with data used in this study originally purchased for use on the Shoreline Management Plans in this area (Bullen Consultants 1999a and 1999b). No other long-term records of offshore data are believed to exist. Interpolation between Met Office data points to specify offshore conditions for each data point was considered based on a linear interpolation of offshore wave direction at each point as demonstrated on Figure 4.8 (Section 4.7). There were several periods of missing data for the Met Office records, which are outlined in Table 3.9. These are heavily weighted to the winter months when more extreme conditions would be expected. However, with missing records only accounting for approximately 1% of the total record, it is unlikely that these missing records would result in reduced extreme predictions. No correction was therefore considered or applied to the records or results to account for missing data.

Unlike the sea level data, no pre-processing of the Met Office wave data could be carried out. Although the Met Office do verify model predictions against observations from moored buoys and weather ships (Met Office 1995), no verification points exist in the vicinity of the Irish Sea. However, the accuracy of the Met Office model for $MO_2$ was validated against actual wave measurements by Reeve and Bin (1994), who concluded that model predictions provided a reasonable estimate of the measured wave climate

(see Section 3.3.3). Validation of the predictions for this study could have been made against the wave measurements by Reeve and Bin with a slight modification of the software used. However, this would have significantly added to the total run time of the model runs and was therefore not practical[1]. This could be looked at in the future as results are available, although not easily extracted. However, this is not currently recommended, unless some future doubt is expressed on the wave modelling or the interpolation.

The Met Office wave model is based on a coarse grid which does not include the Isle of Man. This is shown on Figure 6.4 which shows the approximate position of the Met Office coastline superimposed on a map of the United Kingdom.

[1] Computational run times in this study were considerable (as discussed in Section 4.6.1). A judgement therefore often had to be made on the benefit of individual runs, and their perceived importance to this study. In some cases, as was the case here, some results were not pursued as this could have noticeably hampered the production of results.

**Figure 6.4** : Approximate position of Met Office coastline superimposed on UK coastline

With the most significant wave activity from the south-west quadrant, it is not likely that the absence of the Isle of Man will significantly affect results along the Cumbrian coastline as it does not directly interfere with wave activity from this quadrant (see Figure 4.5). However, significant wave activity from the east coast of Ireland would be over-predicted for regions below St. Bees Head, which is sheltered from the west by the Isle of Man.

For this region, the most extreme wave heights are likely to emanate from the south-west quadrant, therefore over-predictions for waves from the west should not noticeably affect the joint probability relationship. However, sample model output given in Appendix C indicates that waves from the west may produce the most significant wave activity above St Bees Head (Figures C.4 and C.7). Although the Isle of Man would not be anticipated to noticeably affect these waves, it is possible that extreme wave heights above St Bees Head may be over-predicted, resulting in an over-estimate of the wave heights in the joint probability relationships.

Applying an offshore boundary south of the Isle of Man may have been appropriate. However, little benefit would have been achieved, and this was not practical as current computing power would not have been able to cope with the grid size or number of runs required. It may be appropriate to consider the effect of the Isle of Man on predictions in the future, however, this is not currently recommended due to the intense computing power that would be required to match, or replace the results in this study.

The Isle of Anglesey is represented as part of the mainland in the Met Office model. However, the southern area of the Island, a distance of 23km, is only 180m to 3.2km from the Welsh mainland. Its effect on waves propagating from the Atlantic Ocean will therefore in reality be the same whether the Island was attached to the Welsh mainland or not. Its inclusion as part of the mainland therefore has to be considered as part of the natural coarseness of the coastline. This is an inherent problem within the Met Office model that cannot be currently taken into account.

Future modifications of the Met Office model, that reduce the coarseness shown in Figure 6.4, may possibly take into account the Isle of Man. If this is the case, inshore wave heights for this study could easily be re-specified.

Similar to sea levels, without even considering anthropogenic activity[2], it is unlikely that wave heights are stationary. Indeed, decadal as well as

[2] The IPCC (2001) state that recent, and current changes in climate are mostly a result of anthropogenic activity. This is anticipated to result, amongst other things, in changes in the wind climate, and therefore wave heights.

secular variability is high probably as a result of the North Atlantic Oscillation. As indicated in Section 3.3.6, there is no clear evidence yet of any long term trend in wave heights, whether mean or extreme, positive or negative, therefore wave heights were assumed to be stationary over the analysis period.

Waves approaching the Cumbrian coastline were considered as the vector sum of the wind generated and swell components. Both types of waves were analysed with no directional spreading, with wind waves considered as having 13 frequency components and swell waves 1. The reasons were outlined in Section 4.6. The TMA spectrum was used to describe offshore wind wave conditions, the justification for which was given in Section 4.6.1.

The modelling of offshore conditions for both wind and swell waves was performed on an array of standard values, with results interpolated based on the model results for inshore conditions (see Section 4.6). Modelling conditions as an array of standard values was based on the logistical problems of running different wave conditions at different sea levels which current computing power would not be able to cope with (see Section 4.6.1). The discretization chosen for both the wind and swell waves is shown in Tables 4.1 and 4.2. Results from these two arrays of values could not be combined as swell waves considered energy dissipation, which wind waves didn't (see Section 4.5.3). For both wind and swell waves, the discretization was chosen so as to be as fine as possible, but without being too fine so that model runs would take too long. For wind waves, which are the most important in a joint probability assessment, discretization was reduced at higher wave heights, periods and sea levels to reflect potential increasing importance of these factors as they increased. For swell waves, the same criterion was applied except for wave periods. This was because unlike wind waves, a large swell period would not necessarily mean a 'relative' large wave height, which could easily occur at a much smaller wave period. With a large range of long period waves, a small discretization for large wave periods would have resulted in a lot of model runs shared amongst few offshore conditions. Discretization was therefore reduced at higher periods to reflect the fewer runs accessing these results. This is demonstrated, for example, on Figure 6.5 below which is a scatter

plot of swell wave heights against swell wave periods for offshore point 542240N. This shows a large number of wave conditions in the range 5-12s, noticeably reducing beyond this region. For wave periods greater than 16s, few records exist, and discretization would have likely been shared only between one or two conditions per offshore point.

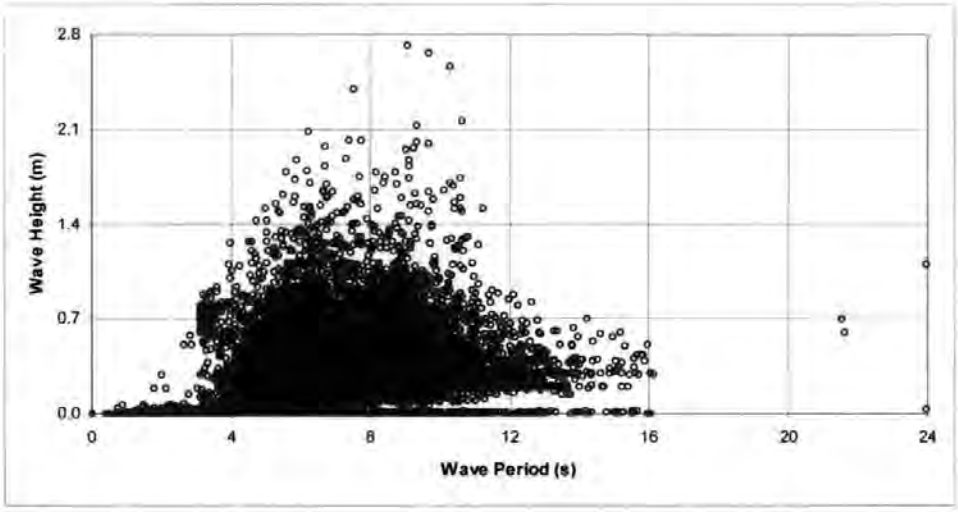


**Figure 6.5** : Scatter plot of wave heights and wave periods for swell conditions (offshore point 542240N)

Despite the relative lack of importance in a joint probability assessment for certain wave / sea level combinations, discretization at small wind wave heights and (or) sea levels (for example) was not reduced. However, wind waves less than 0.5m were modelled as a monochromatic wave to reduce run times, as results would be insignificant in a joint probability assessment.

The directional discretization was probably too fine, and results would be expected to show little variation over a 1° range. A discretization of 3° would probably have been preferable, which would have resulted in the reduction in the number of runs required by almost $^{2}/_{3}^{rd}$. This also probably meant that a number of wind wave runs below 1.0m could not be run, often resulting in an increased discretization below 1.0m. However, this is unlikely to have had a noticeable effect on results. A final, although minor factor to consider was that the lowest sea level on the Cumbrian coast in the analysis period was greater than 1.4m@OD. The lowest sea level should therefore have been set at 1.4m@OD (the same as for swell waves), not 1.2m@OD.

Based on the discretization outlined above, six model grids were established to transfer offshore conditions inshore (see Figure 3.12). These modelled wave conditions based on offshore conditions from 165° to 345° (where 0° corresponds with waves from the North, and clockwise is positive). Wave heights outside these ranges are rare and of small amplitude. It is also likely that they would be travelling away from the coastline. Their effect on a joint probability assessment would therefore be negligible, and they were not considered. Where possible, the offshore boundaries were set at a consistent deepwater boundary (such as -30m@CD for the 240° model grid). Although some boundaries corresponded with land, the effects on inshore predictions were generally restricted to the 20° lateral boundary for edge effects. The exceptions to this were for the 270°, 300° and 300° grids. However, this generally corresponded to regions where minimal wave activity would exist, and these would have little effect on a joint probability analysis. The effect of land, or shallow water depths near lateral boundaries could have been negated by specifying a variable wave height along the offshore boundary, an option available in REFDIF. However, this was discounted, as its effect on the joint probability relationship would have been minimal. A re-assessment of wave conditions in the future could consider this though.

## 6.4 Model Grids

To determine the model grids used in this study, all bathymetric survey information available was identified and obtained (Tables 3.9 and 3.10). Ordnance Survey strategi tiles were used to define the coastline and islands, replaced with local surveys (for example Allonby Bay) where more detailed survey information was available.

All surveys used in the model grids were checked, with grid co-ordinates of localised surveys correlated against known features.

Considerable difficulty was observed in obtaining the Chapelcross Survey, which was owned by BNFL, and as a result was confidential. Although two

different sources were identified, it took almost 6 years and several attempts to secure permission to use this survey. This survey covered the most complex bathymetry of the whole study area, and apart from the region around Allonby Bay, and limited bathymetric data around the ports of Silloth and Maryport, was the only known survey carried out in this area for over 150 years. With surveys from different sources, and of varying quality, particular attention was paid to regions where surveys overlapped. The survey that was considered the most accurate in overlapping regions was given precedence. A zone was also applied to this survey within which bathymetric data from the overlapping survey was removed. This was to prevent sudden gradients in the bathymetry as a result of bathymetric survey accuracy, as indicated in Table 3.11, and different survey dates, between which there may have been noticeable localised changes in bathymetry. This is indicated (for example) on Figure 6.6 which shows the overlap between the survey for Maryport Harbour for Admiralty Chart 2013 and the Chapelcross survey. In this case, precedence was given to the Chapelcross survey. A typical zone around this survey is indicated within which all bathymetric data from the survey for Maryport Harbour would have been removed.

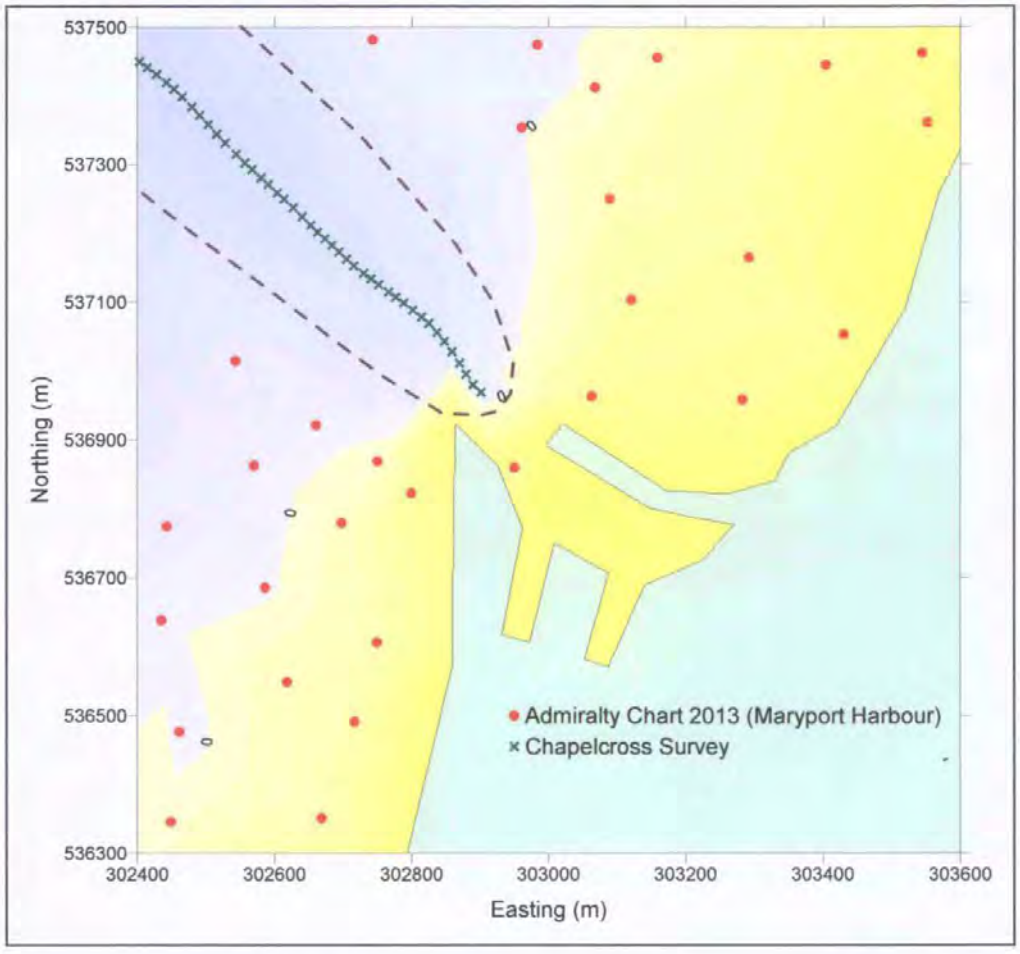


**Figure 6.6** : Overlapping surveys at Maryport Harbour

The vast majority of the bathymetric data acquired for this study came from digitised surveys carried out using GPS or local benchmarks. Apart from Ordnance Survey strategi maps, these are believed to have a relative high level of accuracy, and any errors would be expected to have a negligible effect on wave height predictions. Ordnance Survey strategi tiles, although likely to have errors in vertical alignment of up to 2m, were mainly used to fix the shoreline, where their influence on predictions are likely to be restricted at most to the last one or two grid points. The vast majority of spatial survey information (apart from the Solway Firth) came from Admiralty Charts which, depending on the Chart scale, could have a large horizontal error. Offshore (beyond -10m@OD), where variations in seabed slopes are small, this would not be significant. However, nearshore where seabed slopes are steeper and where wave heights are more influenced by water depths and changes in gradients, errors in the horizontal alignment could have a significant effect on wave predictions. Details checks were

therefore carried out on the nearshore bathymetry (above -5m@OD) to check for any likely anomalies or excessive beach slopes. This involved looking at the modelled bathymetry in small sections taking into account the type of coastline at each section and the expected contour shape. This would involve, for example, checking for parallel contours between the Ravenglass Estuary and St. Bees Head which has a similar coastline of similar exposure conditions and parallel offshore contours.

Despite the extensive checks outlined above, subsequent model runs revealed an erroneous survey point near Sandscale Haws. This has resulted in a steep beach slope in this region resulting in unreliable predictions (see Section 5.2.3).

Triangulation was used to determine the bathymetry, which was the same method used in KrKs to determine beach depths and slopes (see Section 4.3.1). This was deemed the most appropriate gridding method as other methods (based on curve fitting techniques for example) could have resulted in sharp and false seabed gradients, particularly with close survey points of noticeably different levels. The figures used in this report have also been produced using triangulation so as to maintain consistency with the results. Six model grids were specified, which are given in Section 3.5.2. Subsequent to initially setting up these model grids, additional survey information was required around the region of the Isle of Man and South of Walney Island. These were added based on current Admiralty Chart information which was different from the Admiralty Charts originally used to set up the bathymetric model, which were no longer available. Even though this survey information has probably not changed for the later versions of the Charts, with these additional areas in the region of the 15° edge effects, there will have been no noticeable effect on inshore wave height predictions.

## 6.5 Wave Modelling

The wave model used in this study to transform wave heights inshore was REFDIF, Kirby and Dalrymple (1994). Apart from REFDIF, two other WTMs

were considered, SWAN, Holthuijsen et al (2004) and a model developed by the author, KrKs. With KrKs deemed not suitable due to significant problems with caustics (see Section 4.5), REFDIF was favoured over SWAN mainly for its ability to consider diffraction, which was not modelled in the version of SWAN considered. The literature review of comparisons between the two models also indicated that for this study REFDIF was the most suitable model. A direct comparison of the two models for the Cumbrian coastline was not considered as it would have been difficult to evaluate results with little recorded data available. A comparison would also have required two models to be established, with the author required to attain an appropriate level of understanding for both WTMs. Boundary conditions for SWAN may also have been difficult to define.

Since starting this study, diffraction has been added to SWAN, and with its ability to consider further wave growth, it may now be a more suitable model for the Cumbrian coastline than REFDIF. However, regardless of potential problems with computer memory and speed, it is not possible to consider SWAN (or any other WTM) as a present or future alternative to REFDIF due to the sheer scale of model results that already exist from the REFDIF modelling.

Having adopted REFDIF as the WTM for this study, limitations were imposed on model runs based on stated limitations of the model, and limitations detected in sample runs. These limitations are outlined in 4.5.1. These include problems of instability of the model, which it is believed had not previously been noted.

Despite the conditions imposed on runs outlined above, REFDIF was noted to become unstable for some runs on some of the grids when wind waves in the region 7.4s to 9.0s were considered (see Table 4.1). This was more noticeable at higher sea levels, particularly for periods in the range 7.8s to 8.6s. These became even more significant when currents were considered, although for the reasons outlined in Section 4.5.2, currents were not considered in the REFDIF modelling. To overcome the problems of instability, wave heights for the runs affected were interpolated between the nearest available runs. Although this did cause considerable problems

initially (due to the number of conditions affected, and the 'random' interruption of model runs), this will have affected considerably less than 0.1% of all results, and will not have made any noticeable difference to the chosen discretization (Section 4.6.1) or the accuracy of results. As the nature of problems with these runs became apparent, computerised checks on later model runs were also carried out to identify runs 'on the point' of becoming unstable. These were then stopped, and identified so that a separate interpolation could be made to simulate the results.

## 6.6 Investigation of Joint Probability Relationship

### 6.6.1 Marginal Distributions

In the estimation of marginal extremes, two techniques are generally considered. These are annual maxima methods, and peaks over threshold methods. In relation to coastal engineering, annual maxima methods have traditionally been used to estimate extreme sea levels. However, these methods have almost certainly been favoured as data is readily available going back many years. Data for a peaks over threshold analysis are available for many locations, however, these have usually not been digitised, and it is not considered economic to do so. Annual maxima, particularly for the largest events are also well documented historically. This is likely to give more confidence in the accuracy of the values recorded (also see below). As regards nearshore wave heights, little analysis has been done for extremes as long term records are either not available, or are not economic to generate from offshore records.

In relation to the Cumbrian coastline, annual maxima sea level data is available for Barrow since 1920, Workington since 1992 and Silloth since 1928, JBA (1998). Apart from the data digitised at Whitehaven for this study, it is believed that no other annual maxima sea levels are available for the Cumbrian coastline. Despite data being available since 1920 for Barrow, large gaps are present, with no records available over the period 1924 to 1961. Gaps are also present in the Silloth records, with about 20% of the annual maxima records missing. The annual maxima records

available for Workington are based on the POL records which have been used in this study. Supplementing available records using the data in this study would produce annual maxima time series for Barrow of 27 years, Silloth of 52 years and Workington of 13 years.

These supplemented records could therefore be used to produce estimates of extremes that could be considered with more confidence than those given by other authors, including JBA (1998), outlined in Section 5.2.1. Despite the improved predictions using updated annual maxima data and the length of data sets analysed, the predictions used in this study using peaks over threshold techniques are however based on significantly more extensive data sets, and are therefore preferred. Another factor that favours the peaks over threshold method using the data collected for this study is the quality of past annual maxima records. Despite the comments given above about confidence in the most extreme events, errors in the recording or digitising of annual maxima events may be present, and if the original records are not available, could not be checked[3]. These errors could be significant, and a sea level recorded 1m too high (for example) may not be spotted if the records were digitised many years later, as indicated for example in Hames (2004).

For nearshore extreme wave heights, no previously recorded or predicted wave heights are available.

The marginal distributions of sea level and wave height were therefore modelled based on the GPD outlined in Section 2.6. The use of this formula gave more flexibility to the prediction of extremes as it allowed the data itself to determine the most appropriate distribution (as outlined in Section 5.2).

Spatial estimates of standard extremes sea levels along the Cumbrian coastline are given in Figure 5.8. The values on this figure have to be considered in relation to comments on quality of secondary port information

[3] Hames (2001), for example, identified an error rate of up to 25% for the translation of sea levels digitally and on paper charts for two locations along the River Dee in Cheshire.

given in Section 6.2. These indicate that away from locations where sea levels are recorded, extremes could be estimated in error by at least 0.25m.

Offshore extremes were considered for the two Met Office data points. Unlike sea levels, apart from extreme estimates of offshore points which can be produced by the Met Office (which were not obtained for this study), there are no known published estimates of extremes in the East Irish Sea. For $MO_1$, extreme predictions appeared to be fairly robust. However, extreme predictions for $MO_2$, were a poor fit to the data, indicating a lack of confidence in extreme predictions at this location. Considering the agreement between wave heights at $MO_1$ and $MO_2$ (Figure 5.12), it is considered that offshore predictions above approximately 3m for $MO_2$ can be viewed with suspicion. These are the waves that will mostly dictate the extreme predictions. $MO_2$ is sheltered from the most extreme wave heights from the south west quadrant (as indicated on Figure 4.5), and it is unlikely that the most extreme wave heights at this location would exceed those at $MO_1$, which predictions do. Despite this, there is no means of confirming the values at $MO_2$ or otherwise. However, Reeve and Bin (1994) do indicate that predictions at $MO_2$ deteriorate with increasing wave height. No indication of how these deteriorate is given. However, an analysis of the most extreme storms analysed indicate an over prediction of approximately 10-15%, although based on too little data to draw any concrete conclusions. The threshold chosen for $MO_2$ produced the lowest estimates, and the closest to those at $MO_1$. With no means of indicating with certainty whether extreme predictions for $MO_2$ are correct or not (or to what level), no correction was made to extreme estimates at $MO_2$.

The effect of data from $MO_2$ on inshore predictions is likely to produce an overestimate of inshore extremes from the southernmost boundary, up to an area around St. Bees Head. This would become less pronounced the further north you go. This is demonstrated for example on Figure 6.7 which shows quantile plots for 4 equally spaced locations (for -2m@OD) along the coastline (also see below). This shows poor agreement approaching the extremes for the first point (469840N), although significantly better than offshore, with increasing confidence at the more northern points. For the last point, which would be mostly described using wave conditions from

$MO_1$, strong agreement is observed between the model and the empirical distribution. Agreement between model and empirical predictions generally improved at higher beach levels.

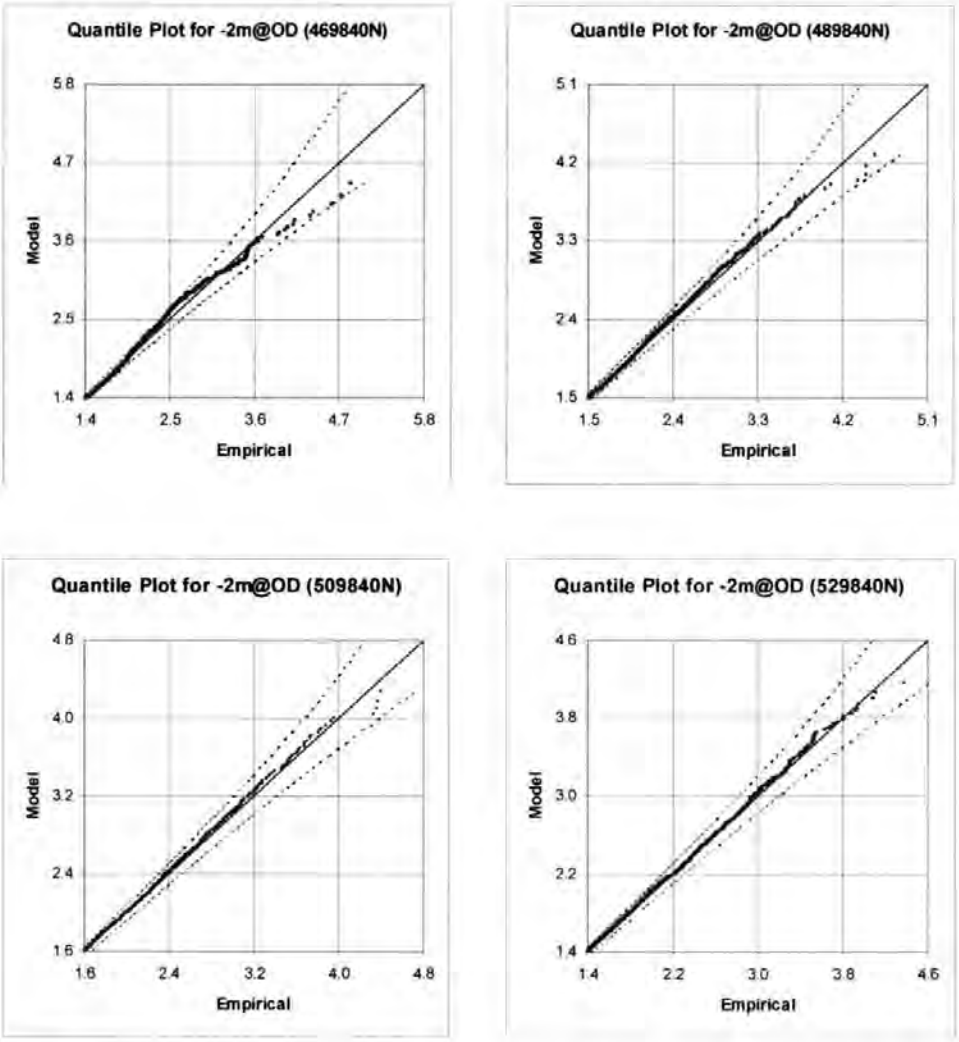


**Figure 6.7** : Quantile plots for waves heights at a beach level of -2m@OD for selected inshore locations

For inshore extremes, predictions were made at five beach levels (-2, -1, +0, +1 and +2m@OD). However, as stated in Section 5.2.3, nearshore extremes need to account for depth limited effects which are not implicitly included in the GPD distributions. Inshore extremes were therefore determined based on 'counting back' to the required return period for a simulation of 10,000 years of wave and sea level data (see Section 6.6.5). This produced little difference in extremes as demonstrated in Figure 5.20 (based on extrapolation of the GPD), and Figure 5.24 (based on 'countback'). This was except at Whitehaven, where as a result of the large

breakwater arm protecting the port, deep waters enable large wave heights to approach into nearshore regions. With inshore predictions at 229 locations and 5 depths, it was not practical to rigorously consider the detailed methods outlined in Section 5.2 to determine extremes. The choice of threshold was therefore based on a spatial comparison at a number of locations for different thresholds. This indicated general stability of estimates in the region 0.80 to 0.82, with a threshold of 0.82 appearing to give slightly better stability spatially at all 5 depths than a lower threshold. This threshold was therefore adopted for inshore predictions. Figures 6.8 and 6.9 below show two of the sections considered for -2m@OD. This shows some scatter in estimates, particularly at the higher return period events. The general consistency for estimates using thresholds between 0.80 and 0.82 was a consistent pattern through all of the locations considered.

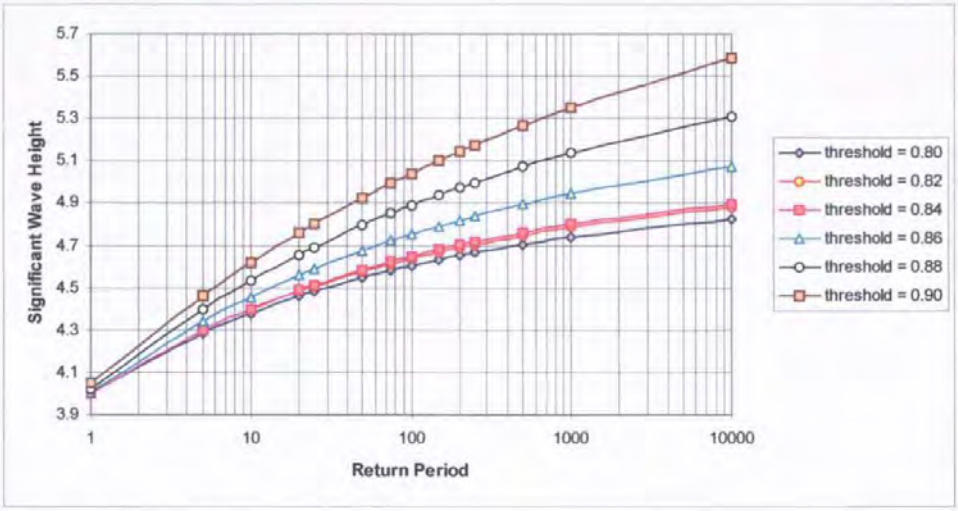


**Figure 6.8** : Extreme estimates of $H_s$ for different thresholds (-2m@OD, Northing coordinate 477440N)

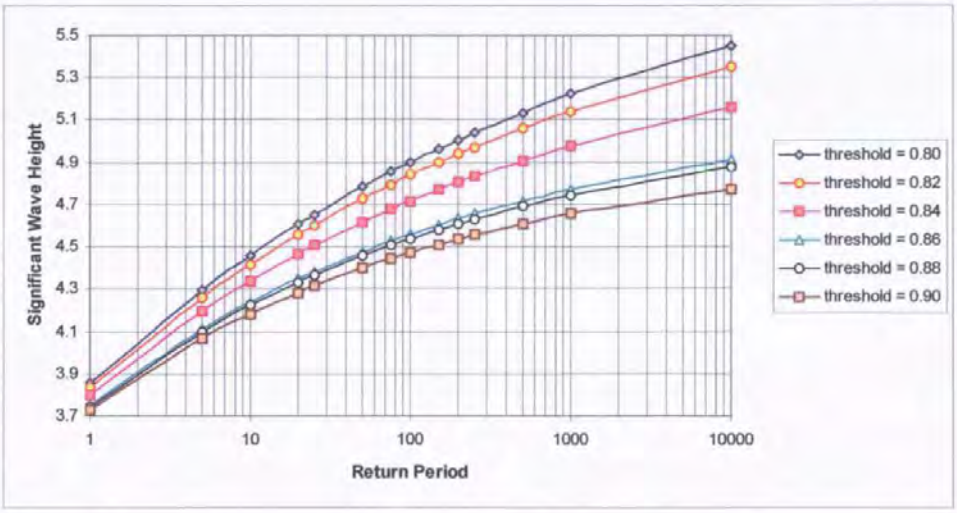


**Figure 6.9** : Extreme estimates of $H_s$ for different thresholds (-2m@OD, Northing coordinate 538240N)

Considering extreme estimates of inshore wave heights in detail, the following points were noted. These comments are based on Figure 6.10 below which is an expanded version of Figure 5.24, but for just the 100 year return period event showing the different levels considered. Locations referred to are also shown on Figure 1.2.

1. Extremes from the southernmost boundary are generally constant, possibly decreasing slightly until a region opposite approximately Barrow. From here until Whitehaven Harbour, extremes are generally consistent, although reducing slightly.
2. There is an increase in extreme wave activity at the northern head of Walney Island possibly as a result of localised sand banks just offshore of this region.
3. There is an increase in extremes at Haverigg Point probably as a result of a concentration of wave energy at this (effective) headland.
4. At St. Bees Head, there is a noticeable increase in extreme predictions, and a noticeable reduction in the lee of St. Bees Head in Saltom Bay. The increase in extreme predictions at St. Bees Head is probably as a result of concentration of wave energy at the headland due to refraction. This will result in less wave energy behind the headland which combined with refraction in the Bay would be expected to reduce wave heights.

5. At all ports on the coastline with the possible exception of Silloth (Whitehaven, Harrington, Workington and Maryport), there is a noticeable increase in extreme predictions. This is particularly noticeable at Whitehaven. This is anticipated to be as a result of protruding coastal structures at these locations leading to steep beach slopes which are not present at Silloth.
6. For Allonby Bay, there is a reduction in extreme wave heights centred on coordinate 541240N for a radius of approximately 1.5km. This is probably as a result of refraction into the Bay past Maryport.
7. Extremes from approximately Allonby to approximately 2km past Dubmill Point are generally constant. From this point on, extremes tend to reduce, apart from a region around Beckfoot, until Silloth.

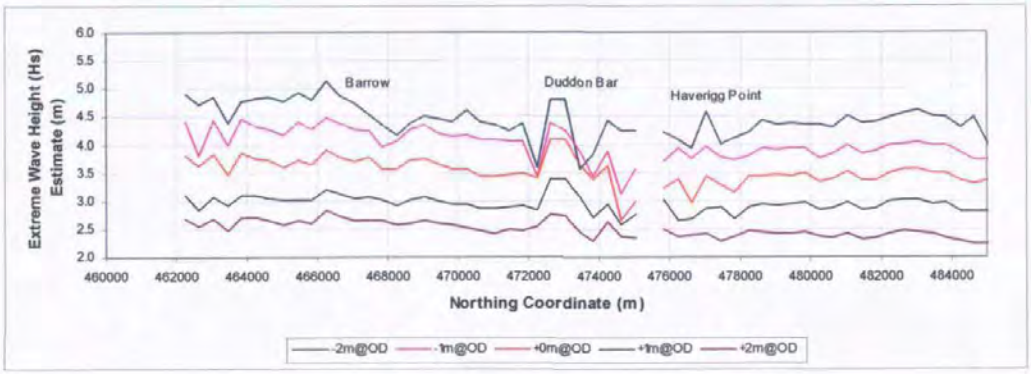


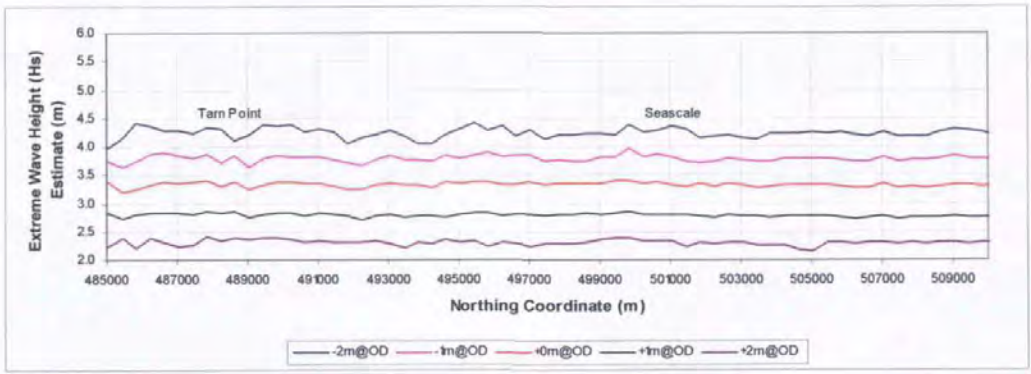


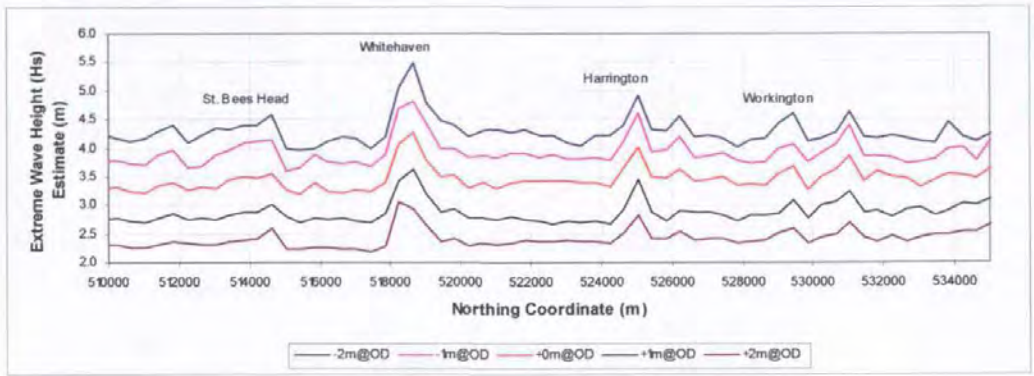


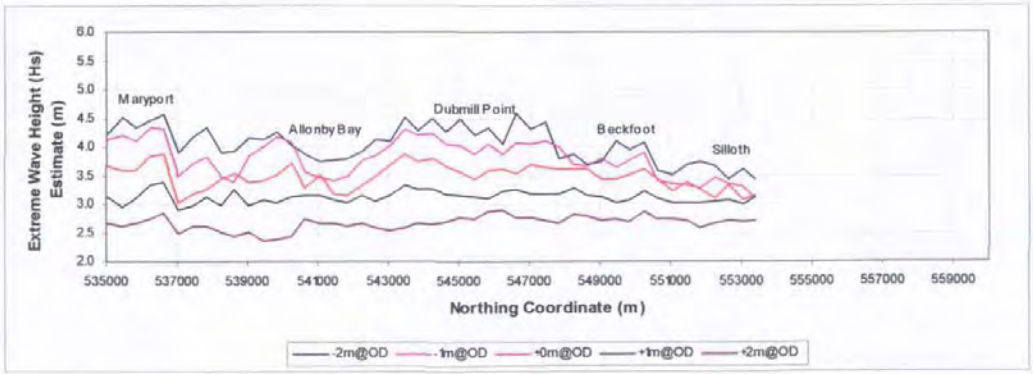


**Figure 6.10** : Spatial variation of extreme wave heights (100 year return period event)

### 6.6.2 Model Selection

Within JOIN-SEA, two types of model are available dependent on the level of correlation between wave heights and sea levels above increasing levels of thresholds of non-exceedance. For this study, for both offshore and inshore conditions the threshold varied as the threshold of non-exceedance increased (Figures 5.31 to 5.36), therefore the mixture model was used to determine the joint probability relationship (Section 2.6).

To consider the variation in correlation in detail, and also to look at its effect on the joint probability relationship, Figures 6.11 to 6.13 below show sections through Figures 5.31 to 5.36 at thresholds of non-exceedance of the high sea level of 0.90, 0.95 and 0.99. From these graphs, the following conclusions can be drawn:

1. There is a general linear increase in correlation from the southernmost boundary until the start of St. Bees Head (515000N).
2. There is a general reduction in correlation from approximate coordinate 472240N to 477040N corresponding to the northern head of Walney Island and prediction points within the Duddon Estuary.
3. Correlation at Tarn Point and to the south varies slightly probably as a result of the small headlands in these regions.
4. There is a general variation in correlation at St. Bees Head, lower at the southern end, consistently reducing as you enter Saltom Bay.
5. There is a reduction in correlation at Whitehaven. This would be as a result of the steep beach slope in this region meaning that wave heights break at higher beach levels.
6. To the immediate south of Workington, there is a slight reduction in correlation corresponding to what appears to be protruding sand banks in this region.
7. There is a general linear reduction in correlation between approximate coordinates 519440N (north of Whitehaven) and 536000N (just below Maryport).
8. There is a general reduction in correlation for Allonby Bay between the headlands centred on approximate coordinate 540440N.
9. Correlation from Dubmill Point generally reduces until Silloth.

10. Correlation at -2m@OD shows good general agreement with offshore conditions except at a threshold of exceedance of 0.99.
11. Generally correlation for offshore conditions is less than nearshore conditions below approximate Northing coordinate 520000N, although often higher above 520000N for -2, -1 and +0m@OD.

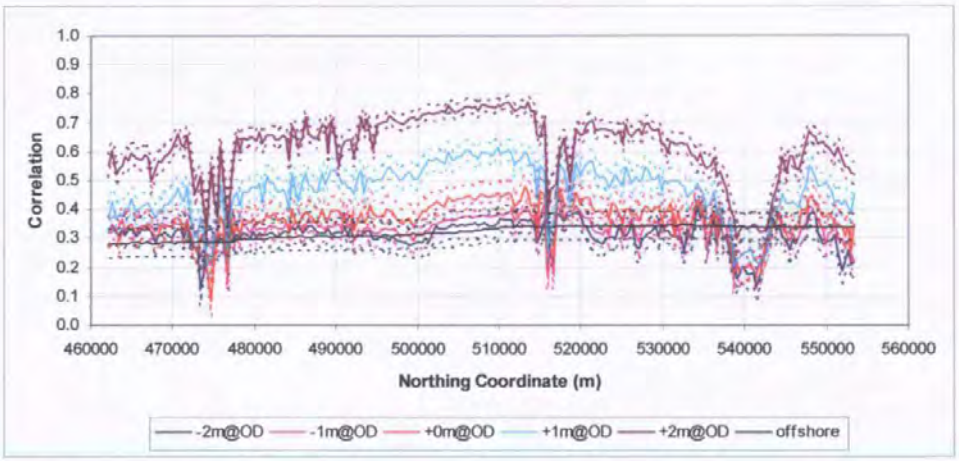


**Figure 6.11** : Spatial variation in correlation for threshold of exceedance of 0.90 (with 95% confidence limits)

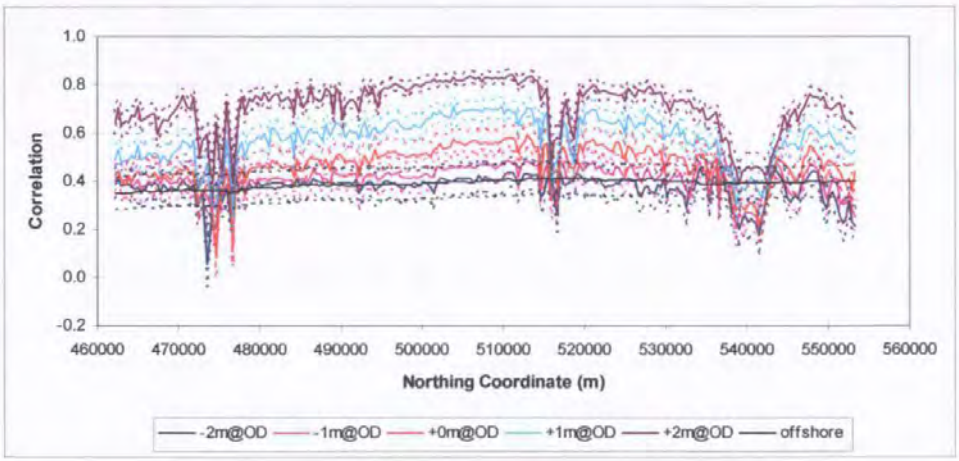


**Figure 6.12** : Spatial variation in correlation for threshold of exceedance of 0.95 (with 95% confidence limits)

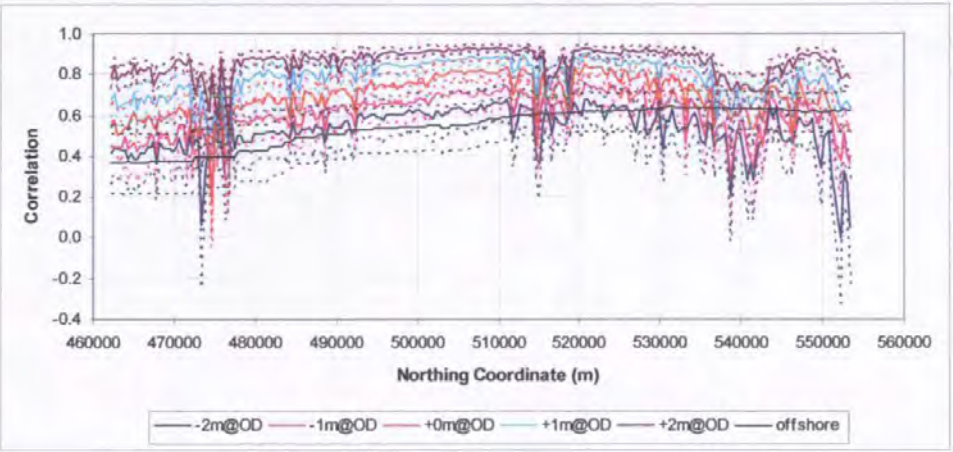


**Figure 6.13** : Spatial variation in correlation for threshold of exceedance of 0.99 (with 95% confidence limits)

### 6.6.3 Spatial Variation in Joint Probability at -2m@OD

Considering the comments about the spatial variation in extremes and correlation outlined in Sections 6.6.1 and 6.6.2, the spatial variation in joint probability between waves and high sea levels has been considered for the sections outlined in Table 6.3 below. The choice of these sections has also been made with reference to Figures 5.32 to 5.36 which show the spatial variation across all thresholds. Typical joint probability curves for these sections are shown in Appendix D.

Generally the comments given below refer to joint probability curves at a beach level of -2m@OD. Above this beach level, joint probability curves become noticeably steeper approaching the extremes, the shapes becoming increasingly more uniform at higher beach levels. The comments given below relate specifically to the shape of the joint probability curves, not the values although comments on the values are made where considered appropriate.

| Northing Coordinates | Region |
|---|---|
| 462240N to 471840N | Middle and Southern Sections of Walney Island |
| 472240N to 473840N | Northern head of Walney Island |
| 474240N to 477440N | Sandscale Haws and prediction points within the Duddon Estuary. |
| 477840N to 511040N | Haverigg Point to just below St. Bees Head |
| 511440N to 518240N | St. Bees Head and Saltom Bay |
| 518640N to 519040N | Whitehaven |
| 519440N to 537840N | North of Whitehaven to just north of Maryport |
| 538240N to 546640N | Allonby Bay |
| 547040N to 553360N | Dubmill Point to Silloth |

**Table 6.3** : Sections where spatial variation in joint probability was considered.

## 1. Northing coordinates 462240m to 471840m (see Figure 1.2)

This section of the coast was split between two parts. For the southern part (462240m to 467440m), the joint probability curves were steeper approaching the extremes, indicating stronger correlation between wave heights and sea levels. A typical section is shown on Figure D.1. For the northern part, (467840m to 471840m), the joint probability curves were shallower approaching the extremes, indicating weaker correlation between wave heights and sea levels. A typical section is shown on Figure D.2. There is a slight change in the orientation of the coastline between these two sections (about 17°) with the southern section more orientated towards the predominant wave direction. This results typically in reduced extreme wave heights for the northern section as indicated on Figure 6.10.

2. **Northing coordinates 472240m to 473840m (see Figure 1.2)**

There was a constant joint probability relationship along this coastline, a typical section of which is shown on Figure D.3. Joint probability curves for this section were shallower approaching the extremes than curves to the south. With the largest sea levels corresponding to waves from the south-west, this area possibly suffers from the most significant wave activity from the west resulting in the shape of the curves shown.

Marginal extreme wave heights are significantly reduced for 472240m probably as a result of raised sandbanks either side of the prediction points nearshore and 473440m and 473840 which are more shielded from the predominant wave direction.

3. **Northing coordinates 474240m to 477440m (see Figure 1.2)**

Generally there was a constant joint probability relationship along this coastline, similar to the joint probability relationship between 462240m and 467440m (see Figure D.4). However, sections 476240m and 476640m were noticeably flatter approaching the extremes (see Figure D.5) with significantly reduced marginal extreme wave heights. These sections are within the Duddon Estuary and will be protected from the largest wave activity coinciding with the largest wave heights from the south west. This would result in a flatter joint probability curve approaching the extremes, and reduced wave heights. However, sections 477040m and 477440m are also similarly exposed (although further north), yet have a joint probability relationship (and marginal extreme wave heights) similar to the remaining sections.

4. **Northing coordinates 477840m to 511040m (see Figure 1.2)**

Joint probability curves around Haverigg Point (477840m and 478240m) are noticeably flatter approaching the extremes compared to remaining curves in this section (see Figure D.6). For the rest of

this section, two types of joint probability curve exist, examples of which are shown on Figures D.7 and D.8. These types of joint probability curve are typical for most of the coastline above Haverigg Point. There appears to be no noticeable reason why one curve is more likely to occur than any other. However, considering the comments below regarding long shore drift with regards to Allonby Bay, it is noticeable that curves that are flatter approaching the extremes exist in the region from south of Tarn Point to just south of the Ravenglass Estuary. This is except for regions sheltered by protruding land, for example in the northern lee of Tarn Point. These curves, flatter approaching the extremes, correspond to land that is apparently suffering from significant erosion (Williams 2005). This is probably as a result of the orientation of this area of coastline, which faces further west (20°) than the coastline north of the Ravenglass Estuary which is not believed to be eroding. This results in waves from the predominant south west approaching the coastline at a more oblique angle than regions to the north.

The curves termed steeper approaching the extremes, e.g. in the lee of the predominant wave direction, correspond to regions where waves at lower sea levels would be expected to be reduced comparatively more as a result of refraction compared to waves at higher sea levels.

Marginal extreme wave heights show little variation over this section, with a maximum range of 0.45m, and a typical range of less than 0.12m for the 5 year return period event.

**5. Northing coordinates 511440m to 518240m (see Figure 1.2)**

This region covers the joint probability curves either side of the headland of St. Bees Head, where the coastline has its most noticeable change in direction. Generally the joint probability curves are similar in this region (see for example Figure D.9), but steeper approaching the extremes in the lee of the predominant wave direction in Saltom Bay (see for example Figure D.10). However,

marginal extreme wave heights in this region are lower. This will probably be as a result of increased refraction within Saltom Bay at lower sea levels.

Marginal extreme wave heights show little variation over this section except for section 518240m with marginal extremes noticeably larger. This section is in the lee of the southern breakwater arm at Whitehaven, and will be affected by the large beach slopes in this region.

**6. Northing coordinates 518640m to 519040m (see Figure 1.2)**

This covers the region near Whitehaven harbour where the beach is at its steepest. Typical joint probability curves for this region are given in Figure D.11. These curves can be considered shallow approaching the extremes probably as a result of extreme wave heights at lower sea levels being less affected by steeper beach levels than shallower beach levels observed elsewhere.

**7. Northing coordinates 519440m to 537840m (see Figure 1.2)**

Joint probability curves from 519440m to 529840m (Port of Workington) are generally consistent, with typical curves given by Figure D.12. The range of marginal extreme wave heights is generally small (less than 0.30m for the 5 year return period event) although noticeably higher for section 525040m (at Harrington harbour), where beaches in this region are at their steepest.

North of this region, where there is a slight change in the orientation of the coastline away from the predominant wave direction joint probability curves become flatter as demonstrated for example on Figure D.13. However, for higher beach levels, joint probability curves tend to become steeper approaching the extremes, approaching the same shape as joint probability curves observed below 529840m.

## 8. Northing coordinates 538240m to 546640m (see Figure 1.2)

Joint probability curves from 519440m to 543040m (Allonby) are generally consistent, with typical curves given by Figure D.14. These are noticeably flat approaching the extremes. Beyond this point, joint probability curves tend to be steeper approaching the extremes, as indicated by Figure D.15. These joint probability curves that are flat approaching the extremes correspond to regions in the Bay that suffers from significant erosion as a result of long shore drift. This is also noted for the region between Tarn Point and the Ravenglass Estuary, although not as 'flat'. Similar to this region, the orientation of the coastline is further away from the predominant wave direction than the adjacent coastline, therefore being exposed to direct wave attack from waves at lower (extreme) sea levels.

Beyond Allonby, with no noticeable long shore drift occurring, steeper joint probability curves approaching the extremes are noted. This also results in larger marginal extreme wave heights in this region, which for the 5 year return period are typically 0.2-0.25m higher.

## 9. Northing coordinates 547040m to 553360m (see Figure 1.2)

Joint probability curves at the start of this section correspond to the headland of Dubmill Point. For the sections 547040m to 548240m, joint probability curves are steep approaching the extremes as given by Figure D.16. However, marginal extreme wave heights for sections 547840m and 548240m, which are in the lee of the rock outcrops at this headland are noticeably reduced (over 0.3m for the 5 year return period event).

Beyond Dubmill Point, joint probability curves are flat approaching the extremes (typical example shown on Figure D.17), probably for the same reasons as given above for joint probability curves before Allonby. This area of coastline is also believed to be eroding (Bullen Consultants 1999b). Marginal extreme wave heights are the lowest

for the Cumbrian coastline, generally reducing the further north you go. This would be expected as a result of the reduced exposure expected the further into the Solway Firth you progress.

Considering the comments given above, generally for the Cumbrian coastline joint probability curves appear to show a consistent spatial relationship. This usually applies if the orientation and exposure conditions of the two sites are similar. Headlands or steep beaches appear to produce joint probability curves that are shallow approaching the extremes probably as a result of more concentration of wave energy at headlands and less wave breaking on steep beaches respectively for lower sea levels. Bays appear to produce joint probability curves that are steep approaching the extremes probably as a result of comparatively more reduced wave heights at lower sea levels as a result of increased refraction into the Bay. However, marginal extreme wave heights were generally larger at headlands or on steep beaches. The two regions of the coastline that are known to suffer from significant erosion had joint probability curves that were shallower in the extremes than adjoining areas that did not suffer from significant erosion. It is noticeable that for these two regions the coastline is orientated 'away' from the predominant wave direction compared to adjacent areas of the coast. This would result in direct wave attack from waves that are at lower (extreme) sea levels. This should explain the shape of the curves shown with waves at the higher sea levels being subject to more refraction into the coastline, resulting in a reduction in wave heights. This would also explain the increased sediment movement at these locations.

Based on the strong linear relationship between similar stretches of coastline (outlined above), it was noted that given the joint probability relationship at one point on the coastline, the joint probability relationship at a point further up or down the coastline could be estimated by the relationship given by Equation 6.1 below.

$$(H_s)^h_{P2} \approx (H_s)^h_{P1} \frac{(H_s)^{\max}_{P2}}{(H_s)^{\max}_{P1}} \qquad \textbf{(6.1)}$$

$(H_s)^h_{Pi}$ = wave height at sea level percentile *h* on *i*th joint probability curve.

$(H_s)^{max}_{Pi}$ = maximum wave height for *i*th joint probability curve.

This relationship appeared to become more applicable at higher beach levels as the correlation between wave heights and sea levels became stronger, and waves became depth limited. As the beach levels increased, this relationship also became more applicable over wider areas. This is particularly noticeable for example for the region analysed from Haverigg Point to just below St. Bees Head. For this stretch of coastline, with no noticeable changes in directions, headlands or bays it was noted for example that for a beach level of +2m@OD, given the joint probability relationship at one location and using the relationship given by Equation 6.1, the joint probability relationship at any other location on this stretch of coast could, for the same beach level, be estimated to a high degree of confidence.

Using the relationship given by Equation 6.1, joint probability curves could generally be considered to follow the type given by for example Figures 5.42 to 5.46. These are the type of curves that can be considered steeper approaching the extremes, also shown by for example Figures D.7 to D.12. Therefore, generic curves could be constructed for the Cumbrian coastline based on these types of curves. Generally, more confidence can be given to these generic relationships at higher beach levels, which would also give a degree of conservatism if a joint probability curve shallower approaching the extremes was appropriate.

Based on the comments given above, Figures 6.14 and 6.15 below show generic curves typical for the Cumbrian coastline at -2m@OD and +0m@OD, where:

$$\text{Wave Height Ratio} = \frac{(H_s)^h_{Pi}}{(H_s)^{max}_{Pi}} \qquad \textbf{(6.2)}$$

$$\text{Sea Level Ratio} = \frac{\eta - msl}{\eta_e - msl} \qquad (6.3)$$

$\eta_e$ = extreme sea level

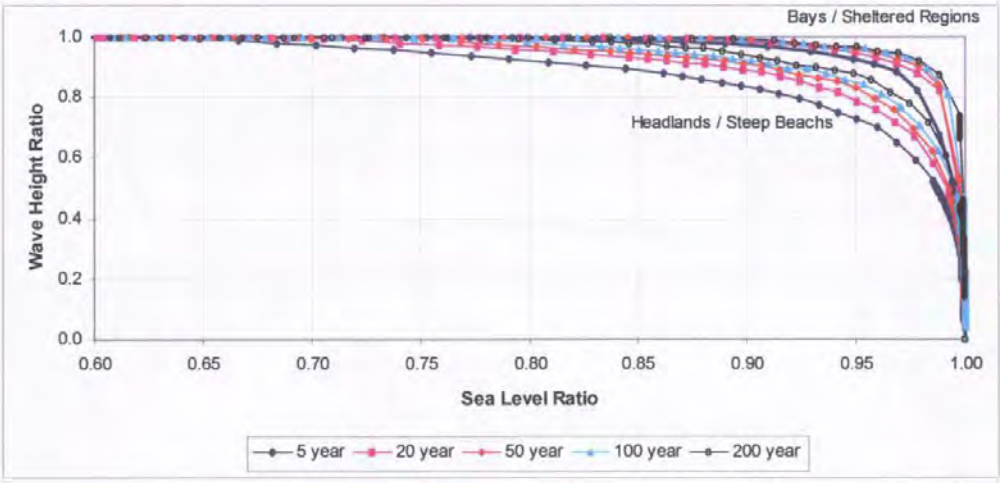


**Figure 6.14** : Generic joint probability curves for Cumbrian coastline (-2m@OD)

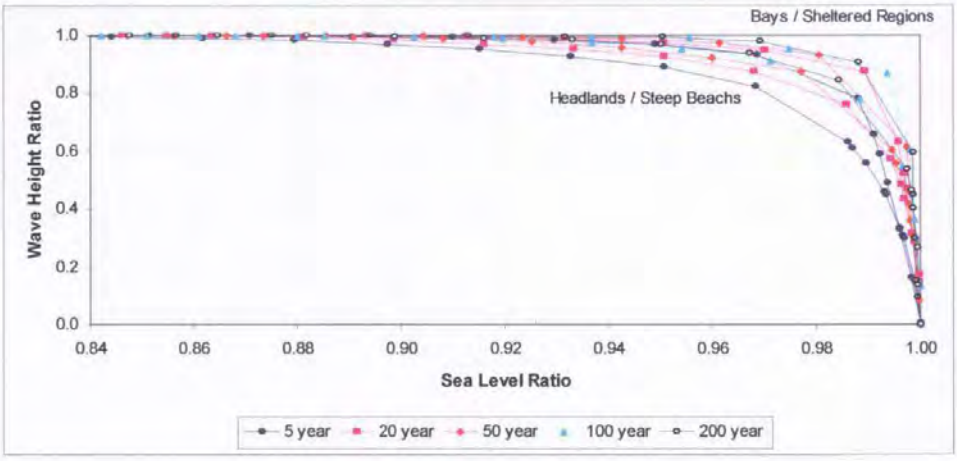


**Figure 6.15** : Generic joint probability curves for Cumbrian coastline (+0m@OD)

Therefore, knowing the type of coastline, the joint probability curve could be estimated using these curves and the marginal extremes given by Figures 5.8 and 5.24 (or Figure 6.10). The types of curves that do not follow this

relationship (see comments above regarding for example Figures D.3 and D.17) would result in a conservative estimate of the joint probability curve.

Although these specific generic curves represent the whole of the Cumbrian coastline, more specific curves could be generated over smaller areas, thus giving more confidence in predictions for these areas. This is the case for example from Maryport to Allonby where curves approaching the extremes are much shallower than the generic curves shown above.

### 6.6.4 Spatial variation in Joint Probability at Higher Beach Levels

As indicated in Section 6.6.3, joint probability curves were noted to become more generic as the beach level increased. Therefore for example, Equation 6.1 was more applicable at a beach level of -1m@OD, than it would be at -2m@OD, yet less so than at +0m@OD.

However, no clear relationship between the joint probability curve at a beach level of -2m@OD and higher was observed. However, approaching the extreme sea level the joint probability curves became steeper, indicating that at the highest sea levels the largest wave heights often occurred at higher beach levels. This is indicated for example on Figure 6.16 which shows the relationship between wave heights at -2m@OD and +0m@OD. This indicates that for a sea level ratio greater than approximately 94%, wave heights are usually larger at +0m@OD than at -2m@OD.

In this figure, wave height beach level ratio is given by:

$$\text{Wave Height Beach Level Ratio} = \frac{(H_s)^h_{+0m@OD}}{(H_s)^h_{-2m@OD}} \qquad \textbf{(6.4)}$$

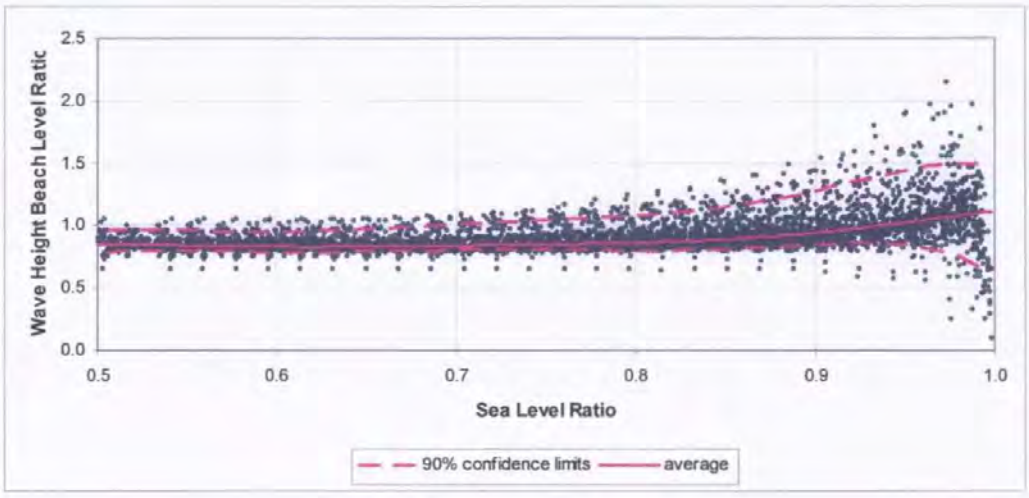


**Figure 6.16** : Wave height ratio at +0m@OD compared to -2m@OD

Obviously, however, there must come a point where wave heights at the most extreme sea level in a joint probability curve are depth limited. The joint probability relationship is then described by the depth limited wave at the extreme sea level. Considering the relationship between the extreme sea level and the highest sea level where the maximum wave height occurs on the joint probability curve, Figure 6.17 below gives an estimate of the point where the joint probability curve can be considered to be given by the depth limited wave at the extreme sea level. This curve was estimated by an analysis of this relationship at all five beach levels at all 229 prediction points. This indicated that the joint probability relationship could be described by depth limited conditions at the extreme sea level at lower beach levels as the return period increased. This seems to be confirmed by analysis of all the Figures given in Section 5.4 and Appendix D. However, as indicated, there is a large error band on these results.

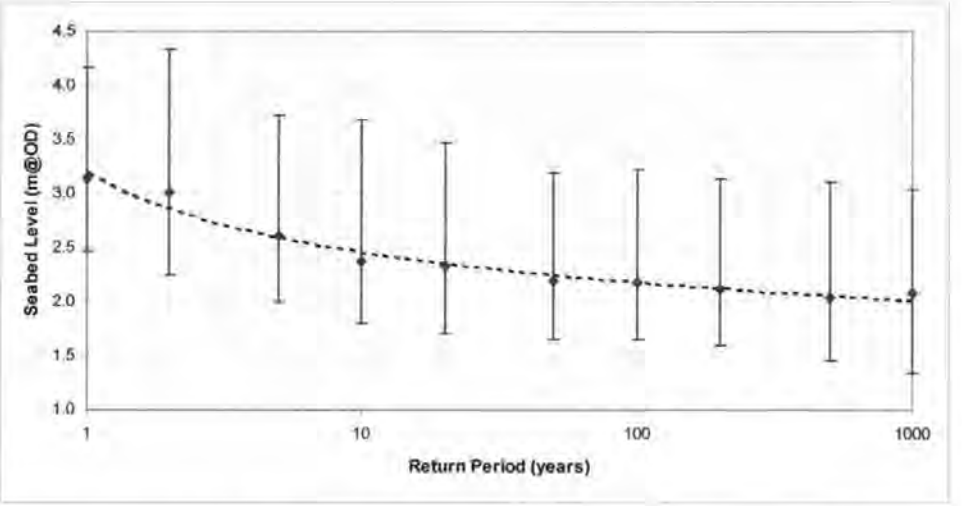


**Figure 6.17** : Estimate of seabed level where joint probability curve is depth limited at extreme sea level (with 95% error bands)

### 6.6.5 Accuracy of JOIN-SEA Estimates

Considering the typical joint probability curves shown against the recorded data (Figures 5.42 to 5.46 and 5.48 to 5.52), there appears to be a disproportionate number of values that exceed the joint probability curves. For example, considering Figure 5.42, with 13.2 years of data, the 20 year return period curve is exceeded at all high sea levels. However, statistically you would expect the 20 year return period curve to be exceeded by at least 1 wave height / high sea combination for only approximately 50% of high sea levels.

Figure 6.18 below shows the 1 year return period curve determined by JOIN-SEA and based on countback of the wave height / sea level combinations for -2m@OD at Northing coordinate 546240m (see Figure 5.48). This indicates that the joint probability curve using JOIN-SEA appears to underestimate the joint probability curve at low high sea levels, yet overestimate the joint probability curve at high sea levels. This is confirmed by an assessment of the joint probability curves at all locations and beach levels, which indicate that the 1, 2 and 5 year return period curves are typically exceeded 1-1.5, 1.5-3 and 2-3 times respectively more than expected. These reduce at the more extreme high sea levels (>5m@OD) as indicated on Figure 6.18 below. The offshore joint probability curves are also exceeded more times than expected, although

not as much as predictions nearshore. However, the linear specification of offshore wave heights (see Section 4.7) means that no conclusions on accuracy of JOIN-SEA fits to offshore extremes can be made.

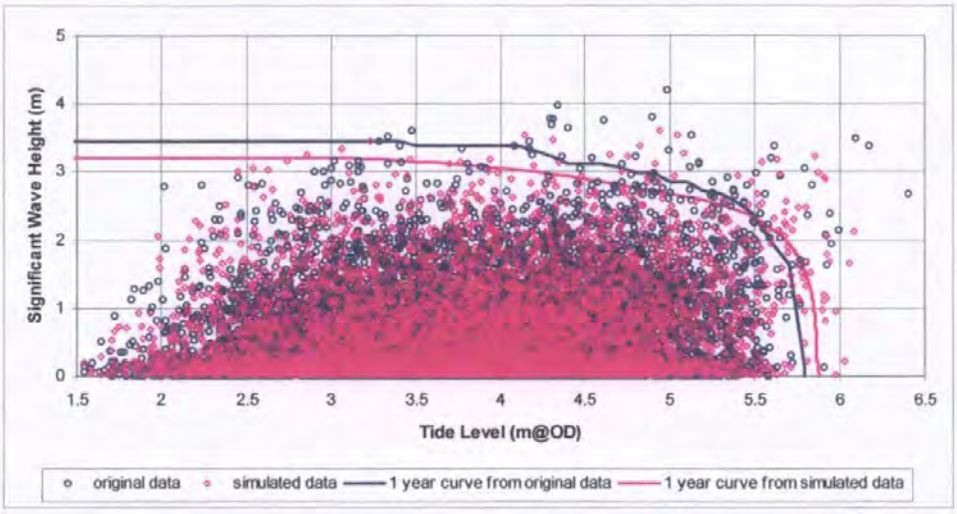


**Figure 6.18** : 1 year return period curve determined by JOIN-SEA and countback of original time series (-2m@OD Northing coordinate 546240m)

Although the accuracy of the JOIN-SEA method could be questioned based on these apparent poor fits, this is probably as a result of the fits to the marginals approaching the extremes, particularly for the wave heights. Considering the offshore extremes, Figures 5.16 and 5.17 indicate that model predictions are under-predicted approaching the extremes, particularly for $MO_2$. Inshore, model predictions appear to be more accurate, but also appear to be under-predicted. This is particularly the case for prediction points to the south of the study area, corresponding to predictions dominated by offshore predictions from $MO_2$, as indicated by Figure 6.7. For sea levels, model predictions are typically greater than the empirical distributions as indicated by Figures 5.5, 5.6 and 5.6 for Barrow, Workington and Silloth. Both of these factors are likely to result in a joint probability curve that appears to under-predict the joint probability curve at low high sea levels, yet over-predict the joint probability curve at high sea levels. Away from the extremes, it is difficult to estimate the accuracy of the joint probability curves unless the extreme wave heights and extreme sea levels are exceeded by a similar number of events, and this has therefore not been considered.

Considering the 1 year return period curve in Figure 6.18 above determined from the original data, it appears to be rather noisy. This indicates that using 13.2 years of data to estimate the 1 year return period event is probably not sufficient. For this study, 10,000 years of data have been simulated to estimate a maximum return period event of 200 years. This is $1/50^{th}$ the size of the simulation and the equivalent of almost 4 times more than considered for Figure 6.18. Considering the 200 year return period curves shown on Figures 5.41 to 5.52 these appear to be a little noisy, although not as noisy as Figure 6.18. This would indicate that a larger simulation would be appropriate. However, with over 1,000 simulations required for this study, it was not practical to consider more simulations due to the amount of storage required. Although these can be reproduced relatively easily, by their very nature, simulations are always different, and the original data sets used for this study would have been lost. Hawkes et al (2005) also indicate that a sensitivity check on a simulation 740 times the required return period event produces results whose differences were insignificant. A simulation 50 times the size of the maximum return event would probably produce results whose differences are approximately 4 times bigger, yet considering the number of results required for this study still insignificant.

### 6.6.6 Effect of Wave Period on Damage and Overtopping / Sea Level Rise

In this study, wave period, and therefore wave steepness, has only been used in the determination of wave breaking conditions. However, as mentioned in Section 5.3.2, the accurate specification of wave steepness is of vital importance in coastal defence work.

For offshore conditions, wave steepness in the East Irish Sea for significant wind wave activity is typically in the range 0.040-0.043, and for coastal defence work under extreme conditions, it would not be necessary to consider a value outside this range. However, inshore, wave steepness (based on inshore wave heights) varies significantly due to the potential eclectic mix of wind and swell waves, and the different breaking characteristics of waves at different frequencies. Within this study, wave heights, and therefore wave periods inshore have been assumed to follow

the Rayleigh distribution, with wave periods given by Equation 4.3. This has produced a range of wave periods and therefore steepnesses as indicated on Figure 6.5. Although more work on the definition of inshore wave period could be considered, the work produced in this study indicates that inshore wave steepnesses on the joint probability curve could, for the same wave height, produce a range of wave periods.

This effect on coastal defences can be demonstrated for a typical coastal defence structure on the Cumbria coastline. For example, consider a 3m wave acting on a 1 in 2, 2 layered rock armoured revetment designed to suffer minimal damage and to restrict overtopping to a value of $0.05m^3/s/m$. Using a typical offshore steepness of 0.04, this would require a minimum rock weight of approximately 2.7 tonnes, and a defence structure in the region of 3.2m higher than the sea level[4]. Considering a potential inshore steepness of 0.015, the minimum rock weight would increase to approximately 4.0 tonnes, and the coastal defence structure in this case would need to be in the region of 6.0m higher than the sea level. These are significant differences resulting in structures not only of different proportions, but also increased costs possibly of several factors. Also, based on a joint probability assessment, 'larger' structures would stretch out to sea more and be in deeper depths. This would probably increase the values given above for a steepness of 0.015 even more, particularly for steep beaches, where the biggest design wave heights have been observed.

Therefore, although wave steepness has not been implicitly considered in this study, it is important in coastal defence work and more work is required to specify wave steepness on joint probability curves inshore. However based on the technique used in this study, it was generally noted that wave period varied little between offshore and inshore, particularly for larger wave heights on the joint probability curve likely to be considered in design. It is therefore suggested that inshore wave periods be assumed to not change from offshore conditions. Inshore wave periods would therefore be evaluated by overlaying the joint probability curves for offshore conditions

[4] Rock sizes have been estimated based on Van Der Meer's formulae (1988). Overtopping values have been estimated based on Owen's formulae (1980).

over the joint probability curves for inshore conditions. Wave steepness would then be determined by assuming a typical wave steepness for offshore conditions and multiplying it by the ratio of the inshore wave height to the offshore wave height. These curves have been produced, but have not been presented in this study.

A further factor to consider in coastal defence work that has not been considered in this study is the effect of sea level rise on joint probability curves. Although a major consideration in coastal defence work, analysing the effect of rises in sea levels would have vastly increased the number of runs required, and was therefore not considered. A rise in sea levels would increase the depths of water at a structure, which, in terms of the work presented in this study, would effectively reduce the beach level. This would probably result in larger wave heights on the joint probability curves, although, considering the results from Figure 6.1, not necessarily. It is therefore recommended that sea level rises should be considered by adding the additional depth of water onto sea levels for the joint probability curve considered. The joint probability curves should then be examined at the different beach levels and where considered appropriate, extrapolated to estimate any likely increase in wave height. However, despite the comments given above, wave heights should not be reduced.

# 7 Conclusions

Before considering a joint probability assessment, the 'base data' i.e. sea levels and wave heights have to be obtained. For this study, sea level data was obtained from a number of sources, and wave heights were determined based on model transformation from offshore conditions of Met Office model data.

Sea level data from the EA gauge at Workington was of poor quality, and considering the data obtained for Workington from POL, it is unlikely that a reliable representation of sea levels at Workington could have been obtained at this location without this data set. This would have had a subsequent effect on predictions at Silloth and Whitehaven as well as spatially. The POL data set at Workington could be considered of very good quality, although the datum prior to 27/05/94 which has had to be estimated may be in error by 1-2cms. Based on the three data sets of sea levels at Workington and the analysis carried out, it is likely that sea level measurements at Workington are correct and accurate to the accuracy of the measuring devices. This is unlikely to be the 1cm accuracy required of the POL tide gauge by the GLOSS standard (see Section 3.3.2) as a result of the likely water density variation at this location due to the outfall of the nearby River Derwent.

With the tide gauges at Barrow originally installed for the BAE trident submarine programme, the quality of these gauges and records could be considered to be good when not affected by quality issues such as siltation. This is confirmed by a comparison of sea levels at these three locations which show very good agreement (see Figures 3.4 – 3.6). Despite the pressure differentials observed (see Section 3.2.4), it is not believed that this has a noticeable effect on measurements of sea levels. In a similar manner to Workington, it is considered that the sea level records used for Barrow are correct and accurate to a similar degree, although not affected by any likely density variations.

For Silloth, the sea level simulation from the Workington record (Equation 3.1) is considered to be a more accurate representation of sea levels at this location than the records recorded manually. This is related to the variability expected in manually recorded sea level records outlined for example in Hames et al (2004). This is particularly true for Silloth where the tide boards are subject to significant swell. For Whitehaven, the manually recorded sea levels at this location are considered of poor quality with a significant number of incorrectly recorded sea levels. However, as at Silloth, the sea level simulation based on records at Workington would be expected to give an accurate representation of sea levels at this location.

Spatially, it is anticipated that sea level estimations along the Cumbrian coastline could be significantly incorrect. The secondary port information can be considered to be unreliable to an unknown degree, particularly for Tarn Point and Duddon Bar where the relationship between Ordnance and Chart datum has had to be estimated. Considering the comparison between secondary port information at Silloth and Whitehaven with the records established for this study, it is likely that spatially sea levels are likely to be in error by about 0.25m, or possibly more. This will probably have a noticeable effect on the joint probability results, although no sensitivity checks have been carried out.

Sea levels over the analysis period have been estimated to be rising at an average rate of 2mm/year. Based on an analysis of records around the Irish Sea, but mainly on published results, this is likely to be accurate to ±0.5mm/year. Using this estimate of sea level rise, and isostatic rebound estimates given by Shennan (1989), sea level records have been standardised to the start of 2004, which was the latest date that this study could practically be based on. The 18.61 year nodal variation caused by the moon's declination to the earth has not been considered in the standardisation of sea level records, although this is likely to have an effect. Standardisation of records is considered necessary to give a stationary data set.

Offshore records were based on Met Office data from prediction points 54.5°N 4.06°W (northern limit) and 54.0°N 3.26°W (southern limit). These,

together with a third prediction point (54.25°N 3.66°W) are the nearest Met Office prediction points to the Cumbrian coast. No other long term records of waves offshore of the Cumbrian coastline are available. Little added benefit was expected to be achieved with the third prediction point, and this was not pursued. Unlike the sea level data, with Met Office data based on predictions, no pre-processing could be carried out. No standardisation of records was carried out, as no consistent or reliable information is available to indicate any non-stationarity in offshore wave records.

Based on available sea level and offshore wave data, the analysis period was determined from 23/05/91 to 31/10/04. Taking missing records into account this gave an analysis period of 13.2 years.

The wave model chosen to model inshore conditions was the REFDIF model. This was run in monochromatic form for an array of wave heights, periods, directions and sea levels with individual wave components combined based on 13 frequency components. Discretization of the offshore spectrum was based on equal energy bins to ensure good resolution near the spectral peak, with computational effort not being taken up by runs in the low energy spectral tails. Consistency of wave height predictions was observed for at least 9-10 frequency components, and 13 were chosen as this matched the number of frequency components used by the Met Office to predict offshore wave heights. No directional variation was considered as the largest waves from the south west can be considered to be uni-directional as a result of the narrow gap between the North Welsh coast and Southern Ireland.

Three wave models were initially considered to model nearshore wave conditions, with REFDIF mainly chosen due to its ability to model diffraction. This is considered particularly important for the low lying irregular bathymetry of the Solway Firth. Verification tests on REFDIF against published benchmark tests, Lawson et al (1994) and Lawson and Gunn (1996), indicated that it performed well on the types of bathymetry observed along the Cumbrian coastline.

Marginal extremes were modelled based on the GPD, with a minimum threshold of 0.80. Use of the GPD is considered to give more flexibility in the prediction of extremes, especially considering the large data sets used in this study. The 0.80 threshold was chosen to ensure that the asymptotic assumption for the GPD was held. Stability of extreme estimates was observed for sea levels at a threshold below 0.89, and a threshold of 0.80 was chosen. Little variation in extreme estimates was noted for a threshold choice between 0.80 and 0.89. For $MO_1$, stability of extremes was noted for thresholds below 0.90. For $MO_2$, little stability of extremes was noted above any threshold, with model predictions typically increasing with threshold. However, based on the recommended distribution to describe extreme wave heights by Mathiesen et al (1984), a threshold below 0.84 for $MO_2$ was considered appropriate (i.e. a Weibull distribution). The threshold adopted for $MO_1$ and $MO_2$ was 0.80. This was a particularly poor fit to the $MO_2$ data set, which was the same whichever threshold was chosen. However, based on an analysis of wave records for $MO_1$ and $MO_2$, it is believed that wave height records for $MO_2$ particularly above 3m can be viewed with suspicion, although there is presently no means of confirming this or otherwise. This is likely to result in overestimates of extreme wave height conditions inshore, mainly to the south of the study area, which would be reduced at higher beach levels as a result of depth limited effects. This appeared to be confirmed by a visual comparison of predictions from nearshore extremes at regularly spaced inshore locations. For inshore locations, stability of extremes was observed over the range 0.80 to 0.82 and a threshold of 0.82 was chosen.

Considering extreme estimates of inshore wave heights, these were generally constant from the southernmost boundary, possibly decreasing slightly until a region around Barrow. From here until Whitehaven Harbour, little variation in extremes was noted, apart from around the northern limit of Walney Island and Haverigg Point (see below), where there were noticeable increases, and just before Sandscale Haws where they were noticeably lower. Extreme estimates were generally noted to increase at headlands (e.g. Haverigg Point and St. Bees Head), and reduce within bays (e.g. Saltom Bay and Allonby Bay). This was particularly the case for bays north of the predominant wave direction (such as Saltom Bay) which are in

the shelter of protruding land (in this case St. Bees Head). Increased extremes at headlands are probably as a result of concentration of wave energy at these locations due to refraction. Reduced extremes in bays are probably due to the spread of wave energy at these locations due to the same reason, but with the opposite effect. All ports along the coastline, with the exception of Silloth, were noted to have a notable increase in extremes. This is probably due to the large offshore structures at these locations, resulting in steep beach slopes which are not present at Silloth. Whitehaven has particularly large extreme predictions, the largest for Cumbria. Despite the limitation placed on beach slopes in this region (see Section 5.2.3), this is probably as a result of the relative deep waters immediately seaward of the prediction points, which allows large wave heights to approach the harbour relatively unaffected by depth limitation effects.

The model chosen to model joint probability conditions along the study area was the MIX model. This was as a result of a general increase in the correlation between wave heights and sea levels above increasing levels of non-exceedance for the sea level.

Based on an analysis of the joint probability curves along the Cumbrian coastline, there were consistent patterns noted. The 'shape' of the joint probability curves are approximately the same shape for coastlines that could be considered similar. This would mainly include coastlines at the same orientation, but also included bays and headlands. The shapes of the curves generally followed one of three patterns. These consisted of curves that could be considered steep, or steeper approaching the extremes, generic curves of which are shown on Figures 6.14 and 6.15, and curves that could be considered shallow approaching the extremes.

The steepest curves were typically noted to occur within small bays, or regions sheltered from the predominant wave direction by headlands. This is believed to be as a result of extreme wave heights at lower beach levels being subject to more refraction 'into the bay' at lower sea levels. The 'steep' curves were typically noted to occur at headlands or on steep beaches, probably as a result of increased concentration of wave heights at

lower sea levels for headlands, and reduced wave breaking at lower sea levels for steep beaches. Where coastlines were noted to have a change in direction, the joint probability curves for the section of coastline facing further away from the predominant wave direction were noted to have joint probability curves that were flatter approaching the extremes than the section of coastline facing nearer the predominant wave direction. This is generally believed to be as a result of these sections of coastline being exposed to direct wave attack from waves at lower 'extreme' sea levels.

Curves that were noted to be flat approaching the extremes were typically noted at two types of locations. These were locations that could be considered to be within estuaries, sheltered from the predominant wave direction, and sections of the coastline subject to oblique wave attack with a change in coastal orientation 'away' from the predominant wave direction (also see comments above). As this study has concentrated on joint probability curves at the coastline, and not estuaries, few locations, for example within the Duddon Estuary, and the 'effective estuary' at the northern entrance to the Scarth Channel (behind Walney Island), are within estuaries. However, these do have joint probability curves that are flat approaching the extremes, probably as a result of them being sheltered from the predominant wave activity at the largest sea levels. Sections of the coastline subject to an oblique wave attack with a change in coastal orientation 'away' from the predominant wave direction included the sections between Workington and Maryport, Maryport to Allonby and Dubmill Point to Silloth. All three of these sections are either eroding (Maryport to Allonby), protected by a seawall to prevent erosion (Workington to Maryport), or believed to be eroding (Dubmill Point to Silloth). The shape of these curves, and the sediment movement is consistent with the joint probability curves, where direct wave action would be expected at lower 'extreme' sea levels, with the largest waves from the predominant direction approaching at an oblique angle.

At higher beach levels the shapes of the curves given above became increasingly more generic. The difference between, for example, the 'steep' and 'steeper' curves became less noticeable, and the 'flat' curves became 'steep'. At a beach level of +2m@OD, curves for the Cumbrian coastline

could generally be considered to follow the same shape (see below). Despite depth limitation effects at higher beach levels, it was also generally noted that for the most extreme sea levels, wave heights were larger at higher beach levels than at -2m@OD. This could result in damage to coastal defence structures at higher beach levels, and vastly increased levels of overtopping. In the design of coastal defence structures, joint probability curves should therefore be considered at a range of beach levels, rather than one, usually specified at the structure toe. However, more work is required into the change of joint probability curves at higher beach levels.

Given the shape of the curves at a coastline, joint probability curves could be estimated at a location based on joint probability curves at a second location using extreme estimates of wave heights given by Figures 5.24-5.28 and 6.10, and Equation 6.1. Where joint probability curves were not available, which for this study they are, but not necessarily included in this study, the generic curves given by Figures 6.13 and 6.14 could be used based on an estimate of the marginal extreme wave height.

Although this study has concentrated on the analysis of joint probability curves at nearshore locations along the Cumbrian coastline, the main aim of this study was to give guidance to the applications of joint probability at any location. Clearly, the similarity of joint probability curves at similar stretches of coastline means that if a joint probability curve is available at one location, the curve at a location further up or down the coastline could be estimated with a high degree of confidence. The change in the 'shape' as the coastline changes direction also means that a good indication of the regions where the joint probability relationship changes can be made. The standardised 'generic' curves produced at -2m@OD and +0m@OD should help in the choice of the joint probability curve, although it is anticipated that different coastlines would have different generic curves.

An interesting point to emerge from the joint probability curves was the strong agreement noted to eroding coastlines. These tended to coincide with noticeably flatter curves, particularly the more oblique the angle of the coastline to the predominant wave direction. However, this is probably

more related to the angle of predominant wave attack to the coastline than the fact that the coastline is eroding. Curves of these type are therefore probably appropriate to areas of the coast where the predominant wave attack direction is at an oblique angle to the coastline, and coincides with the highest sea levels such as certain areas on the north east coastline of England.

# 8 Recommendations

The original intention in terms of wave modelling at the start of this study was to generate combinations of wave height and sea level records at regularly spaced intervals along the Cumbrian coastline. These were then to be smoothed to reduce the effects of any potential spurious results before looking at the spatial variation. Although the intervals weren't specified at the start of this study, 40m intervals were later decided upon to match the grid spacing of the numerical models. This would have given 2279 prediction points, with 5 inshore prediction beach levels per point, plus one offshore. Smoothing would then have been considered over approximately 5 points, although neither this figure nor method had been decided upon. However, early on in the wave modelling, it became clear that it would not be possible to consider 40m intervals due to the considerable length of time it took to establish inshore conditions from the wave model output. For 2279 predictions points, this would have taken over 100 days, which could not be shared amongst different machines. Therefore 400m intervals were specified, and no smoothing considered. The time to generate the model predictions also meant that a number of runs for wave heights less than 1.0m could not be completed, although all runs for the other three variables were.

Despite the problems experienced with computer run time, the computer models are set up to consider results at 40m intervals. Therefore it is proposed to continue the modelling at these finer intervals so as to give more confidence in the results. These have already started, and at the time of writing, results from over 1900 locations are available. It is also proposed to complete any missing model runs.

A factor not considered in this study was the effect of sea level rise on joint probability curves. To consider sea level rise will result in a considerable number of additional model runs as a result of different sea levels for which model results may not be available. This is particularly the case at the extreme sea levels where the discretization is at its finest, and yet currently the fewest model runs exist. It is proposed to consider this in the future, but

not until further work on the current joint probability curves, plus any additional ones generated, have been completed.

Regardless of whether any additional results are made available or not, the data sets generated are of considerable benefit to the coastal community along the Cumbrian coastline. Results from this study have already been used by third party consultants on at least five projects, including two large scale modelling studies. The joint probability curves will enable coastal defences to be built to a design standard with considerable more confidence, and benefit cost calculations could be considered more robust. These results should be of particular importance to Railtrack as the west coast mainline runs along most of the coastline considered in this study. However, coastal authorities, ports and government agencies (the EA and MAFF) should also benefit to a noticeable degree. It is therefore proposed that the full results for this study are published on a web site. However, this will take a considerable period of time and funding may need to be sought. A further issue to consider is the cost and release of the results themselves. Much of the data used in this study was provided free for research purposes only (such as the Met Office wave data). Although these data could retrospectively be paid for, essential data, such as the Chapelcross hydrographic survey, which belongs to BNFL may not be released. Without permission to use this survey, no results could be made available for potential commercial use. Therefore, before consideration to the results being published is made, it is proposed to investigate potential funding for the data used in this study, and to look into receiving permission to use all data supplied. Several presentations to organisations with an interest in the results was made at the start of this study, and it is proposed to return to these and other organisations to present the final findings and to investigate their interest, and where necessary, any funding available.

# References


Abernethy C.L. and Gilbert G. 1975. Refraction of Wave Spectra. Hydraulics Research Station. Report No. INT 117. May 1975.

Admiralty Tide Tables. 2001. Volume 1, United Kingdom and Ireland (including European Channel Ports). Hydrographer of the Navy.

Alexandersson H., Tuomenvirta H., Schmith T. and Iden K. 2000. Trends of Storms in NW Europe Derived from an Updated Pressure Data Set. Climate Research. Volume 14. pp 71-73.

Andrew C.J.F. 1999. Bibliographic Review of Nearshore Wave Models. Report DSTO-GD-0214. Maritime Operations Division. Aeronautical and Maritime Research Laboratory.

Berkhoff J.C.W. 1972. Computation of Combined Refraction-Diffraction. *Proceedings of the 13th International Conference on Coastal Engineering.* American Society of Civil Engineers. Vancouver. pp 471-490.

Besley P. 1999. Overtopping of Seawalls – Design and Assessment Manual. R&D Technical Report W178. Environment Agency. Bristol.

Booij N. 1983. A Note on the Accuracy of the Mild Slope Equation. *Coastal Engineering.* Volume 7. pp 191-203.

Boon J. (retired member of Virginia Institute of Marine Science, VIMS), Kim S.C. (US Army Cops of Engineers) and Maa J (VIMS). 2004. Personal Communications.

Borgman L.E. 1979. Directional Wave Spectra from Wave Sensors. Ocean Wave Climate. Plenum Press. New York. pp 269-300.

Bouws E., Gunther H., Rosenthal W. and Vincent C. 1985. Similarity of the Wind Wave Spectrum in Finite Depth Water. *Journal of Geophysical Research.* Volume 90(c1).

Bullen Consultants. 1999a. Shoreline Management Plan: sub-cell 11d: St. Bees Head to Earnse Point, Isle of Walney. Volume I. Core Report.

Bullen Consultants. 1999b. Shoreline Management Plan: sub-cell 11e: St. Bees Head to River Sark, Scottish Border, Volume I. Core Report.

Carter D.J.T. and Draper L. 1988. Has the North-East Atlantic Become Rougher? *Nature.* Volume 332. Number 6164. p 494. 7th April 1988.

Chawla A. 2004. Private Communication. Center for Coastal and Land Margin Research. Oregon Health and Science University.

Chawla A. and Baptista A. 2004. Wave-Current Bathymetry Interactions around the Mouth of the Columbia River Estuary. Center for Coastal and Land Margin Research. Oregon Health and Science University.

Coastal Engineering Manual. 2002. Coastal and Hydraulics Laboratory, Engineer Research Center, Waterways Experiment Station, Vicksburg, Mississippi. Part II (Coastal Hydrodynamics). Chapter 3. Section 5.

Coles S. 2001. An Introduction to Statistical Modelling of Extreme Values. Springer Series in Statistics.

Coles S.G. and Tawn J.A. 1990. Statistics of Coastal Flood Prevention. *Philosophical Transactions of the Royal Society of London Series A.* Volume 332. pp 457-476.

Dalrymple R.A., Kirby J.T. and Mann D.W. 1984. Wave Propagation in the Vicinity of Islands. *Proceedings of the 16th Offshore Technology Conference.* Number 4675. Houston. May.

Davison A.C. and Smith R.L. 1990. Models foe Exceedances over High Thresholds. Journal of the Royal Statistical Society Series B. Volume 52. Number 3. pp 393-442.

Defra. 2001. Shoreline Management Plans. A Guide for Coastal Defence Authorities. June 2001.

Defra / Environment Agency. 2005. Joint Probability : Dependence Mapping and Best Practice. Defra / Environment Agency Flood and Coastal Defence R&D Programme. R&D Technical Report FD2308/TR1. March 2005.

DETRA. 1999. Indicators of Climate Change in the UK. Report by Climate Research Unit and Centre for Ecology and Hydrology.

Dingemans M.V. 1983. Verification of Numerical Wave Propagation Models with Field Measurements. Report No. W488. CREDIZ Verification, Haringvliet. Delft Hydraulics Laboratory.

Dingemans M.W. 1997. Water Wave Propagation over Uneven Bottoms. Advanced Series on Ocean Engineering. Volume 13. Part 2 – Non-Linear Wave Propagation. World Scientific Press. Singapore.

Dixon M.J. and Tawn J.A. 1994. Extreme Sea-Level at the UK A-Class Sites : Site-by-Site Analyses. Proudman Oceanographic Laboratory. Internal Document Number 65, March 1994.

Dixon M.J. and Tawn J.A. 1995. Extreme Sea-Levels at the UK A-Class Sites : Optimal Site-by-Site Analyses and Spatial Analyses for the East Coast. Proudman Oceanographic Laboratory. Internal Document Number 72. August 1995.

Dixon M.J. and Tawn J.A. 1997. Spatial Analyses for the UK Coast. Proudman Oceanographic Laboratory. Internal Document Number 112. June 1997.

Douglas B.C. 1991. Global sea level rise. *Journal of Geophysical Research.* Volume 96 (C4). pp 6981-6992.

Dwarko R. 2004. Ocean Tide Loading Monitored by GPS in the British Isles. MSc. Thesis. University of East London.

Foskett N. 2006. Private Communication. Harbour Master, Whitehaven Harbour. 20/04/2006.

Goda Y. 2000. Random Seas and Design of Maritime Structures. Advanced Series on Ocean Engineering. Volume 15. World Scientific Press.

Goda Y., Hawkes P.J., Mansard E., Martin M.J., Mathiesen M., Peltier E., Thompson E.F. and Van Vledder G. 1993. Intercomparison of Extremal Wave Analysis Methods using Numerically Simulated Data. *Proceedings of the Second International Symposium on Ocean Wave Measurement and Analysis.* New Orleans. Louisianna.

Golding B. 1983. A Wave Prediction System for Real Time Sea State Forecasting. *Quarterly Journal of the Royal Meteorological Society.* Volume 109. pp 393-416.

Graff J. 1981. An Investigation of the Frequency Distributions of Annual Sea-Level Maximum at Ports around Great Britain. *Estuarine, Coastal and Shelf Science*, Volume 12. pp 389-449.

Grimshaw S.D. 1993. Computing Maximum Likelihood Estimates for the Generalised Pareto Distribution. *Technometrics.* American Statistical Association and the American Society for Quality Control. May 1993. Volume 35. Number 2. pp185-191.

Hames D. 1997. KrKs User Manual. Bullen Consultants Ltd. Birkenhead. Internal Document.

Hames D.P. 2001. Assessment of Tide Levels at Wepre Brook. University of East London. Confidential Letter Report for Bullen Consultants. March 2001.

Hames D.P. 2002. Coastal Erosion at Bootle – Flooding Assessment. University of East London. Confidential Report for Bullen Consultants. July 2002.

Hames D., Reeve D., Marriott M. and Chadwick A. 2004. Effect of Data Quality on the Analysis of Water Levels along the Cumbrian Coastline. *International*

*Conference on Flood Risk Assessment.* Institute of Mathematics and its Applications. University of Bath. April 2004.

Harford C.M. 1998. A Catalogue of Instrumentally Measured Wave Data around the Coast of England and Wales. HR Wallingford Ltd. Report Number TR 51. October 1998.

Hawkes P.J. and Hague R.C. 1994. Validation of Joint Probability Methods for Large Waves and High Water Levels. HR Wallingford Report SR 347.

Hawkes P., Gouldby B., Weidong S., Tawn J., Hames D., Reeve D., Blackman D., Sproson R. and Mavronasos K. 2004. A Comparison of Marginal and Joint Extremes Predicted from Synthesised Wave and Water Level Data. *International Conference on Flood Risk Assessment.* Institute of Mathematics and its Applications. University of Bath. April 2004.

Hedges T.S. 1976. An Empirical Modification to Linear Wave Theory. *Proceedings of the Institution of Civil Engineers.* Volume 61. pp 575-579.

Holt M. 1999. Private Communication. Manager Operational Ocean Model Development, the Met Office 18/08/99.

Holthuijsen L.H., Booij N., Ris R.C., Haagsma I.J.G., Kieftenburg A.T.M.M., Kriezi E.E., Ziilema M. and Westhuysen A.J. 2004. SWAN Cycle III version 40.31 User Manual. Delft University of Technology.113 pp.

Hulme M. and Jenkins G.J. 1998. Climate Change Scenarios for the UK: Scientific Report. UKCIP Technical Report No 1. Climate Research Unit. Norwich. 88pp.

Hydraulics Research Limited. 1990. Joint Probability of Waves and Water Levels on the North Wales Coast. Report Number EX 2133. May 1990.

HR Wallingford. 1992. UK South Coast Shingle Study - Joint Probability Assessment. Report Number SR 315. July 1992.

HR Wallingford. 2000a. The Joint Probability of Waves and Water Levels : JOINSEA – A Rigorous but Practical New Approach. Report SR537. May 2000.

HR Wallingford. 2000b. The Joint Probability of Waves and Water Levels : JOINSEA – Version 1.0. User Manual. Report TR71. May 2000.

Intergovernmental Panel on Climate Change (IPCC). 2001. Climate Change 2001, The Scientific Basis. Contribution of Working Group 1 to the Third Assessment Report of the Intergovernmental Panel on Climate Change, (editors Houghton J.T., Ding Y., Griggs D.J., Noguer M., Van Der Linden P.J., Dai X. Maskell K. and Johnson C.A.). Cambridge University Press. Cambridge.

Jeremy Benn Associates Limited. 1998. Extreme Sea Levels for Section 105 Surveys - Final Report for Environment Agency North West Region, July 1998.

Jones J.E. and Davies A.M. 2003. Processes Influencing Storm-Induced Currents in the Irish Sea. *Journal of Physical Oceanography.* Volume 33. Number 1. pp 88-104.

Kelley S.W., Ramsey J.S. and Byrnes M.R. 1999. Comparison of Numerical Spectral Wave Transformation Models for Evaluating the Physical Environmental Impacts of Offshore Sand Mining. Applied Coastal Research and Engineering, Inc. Technical Report for U.S. Department of the Interior. 24 pp.

Kirby J.T. 1986a. Rational Approximations in the Parabolic Equation Method for Water Waves. *Coastal Engineering.* Volume 10. pp 355-378.

Kirby J.T. 1986b. Open Boundary Condition in Parabolic Equation Method. *Journal of Waterways, Port, Coastal and Ocean Engineering.* Volume 112. pp 460-465.

Kirby J.T. and Dalrymple R.A. 1986. Modelling Waves in Surfzones and around Islands. *Journal of Waterways, Port, Coastal and Ocean Engineering*, Volume 112. pp 78-93.

Kirby J.T. and Dalrymple R.A. 1994. Combined Refraction / Diffraction Model REFDIF-1. Version 2.5. Documentation and User's Manual. CACR Report 94-22. Center for Applied Coastal Research. University of Delaware. 122 pp.

Kobune K. and Konube K. 1986. Estimation of Directional Spectra from the Maximum Entropy Principle. *Proceedings of the 5th Offshore Mechanics and Artic Engineering'86 Conference.* Tokyo. pp 80-85.

Kotz S. and Nadarajah S. 1999. Extreme Value Distributions, Theory and Applications. Imperial College Press.

Krogstad H., Barstow S.F., Haug O. and Peters D.J.H. 1998. Directional Distributions in Wave Spectra. *Proceedings of the third international symposium Waves 97. Ocean Wave Measurements and Analysis.* November 3-7 1997. Virginia. Volume 2.

Lawson J., Smallman J.V. and Watson G.M. 1994. Application of Appropriate Wave Transformation Models. HR Wallingford R&D Note 272 for National Rivers Authority.

Lawson J. and Gunn I.J. 1996. Guidelines for the use of Computational Models in Coastal and Estuarial Studies - Wave Transformation and Wave Disturbance Models. HR Wallingford Report SR 450. March 1996.

Ledford A.W. and Tawn J.A. 1996. Statistics for Near Independence in Multivariate Extreme Values. *Biometrika.* Volume 83. Number 1. pp 169-187.

Ledford A.W. and Tawn J.A. 1997. Modelling Dependence within Joint Tail Regions. *Journal of the Royal Statistical Society.* Series B. Volume 59. Number 2. pp 475-499.

Lee D.T. and Schachter B.J. 1980. Two Algorithms for Constructing a Delaunay Triangulation. *International Journal of Computer and Information Sciences.* Volume 9. Number 3. pp 219-242.

Lloyd R. 2000. Private Communication. Chief Hydrographer Mersey Docks and Harbours.

Longuet-Higgins M.S., Cartwright D.E. and Smith N.D. 1962. Observations of the Directional Spectrum of Sea Waves using the Motions of a Floating Buoy. Ocean Wave Spectra. Proceedings of a Conference, Maryland May 1-4 1961. Prentice-Hall. Englewood Cliffs. NJ. pp 111-132.

Maa J.P-Y., Hobbs C.H., Kim S.C. and Wei E. 2004. Potential Impacts of Sand Mining Offshore of Maryland and Delaware: Part 1 – Impacts on Physical Oceanographic Processes. *Journal of Coastal Research.* Volume 20. Part 1. pp 44-60.

Martin C.J., Dalrymple R.A. and Miller M.C. 1987. A Verification Procedure for Wave Propagation Models. In: Modelling the Offshore Environment. Society for Underwater Technology. Graham and Trotman.

Mathiesen M., Goda Y., Hawkes P.J., Mansard E., Martin M.J., Peltier E., Thompson E.F. and Van Vledder G. 1994. Recommended Practice for Extreme Wave Analysis. *Journal of Hydraulic Research.* Volume 32. Number 6.

The Met Office. 1995. Numerical Weather Prediction (NWP) Gazette. Met Office Research and Development Publication. September 1995.

Míguez B.M., Begoña P.G. and Fanjul E.A. 2005. The ESEAS-RI Sea Level Test Station : Reliability and Accuracy of Different Tide Gauges. *International Hydrographic Review.* Volume 6. Number 1. April 2005.

Owen M.W. 1980. Design of Sea Walls Allowing for Wave Overtopping. Hydraulics Research Station. Report No. EX 924.

Peregrine D.H. 1967. Long Waves on a Beach. *Journal of Fluid Mechanics.* Volume 27. Part 4. pp 815-827.

Pirazzoli P.A. 2000. Sea-Level Changes. The Last 20000 Years. Wiley.

Proudman Oceanographic Laboratory. Coastal Observatory, Liverpool Bay, Irish Sea (UK). Irish Sea Model. www.cobs.pol.ac.uk/modl. Date accessed 16/05/05.

Proudman Oceanographic Laboratory. 1998. POLTIPS.2 Tide Prediction Program. (Leisure Version). Version 2. [3½in disk]. Bidston.

Proudman Oceanographic Laboratory. 2001. POLTIPS.3 Tide Prediction Program. (Customised / Publishers Version). Version 3. [CD-ROM]. Bidston.

Ramsey D.L. and Harford C.M. 1995. A Catalogue of Synthetic Wave Data around the Coast of England and Wales. HR Wallingford Report Number SR 373. November 1995.

Reeve. D.E. 1992. Bathymetric Generation of an Angular Wave Spectrum. *Wave Motion.* Volume 16. pp 217-228.

Reeve D. and Bin L. 1994. MAFF/NRA Joint Wave Measurement and Validation. Phase II : Modelling, Comparison and Validation. Final Study Report. Ministry of Agriculture, Fisheries and Food Flood and Coastal Defence Division. October 1994.

Reeve D., Chadwick A. and Fleming C. 2004. Coastal Engineering Processes, Theory and Design Practice. Spon Press.

Schröter A., Mayerle R., Kahlfeld A. and Zielke W. 1995. Assessment of a Boussinesq Wave Model for the Design of a Harbour. Proceedings of the 4th International Conference on Coastal and Port Engineering in Developing Countries (COPEDED IV). Rio de Janeiro.

Shennan I. 1989. Holocene Crustal Movements and Sea-Level Changes in Great Britain. *Journal of Quaternary Science.* Volume 4. pp 77-89.

Shennan I. and Horton B. 2002. Holocene Land and Sea Level Changes in Great Britain. *Journal of Quaternary Science.* Volume 17. Parts 5-6. pp 511-526.

Shennan I. and Woodworth P.L. 1992. A Comparison of late Holocene and Twentieth Century Sea Level Trends from the UK and North Sea Region. *Geophysical Journal International.* Volume 109. pp 96-105.

Tsimplis M.N. and Spencer N.E. 1997. Collection and Analysis of Monthly Mean Sea Level Data in the Mediterranean and the Black Sea. *Journal of Coastal Research.* Volume 13. Number 2. pp 534-544.

UNESCO. 1985. Manual on Sea Level Measurement and Interpolation, Basic Procedures. Intergovernmental Oceanographic Commission, Manuals and Guides. Volume I. Number 14. 83 pp.

UNESCO. 2002. Manual on Sea Level Measurement and Interpolation, Reappraisals and recommendations as of the year 2000. Intergovernmental Oceanographic Commission, Manuals and Guides. Volume III. Number 14. 47 pp.

Van Der Meer J.W. 1988. Rock Slopes and Gravel Beaches under Wave Attack. Ph.D. Thesis. Department of Civil Engineering. Delft Technical University. Delft. The Netherlands.

Van Vladder G., Goda Y., Hawkes P.J., Mansard E., Martin M.J., Mathiesen M., Peltier E. and Thompson E.F. 1993. Case Studies of Extreme Wave Analysis : A Comparative Analysis. *Proceedings of the Second International Symposium on Ocean Wave Measurement and Analysis.* New Orleans, Louisianna.

Williams A. 2005. Private Communication. Faber Maunsell (Birkenhead). 27/09/05.

Woodworth P., Smith D., Flather R., Baker T., Rickards L. 2004. Proposals for the Development of the UK National Tide Gauge Network. Proudman Oceanographic Laboratory Internal Document 161.

Woodworth P.L., Tsimplis M.N., Flather R.A. and Shennan I. 1999. A Review of the Trends Observed in British Isles Mean Sea Level Data Measured by Tide Gauges. *Geophysical Journal International.* Volume 136. pp 651-670.

# Appendix A : History of Known Sea Level Records for the Cumbrian Coastline

**Silloth**

Sea level readings at Silloth are usually taken off one of two tide boards located on the outside of the Dock Gate and overlooked by the Port Operations Office (see Figure A.1). Only readings at high sea levels are taken, and these are probably taken within 5-10 minutes of the predicted high tide, and not necessarily when the highest sea level occurs. This will lead to a negligible maximum error in the tidal readings, less than 0.5% of the tidal range. If the dock gate is closed at high tide, tide readings are sometimes taken off the tide board located within the dock[1]. Manually recorded sea level records are available for Silloth from 01/11/87 to date, and have been digitised to 31/10/04.

**Figure A.1a** : Internal tide board

**Figure A.1b** : External tide board

The tide boards at Silloth are located 1.8m above Chart Datum. This is 2.6m below Ordnance Datum. The tide boards at Silloth were re-levelled as a result of initial reservations regarding their quoted level. This confirmed the level to an accuracy of 11mm (2.589m below Ordnance

[1] Private Communications with Deputy Harbour Master, Port of Silloth 18/09/02.

Datum)[2]. The tide boards are metric, with graduations every 10 centimetres. Readings are typically recorded to the nearest 0.05m.

**Workington**

Two tide gauges are located at Workington, one maintained by the EA, and one maintained by POL. The EA gauge is a pressure gauge which dries out at -3.4m@OD. The POL gauge is a pneumatic bubbler system supplying two full tide pressure points. Both tide gauges are calibrated for salt water conditions. There are no mid tide probes at Workington. The tide gauges are contained in the same building (shown on Figure A.2 below), which is overlooked by the Port Operations Office. The measuring points are located seaward of the Dock Gates by the Lifeboat Station behind fender piles with very limited access. Despite this region being dredged, the POL measuring points are only 2cms below Chart Datum, sitting on the mud. No details on the EA measuring points are available. The tide gauge bench mark is set 0.7m above ground level on the south west face of the Port Operations Office. Temperature / conductivity tests show that the density of water near the port entrance is very 'fresh' as a result of the outfall of the River Derwent immediately to the south of the tide gauges[3] (see Figure 3.1). The POL tide gauge gives a real time reading of the sea level in the harbour offices, although this is not used in the manual recording of the sea level at high water.

Manual sea level readings are taken off the internal tide board, which is in imperial units. Graduations are every 6ins, and they are located 1.16m below Chart Datum (5.36m below OD). Readings are taken at the time of predicted high tide, typically to the nearest 3ins. The external tide board is not used except to fix the tide gauges. It is very dirty, and is not cleaned by the harbour authorities.

---

[2] Survey carried out by Alex Williams of Bullen Consultants Ltd on 14/11/02 on behalf of Dominic Hames.

[3] Based on observations and private communications with Capt. Ashbridge, Harbour Master, Port of Workington, Martin Wilson, Environment Agency Penrith and David Smith, Manager Tide Gauge Inspectorate, POL.

As a result of the difficulties in checking the tide board, data recorded by the EA from January 2001 to February 2003 inclusive remained unchecked. The EA were looking to replace the external tide board before the end of October 2002. It is likely that the external tide board was replaced in late February 2003, although this has not been confirmed.

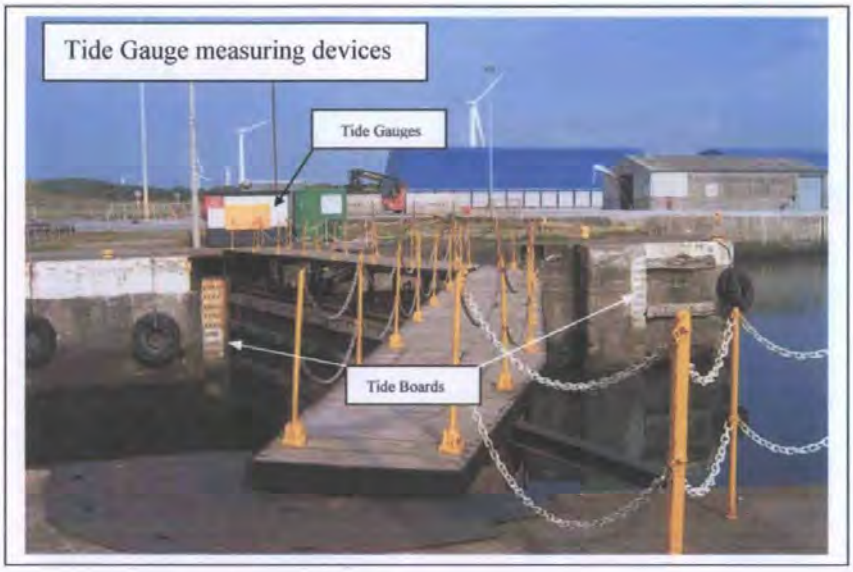


**Figure A.2** : Tide boards at Workington

The POL tide gauge was initially set up to record sea levels approximately 0.11m too high. At the start of 1993, digital readings were recording 0.18m lower, giving a net effect of recording sea levels approximately 0.07m too low. Around 27/05/94, digital readings started recording approximately 0.11m lower, a net effect of recording sea levels about 0.18m too low. This tide gauge was re-levelled on 24/09/02, and the entire POL Workington tidal record was initially adjusted to record 0.18m higher, including (incorrectly) the period till 27/05/94. Subsequent to this initial readjustment, readings for 1992 have been reset to their original levels, approximately 0.11mm too high. POL are aware of the concerns expressed relating to the sea levels at Workington prior to 27/05/94, which were also commented on in Hames et al (2004), and it is believed that these may be revisited as part of a general review of recorded sea levels sometime in the future.

**Whitehaven**

Up until August 1998, only high sea level records were recorded at Whitehaven. This was done based on manual readings off the tide board located seaward of the Queens Dock Gates at the entrance to the Harbour. As a result of a major development of the Harbour in 1998, three radar reflection tide gauges were installed for the harbour. These were inside the harbour (shown on Figure A.3), within the dock gate system (overlooked by the Port Operations Office) and on the outside of the external harbour wall. Although high sea levels are still recorded (as well as low sea levels), this is done based on a real time digital readout from the external tide gauge. High sea levels up to 02/01/98 are in imperial units, and were typically recorded to the nearest 3ins. High sea levels from this date are in metric units, and are typically recorded to the nearest 0.1m. The changeover from imperial to metric measurements in early 1998 is believed to be as a result of the lead in to the harbour development in that year.

Availability and ownership of the digital records is not known, and it has not been possible to obtain these records for this study. However, it is believed, based on several unrecorded communications that these records are of poor quality, and could well be of little use. This was partly confirmed by observation of the erratic nature of the real time display in the Port Operations Office.

The zero datum of the imperial manual readings off the old Queens Dock gate is not available, but has been estimated at 1.4m above CD. The original manual sea level readings at Whitehaven used for this study are now believed to be lost.

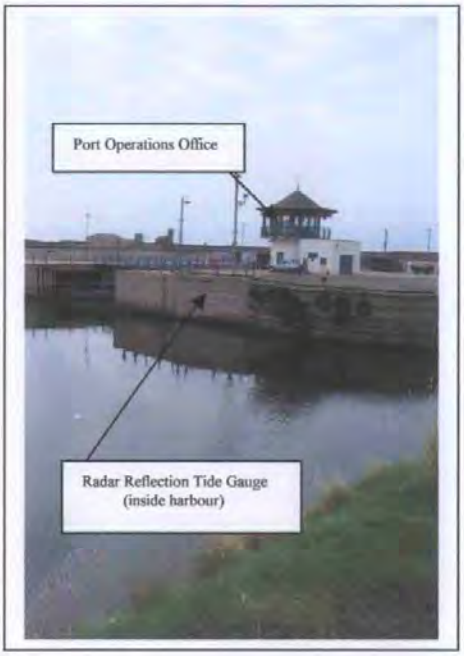


**Figure A.3** : Radar reflection tide gauge (inside harbour).

**Barrow (Ramsden Dock, Roa Island and Halfway Shoal)**

Sea levels at Barrow are / have been digitally recorded at three locations; Ramsden Dock, Halfway Shoal and Roa Island since 01/05/92 (see Figure A.4). The reduction in the BAE trident submarine programme now means that until the end of 2004 only the tide gauges at Ramsden Dock had been operational. The tide gauge bench mark for Ramsden Dock is a pin on the north-west side of the old Dock Entrance, 1.2m south-west of the lock gates' south-west face. The tide gauge bench mark for Roa Island is an Ordnance Survey Bolt on the curb on the east side of Piel Street. The tide gauge bench mark for Halfway Shoal is the top of the platform.

Sea levels are also recorded manually off one of four tide boards every hour since about 2001. These are located either side of the Dock Gates, two inside the Dock Gates and two outside the Dock Gates and overlooked by the Port Operations Office. High and low sea levels have been recorded for many years, the exact duration of which is not known. Awareness of the existence of these records came too late for them to be included in this study. A real time reading of the sea level in the harbour offices is also given from the Ramsden Dock tide gauges.

The tide boards on their last levelling in were recorded as being 2.3cm too high, and record higher visually than the digital readouts from the Ramsden Dock tide gauges[4]. However, this is not confirmed by analysis of the sea level records, which have not been changed.

The digital sea levels at Ramsden Dock, Roa Island and Halfway Shoal have been recorded based on two gauges placed side by side (pneumatic bubbler for Ramsden Dock and Roa Island and pressure for Halfway Shoal). These gauges have been in operation since 01/05/92 for Ramsden Dock and Roa Island, and since 22/08/92 for Halfway Shoal. The tide gauges at Roa Island and Halfway Shoal have not been in operation since February 2000 and June 2001 respectively, and will not be used again (see below).

**Figure A.4a** : Location of tide gauge at Ramsden Dock

The tide gauges at Ramsden Dock are located near the Dock Gates behind the fender wall. The location of the tide gauges is indicated on Figure A.4a above. Originally this tide gauge was placed on the inside of the Dock wall, but had to be moved to the outside of the Dock wall as this location was found to be less prone to siltation. The tide gauge at Roa Island is located on the old Lifeboat slipway near the new Lifeboat station on Roa Island.

[4] Private Communication with David Carpenter, Harbour Master, Ramsden Dock 17/06/04.

The old cable leading off from the tide gauge is now cut in two as shown on Figure A.4b below. The tide gauge at Halfway Shoal is located on the Beacon in the dredged channel entrance to the port (see Figure A.4b).

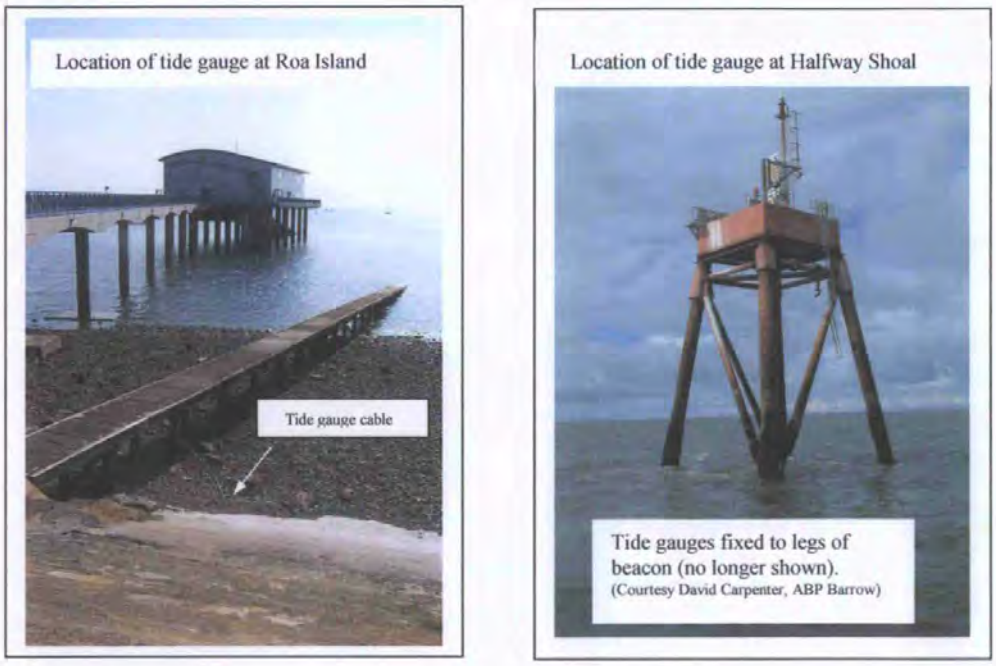


**Figure A.4b** : Location of tide gauges at Roa Island and Halfway Shoal.

The tide gauges at these locations are prone to siltation, especially Ramsden Dock, as indicated in Hames et al (2004).

The 'Barrow' data sets have not been maintained for a number of years. Since the Roa Island and Halfway Shoal tide gauges ceased to be operational, maintenance on the Ramsden Dock tide gauges only appears to have been carried out when the gauges break down. The tide gauges at Ramsden Dock now appear to be silted up, and readings since 07/01/01 are considered unreliable, and are not included in this study.

A completely new set of tide gauges was installed at all three stations in mid 2005 to support Navigation Channel modelling for future nuclear submarine access. These were expected to be operational before the end of 2005.

# Appendix B : Verification of REFDIF

To verify the use of REFDIF in this study, it was tested against four of six benchmark tests which were outlined in Lawson et al (1994) and Lawson and Gunn (1996). The range of tests chosen consisted of a simple test with an analytical solution, two real situations for which field measurements exist and a test case based on a physical model, for which physical model test data exists.

The results from the verification were compared with the original comparisons done against sixteen wave transformation models and the monochromatic form of KrKs for 3 of the 4 test cases. The models for which the comparisons were made are given in Table B.1 below.

| Program | Developer | Year | Type |
|---|---|---|---|
| ORCAWAVE | Orcina Ltd | 1990 | Forward Tracking |
| OUTRAY | HR Wallingford Ltd | 1989 | Back Tracking |
| PORTRAY | HR Wallingford Ltd | 1988 | Forward Tracking |
| REFRAC | Delft Hydraulics | 1990 | Forward or Back Tracking |
| W-RAY | Scott Wilson Kirkpatrick | 1993 | Back Tracking |
| ENDEC | Delft Hydraulics | 1990 | Finite Difference Refraction |
| HISWA | Delft University | 1992 | Finite Difference Refraction |
| LINDAL | Applied Wave Research | 1988 | Finite Difference Refraction |
| MIKE 21 NSW | Danish Hydraulic Institute | 1991 | Finite Difference Refraction |
| ARMADA | Li and Anastasiou | 1992 | Finite Difference Refraction / Diffraction |
| MIKE 21 PMS | Danish Hydraulic Institute | 1993 | Finite Difference Refraction / Diffraction |
| MULTIGRID | Li and Anastasiou | 1992 | Finite Difference Refraction / Diffraction |
| PARAB | HR Wallingford Ltd | 1992 | Finite Difference Refraction / Diffraction |
| Wc2D | University of Liverpool | 1990 | Finite Difference Refraction / Diffraction |
| CGWAVE | University of Maine | 1993 | Finite Element Refraction / Diffraction |
| ARTEMIS 2.0 | L'aboratoire d'Hydraulique de France | 1992 | Finite Element Model |

**Table B.1** : Wave transformation models used in verification exercise

## B.1 Benchmark Tests

For each benchmark test, REFDIF and KrKs were tested and the results compared with each model tested. The comparisons were made with the versions of these models which would have existed between February and September 1993. Although many of these models will have been updated since then, more up to date comparisons are not available. It should also be remembered that this exercise was to investigate the accuracy and suitability of REFDIF to predict nearshore wave conditions along the Cumbrian Coast and not to determine whether it was better or worse than any of the other models tested.

**Test A - Linear Beach**

The bathymetry for this test consisted of a plane slope rising from a region of constant depth, the solution of which is given by Snell's law. The definition of the model bathymetry and the analysis points is given in Lawson et al (1994) and Lawson and Gunn (1996), and shown in Figure B.1a below.

The incident wave conditions were a monochromatic wave with an amplitude of 0.58m and a period of 3.7 seconds with an incident direction of 0° to the 'y' axis. Model results were compared against the analytic solution.

**Test B - Elliptic Shoal**

The bathymetry for this widely used test case is similar to that used in the linear beach example but with an elliptic shoal on the slope. The definition of the model bathymetry and the analysis points is given in Lawson et al (1994) and Lawson and Gunn (1996), and shown in Figure B.1b below.

The incident wave conditions were a monochromatic wave with an amplitude of 0.58m and a period of 5 seconds with an incident direction of 0° to the 'y' axis. Model results were compared against physical model test results.

**Test C - Harbour Approach**

The bathymetry for this test case is based on a physical model and represents bathymetry typical of a dredged harbour approach channel. Four different incident wave conditions were specified (shown in Table B.2 below), with wave heights predicted at ten analysis points. The definition of the model bathymetry and the analysis points is given in Lawson et al (1994) and Lawson and Gunn (1996), and shown in Figure B.1c below. All test cases were specified to be run at a sea level of +1.9m@CD.

This test was not considered a suitable test case for KrKs due to the large diffraction effects at the channel, and was therefore not tested against this model.

| Storm Number | Offshore Wave Conditions | | |
|---|---|---|---|
| | $H_s$ | $T_m$ | Direction (°) |
| 1 | 4.3 | 8.6 | 0 |
| 2 | 1.9 | 6.0 | 0 |
| 3 | 6.0 | 10.0 | 25 |
| 4 | 3.2 | 7.5 | 25 |

**Table B.2** : Incident wave conditions for harbour approach

Model runs for REFDIF were carried out assuming a JONSWAP spectrum and a wrapped normal distribution for 5 frequency and 5 directional components.

**Test D - Perranporth**

This test was based on a site near Perranporth which lies on the north coast of Cornwall. Wave measurements from an offshore waverider buoy were used as the incident wave conditions with actual measured data available from an inshore waverider buoy. Wave spectra, with both directional and frequency components for ten storms were used, which are shown in Table B.3 below. The bathymetry for this location together with the positions of the offshore and the inshore waverider buoys are shown in Figure B.1d.

Lawson et al (1994) and Lawson and Gunn (1996) state that a previous study at Perranporth indicated that the effect of the tidal range was small. Therefore all runs were to be run at mean sea level (+0.25m@OD).

| Storm Number | Offshore Wave Conditions | | |
|---|---|---|---|
| | $H_s$ | $T_m$ | Direction (°) |
| 1 | 4.0 | 7.0 | 259 |
| 2 | 3.2 | 7.3 | 253 |
| 3 | 7.1 | 10.5 | 253 |
| 4 | 3.2 | 6.1 | 11 |
| 5 | 3.4 | 8.0 | 255 |
| 6 | 4.2 | 7.3 | 271 |
| 7 | 4.5 | 7.2 | 273 |
| 8 | 5.8 | 7.7 | 343 |
| 9 | 3.6 | 6.7 | 276 |
| 10 | 3.4 | 6.2 | 279 |

**Table B.3** : Storm conditions recorded by offshore waverider buoy at Perranporth

Model runs using REFDIF were carried out assuming a JONSWAP spectrum and a wrapped normal distribution for 5 frequency and 5 directional components.

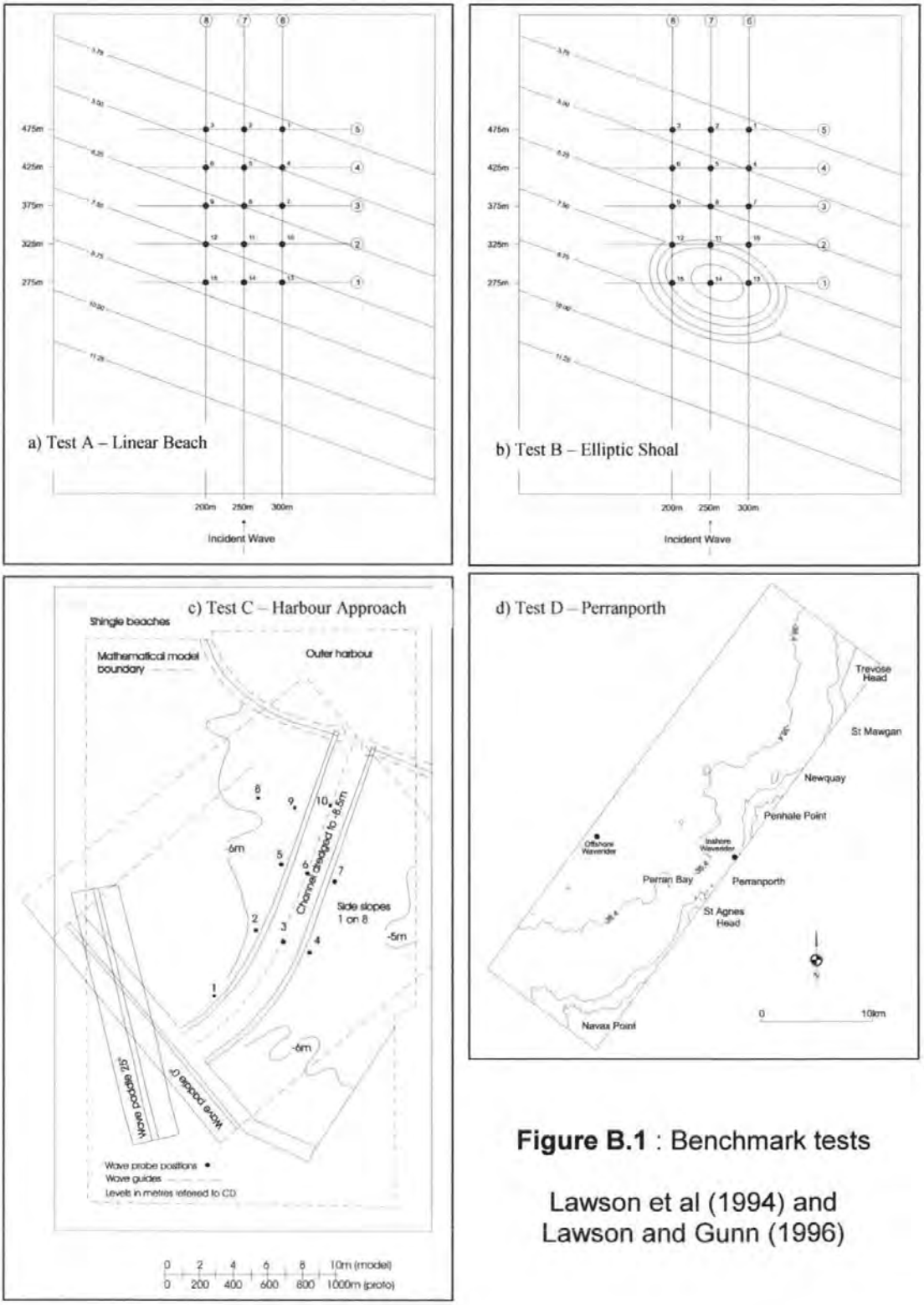


**Figure B.1** : Benchmark tests

Lawson et al (1994) and
Lawson and Gunn (1996)

## B.2 Benchmark Test Results

The tests comparisons carried out and the participants are given in Table B.4. Wave height coefficients (WHC), given as the ratio of the modelled wave height to the input wave height, are quoted to the same degree of accuracy as the field, physical model or analytic data with the percentage errors computed using the results supplied. The original supplied results are no longer available from HR Wallingford Ltd.

| Participant | Key | Model | Test Case | | | |
|---|---|---|---|---|---|---|
| | | | A | B | C | D |
| ABP Research and Consultancy | ABP | MULTIGRID | | ✓ | ✓ | ✓ |
| Acer Consultants Ltd | ACER | OUTRAY | | | | ✓ |
| Applied Wave Research | AWR | LINDAL | ✓ | ✓ | | ✓ |
| Binnie and Partners | BIN | Wc2D | | | ✓ | ✓ |
| Halcrow | HC | ARMADA | ✓ | ✓ | | |
| HR Wallingford Ltd | HR | OUTRAY | ✓ | ✓ | ✓ | ✓ |
| | | PORTRAY | ✓ | ✓ | ✓ | ✓ |
| | | PARAB | ✓ | ✓ | ✓ | ✓ |
| Kirk McClure Morton | KMM | CGWAVE | | ✓ | | |
| | | OUTRAY | | | | |
| L'aboratoire d'Hydraulique | LHF | ARTEMIS 2.0 | ✓ | ✓ | | |
| Orcina Ltd | ORC | ORCAWAVE | ✓ | ✓ | | ✓ |
| Posford Duvivier | PD | ENDEC | ✓ | ✓ | | |
| | | HISWA | ✓ | ✓ | | ✓ |
| | | REFRAC | ✓ | ✓ | | |
| Scott Wilson Kirkpatrick | SWK | MULTIGRID | ✓ | ✓ | ✓ | |
| | | W-RAY | | | ✓ | ✓ |
| W.S. Atkins | WSA | MIKE21NSW | | | | ✓ |
| | | MIKE21PMS | ✓ | ✓ | ✓ | |
| N/A | | REFDIF | ✓ | ✓ | ✓ | ✓ |
| N/A | | KrKs | ✓ | ✓ | | ✓ |

**Table B.4** : Test comparisons carried out together with participants.

| Analysis Point | Analytic Solution | OUTRAY (HR) | PORTRAY (HR) | REFRAC (PD) | ENDEC (PD) | HISWA (PD) | LINDAL (AWR) | ORCAWAVE (ORC) |
|---|---|---|---|---|---|---|---|---|
| 1 | 0.91 | 0.92 (+1%) | 0.88 (-3%) | 0.92 (+1%) | 0.94 (+3%) | 0.78 (-14%) | 0.92 (+1%) | 0.91 (0%) |
| 2 | 0.91 | 0.95 (+4%) | 0.88 (-3%) | 0.93 (+2%) | 0.96 (+5%) | 0.80 (-12%) | 0.92 (+1%) | 0.92 (+1%) |
| 3 | 0.92 | 0.96 (+4%) | 0.88 (-4%) | 0.93 (+1%) | 0.96 (+4%) | 0.82 (-11%) | 0.93 (+1%) | 0.92 (0%) |
| 4 | 0.92 | 0.94 (+2%) | 0.91 (-1%) | 0.94 (+2%) | 0.97 (+5%) | 0.84 (-9%) | 0.93 (+1%) | 0.93 (+1%) |
| 5 | 0.93 | 0.93 (0%) | 0.90 (-3%) | 0.94 (+1%) | 0.97 (+4%) | 0.85 (-9%) | 0.93 (0%) | 0.93 (0%) |
| 6 | 0.93 | 0.98 (+5%) | 0.91 (-2%) | 0.95 (+2%) | 0.97 (+4%) | 0.85 (-9%) | 0.94 (+1%) | 0.94 (+1%) |
| 7 | 0.94 | 0.95 (+1%) | 0.91 (-3%) | 0.95 (+1%) | 0.97 (+3%) | 0.87 (-7%) | 0.95 (+1%) | 0.94 (0%) |
| 8 | 0.94 | 0.95 (+1%) | 0.91 (-3%) | 0.96 (+2%) | 0.97 (+3%) | 0.88 (-6%) | 0.95 (+1%) | 0.95 (+1%) |
| 9 | 0.95 | 1.00 (+5%) | 0.92 (-3%) | 0.96 (+1%) | 0.97 (+2%) | 0.89 (-6%) | 0.96 (+1%) | 0.96 (+1%) |
| 10 | 0.95 | 0.96 (+1%) | 0.93 (-2%) | 0.97 (+2%) | 0.97 (+2%) | 0.91 (-4%) | 0.96 (+1%) | 0.96 (+1%) |
| 11 | 0.96 | 0.97 (+1%) | 0.93 (-3%) | 0.97 (+1%) | 0.98 (+2%) | 0.91 (-5%) | 0.97 (+1%) | 0.97 (+1%) |
| 12 | 0.96 | 1.03 (+7%) | 0.92 (-4%) | 0.98 (+2%) | 0.98 (+2%) | 0.92 (-4%) | 0.97 (+1%) | 0.97 (+1%) |
| 13 | 0.97 | 0.97 (0%) | 0.93 (-4%) | 0.98 (+1%) | 0.98 (+1%) | 0.94 (-3%) | 0.97 (0%) | 0.97 (0%) |
| 14 | 0.97 | 0.97 (0%) | 0.94 (-3%) | 0.99 (+2%) | 0.98 (+1%) | 0.94 (-3%) | 0.98 (+1%) | 0.97 (0%) |
| 15 | 0.97 | 0.99 (+2%) | 0.95 (-2%) | 0.99 (+2%) | 0.98 (+1%) | 0.95 (-2%) | 0.98 (+1%) | 0.98 (+1%) |

**Table B.5a** : Wave height coefficients and percentage errors for Test A - Linear Beach.

| Analysis Point | Analytic Solution | ARMADA (HC) | M21PMS (WSA) | MULTIGRID (SWK) | PARAB (HR) | ARTEMIS (LHF) | REFDIF (V2.6) | KRKS |
|---|---|---|---|---|---|---|---|---|
| 1 | 0.91 | 0.91 (0%) | 0.76 (-16%) | 0.91 (0%) | 0.92 (+1%) | 0.98 (+8%) | 0.92 (+1%) | 0.91 (0%) |
| 2 | 0.91 | 0.91 (0%) | 0.77 (-15%) | 0.91 (0%) | 0.93 (+2%) | 1.00 (+10%) | 0.92 (+1%) | 0.91 (0%) |
| 3 | 0.92 | 0.91 (-1%) | 0.78 (-15%) | 0.93 (+1%) | 0.95 (+3%) | 0.94 (+2%) | 0.92 (0%) | 0.92 (0%) |
| 4 | 0.92 | 0.93 (+1%) | 0.79 (-14%) | 0.93 (+1%) | 0.95 (+3%) | 0.96 (+4%) | 0.93 (+1%) | 0.92 (0%) |
| 5 | 0.93 | 0.93 (0%) | 0.80 (-14%) | 0.93 (0%) | 0.96 (+3%) | 0.96 (+3%) | 0.93 (0%) | 0.93 (0%) |
| 6 | 0.93 | 0.93 (0%) | 0.81 (-13%) | 0.95 (+2%) | 0.97 (+4%) | 0.95 (+2%) | 0.94 (+1%) | 0.93 (0%) |
| 7 | 0.94 | 0.95 (+1%) | 0.82 (-13%) | 0.95 (+1%) | 0.97 (+3%) | 0.98 (+4%) | 0.94 (0%) | 0.94 (0%) |
| 8 | 0.94 | 0.95 (+1%) | 0.83 (-12%) | 0.95 (+1%) | 0.98 (+4%) | 0.95 (+1%) | 0.95 (+1%) | 0.94 (0%) |
| 9 | 0.95 | 0.95 (0%) | 0.84 (-12%) | 0.95 (0%) | 0.98 (+3%) | 0.99 (+4%) | 0.96 (+1%) | 0.95 (0%) |
| 10 | 0.95 | 0.97 (+2%) | 0.85 (-11%) | 0.97 (+2%) | 0.98 (+3%) | 1.00 (+5%) | 0.96 (+1%) | 0.95 (0%) |
| 11 | 0.96 | 0.97 (+1%) | 0.85 (-11%) | 0.97 (+1%) | 0.99 (+3%) | 0.99 (+3%) | 0.97 (+1%) | 0.96 (0%) |
| 12 | 0.96 | 0.97 (+1%) | 0.86 (-10%) | 0.97 (+1%) | 0.99 (+3%) | 1.02 (+6%) | 0.97 (+1%) | 0.96 (0%) |
| 13 | 0.97 | 0.97 (0%) | 0.87 (-10%) | 0.97 (0%) | 0.99 (+2%) | 0.92 (-5%) | 0.97 (0%) | 0.97 (0%) |
| 14 | 0.97 | 0.98 (+1%) | 0.87 (-10%) | 0.98 (+1%) | 0.99 (+2%) | 1.01 (+4%) | 0.98 (+1%) | 0.97 (0%) |
| 15 | 0.97 | 0.98 (+1%) | 0.88 (-9%) | 0.98 (+1%) | 0.99 (+2%) | 1.01 (+4%) | 0.98 (+1%) | 0.97 (0%) |

**Table B.5b** : Wave height coefficients and percentage errors for Test A - Linear Beach.

| Analysis Point | Physical Model | OUTRAY (HR) | PORTRAY (HR) | REFRAC (PD) | ENDEC (PD) | HISWA (PD) | LINDAL (AWR) | ORCAWAVE (ORC) | ARMADA (HC) |
|---|---|---|---|---|---|---|---|---|---|
| 1 | 0.30 | 1.53 (+410%) | 0.77 (+157%) | 0.70 (+133%) | 0.84 (+180%) | 0.87 (+190%) | 0.46 (+53%) | 0.36 (+20%) | 0.29 (-3%) |
| 2 | 1.65 | 1.48 (-10%) | 1.06 (-36%) | 2.37 (+44%) | 0.84 (-49%) | 0.86 (-48%) | 1.21 (-27%) | 0.83 (-50%) | 1.67 (+1%) |
| 3 | 0.90 | 0.49 (-46%) | 1.34 (+49%) | 1.90 (+111%) | 0.83 (-8%) | 0.85 (-6%) | 0.52 (-43%) | 0.43 (-52%) | 0.76 (-16%) |
| 4 | 0.40 | 0.48 (+20%) | 0.28 (-30%) | 0.69 (+73%) | 0.83 (+108%) | 0.89 (+123%) | 0.50 (+26%) | 0.46 (+15%) | 0.48 (+20%) |
| 5 | 1.85 | 1.62 (-12%) | 2.19 (+18%) | 2.18 (+18%) | 0.81 (-56%) | 0.88 (-52%) | 1.94 (+5%) | 1.16 (-37%) | 1.97 (+6%) |
| 6 | 0.68 | 0.53 (-22%) | 0.41 (-40%) | 0.78 (+15%) | 0.81 (+19%) | 0.86 (+26%) | 0.56 (-18%) | 0.56 (-18%) | 0.66 (-3%) |
| 7 | 0.65 | 0.60 (-8%) | 0.13 (-80%) | 0.85 (+31%) | 0.80 (+23%) | 0.91 (+40%) | 0.60 (-7%) | 0.61 (-6%) | 0.60 (-8%) |
| 8 | 2.00 | 1.13 (-44%) | 2.97 (+49%) | 1.34 (-33%) | 0.80 (-60%) | 0.94 (-53%) | 1.85 (-7%) | 1.28 (-36%) | 2.09 (+5%) |
| 9 | 0.70 | 0.65 (-7%) | 0.71 (+1%) | 0.80 (+14%) | 0.80 (+14%) | 0.88 (+26%) | 0.69 (-2%) | 0.72 (+3%) | 0.66 (-6%) |
| 10 | 0.95 | 0.89 (-6%) | 0.28 (-71%) | 0.99 (+4%) | 0.79 (-17%) | 0.87 (-8%) | 0.95 (0%) | 1.00 (+5%) | 0.83 (-13%) |
| 11 | 1.25 | 1.31 (+5%) | 0.24 (-81%) | 1.15 (-8%) | 0.82 (-34%) | 1.01 (-19%) | 1.27 (+2%) | 1.30 (+4%) | 1.45 (+16%) |
| 12 | 0.90 | 0.90 (0%) | 0.90 (0%) | 0.90 (0%) | 0.86 (-4%) | 0.89 (-1%) | 0.90 (0%) | 0.90 (0%) | 0.88 (-2%) |
| 13 | 1.10 | 1.02 (-7%) | 0.84 (-24%) | 0.95 (-14%) | 0.89 (-19%) | 1.00 (-9%) | 1.03 (-7%) | 1.02 (-7%) | 1.05 (-5%) |
| 14 | 1.10 | 1.07 (-3%) | 1.27 (+15%) | 0.97 (-12%) | 0.96 (-13%) | 0.97 (-12%) | 1.08 (-2%) | 1.08 (-2%) | 1.12 (+2%) |
| 15 | 0.87 | 0.93 (+7%) | 0.98 (+13%) | 0.92 (+6%) | 1.03 (+18%) | 0.96 (+10%) | 0.95 (+9%) | 0.95 (+9%) | 0.95 (+9%) |

**Table B.6a** : Wave height coefficients and percentage errors for Test B - Elliptic Shoal.

| Analysis Point | Physical Model | CGWAVE (KMM) | M21PMS (WSA) | MULTIGRID (ABP) | MULTIGRID (SWK) | PARAB (HR) | ARTEMIS (LHF) | REFDIF (V2.6) | KRKS |
|---|---|---|---|---|---|---|---|---|---|
| 1 | 0.30 | 1.12 (+273%) | 0.58 (+93%) | 0.19 (-37%) | 0.34 (+13%) | 0.71 (+137%) | 0.75 (+150%) | 0.40 (+33%) | 0.34 (+13%) |
| 2 | 1.65 | 1.64 (-1%) | 0.98 (-41%) | 1.70 (+3%) | 1.74 (+5%) | 1.79 (+8%) | 1.62 (-2%) | 1.78 (+8%) | 0.86 (-48%) |
| 3 | 0.90 | 0.83 (-8%) | 0.73 (-19%) | 0.61 (-32%) | 0.66 (-27%) | 0.81 (-10%) | 0.99 (+10%) | 1.00 (+11%) | 0.43 (-52%) |
| 4 | 0.40 | 0.74 (+85%) | 0.71 (+78%) | 0.33 (-18%) | 0.52 (+30%) | 0.58 (+45%) | 0.77 (+93%) | 0.60 (+50%) | 0.41 (+2%) |
| 5 | 1.85 | 2.17 (+17%) | 1.38 (-25%) | 1.88 (+2%) | 1.72 (-7%) | 2.16 (+17%) | 2.13 (+15%) | 2.12 (+15%) | 1.15 (-38%) |
| 6 | 0.68 | 0.34 (-50%) | 0.46 (-32%) | 0.69 (+1%) | 0.62 (-9%) | 0.46 (-32%) | 0.61 (-10%) | 0.63 (-7%) | 0.52 (-23%) |
| 7 | 0.65 | 0.57 (-12%) | 0.61 (-6%) | 0.56 (-14%) | 0.60 (-8%) | 0.54 (-17%) | 0.59 (-9%) | 0.62 (-5%) | 0.53 (-18%) |
| 8 | 2.00 | 2.38 (+19%) | 1.78 (-11%) | 2.11 (+6%) | 2.16 (+8%) | 2.16 (+8%) | 2.33 (+17%) | 2.20 (+10%) | 1.25 (-38%) |
| 9 | 0.70 | 0.45 (-36%) | 0.69 (-1%) | 0.81 (+16%) | 0.66 (-6%) | 0.65 (-7%) | 0.59 (-16%) | 0.70 (0%) | 0.63 (-10%) |
| 10 | 0.95 | 0.71 (-25%) | 0.86 (-9%) | 0.83 (-13%) | 0.86 (-9%) | 0.82 (-14%) | 0.92 (-3%) | 0.90 (-5%) | 0.94 (-1%) |
| 11 | 1.25 | 1.47 (+18%) | 1.09 (-13%) | 1.44 (+15%) | 1.43 (+14%) | 1.30 (+4%) | 1.30 (+4%) | 1.31 (+5%) | 1.25 (0%) |
| 12 | 0.90 | 1.12 (+24%) | 0.90 (0%) | 0.86 (-4%) | 1.79 (+99%) | 0.85 (-6%) | 0.94 (+4%) | 0.90 (0%) | 0.84 (-7%) |
| 13 | 1.10 | 0.53 (-52%) | 1.01 (-8%) | 1.05 (-5%) | 1.05 (-5%) | 0.91 (-17%) | 1.02 (-7%) | 1.00 (-9%) | 0.98 (-11%) |
| 14 | 1.10 | 1.14 (+4%) | 0.98 (-11%) | 1.12 (+2%) | 1.10 (0%) | 0.91 (-17%) | 1.15 (+5%) | 1.10 (0%) | 1.03 (-6%) |
| 15 | 0.87 | 0.81 (-7%) | 0.95 (+9%) | 0.96 (+10%) | 0.95 (+9%) | 0.86 (-1%) | 0.96 (+10%) | 0.95 (+9%) | 0.90 (+3%) |

**Table B.6b.** : Wave height coefficients and percentage errors for Test B - Elliptic Shoal.

| Analysis Point | Model | OUTRAY (HR | PORTRAY (HR) | W-RAY (SWK) | M21PMS (WSA) | | MULTIGRID | | PARAB (HR) | WC2D (BIN) | REFDIF (V2.6) |
|---|---|---|---|---|---|---|---|---|---|---|---|
| | | | | | Reg. | Irreg. | (ABP) | (SWK) | | | |
| 1 | 0.9 | 0.9 (0%) | 0.7 (-22%) | 1.0 (+11%) | 0.8 (-11%) | 0.8 (-11%) | 1.0 (+7%) | 1.0 (+11%) | 0.9 (0%) | 1.0 (+6%) | 1.0 (+11%) |
| 2 | 0.9 | 1.0 (+11%) | 1.1 (+22%) | 1.4 (+56%) | 1.0 (+11%) | 0.9 (0%) | 1.5 (+64%) | 1.5 (+67%) | 0.8 (-11%) | 1.2 (+37%) | 1.3 (+44%) |
| 3 | 0.7 | 0.8 (+14%) | 0.1 (-86%) | 0.6 (-14%) | 0.5 (-29%) | 0.4 (-43%) | 0.6 (-19%) | 0.6 (-14%) | 0.5 (-29%) | 0.7 (-4%) | 0.7 (0%) |
| 4 | 0.6 | 0.8 (+33%) | 0.8 (+33%) | 1.1 (+83%) | 0.6 (0%) | 0.6 (0%) | 0.8 (+38%) | 0.8 (+33%) | 0.5 (-17%) | 0.6 (+5%) | 0.6 (0%) |
| 5 | 0.7 | 1.1 (+57%) | 0.5 (-29%) | 1.6 (+129%) | 0.6 (-14%) | 0.6 (-14%) | 1.4 (+103%) | 1.4 (+100%) | 0.5 (-29%) | 1.0 (+37%) | 1.1 (+57%) |
| 6 | 0.7 | 0.8 (+14%) | 0.4 (-43%) | 0.9 (+29%) | 0.3 (-57%) | 0.4 (-43%) | 0.8 (+11%) | 0.7 (0%) | 0.2 (-71%) | 1.0 (+43%) | 0.9 (+29%) |
| 7 | 0.6 | 0.8 (+33%) | 0.1 (-83%) | 0.3 (-50%) | 0.3 (-50%) | 0.3 (-50%) | 0.4 (-35%) | 0.3 (-50%) | 0.2 (-67%) | 0.6 (-3%) | 0.8 (+33%) |
| 8 | 0.8 | 1.0 (+25%) | 0.7 (-13%) | 1.1 (+38%) | 0.7 (-13%) | 0.7 (-13%) | 1.0 (+25%) | 1.0 (+25%) | 0.6 (-25%) | 1.0 (+23%) | 1.0 (+25%) |
| 9 | 0.7 | 1.0 (+43%) | 0.6 (-14%) | 1.5 (+114%) | 0.8 (+14%) | 0.7 (0%) | 1.0 (+43%) | 1.1 (+57%) | 0.5 (-29%) | 1.1 (+53%) | 1.3 (+86%) |
| 10 | 0.6 | 0.8 (+33%) | 1.4 (+133%) | 1.3 (+117%) | 0.8 (+33%) | 0.7 (+17%) | 1.5 (+145%) | 1.4 (+133%) | 0.8 (+33%) | 1.2 (+97%) | 1.1 (+83%) |

**Table B.7a.** Wave height coefficients and percentage errors for Test C (Case 1) – Harbour Approach Bathymetry

| Analysis Point | Model | OUTRAY (HR | PORTRAY (HR) | W-RAY (SWK) | M21PMS (WSA) | | MULTIGRID | | PARAB (HR) | WC2D (BIN) | REFDIF (V2.6) |
|---|---|---|---|---|---|---|---|---|---|---|---|
| | | | | | Reg. | Irreg. | (ABP) | (SWK) | | | |
| 1 | 1.1 | 1.0 (-9%) | 0.8 (-27%) | 1.0 (-9%) | 1.0 (-9%) | 1.0 (-9%) | 1.0 (-12%) | 1.0 (-9%) | 0.9 (-18%) | 1.0 (-9%) | 1.0 (-9%) |
| 2 | 1.4 | 1.0 (-29%) | 1.0 (-29%) | 1.7 (+21%) | 1.6 (+14%) | 1.5 (+7%) | 1.2 (-13%) | 1.4 (0%) | 1.5 (+7%) | 1.5 (+4%) | 1.5 (+7%) |
| 3 | 0.3 | 0.9 (+200%) | 0.1 (-67%) | 0.6 (+100%) | 0.5 (+67%) | 0.6 (+100%) | 0.8 (+170%) | 0.6 (+100%) | 0.5 (+67%) | 0.6 (+90%) | 0.6 (+100%) |
| 4 | 0.6 | 0.8 (+33%) | 0.8 (+33%) | 1.1 (+83%) | 0.8 (+33%) | 0.8 (+33%) | 1.0 (+60%) | 0.9 (+50%) | 0.9 (+50%) | 0.8 (+37%) | 0.8 (+33%) |
| 5 | 1.0 | 1.0 (0%) | 1.0 (0%) | 1.5 (+50%) | 1.1 (+10%) | 1.0 (0%) | 1.0 (+3%) | 1.0 (0%) | 1.4 (+40%) | 1.0 (-1%) | 1.1 (+10%) |
| 6 | 0.8 | 0.9 (+13%) | 1.8 (+125%) | 1.2 (+50%) | 0.8 (0%) | 1.0 (+25%) | 1.0 (+26%) | 1.0 (+25%) | 0.8 (0%) | 1.2 (+50%) | 1.0 (+25%) |
| 7 | 0.4 | 0.8 (+100%) | 0.2 (-50%) | 0.4 (0%) | 0.4 (0%) | 0.5 (+25%) | 0.7 (+78%) | 0.5 (+25%) | 0.4 (0%) | 0.5 (+20%) | 0.4 (0%) |
| 8 | 0.7 | 0.9 (+29%) | 1.1 (+57%) | 1.1 (+57%) | 1.0 (+43%) | 1.0 (+43%) | 1.0 (+40%) | 1.0 (+43%) | 0.8 (+14%) | 1.0 (+40%) | 0.9 (+29%) |
| 9 | 0.9 | 0.9 (0%) | 1.0 (+11%) | 1.5 (+67%) | 1.1 (+22%) | 1.1 (+22%) | 1.0 (+16%) | 1.1 (+22%) | 1.5 (+67%) | 1.1 (+18%) | 1.4 (+56%) |
| 10 | 0.9 | 0.8 (-11%) | 1.2 (+33%) | 1.3 (+44%) | 0.9 (0%) | 1.0 (+11%) | 1.3 (+40%) | 1.1 (+22%) | 0.9 (0%) | 1.3 (+40%) | 1.2 (+33%) |

**Table B.7b.** Wave height coefficients and percentage errors for Test C (Case 2) – Harbour Approach Bathymetry

| Analysis Point | Model | OUTRAY (HR | PORTRAY (HR) | W-RAY (SWK) | M21PMS (WSA) | | MULTIGRID | | PARAB (HR) | WC2D (BIN) | REFDIF (V2.6) |
|---|---|---|---|---|---|---|---|---|---|---|---|
| | | | | | Reg. | Irreg. | (ABP) | (SWK) | | | |
| 1 | 0.6 | 1.0 (+67%) | 1.0 (+67%) | 1.1 (+83%) | 0.7 (+17%) | 0.6 (0%) | 0.9 (+53%) | 1.0 (+67%) | 0.6 (0%) | 1.0 (+63%) | 1.0 (+67%) |
| 2 | 0.5 | 1.1 (+120%) | 0.5 (0%) | 1.2 (+140%) | 0.6 (+20%) | 0.6 (+20%) | 0.5 (+6%) | 1.1 (+120%) | 0.5 (0%) | 0.9 (+82%) | 0.7 (+40%) |
| 3 | 0.4 | 0.9 (+125%) | 0.9 (+125%) | 1.4 (+250%) | 0.7 (+75%) | 0.7 (+75%) | 1.0 (+160%) | 1.4 (+250%) | 0.7 (+75%) | 1.0 (+155%) | 0.9 (+125%) |
| 4 | 0.6 | 0.9 (+50%) | 0.3 (-50%) | 0.8 (+33%) | 0.5 (-17%) | 0.4 (-33%) | 0.9 (+55%) | 0.8 (+33%) | 0.3 (-50%) | 0.8 (+37%) | 0.8 (+33%) |
| 5 | 0.6 | 1.0 (+67%) | 0.5 (-17%) | 1.1 (+83%) | 0.6 (0%) | 0.5 (-17%) | 0.4 (-27%) | 1.0 (+67%) | 0.5 (-17%) | 0.9 (+47%) | 0.8 (+33%) |
| 6 | 0.5 | 0.9 (+80%) | 0.4 (-20%) | 1.1 (+120%) | 0.6 (+20%) | 0.5 (0%) | 0.6 (+12%) | 1.2 (+140%) | 0.5 (0%) | 0.9 (+74%) | 0.7 (+40%) |
| 7 | 0.4 | 0.8 (+100%) | 0.2 (-50%) | 0.9 (+125%) | 0.4 (0%) | 0.4 (0%) | 1.1 (+183%) | 0.8 (+100%) | 0.4 (0%) | 0.9 (+113%) | 0.5 (+25%) |
| 8 | 0.6 | 0.9 (+50%) | 0.5 (-17%) | 1.1 (+83%) | 0.5 (-17%) | 0.5 (-17%) | 1.4 (+127) | 1.0 (+67%) | 0.4 (-33%) | 0.9 (+50%) | 0.4 (-33%) |
| 9 | 0.6 | 0.9 (+50%) | 0.4 (-33%) | 1.1 (+83%) | 0.5 (-17%) | 0.5 (-17%) | 0.5 (-20%) | 0.9 (+50%) | 0.4 (-33%) | 0.9 (+47%) | 0.6 (0%) |
| 10 | 0.4 | 0.8 (+100%) | 0.8 (+100%) | 1.4 (+250%) | 0.7 (+75%) | 0.6 (+50%) | 0.2 (-58%) | 1.2 (+200%) | 0.6 (+50%) | 1.0 (+140%) | 0.5 (+25%) |

**Table B.7c.** Wave height coefficients and percentage errors for Test C (Case 3) – Harbour Approach Bathymetry

| Analysis Point | Model | OUTRAY (HR | PORTRAY (HR) | W-RAY (SWK) | M21PMS (WSA) | | MULTIGRID | | PARAB (HR) | WC2D (BIN) | REFDIF (V2.6) |
|---|---|---|---|---|---|---|---|---|---|---|---|
| | | | | | Reg. | Irreg. | (ABP) | (SWK) | | | |
| 1 | 0.9 | 1.0 (+11%) | 1.0 (+11%) | 1.1 (+22%) | 1.0 (+11%) | 0.9 (0%) | 1.0 (+7%) | 1.0 (+11%) | 1.0 (+11%) | 1.0 (+9%) | 1.0 (+11%) |
| 2 | 0.9 | 1.1 (+22%) | 0.9 (0%) | 1.2 (+33%) | 0.9 (0%) | 0.9 (0%) | 0.6 (-31%) | 1.1 (+22%) | 0.9 (0%) | 1.0 (+13%) | 1.1 (+22%) |
| 3 | 1.1 | 0.9 (-18%) | 1.3 (+18%) | 1.6 (+45%) | 1.2 (+9%) | 1.1 (0%) | 1.2 (+10%) | 1.4 (+27%) | 1.3 (+18%) | 1.2 (+13%) | 1.4 (+27%) |
| 4 | 0.9 | 0.9 (0%) | 0.7 (-22%) | 1.0 (+11%) | 0.7 (-22%) | 0.7 (-22%) | 1.3 (+47%) | 0.8 (-11%) | 0.6 (-33%) | 0.9 (+1%) | 0.9 (0%) |
| 5 | 0.8 | 1.0 (+25%) | 0.9 (+13%) | 1.2 (+50%) | 0.9 (+13%) | 0.8 (0%) | 0.6 (-20%) | 1.0 (+25%) | 0.8 (0%) | 1.0 (+24%) | 0.7 (-13%) |
| 6 | 0.8 | 0.9 (+13%) | 0.8 (0%) | 1.1 (+38%) | 0.9 (+13%) | 0.9 (+13%) | 0.9 (+11%) | 1.2 (+50%) | 0.9 (+13%) | 1.0 (+21%) | 1.1 (+38%) |
| 7 | 0.8 | 0.9 (+13%) | 0.3 (-63%) | 1.0 (+25%) | 0.8 (0%) | 0.7 (-13%) | 1.7 (+111%) | 0.8 (0%) | 0.6 (-25%) | 0.9 (+11%) | 0.8 (0%) |
| 8 | 0.9 | 0.8 (-11%) | 0.8 (-11%) | 1.1 (+22%) | 0.9 (0%) | 0.8 (-11%) | 1.2 (+34%) | 1.0 (+11%) | 0.8 (-11%) | 1.0 (+10%) | 0.4 (-56%) |
| 9 | 0.9 | 0.9 (0%) | 0.7 (-22%) | 1.1 (+22%) | 0.9 (0%) | 0.8 (-11%) | 0.6 (-29%) | 1.0 (+11%) | 0.7 (-22%) | 1.0 (+8%) | 0.4 (-56%) |
| 10 | 0.6 | 0.8 (+33%) | 1.1 (+83%) | 1.4 (+133%) | 1.1 (+83%) | 1.0 (+67%) | 0.3 (-52%) | 1.2 (+100%) | 1.1 (+83%) | 1.1 (+88%) | 0.7 (+17%) |

**Table B.7d.** Wave height coefficients and percentage errors for Test C (Case 4) – Harbour Approach Bathymetry

| Analysis Point | Field Data | OUTRAY (ACER) | OUTRAY (HR) | PORTRAY (HR) | W-RAY (SWK) | HISWA (PD) | LINDAL (AWR) |
|---|---|---|---|---|---|---|---|
| 1 | 0.9 | 0.8 (-7%) | 0.9 (0%) | 0.9 (0%) | 0.7 (-20%) | 0.9 (-2%) | 0.9 (-3%) |
| 2 | 1.0 | 0.8 (-20%) | 0.8 (-20%) | 0.6 (-40%) | 0.7 (-30%) | 0.8 (-22%) | 1.0 (-3%) |
| 3 | 0.8 | 0.8 (+5%) | 0.8 (0%) | 1.9 (+137%) | 0.7 (-16%) | 0.8 (-3%) | 0.8 (+3%) |
| 4 | 0.6 | 0.5 (-18%) | 0.6 (0%) | 0.7 (+17%) | 0.9 (+50%) | - | 0.7 (+8%) |
| 5 | 0.9 | 0.8 (-10%) | 0.8 (-11%) | 1.0 (+11%) | 0.7 (-24%) | 0.9 (-12%) | 1.0 (+7%) |
| 6 | 0.8 | 0.9 (+10%) | 0.9 (+13%) | 0.9 (+13%) | 0.8 (-6%) | 0.8 (+4%) | 1.0 (+19%) |
| 7 | 0.9 | 0.8 (-6%) | 0.9 (0%) | 0.7 (-22%) | 0.8 (-17%) | 0.8 (-7%) | 0.9 (+4%) |
| 8 | 0.8 | 0.7 (-18%) | 0.8 (0%) | 0.9 (+13%) | 0.9 (+13%) | - | 0.8 (+3%) |
| 9 | 0.9 | 0.9 (-2%) | 0.9 (0%) | 0.9 (0%) | 0.8 (-12%) | 0.8 (-7%) | 1.0 (+6%) |
| 10 | 0.7 | 0.9 (+24%) | 0.9 (+29%) | 0.9 (+29%) | 0.8 (+17%) | 0.9 (+24%) | 1.0 (+39%) |

**Table B.8a** : Wave height coefficients and percentage errors for Test D - Perranporth.

| Analysis Point | Field Data | M21NSW (WSA) | ORCAWAVE (ORC) | MULTIGRID (ABP) | PARAB (HR) | Wc2D (BIN) | REFDIF (V2.6) | KRKS |
|---|---|---|---|---|---|---|---|---|
| 1 | 0.9 | 0.8 (-11%) | 1.1 (+23%) | 0.7 (-19%) | 1.0 (+11%) | 0.9 (+2%) | 0.9 (0%) | 0.9 (-1%) |
| 2 | 1.0 | 0.8 (-20%) | 0.8 (-21%) | 0.7 (-28%) | 0.8 (-20%) | 0.9 (-13%) | 0.9 (-10%) | 0.9 (-11%) |
| 3 | 0.8 | 0.8 (0%) | 0.5 (-33%) | 0.9 (+14%) | 0.9 (+13%) | 0.7 (-11%) | 0.8 (0%) | 0.6 (-31%) |
| 4 | 0.6 | 0.7 (+17%) | 0.9 (+42%) | 0.9 (+53%) | 0.9 (+50%) | 0.6 (-2%) | 1.0 (+67%) | 0.7 (+19%) |
| 5 | 0.9 | 0.8 (-11%) | 0.9 (-3%) | 0.7 (-18%) | 0.8 (-11%) | 0.9 (-6%) | 1.1 (+22%) | 0.8 (-6%) |
| 6 | 0.8 | 0.9 (+13%) | 0.9 (+8%) | 0.8 (+1%) | 0.8 (0%) | 0.9 (+16%) | 0.6 (-25%) | 1.1 (+36%) |
| 7 | 0.9 | 0.9 (0%) | 0.9 (+1%) | 0.8 (-12%) | 0.9 (0%) | 0.9 (+4%) | 0.7 (-22%) | 1.0 (+7%) |
| 8 | 0.8 | 0.8 (0%) | 1.0 (+20%) | 0.9 (+8%) | 0.9 (+13%) | 0.8 (+4%) | 0.8 (0%) | 0.8 (+1%) |
| 9 | 0.9 | 0.9 (0%) | 0.9 (+4%) | 0.8 (-10%) | 0.9 (0%) | 1.0 (+6%) | 0.8 (-11%) | 1.0 (+7%) |
| 10 | 0.7 | 0.9 (+29%) | 1.0 (+39%) | 0.8 (+19%) | 1.0 (+43%) | 1.0 (+39%) | 0.8 (+14%) | 1.0 (+40%) |

**Table B.8b** : Wave height coefficients and percentage errors for Test D - Perranporth.

### B.2.1 Benchmark Test Results

#### Linear Beach

The linear beach is a relatively straightforward test case in which REFDIF and KrKs as well as other models tested would be expected to perform well. From the test results, most models predict WHC to an acceptable degree of accuracy with (considering the simplistic nature of the model) the possible exception of HISWA (PD), M21PMS (WSA) and to a lesser extent ARTEMIS (LHF). KrKs is the only model that predicts all WHC exactly, with REFDIF, together with LINDAL (AWR) and ORCAWAVE (OCR) making predictions to an accuracy of ±1% for all wave prediction points.

#### Elliptic Shoal

The elliptic shoal is a commonly used example to test WTMs, as it subjects the models to significant, and increasing, processes of shoaling, refraction and diffraction. As indicated by the results, this is a much more difficult test case for the models to simulate especially as the wave propagates over and past the shoal. This can be seen by considering the results in two sets, WHC 1-6 (behind the shoal), and WHC 7-15 (over the shoal).

Behind the shoal WHC are significantly in error with the possible exception of ARMADA (a finite difference refraction/diffraction model). Despite this, REFDIF is one of the better performing models in this region, as is KrKs. However results from KrKs should be discounted as, due to ray crossing over the shoal, WHC from KrKs are non quantifiable.

Over the shoal, predictions are significantly better. LINDAL and REFDIF are the only models that give WHC at all predictions points that are within an acceptable 10% of the actual recordings. Of the remaining models, most give WHC that could be considered acceptable, including KrKs.

**Harbour Approach**

The harbour approach channel tests the models in diffraction at the channel, as well as refraction and shoaling. The test runs specified were for relatively shallow water depths, and with significant changes in the sea bed bathymetry near the channel slopes, none of the models would be expected to accurately predict WHC.

Considering the test cases and the relatively shallow water, two conditions could be expected. The first is that model predictions would be more accurate for the shorter wave period events, and that predictions of WHC would, in general, be more accurate at prediction point 1 due to the deeper water depths in this region. This is confirmed by the results.

It is noticeable that predictions for all models are, in general, over-predicted and inaccurate, with no increased or decreased accuracy in, on or away from the channel edges. However, the MIKE21PMS model can be considered accurate for regions not in the channel if differences in predictions up to 20% are allowable. REFDIF generally tends to over predict WHC by at least 25%.

**Perranporth**

The depth contours for Perranporth are relatively straight, with no significant changes in bathymetry on the grid. This test case therefore tests model runs mainly in refraction and shoaling. The storms specified were long period waves, resulting in relatively shallow water at the prediction point. Noticeable refraction would therefore be expected for waves approaching the prediction point at significant angles to the grid, and therefore bathymetry.

Considering the test runs, predictions would be expected to be most accurate for storm number 10. This coincides with the most 'inline' storm at the shortest wave period. However, this storm results in the largest differences, with all models over predicting results by at least 14%

(REFDIF), and typically 25-40%. This storm also has the smallest calculated WHC which would not be expected.

Ignoring storm 10, the LINDAL model predicts WHC to an accuracy of 10% or less in 8 and OUTRAY (HR) correctly predicts WHC in 6 of the remaining model runs. HISWA, OUTRAY (ACER) and M21NSW could also be considered to predict WHC relatively accurately in these remaining model runs.

REFDIF and KrKs generally perform poorly in all model runs.

### B.2.2 Conclusions

The performance of REFDIF and KrKs in the Linear Beach example indicates that in theory in refraction and shoaling these models produce extremely accurate results. Indeed, KrKs gave exact answers and REFDIF within 1% at all 15 prediction points.

For the elliptic shoal, REFDIF gave WHO within 10% over the shoal, and KrKs gave WHC that could be considered acceptable, with reduced accuracy for REFDIF behind the shoal. From both these carefully controlled model runs, REFDIF and KrKs are considered acceptable models for the Cumbrian coastline below the Solway Firth, although the possible generation of caustics in KrKs would be difficult to control in multiple runs. For the Solway Firth, the relatively low lying sand banks would result in significant diffraction in this region, and KrKs would not be an acceptable model which was indicated by preliminary model runs. However, REFDIF can be considered an acceptable model in this region.

Generally for these two test cases, REFDIF can be considered an extremely reliable model when results are compared. KrKs can also be considered reliable where diffraction effects are minimised.

For the Harbour Approach, REFDIF, as with all other models, performs poorly. However, the seabed bathymetry in this example is not of the type

that is encountered on the Cumbrian coastline, and therefore these results are not considered significant.

For Perranporth, both REFDIF and KrKs perform poorly in comparison to the other models. These results are unexpected since the dominant physical processes would be expected to be shoaling and refraction, which both models have already been shown to perform accurately in. There could be several reasons for the poor performance of these models in this test case, including possibly an incorrect specification of the directional spreading and too few frequency components specified for REFDIF (see Section 4.6.1 and Figure 4.7), and the monochromatic treatment of input conditions in KrKs. If this is the case, similar problems would be negated along the Cumbrian coastline using REFDIF due to restricted directional spreading expected, and the use of more (13) frequency components (see Section 4.6.1). However, for all models, predictions are not as accurate as would be expected, especially for storm number 10, which perhaps indicates problems with the test definition (i.e., bathymetry, sea levels or specified offshore or inshore results).

Overall, despite the poor predictions from REFDIF for the Harbour Approach and Perranporth, the accuracy of predictions in the more tightly controlled and realistic conditions compared to the Cumbrian coastline for the linear beach and elliptic shoal indicate that REFDIF is a suitable choice of model for wave height predictions for this study. Also, the subsequent use of 13 as opposed to 5 frequency components is likely to improve accuracy as indicated in Figure 4.8. The inability of KrKs to account for diffraction and the treatment of caustics in multiple runs means that this model is not a realistic option for this study, and KrKs was not considered further.

# Appendix C : Sample Model Output for REFDIF Modelling

This appendix shows sample model output using the REFDIF wave transformation model. Waves at the offshore boundary have been specified using the conditions outlined in Section 4.6 for wind waves. Bathymetric model grids are as specified in section 3.5.2 and Figure 3.12.

These results have been produced using REFDIF/S V1.2, and have not been compiled based on the discretization outlined in Section 4.6.1.

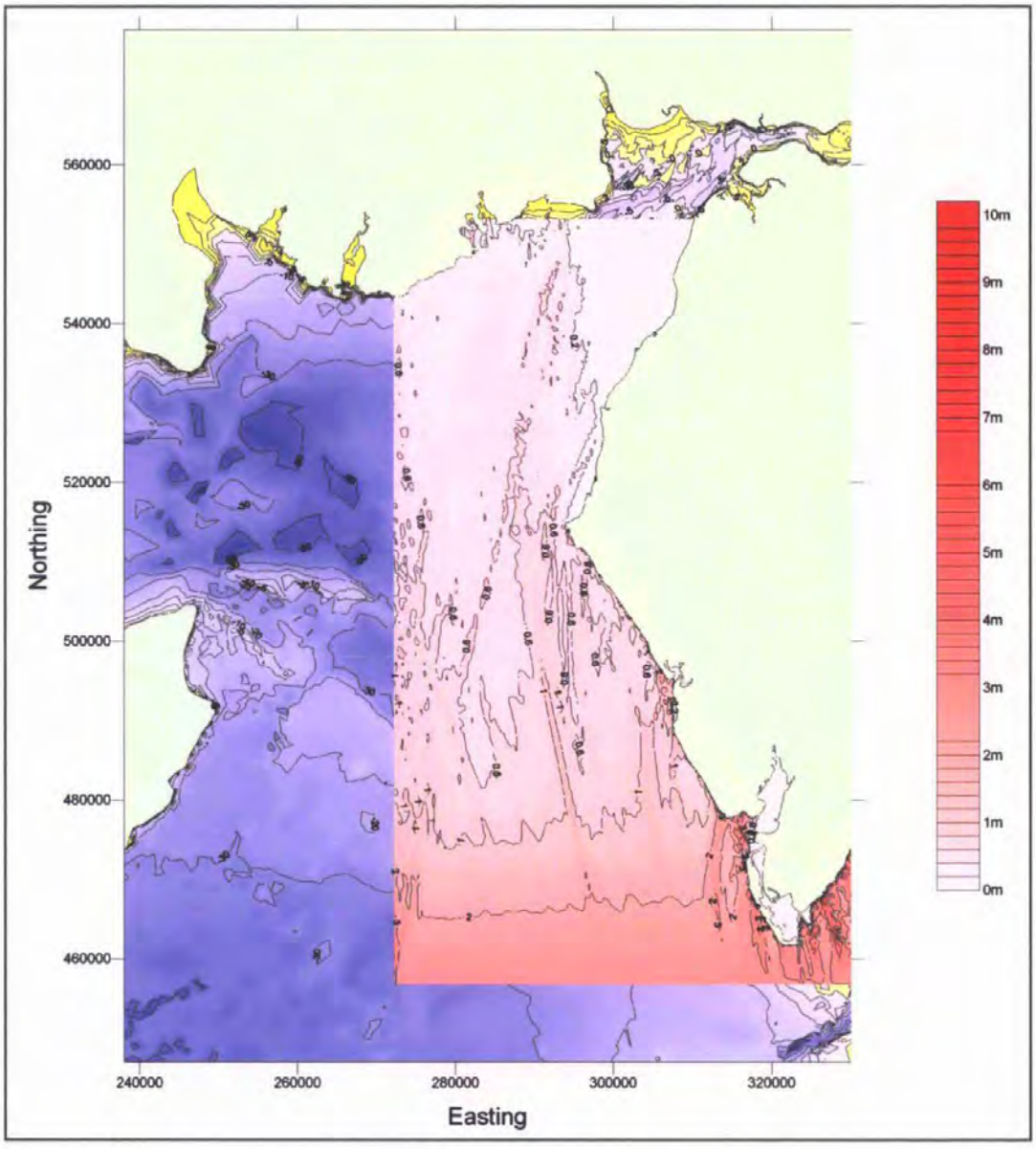


**Figure C.1** : Sample output for 180 grid.

| | | |
|---|---|---|
| Offshore Wave Height | = | 3.0m |
| Offshore Zero Crossing Wave Period | = | 6.5s |
| Wave Direction | = | 194° (0° from north, clockwise positive) |
| Still Water Level | = | 3.8m@OD |

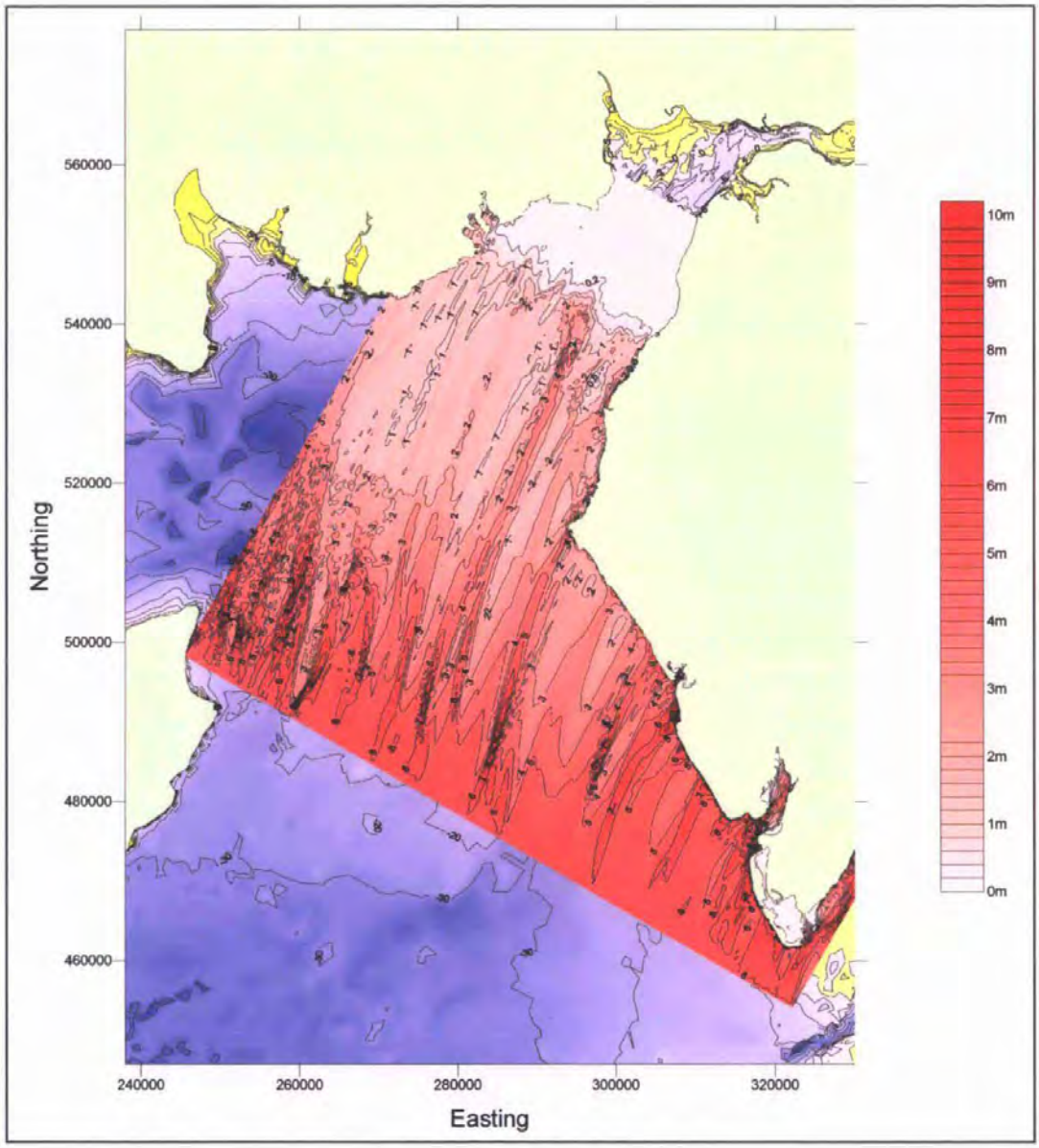


**Figure C.2** : Sample output for 210 grid.

| | | |
|---|---|---|
| Offshore Wave Height | = | 6.0m |
| Offshore Zero Crossing Wave Period | = | 9.5s |
| Wave Direction | = | 224° (0° from north, clockwise positive) |
| Still Water Level | = | 4.0m@OD |

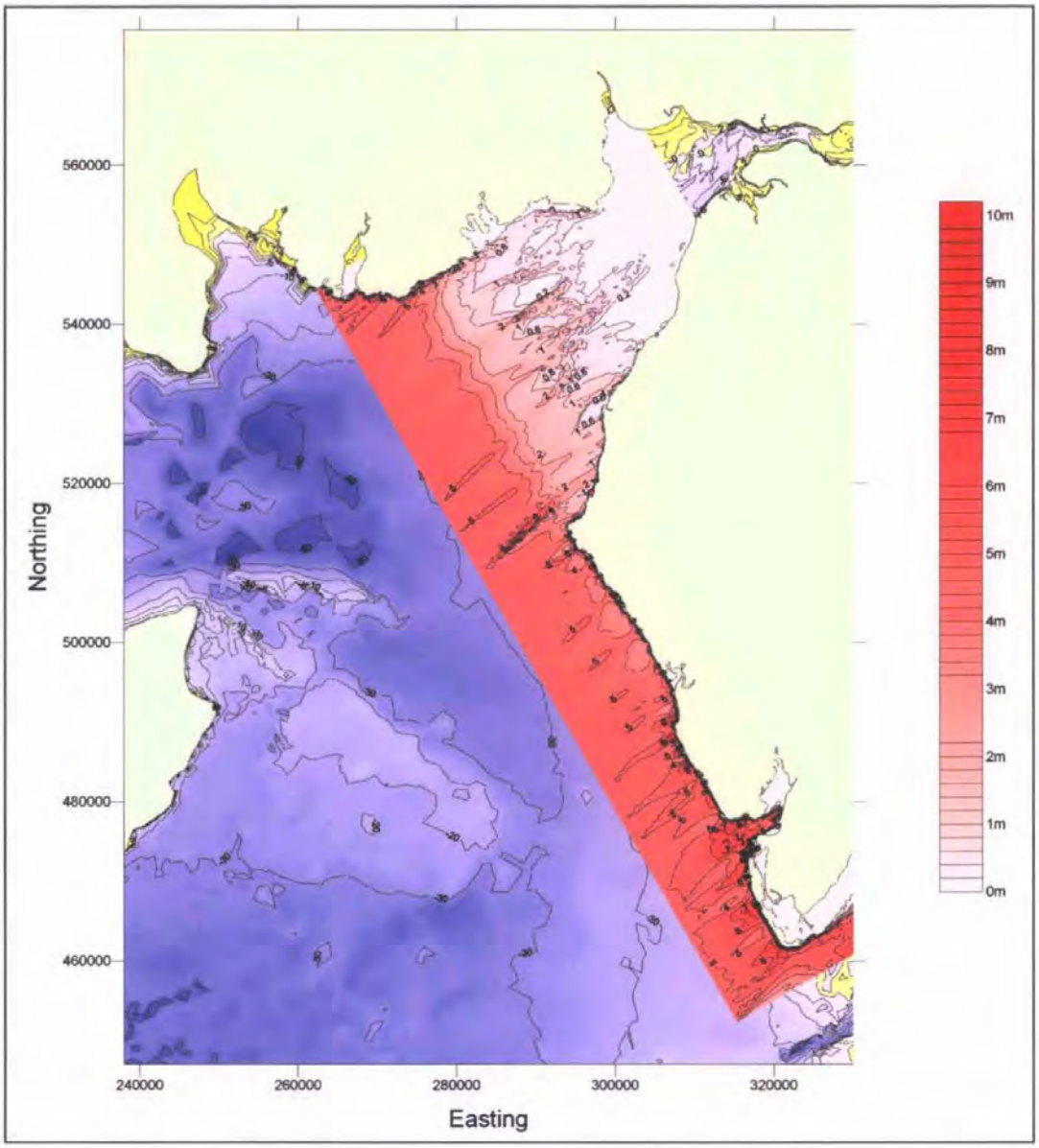


**Figure C.3** : Sample output for 240 grid.

| | | |
|---|---|---|
| Offshore Wave Height | = | 5.0m |
| Offshore Zero Crossing Wave Period | = | 9.0s |
| Wave Direction | = | 230° (0° from north, clockwise positive) |
| Still Water Level | = | 5.0m@OD |

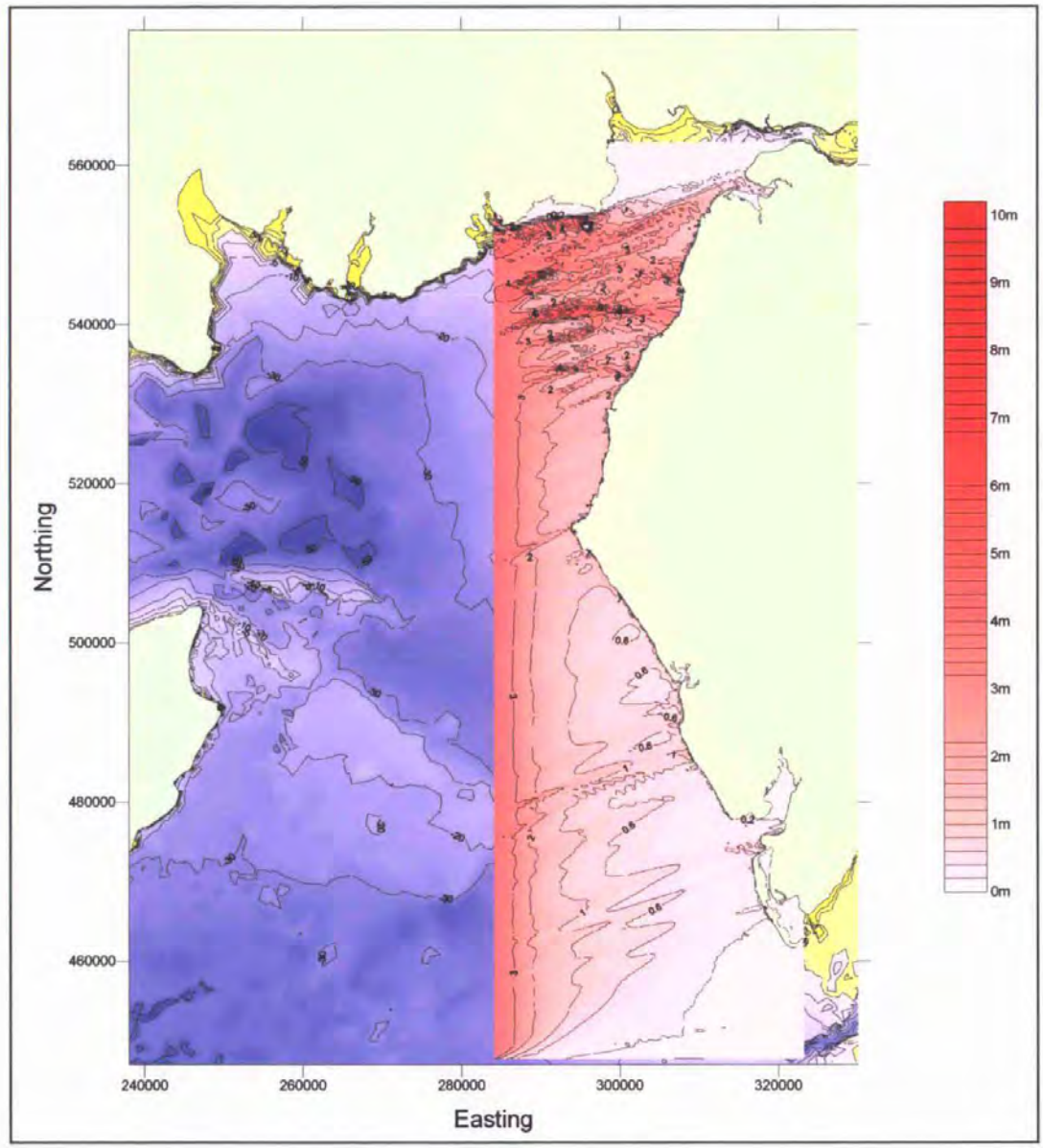


**Figure C.4** : Sample output for 270 grid.

| | | |
|---|---|---|
| Offshore Wave Height | = | 4.0m |
| Offshore Zero Crossing Wave Period | = | 8.0s |
| Wave Direction | = | 261° (0° from north, clockwise positive) |
| Still Water Level | = | 3.0m@OD |

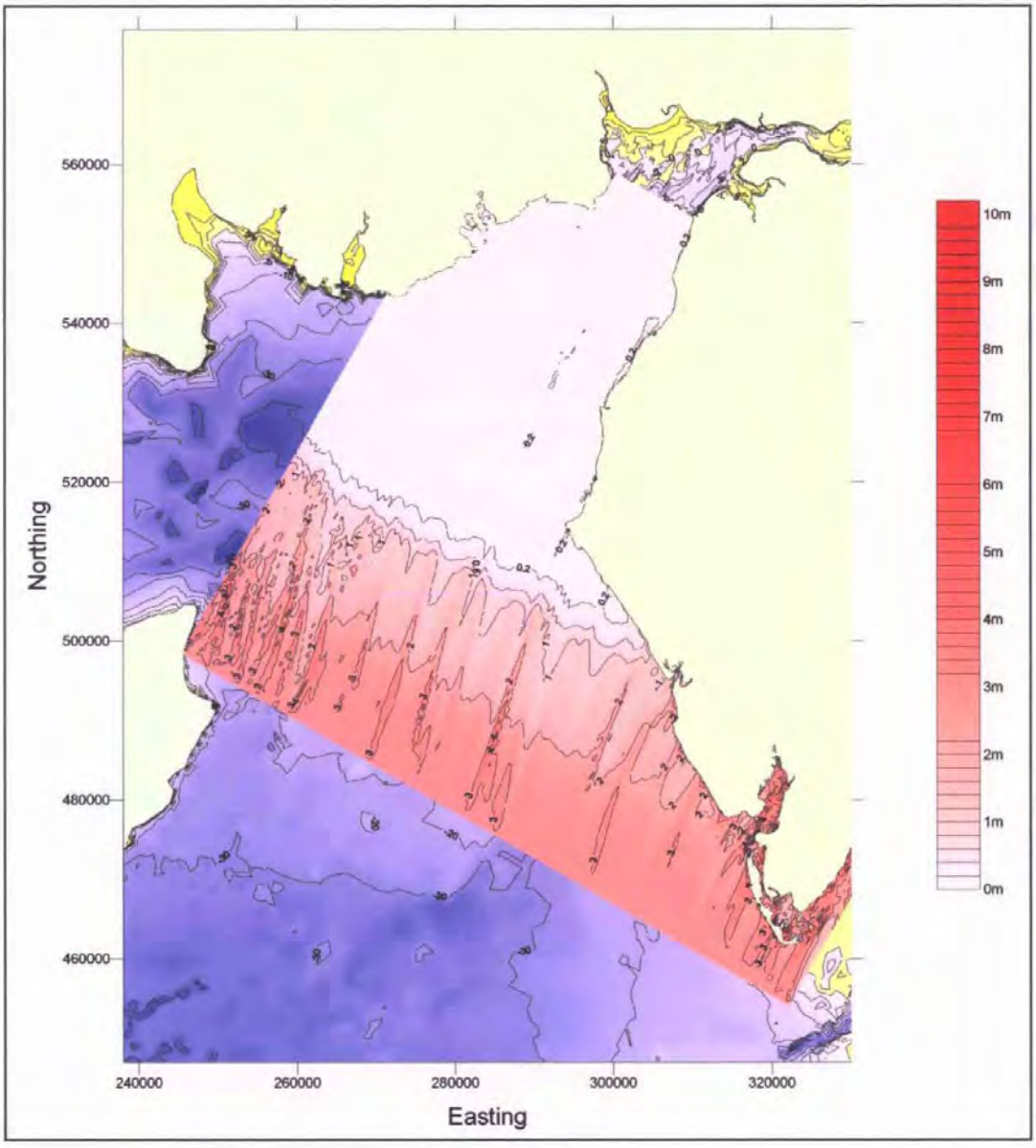


**Figure C.5** : Sample output for 210 grid.

| | | |
|---|---|---|
| Offshore Wave Height | = | 3.0m |
| Offshore Zero Crossing Wave Period | = | 7.0s |
| Wave Direction | = | 201° (0° from north, clockwise positive) |
| Still Water Level | = | 5.5m@OD |

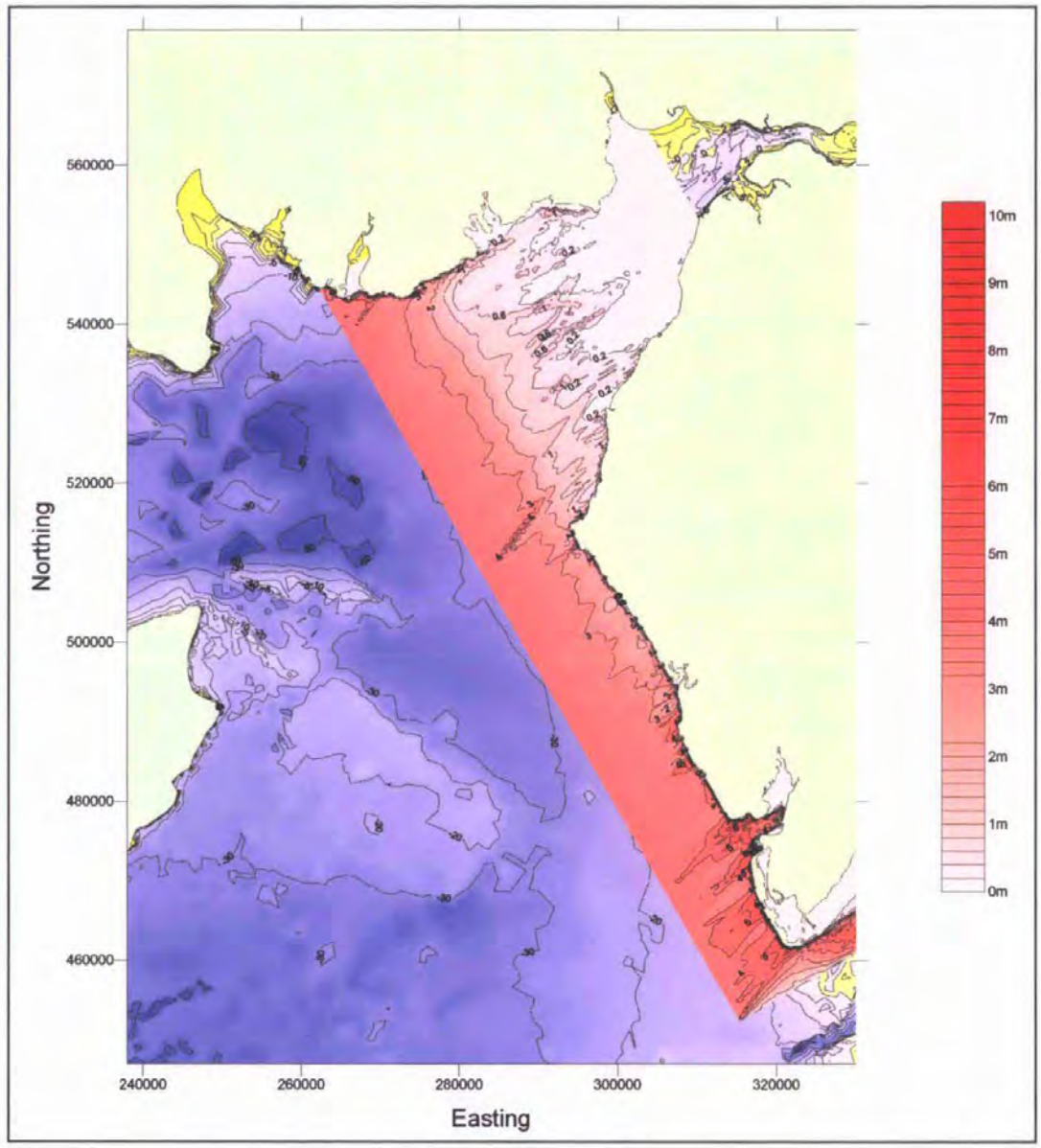


**Figure C.6** : Sample output for 240 grid.

| | | |
|---|---|---|
| Offshore Wave Height | = | 4.0m |
| Offshore Zero Crossing Wave Period | = | 8.0s |
| Wave Direction | = | 221° (0° from north, clockwise positive) |
| Still Water Level | = | 5.5m@OD |

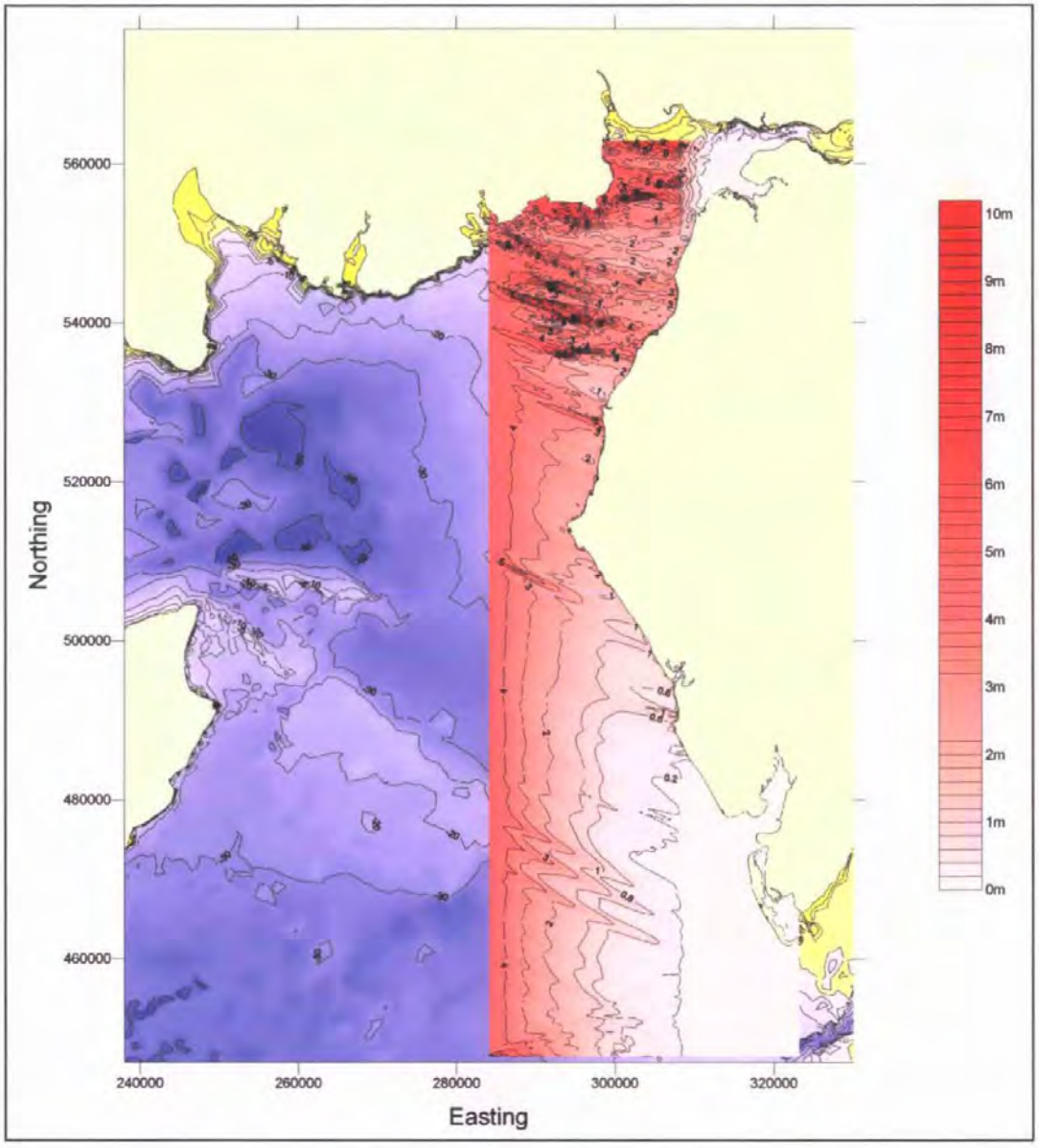


**Figure C.7** : Sample output for 270 grid.

| | | |
|---|---|---|
| Offshore Wave Height | = | 5.0m |
| Offshore Zero Crossing Wave Period | = | 9.0s |
| Wave Direction | = | 281° (0° from north, clockwise positive) |
| Still Water Level | = | 5.5m@OD |

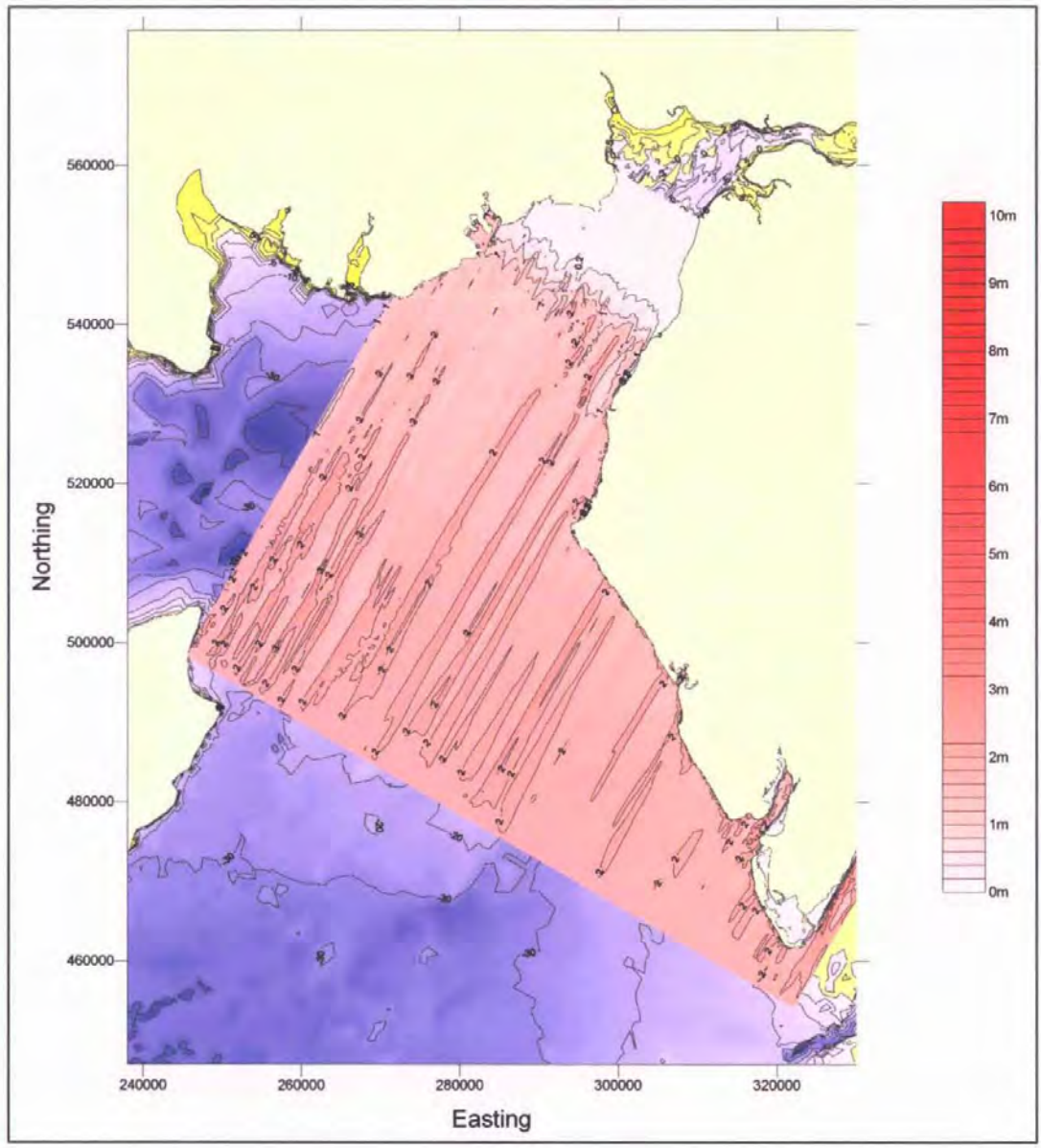


**Figure C.8** : Sample output for 210 grid.

| | | |
|---|---|---|
| Offshore Wave Height | = | 2.0m |
| Offshore Zero Crossing Wave Period | = | 5.5s |
| Wave Direction | = | 210° (0° from north, clockwise positive) |
| Still Water Level | = | 4.0m@OD |

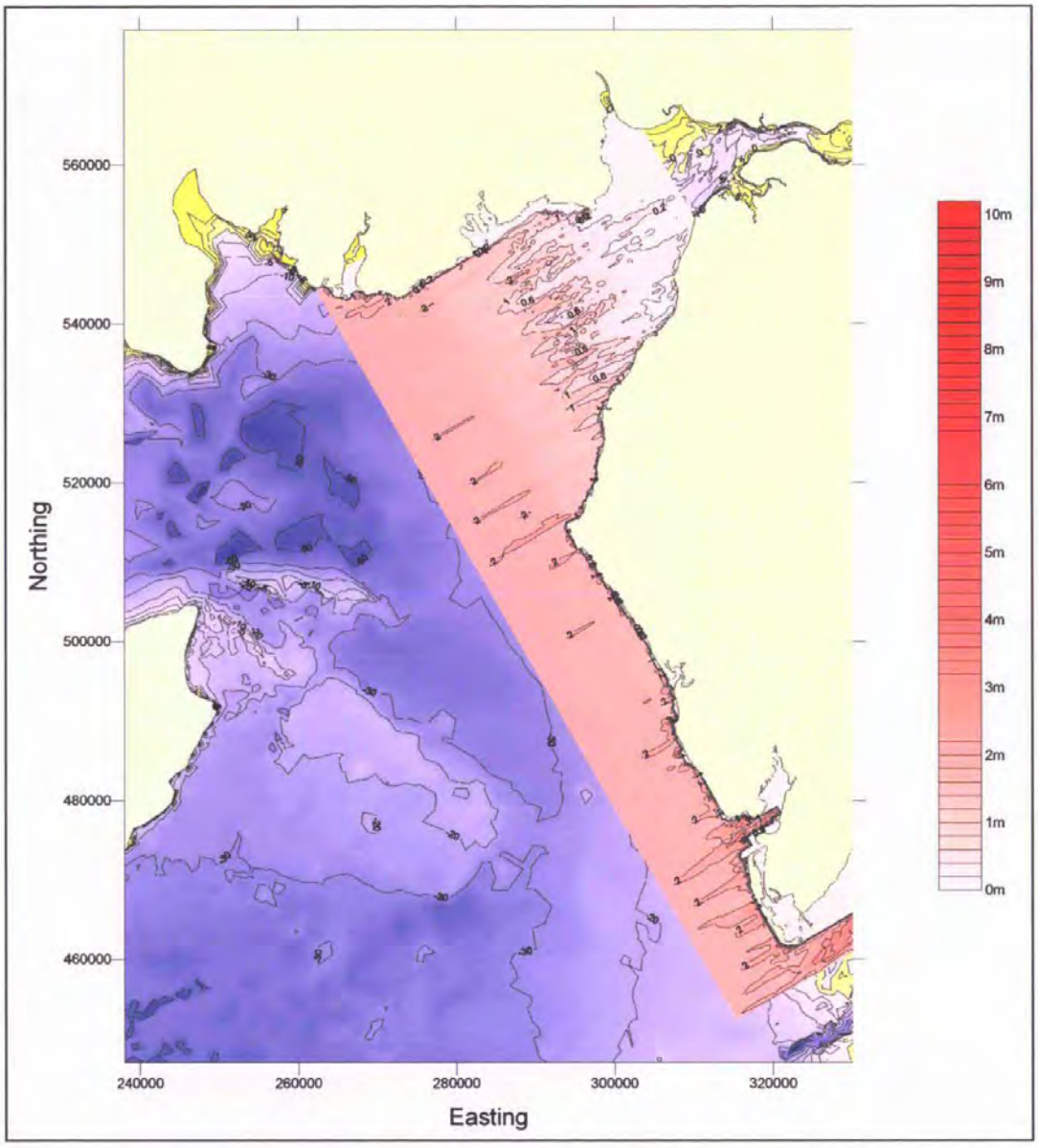


**Figure C.9** : Sample output for 240 grid.

| | | |
|---|---|---|
| Offshore Wave Height | = | 2.0m |
| Offshore Zero Crossing Wave Period | = | 5.5s |
| Wave Direction | = | 240° (0° from north, clockwise positive) |
| Still Water Level | = | 4.0m@OD |

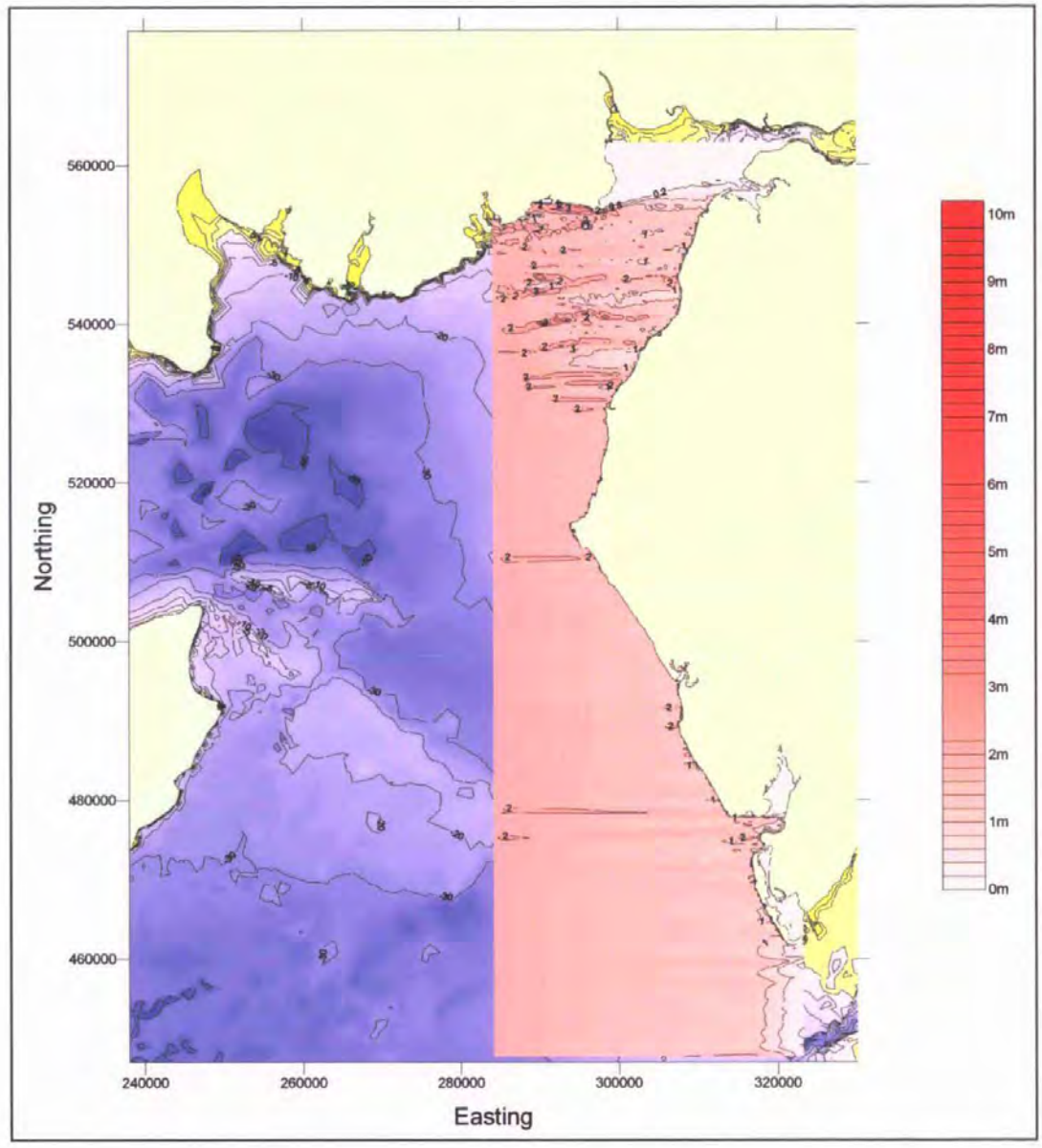


**Figure C.10** : Sample output for 270 grid.

| | | |
|---|---|---|
| Offshore Wave Height | = | 2.0m |
| Offshore Zero Crossing Wave Period | = | 5.5s |
| Wave Direction | = | 270° (0° from north, clockwise positive) |
| Still Water Level | = | 4.0m@OD |

# Appendix D : Joint Probability Curves at Selected Locations

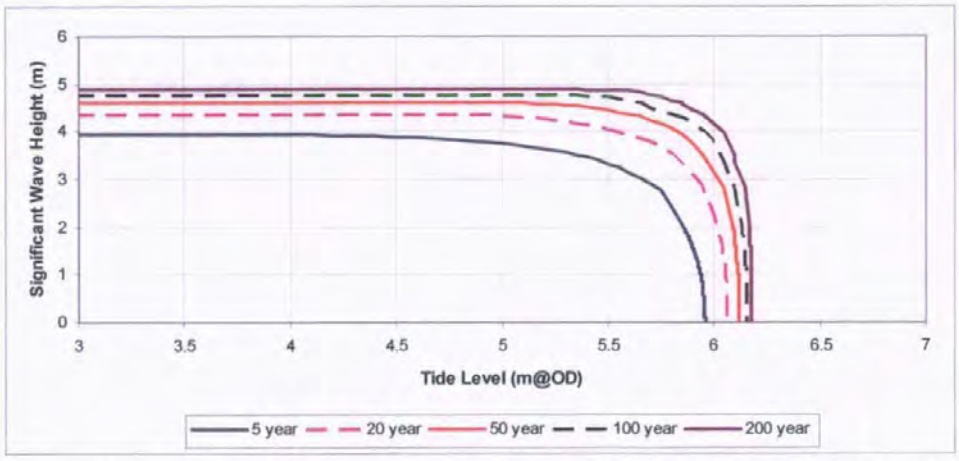


**Figure D.1a** : Joint probability curves for standard return periods for -2m@OD level (Northing coordinate 465040m)

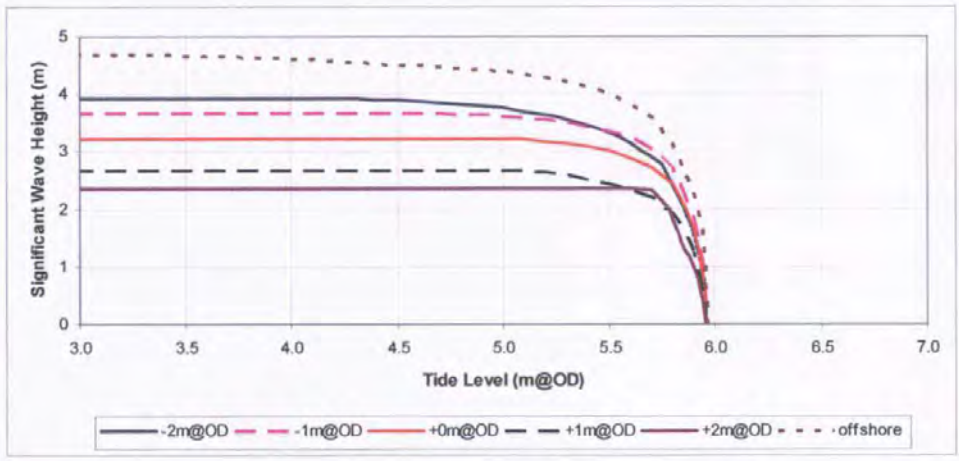


**Figure D.1b** : 5 year joint probability curves for different bed levels (Northing coordinate 465040m)

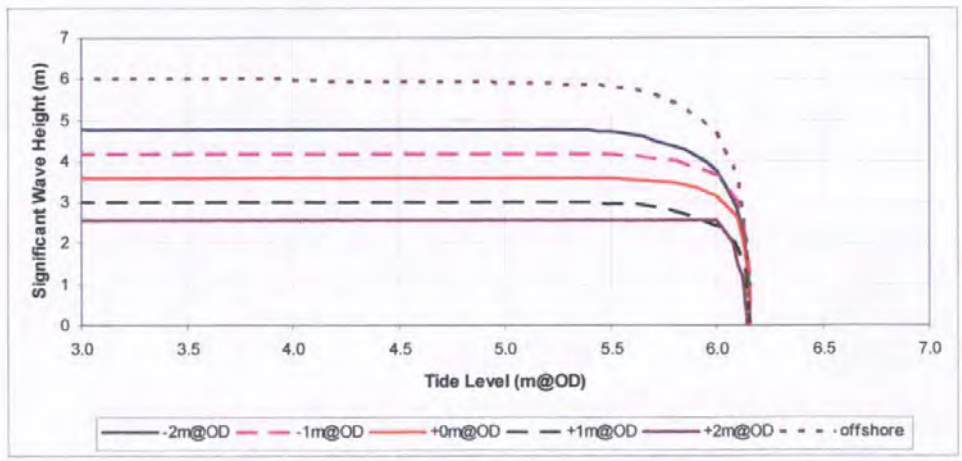


**Figure D.1c** : 100 year joint probability curves for different bed levels (Northing coordinate 465040m)

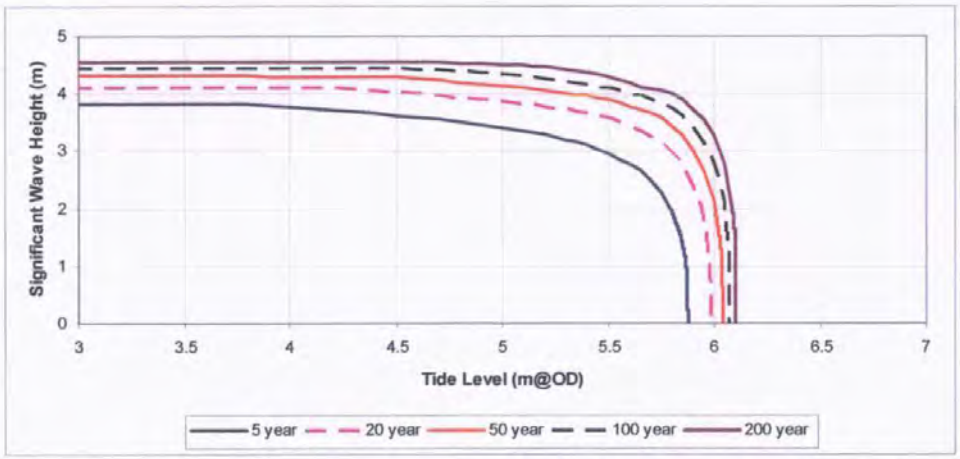


**Figure D.2a** : Joint probability curves for standard return periods for -2m@OD level (Northing coordinate 469440m)

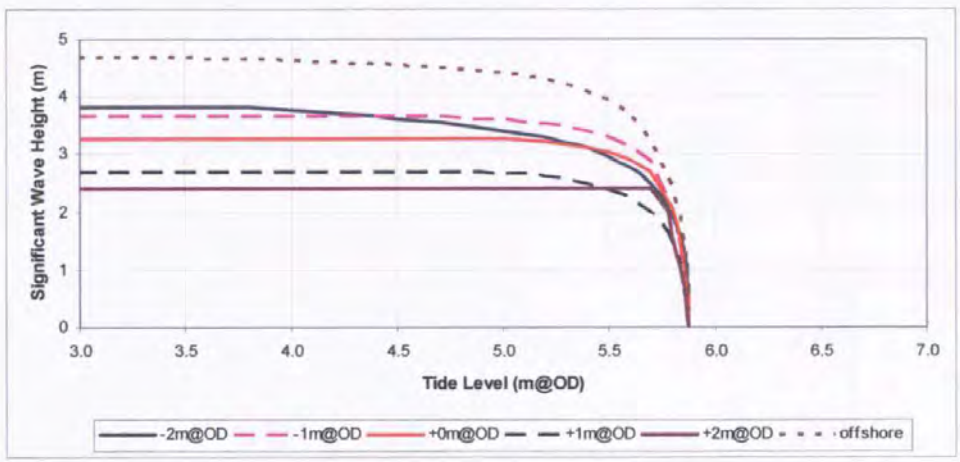


**Figure D.2b** : 5 year joint probability curves for different bed levels (Northing coordinate 469440m)

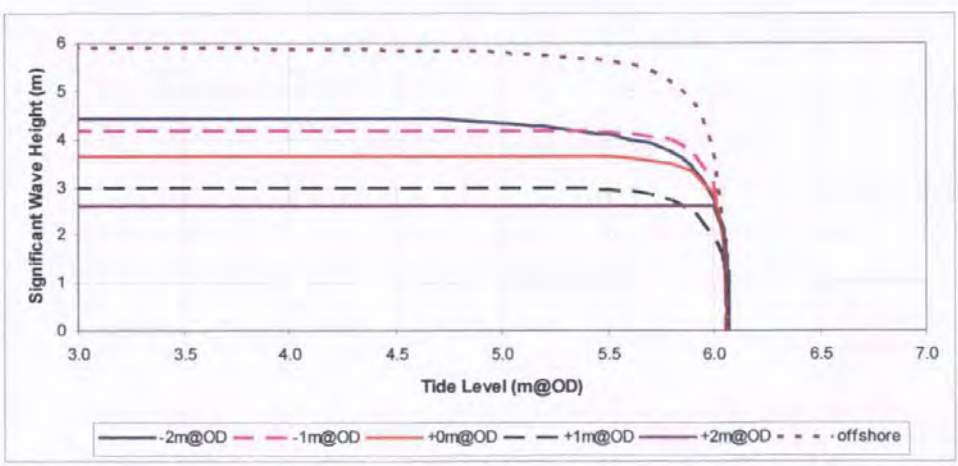


**Figure D.2c** : 100 year joint probability curves for different bed levels (Northing coordinate 469440m)

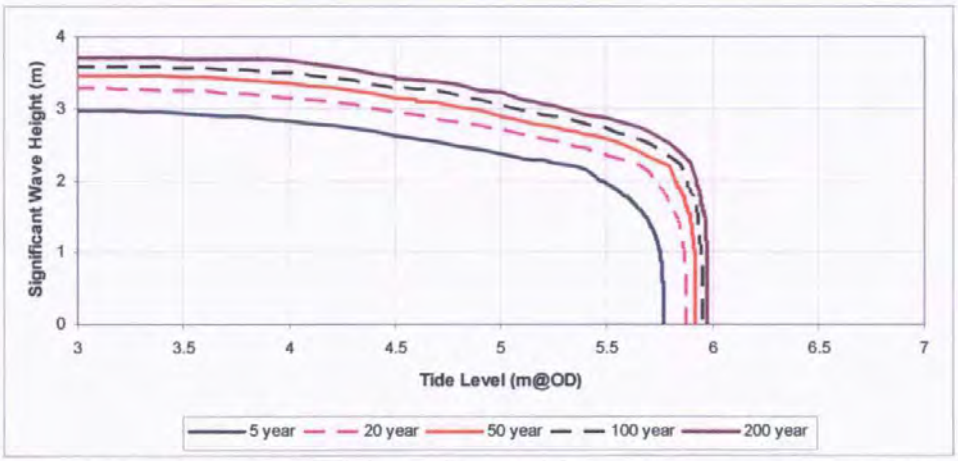


**Figure D.3a**: Joint probability curves for standard return periods for -2m@OD level (Northing coordinate 472240m)

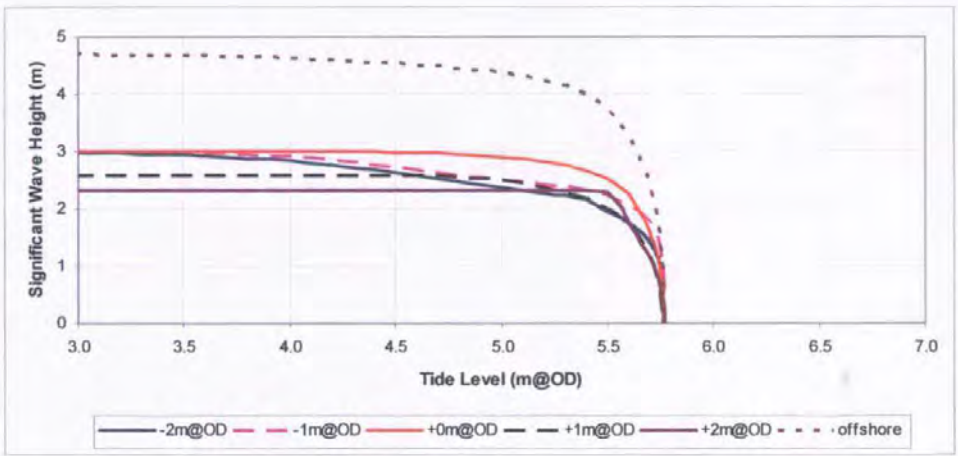


**Figure D.3b** : 5 year joint probability curves for different bed levels (Northing coordinate 472240m)

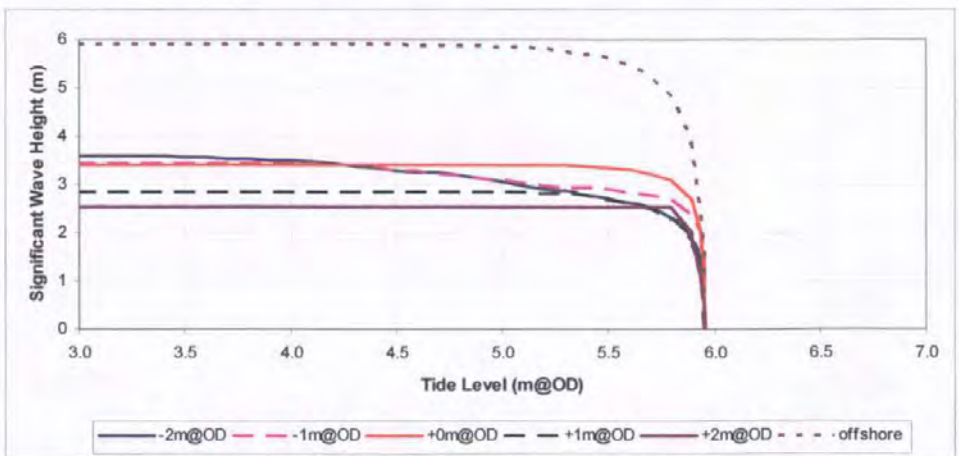


**Figure D.3c** : 100 year joint probability curves for different bed levels (Northing coordinate 472240m)

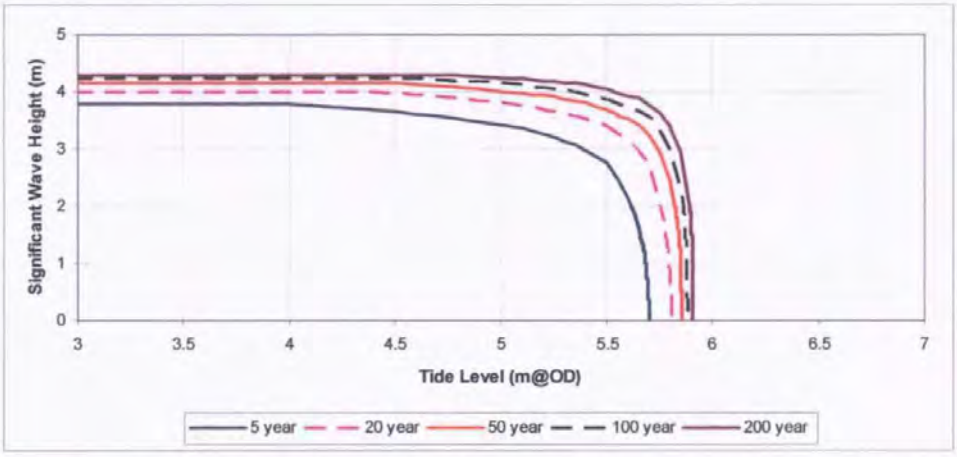


**Figure D.4a** : Joint probability curves for standard return periods for -2m@OD level (Northing coordinate 475840m)

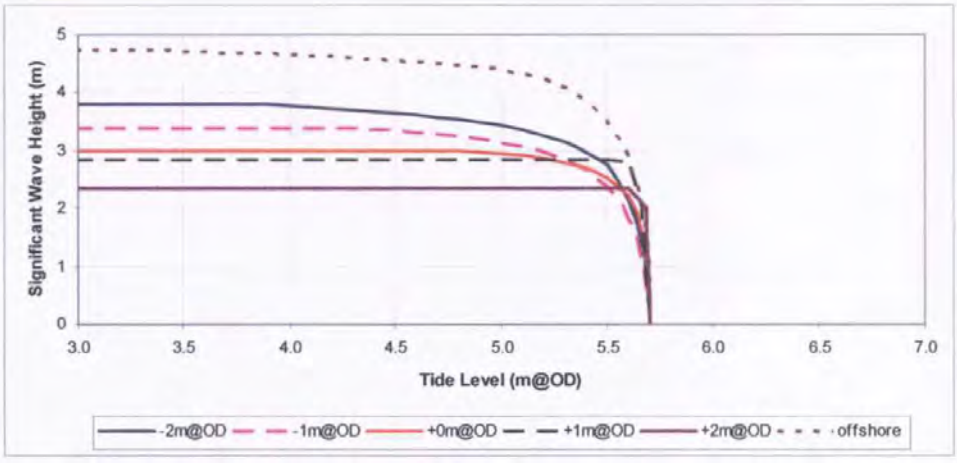


**Figure D.4b** : 5 year joint probability curves for different bed levels (Northing coordinate 475840m)

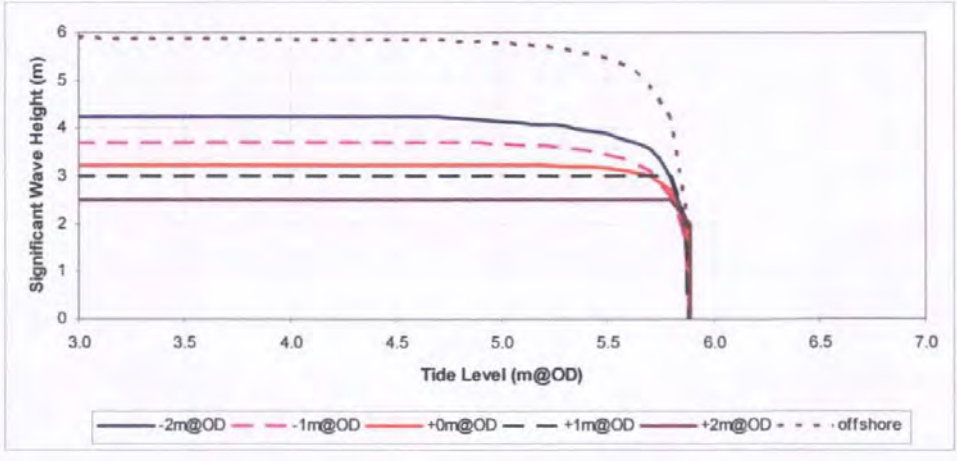


**Figure D.4c** : 100 year joint probability curves for different bed levels (Northing coordinate 475840m)

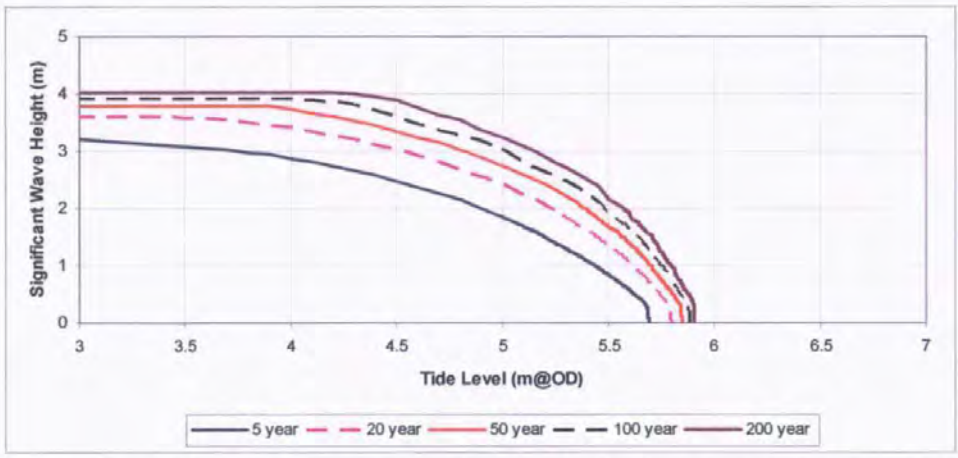


**Figure D.5a** : Joint probability curves for standard return periods for -2m@OD level (Northing coordinate 476640m)

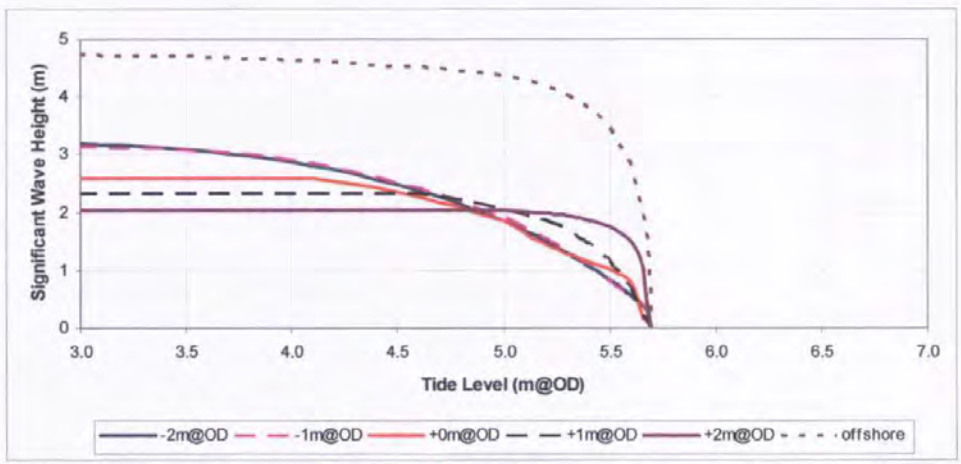


**Figure D.5b** : 5 year joint probability curves for different bed levels (Northing coordinate 476640m)

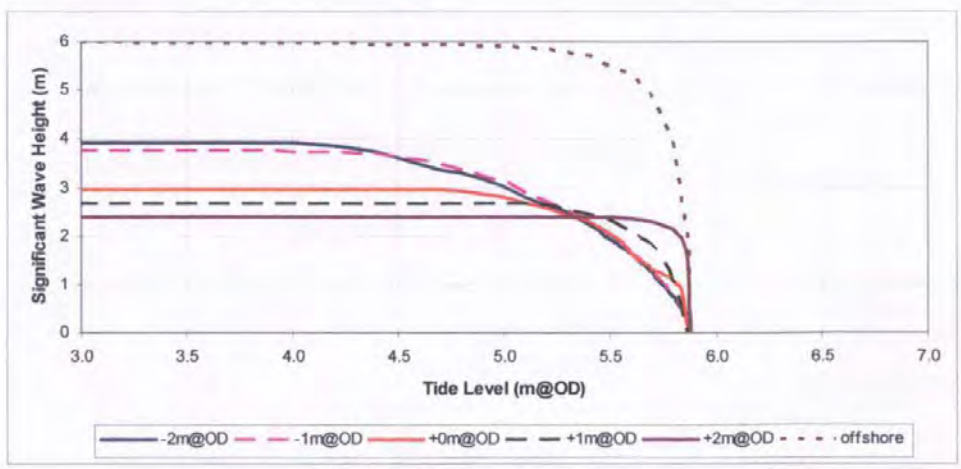


**Figure D.5c** : 100 year joint probability curves for different bed levels (Northing coordinate 476640m)

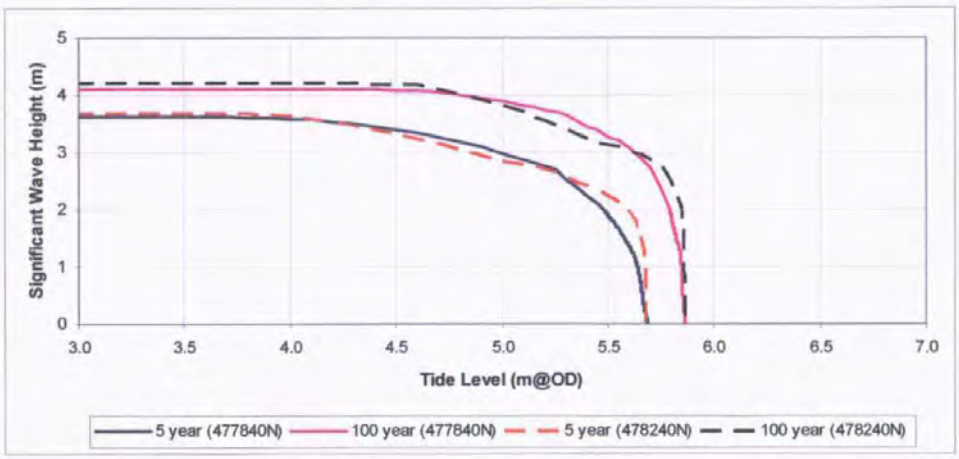


**Figure D.6a** : Joint probability curves for -2m@OD level

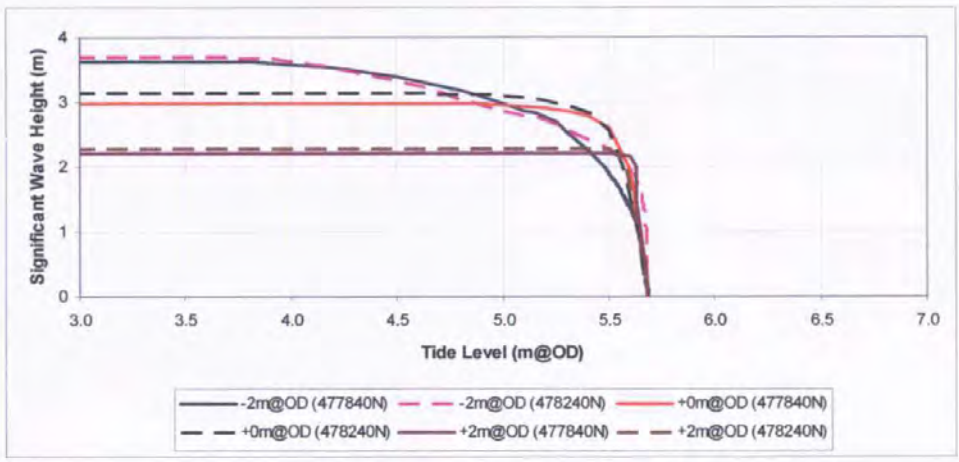


**Figure D.6b** : 5 year joint probability curves

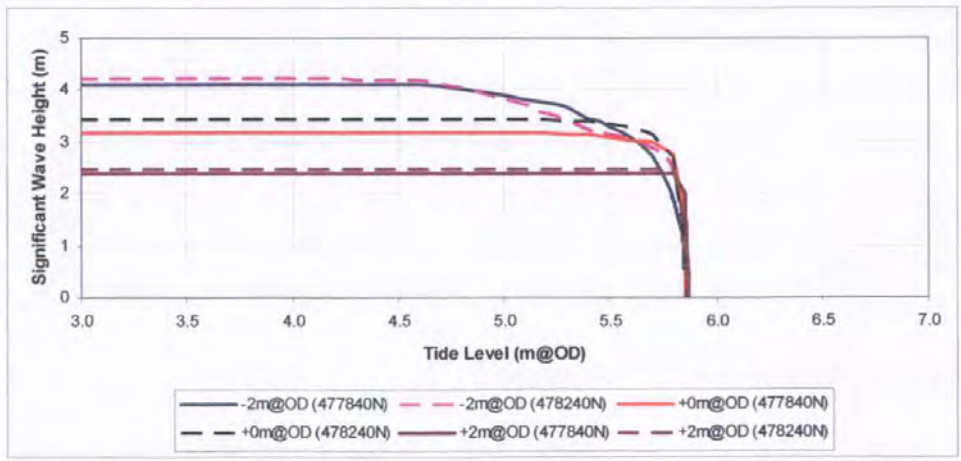


**Figure D.6c** : 100 year joint probability curves

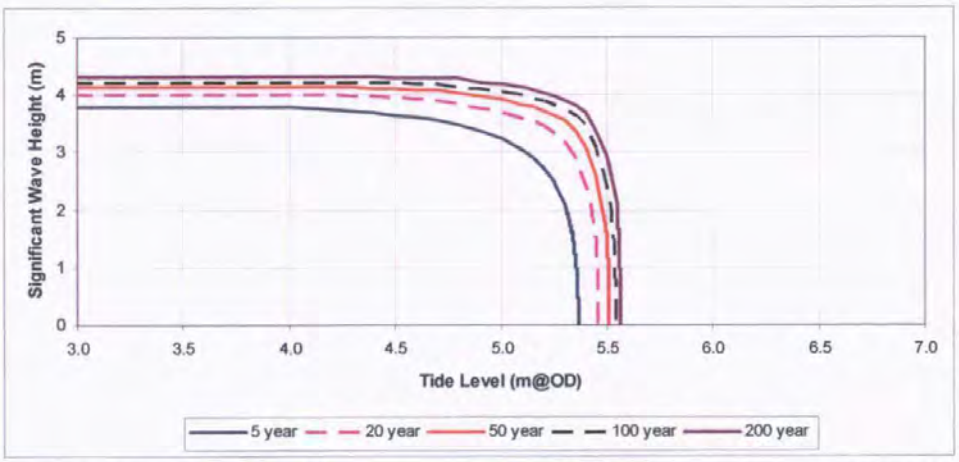


**Figure D.7a** : Joint probability curves for standard return periods for -2m@OD level (Northing coordinate 505440m)

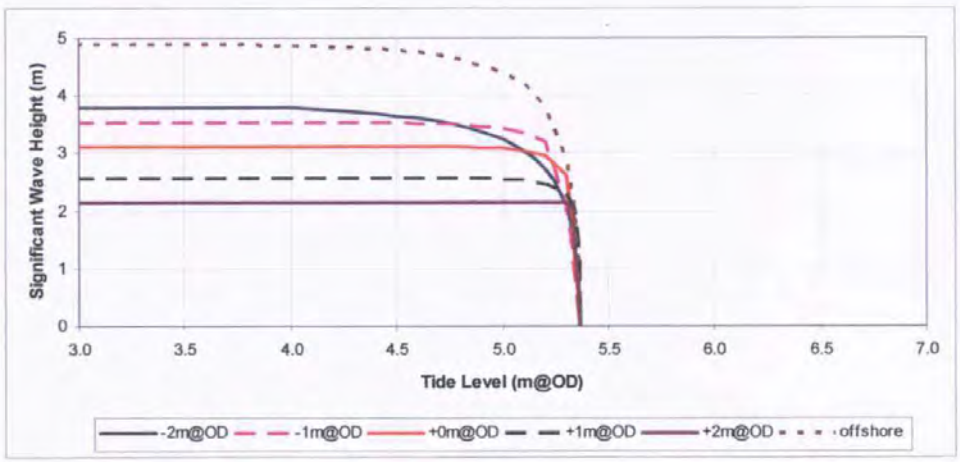


**Figure D.7b** : 5 year joint probability curves for different bed levels (Northing coordinate 505440m)

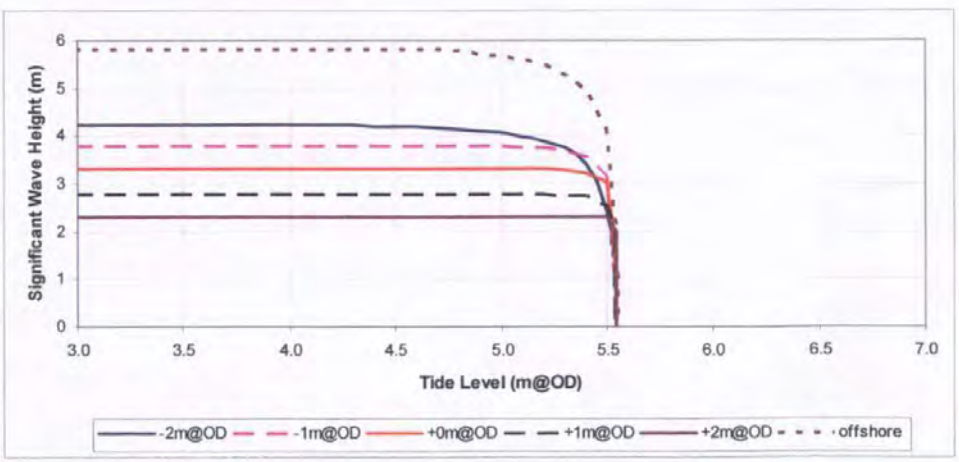


**Figure D.7c** : 100 year joint probability curves for different bed levels (Northing coordinate 505440m)

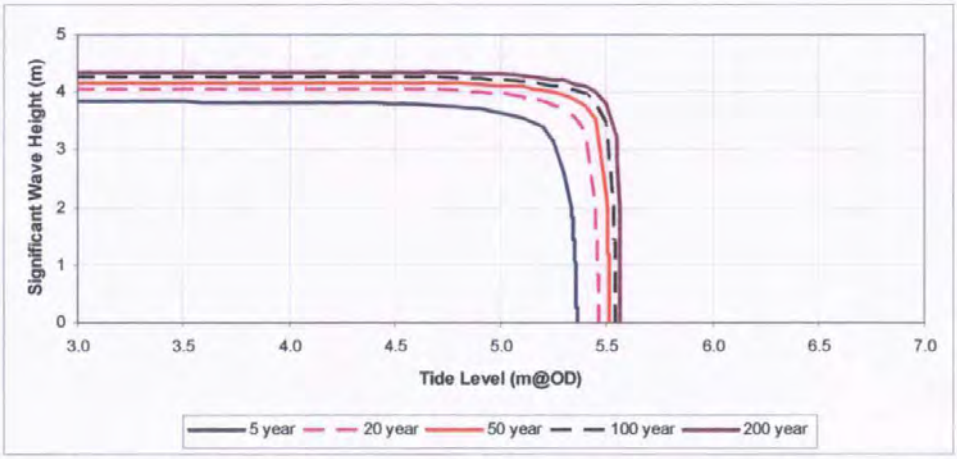


**Figure D.8a** : Joint probability curves for standard return periods for -2m@OD level (Northing coordinate 505840m)

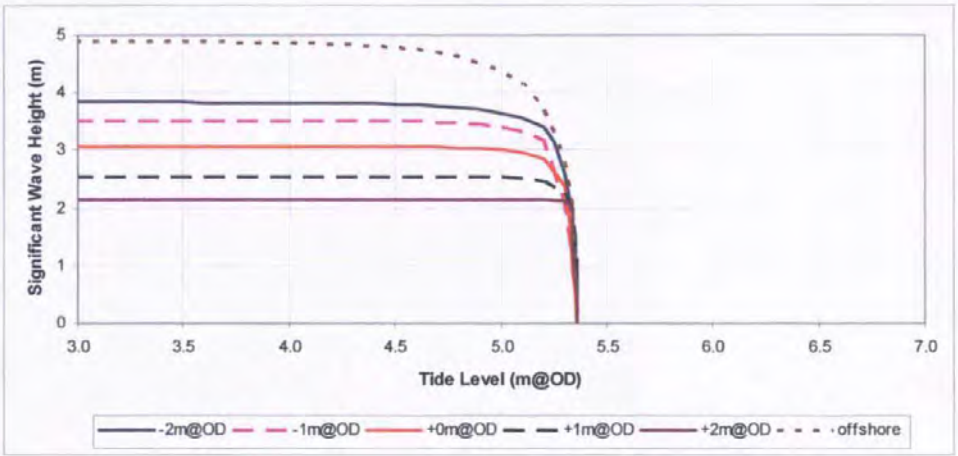


**Figure D.8b** : 5 year joint probability curves for different bed levels (Northing coordinate 505840m)

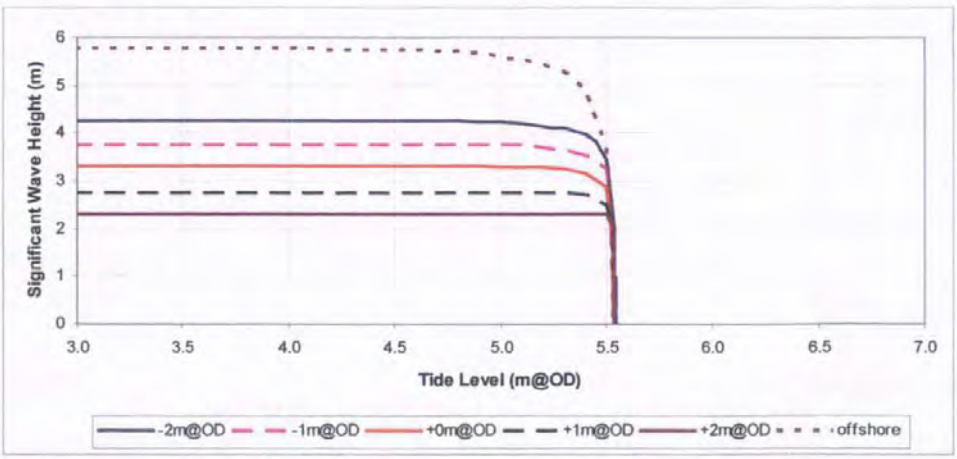


**Figure D.8c** : 100 year joint probability curves for different bed levels (Northing coordinate 505840m)

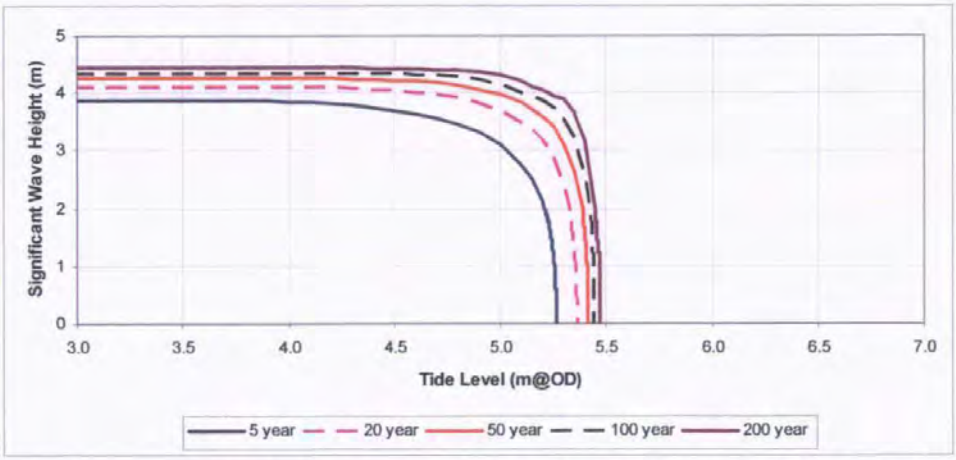


**Figure D.9a** : Joint probability curves for standard return periods for -2m@OD level (Northing coordinate 513040m)

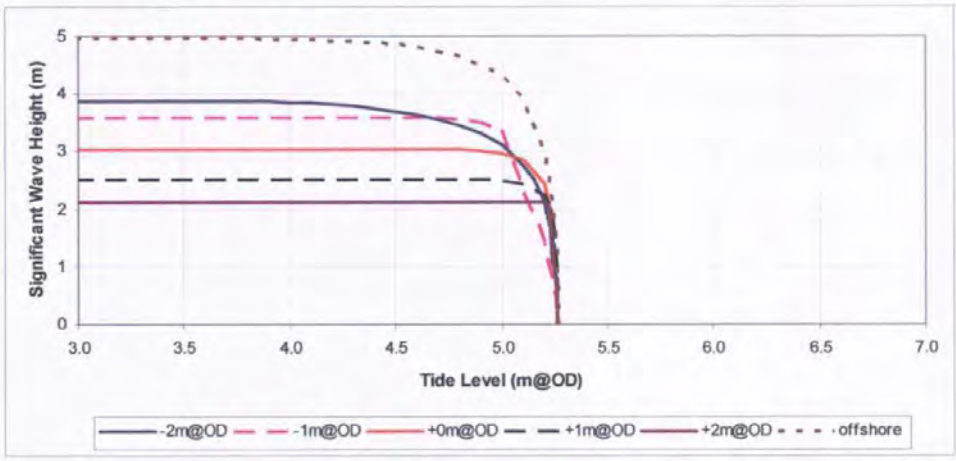


**Figure D.9b** : 5 year joint probability curves for different bed levels (Northing coordinate 513040m)

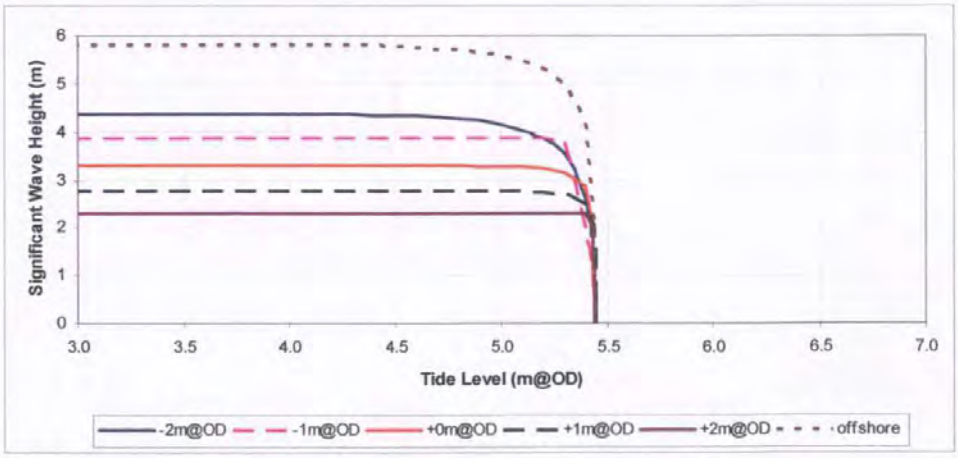


**Figure D.9c** : 100 year joint probability curves for different bed levels (Northing coordinate 513040m)

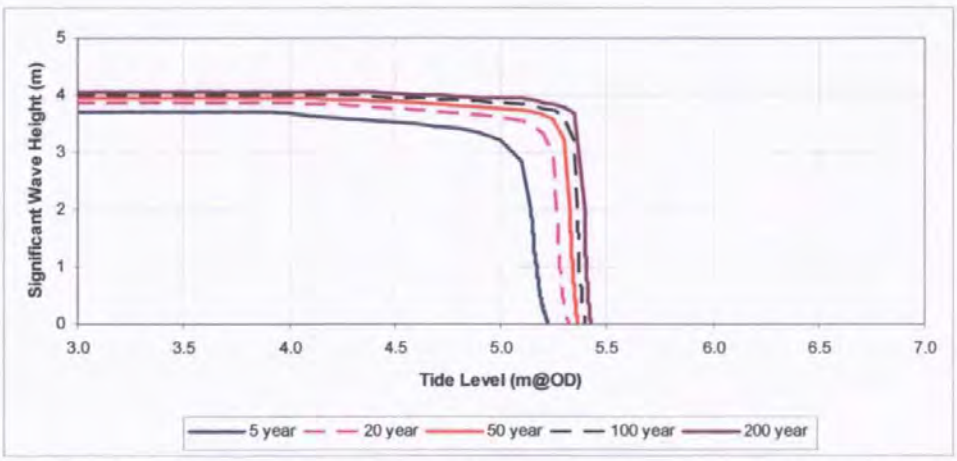


**Figure D.10a** : Joint probability curves for standard return periods for -2m@OD level (Northing coordinate 515840m)

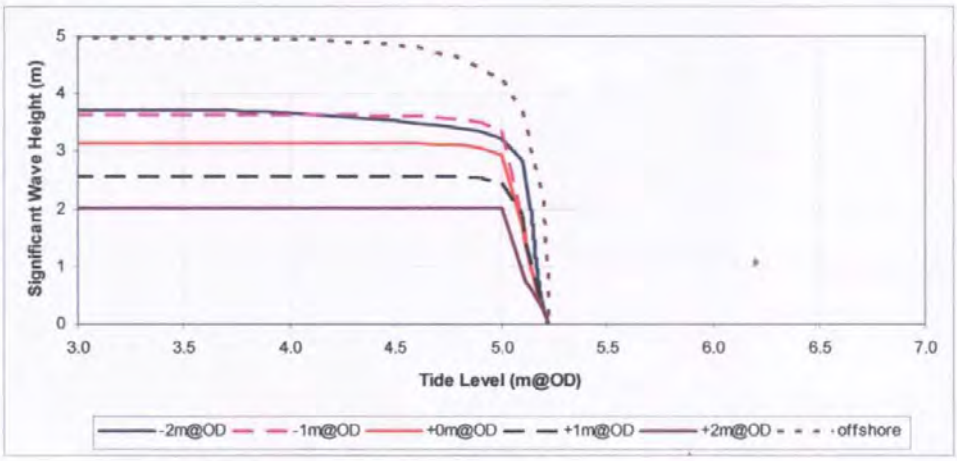


**Figure D.10b** : 5 year joint probability curves for different bed levels (Northing coordinate 515840m)

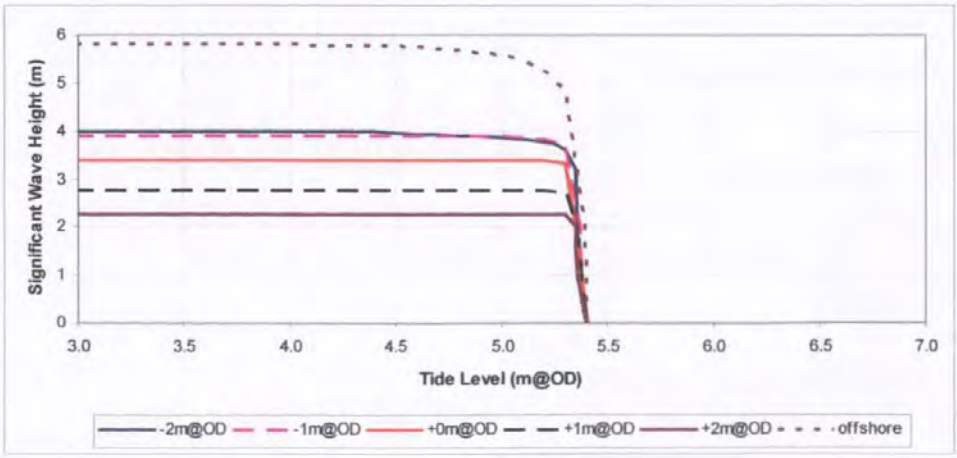


**Figure D.10c** : 100 year joint probability curves for different bed levels (Northing coordinate 515840m)

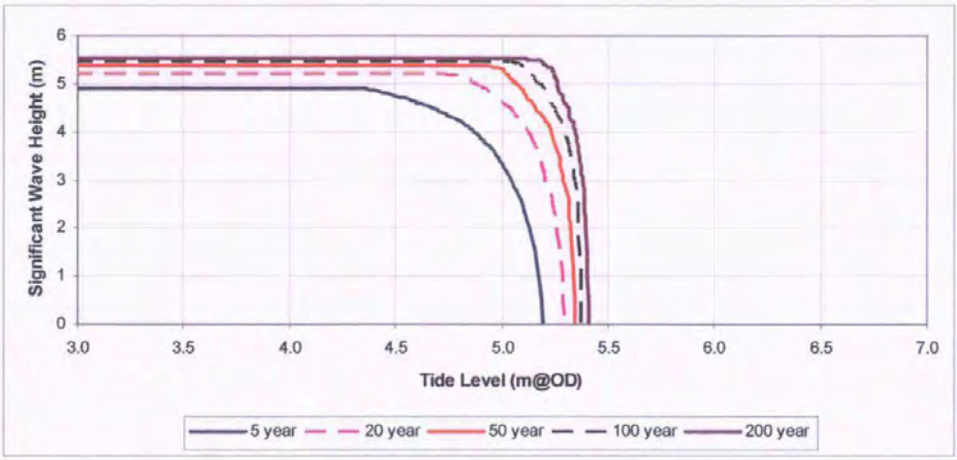


**Figure D.11a** : Joint probability curves for standard return periods for -2m@OD level (Northing coordinate 518640m)

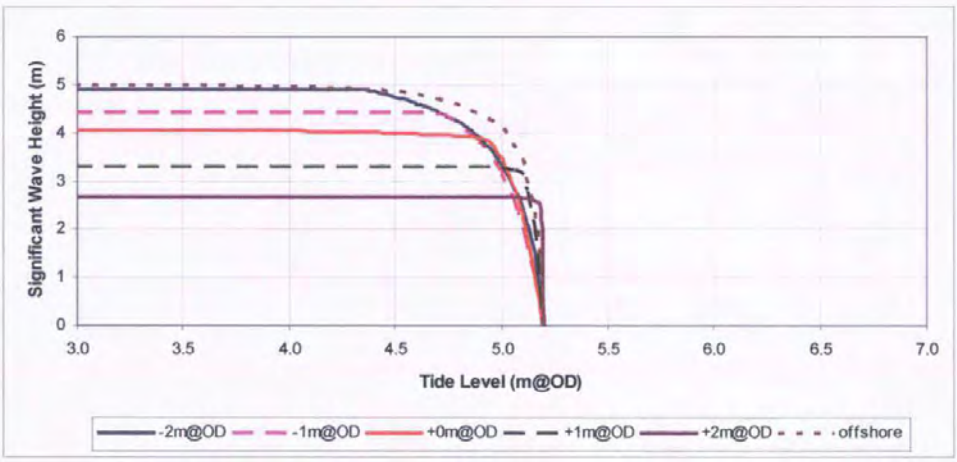


**Figure D.11b** : 5 year joint probability curves for different bed levels (Northing coordinate 518640m)

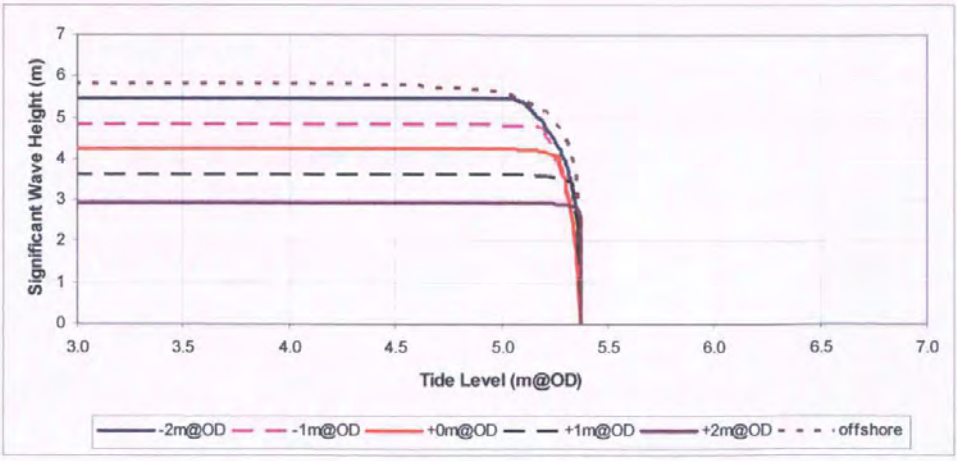


**Figure D.11c** : 100 year joint probability curves for different bed levels (Northing coordinate 518640m)

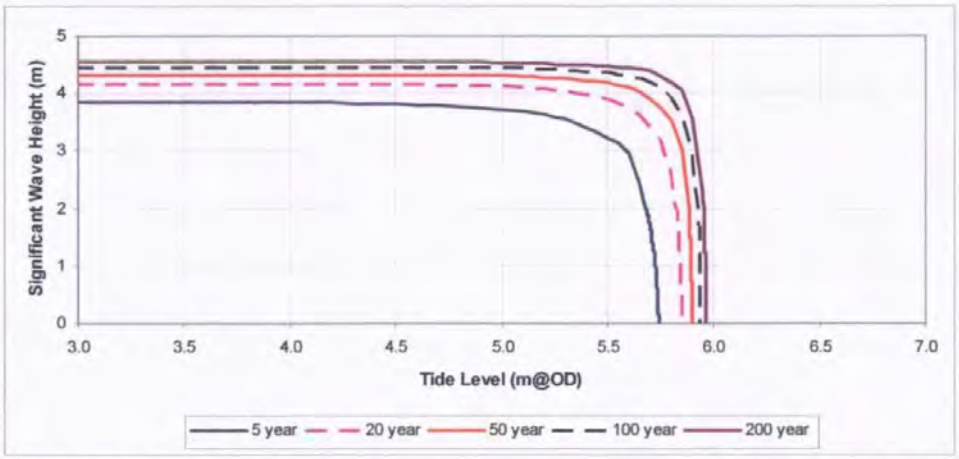


**Figure D.12a** : Joint probability curves for standard return periods for -2m@OD level (Northing coordinate 533840m)

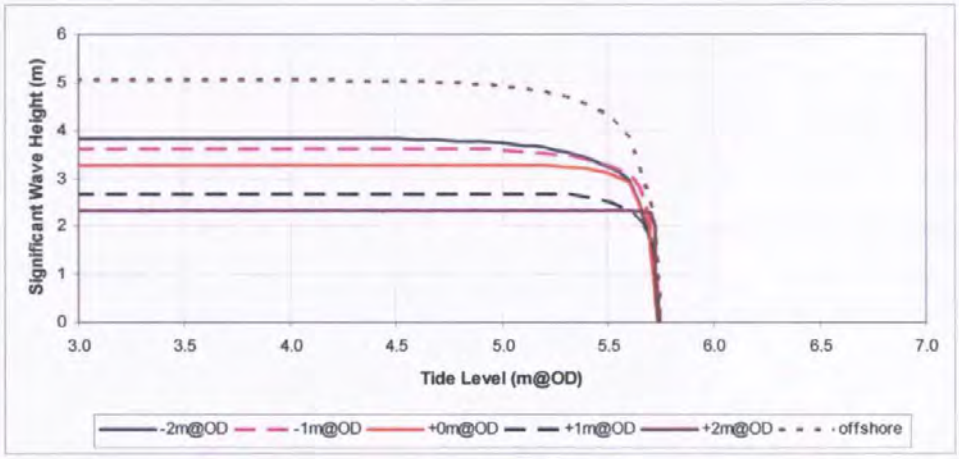


**Figure D.12b** : 5 year joint probability curves for different bed levels (Northing coordinate 533840m)

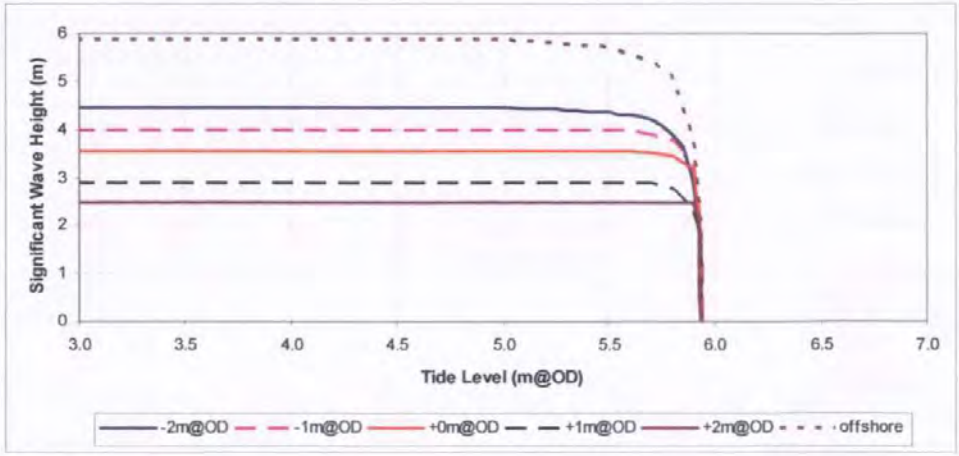


**Figure D.12c** : 100 year joint probability curves for different bed levels (Northing coordinate 533840m)

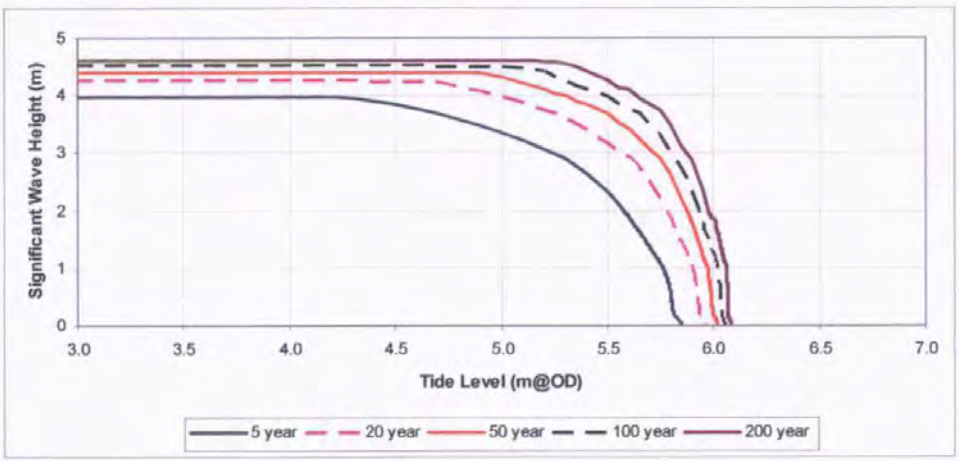


**Figure D.13a** : Joint probability curves for standard return periods for -2m@OD level (Northing coordinate 535440m)

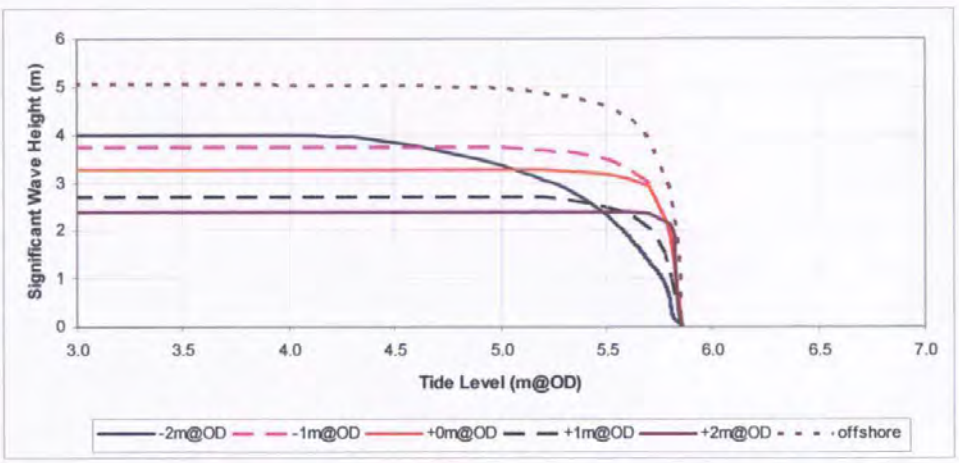


**Figure D.13b** : 5 year joint probability curves at different bed levels (Northing coordinate 535440m)

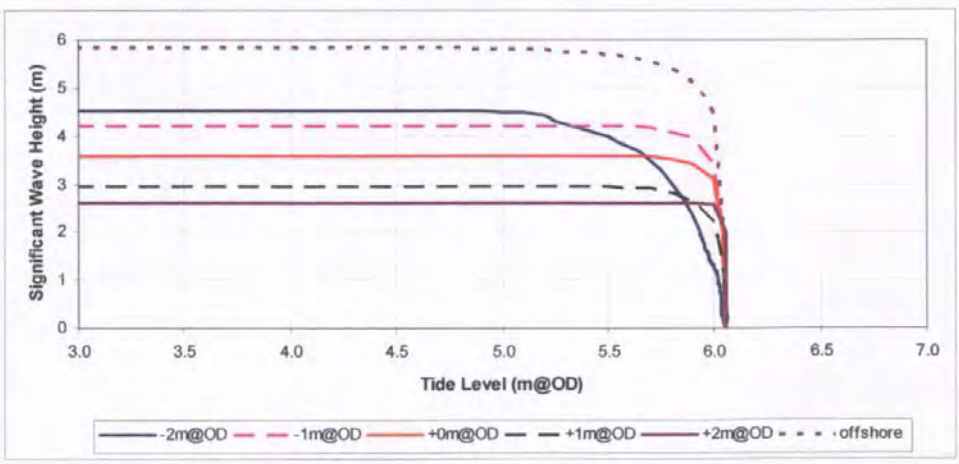


**Figure D.13c** : 100 year joint probability curves for different bed levels (Northing coordinate 535440m)

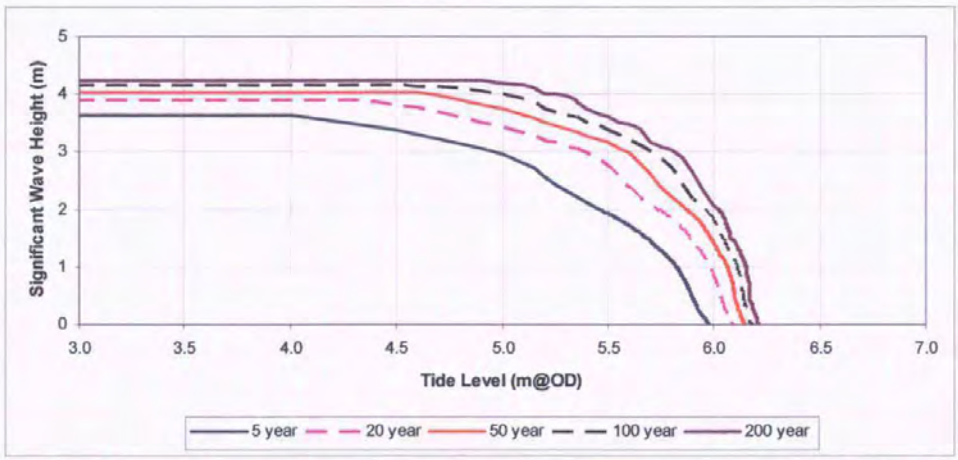


**Figure D.14a** : Joint probability curves for standard return periods for -2m@OD level (Northing coordinate 539040m)

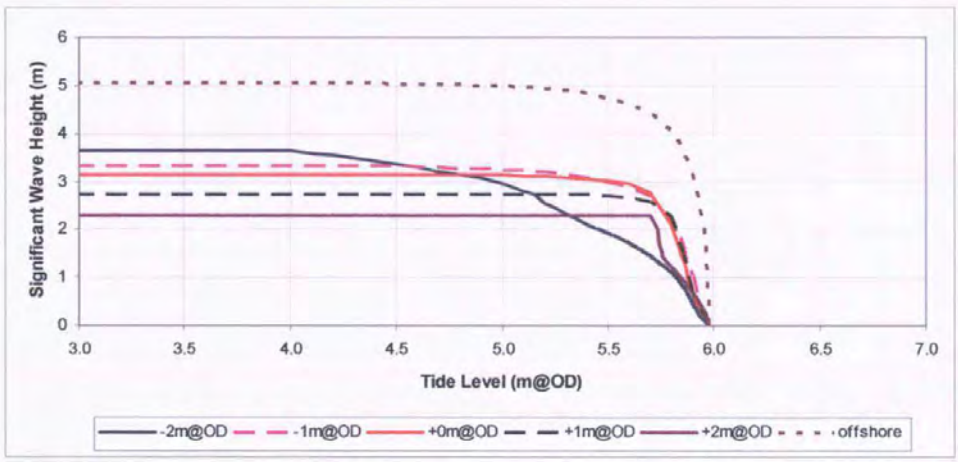


**Figure D.14b** : 5 year joint probability curves for different bed levels (Northing coordinate 539040m)

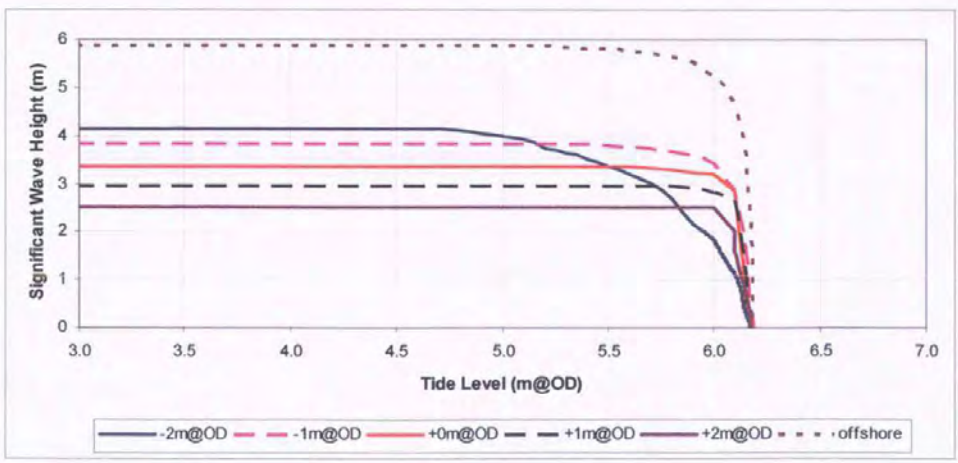


**Figure D.14c** : 100 year joint probability curves for different bed levels (Northing coordinate 539040m)

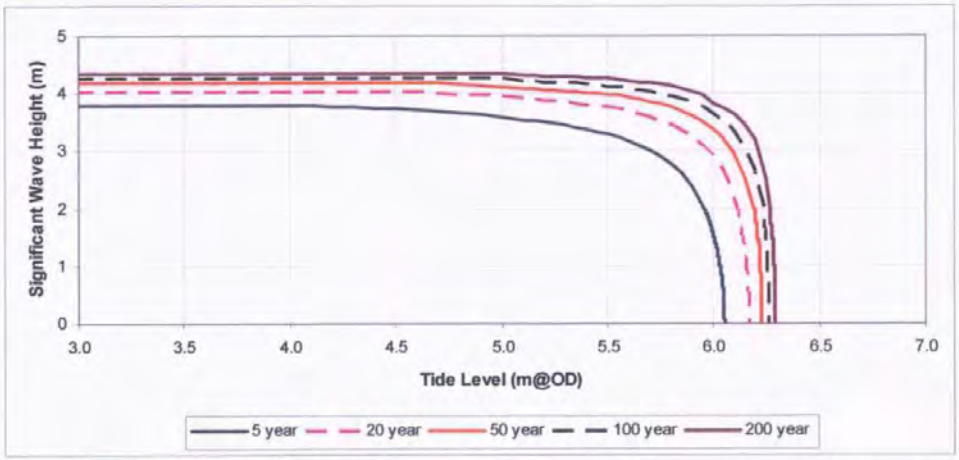


**Figure D.15a** : Joint probability curves for standard return periods for -2m@OD level (Northing coordinate 544640m)

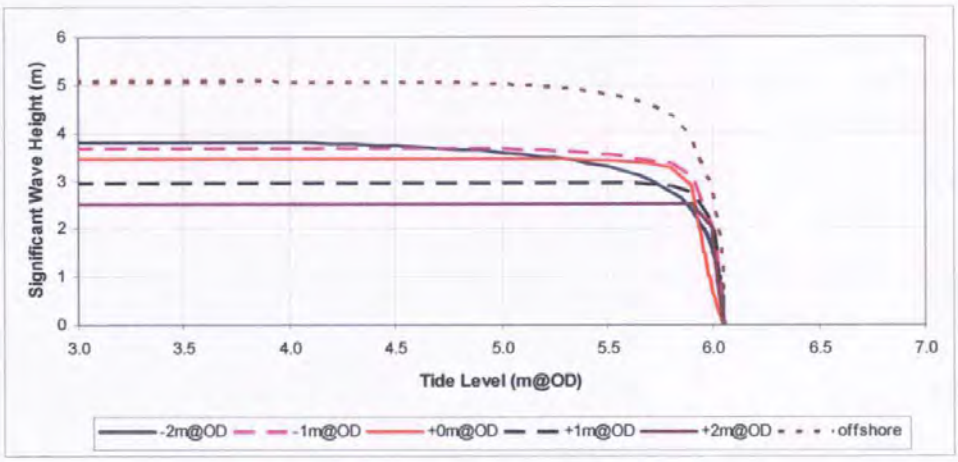


**Figure D.15b** : 5 year joint probability curves for different bed levels (Northing coordinate 544640m)

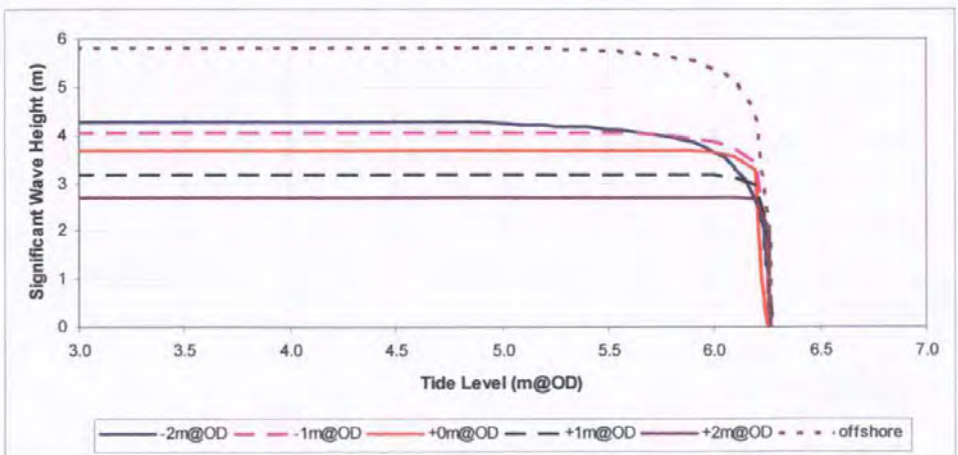


**Figure D.15c** : 100 year joint probability curves for different bed levels (Northing coordinate 544640m)

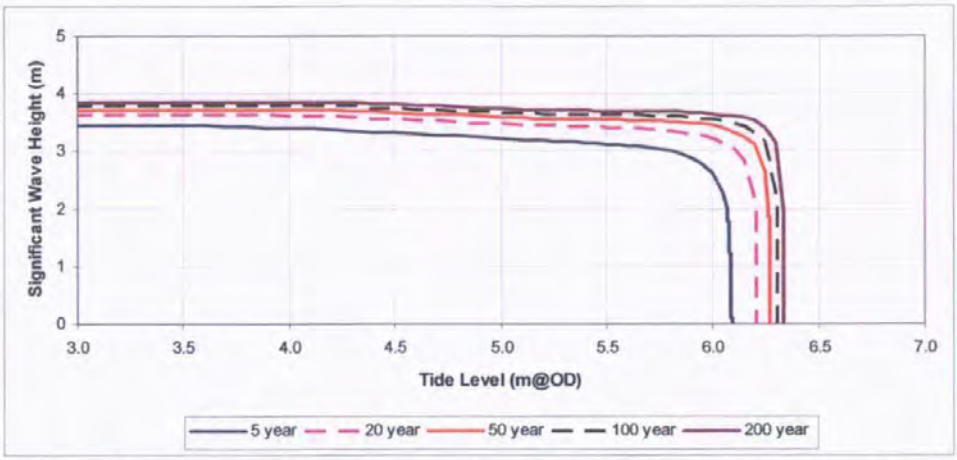


**Figure D.16a** : Joint probability curves for standard return periods for -2m@OD level (Northing coordinate 547840m)

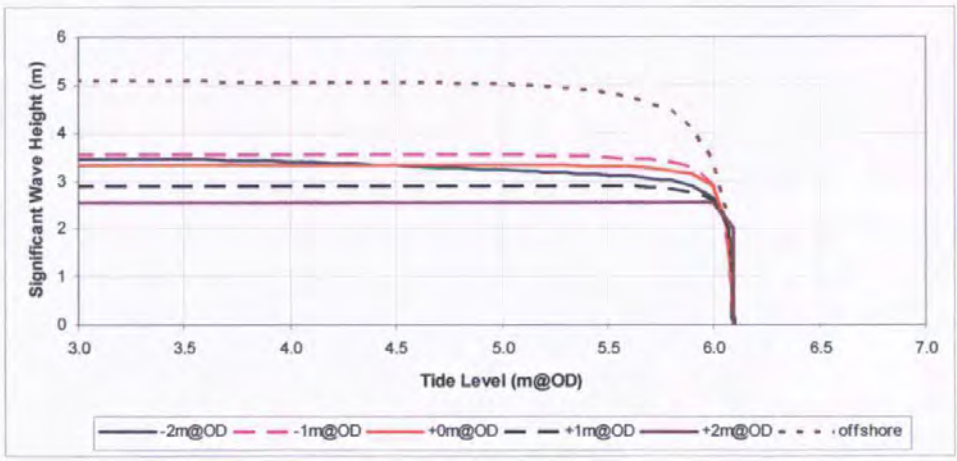


**Figure D.16b** : 5 year joint probability curves for different bed levels (Northing coordinate 547840m)

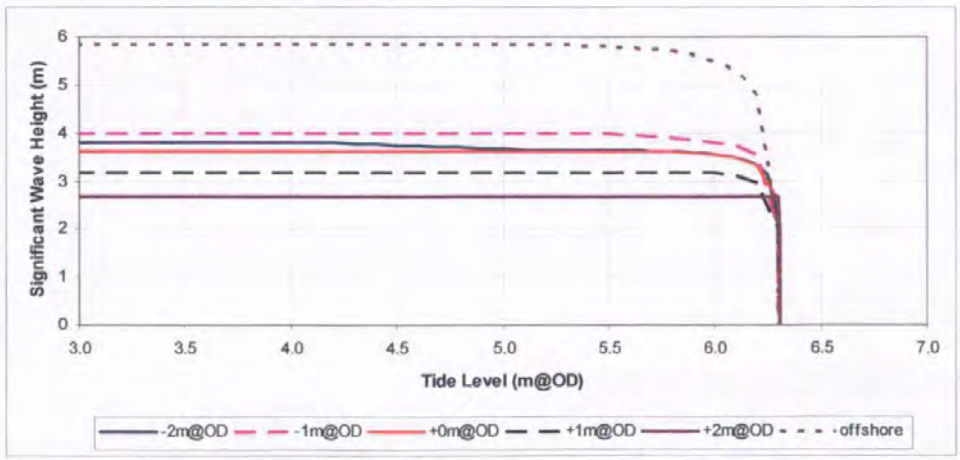


**Figure D.16c** : 100 year joint probability curves for different bed levels (Northing coordinate 547840m)

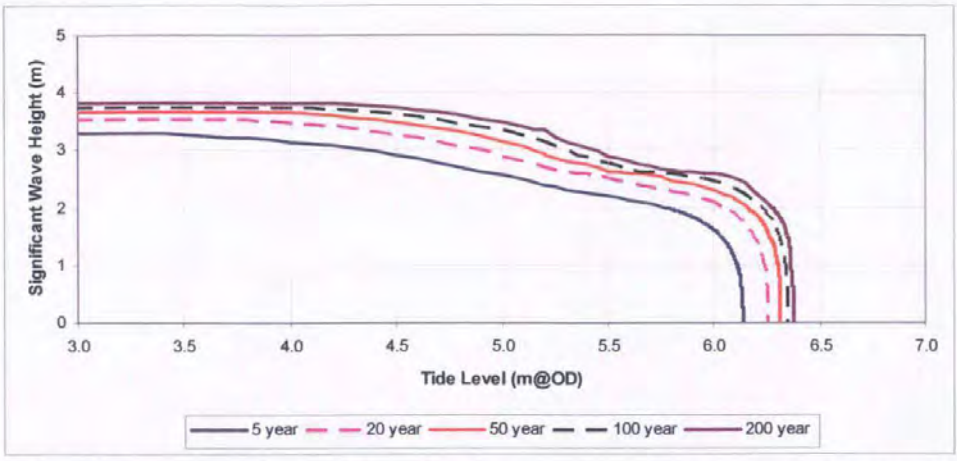


**Figure D.17a** : Joint probability curves for standard return periods for -2m@OD level (Northing coordinate 551840m)

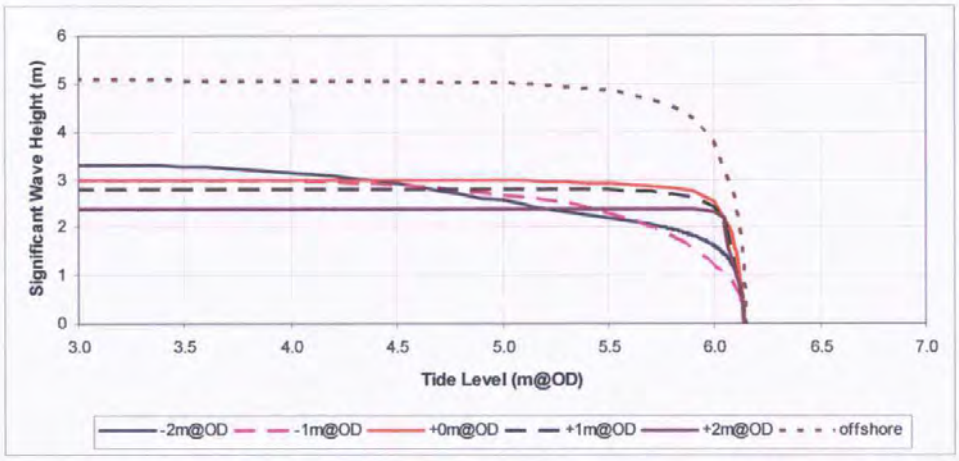


**Figure D.17b** : 5 year joint probability curves for different bed levels (Northing coordinate 551840m)

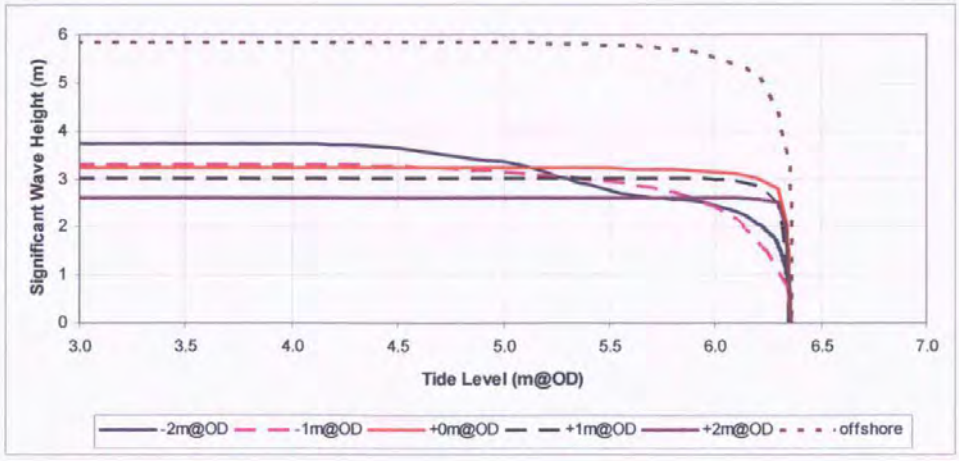


**Figure D.17c** : 100 year joint probability curves for different bed levels (Northing coordinate 551840m)

*This copy of the thesis has been supplied on condition that anyone who consults it is understood to recognise that its copyright rests with its author and that no quotation from the thesis and no information derived from it may be published without the author's prior consent.*